STUDIES ON THE INTERACTION OF SOY ISOFLAVONES WITH PROTEINS

THE

THESIS SUBMITTED TO THE DEPARTMENT OF STUDIES IN BIOCHEMISTRY, UNIVERSITY OF MYSORE IN FULFILLMENT OF THE REQUIREMENTS FOR THE DEGREE OF DOCTOR OF PHILOSOPHY IN BIOCHEMISTRY

BY

MAHESHA H. G.

UNDER THE GUIDANCE OF
DR. A. G. APPU RAO

DEPARTMENT OF PROTEIN CHEMISTRY AND TECHNOLOGY, CENTRAL FOOD TECHNOLOGICAL RESEARCH INSTITUTE

MYSORE-570020, KARNATAKA, INDIA

MARCH 2007

CERTIFICATE

I, **Mahesha H. G.** certify that this thesis is the result of research work done by me under the supervision of **Dr. A. G. Appu Rao** at **Department of Protein Chemistry and Technology, Central Food Technological Research Institute**, Mysore, Karnataka, India. I am submitting this thesis for possible award of **Doctor of Philosophy** (Ph. D.) degree in **Biochemistry** of the University of Mysore.

I further certify that this thesis has not been submitted by me for award of any other degree/diploma of this or any other University.

Mahesha H. G.

Signature of Doctoral candidate

Signed by me on 15th March 2007

Dr. A. G. Appu Rao

Signature of Guide Date: 15th March 2007

Date: 15th March 2007 *Counter signed by*

Dr. A. G. Appu Rao

*Signature of Chairperson/**Head of Department**/*
Institution with name and official seal

ABSTRACT

Genistein, daidzein and their glycosylated forms genistin and daidzin were purified to homogeneity from defatted soy flour. The binding of isoflavones to serum albumin (BSA & HSA) has been investigated by biophysical techniques. One molecule of isoflavone is bound per mole of serum albumin (bovine and human). Temperature and ionic strength dependence and competitive binding measurements of isoflavone with albumin in presence of fatty acids and 8 – Anilino-1- naphthalene sulfonic acid have suggested the involvement of both hydrophobic and ionic interactions in the isoflavone-albumin binding. Binding measurements of genistein with BSA and HSA, and those in the presence of warfarin and 2,3,5-tri-iodobenzoic acid and Förster energy transfer measurements have been used for deducing the binding pocket on serum albumin. Fluorescence anisotropy measurements of daidzein bound and then displaced with warfarin, 2,3,5-tri-iodobenzoic acid or diazepam, reinforced by molecular visualization confirm the binding of daidzein and genistein to sub domain IIA of HSA.

The interaction of isoflavones (genistein and daidzein) with CNBr cleaved albumin fragments – N, M and C was followed by intrinsic protein fluorescence and daidzein fluorescence. Genistein quenched the tryphtophan fluorescence of M domain and was unable to quench the tyrosine fluorescence of N & C domain. Daidzein fluorescence and anisotropy, was unaffected in the presence of N domain, showed enhancement in the

presence of M domain and a marginal increase in the presence of C domain. These studies support our findings with HSA that isoflavones bind to domain IIA of serum albumin.

Isoflavones are found to inhibit the activity of both soy lipoxygenase 1 and human polymorpho nuclear lymphocyte 5-lipoxygenase in a concentration dependent manner. Isoflavones are noncompetitive inhibitors of soy lipoxygenase 1. Spectroscopic studies showed that isoflavones are redox inhibitors inhibiting lipoxygenase by reducing the active state iron to the ferrous state and also prevent the activation of the resting enzyme.

Isoflavones are unable to interact with purified glycinin and conglycinin. Purified glycinin and conglycinin contain tightly bound isoflavones. The presence of intrinsically bound isoflavones was confirmed by the extraction of the pure proteins and quantification of isoflavones present.

ACKNOWLEDGEMENTS

I wish to express my sincere gratitude to my research supervisor Dr. A. G. Appu Rao Head, Department of Protein Chemistry & Technology for suggesting the problem, inspiring with helpful guidance, and forbearing support throughout the course of this investigation.

My sincere thanks to Dr. V. Prakash, Director, CFTRI, Mysore, for permission to use the necessary facilities to work in this institute and to submit the results in the form of a thesis.

The constant help and advice extended by Dr. Sridevi Annapurna Singh during the course of investigation is gratefully acknowledged.

I am indebted to all my colleagues, in the department, both past and present, for ambient working atmosphere all through my research work.

My special thanks to Mr. P. S. Kulashekar for suggestions towards making improvements to the presentation of the material in the thesis.

The patience that my wife, brother and parents exercised during the investigation is acknowledged with immense pleasure.

CSIR, New Delhi, is profoundly thanked for the financial support in the form of fellowship.

MAHESHA H. G.

TABLE OF CONTENTS WITH PAGE REFERENCES

ABBREVIATIONS vii

LIST OF TABLES ix

LIST OF FIGURES x

INTRODUCTION 1

SCOPE AND OBJECTIVES 71

MATERIALS AND METHODS 74

RESULTS AND DISCUSSION 100

SECTION A: INTERACTION OF ISOFLAVONES WITH SERUM ALBUMIN: IDENTIFICATION AND MOLECULAR VISUALIZATION OF THE BINDING SITE ON SERUM ALBUMIN 106

SECTION B: INTERACTION OF ISOFLAVONES WITH DOMAINS OF HUMAN SERUM ALBUMIN 176

SECTION C: INHIBITION OF LIPOXYGENASE BY SOY ISOFLAVONES: EVIDENCE OF ISOFLAVONES AS REDOX INHIBITORS 190

SECTION D: INTERACTION OF ISOFLAVONES WITH GLYCININ AND CONGLYCININ 219

SUMMARY AND CONCLUSIONS 227

BIBLIOGRAPHY 234

PUBLICATIONS 264

ABBREVIATIONS

Ea	Energy of activation
△G	Free Energy
△H	Enthalpy
△S	Entropy
AA	Arachidonic acid
ADH	Alcohol dehydrogenase
ANS	8 – Anilino-1- naphthalene sulfonic acid
BSA	Bovine serum albumin
CA	Carbonic anhydrase
CD	Circular dichroism
CNBr	Cyanogen bromide
DTT	Dithiothreitol
EPR	Electron paramagnetic resonance
HSA	Human serum albumin
HPLC	High performance liquid chromatography
Kcal	Kilo calories
KDa	kilo Daltons

K_i	Inhibition constant
LTB4	Leukotriene B4
LA	Linoleic acid
LDL	Low-density lipoproteins
LOX-1	Lipoxygenase-1
NBS	N-Bromosuccinimide
NDGA	Nor-dihydroguaiaretic acid
PAGE	Poly acrylamide gel electrophoresis
PMNL	Polymorpho nuclear Lymphocyte
SDS	Sodium dodecyl sulphate
RP-HPLC	Reverse phase high performance liquid chromatography
TIB	2, 3, 5 –Tri-iodo benzoic acid
9S-HETE	9*S*-hydroxyeicosatetraenoic acid
5- HETE	5-hydroxyeicosatetraenoic acid
5-LOX	5-Lipoxygenase
IC_{50}	Mid point inhibitor concentration

LIST OF TABLES

NO	TITLE	PAGE NO
1	Corrected fluorescence anisotropy values of the daidzein-BSA complex, when different aliquots of warfarin, diazepam and triiodobenzoic acid were added.	133
2	Corrected fluorescence anisotropy values of the warfarin-BSA complex, when different aliquots of genistein were added.	134
3	Comparison of the genistein (ligand) distance to tryptophan (HSA) measured by Forster non-radiative energy transfer with other ligands bound to HSA.	154
4	Corrected fluorescence anisotropy values of the daidzein-HSA complex, when different aliquots of warfarin, diazepam and tri-iodobenzoic acid were added.	155
5	Corrected fluorescence anisotropy values of the warfarin-HSA complex, when different aliquots of genistein were added.	156
6	Secondary structure analysis of the intact human serum albumin and isolated N, M and C fragments	180
7	IC_{50} values for the inhibition of soy lipoxygenase by isoflavones	195
8	IC_{50} values for the inhibition of human PMNL 5-lipoxygenase by isoflavones	195

LIST OF FIGURES

FIGURE NO	TITLE	PAGE NO
1	Generic structure of isoflavones	3
2	Structure of oestradiol, genistein and daidzein	7
3	X-ray crystal structure of HSA	25
4	Secondary structure scheme of HSA	26
5	Summary of the ligand binding capacity of HSA as defined by crystallographic studies to date.	36
6	Schematic representation of the reaction catalyzed by SLO-1	37
7	Reaction catalyzed by mammalian lipoxygenase	39
8	Ribbon representation of the soybean lipoxygenase1	45
9	Active site structure of soy lox-1	49
10	Molecular model of active center in SLO-1	50
11	Structure of rabbit reticulocyte 15-LOX	53
12	Catalytic mechanism of soy lox-1	58
13	Elution profile of ethyl acetate extract on silica gel column	102
14	Rechromatography of F_1 fraction	102
15	Rechromatography of F_5 fraction	103
16	Adsorption chromatography of F_1 fraction	103
17	Adsorption chromatography of F_5 fraction	104
18	Adsorption chromatography of F_6 fraction	104
19	HPLC Profile of genistin	105
20	HPLC Profile of daidzin	105
21	HPLC Profile of genistein	106
22	HPLC Profile of daidzein	106
23	SDS-PAGE of bovine serum albumin	110
24	Bovine serum albumin interaction with genistein by equilibrium dialysis	
24A	A plot of ν (moles of ligand bound to protein) vs free ligand concentration	111
24B	Scatchard plot depicting the plot of ν / (L) vs ν	111
25	Overlap of emission spectra of BSA with genistein	112
26	Overlap of emission spectra of BSA with daidzein.	112
27	Quantitation of the interaction of BSA with genistein by fluorescence quenching	
27A	% quench of fluorescence intensity, as a function of constituent genistein concentration	113
27B	Double-reciprocal plot of data	114
27C	Job's plot	114
27D	Mass action plot of data	115

28	Quantitation of the interaction of BSA with daidzein by fluorescence quenching	
28A	% quench of fluorescence intensity, as a function of constituent daidzein concentration	116
28B	Double-reciprocal plot of data	117
28C	Mass action plot of data	117
29	Van't Hoff's plot for BSA	118
30	Effect of ionic strength on the binding constant of genistein to BSA	123
31	Emission spectra of daidzein showing blue shift on binding to BSA	124
32	Fluorimetric titration of BSA-ANS complex with genistein	125
33	Fluorimetric titration of BSA-genistein acid complex with palmitic acid	126
34A	Effect of genistein on the tertiary structure of BSA	127
34B	Effect of genistein on near UV CD of warfarin–bound BSA	128
35	Competitive ligand binding interactions of BSA: Genistein and daidzein	
35A	Emission spectra of daidzein with increasing micro molar concentration of BSA	129
35B	Emission spectra of daidzein-BSA complex with increasing micro molar concentration of genistein	130
35C	F_{max} / F vs genistein concentration	131
36	Variation in fluorescence anisotropy of daidzein as a function of BSA concentration	132
37	SDS-PAGE of monomeric HSA	138
38	Human serum albumin interaction with genistein: equilibrium dialysis	
38A	A plot of ν (moles of ligand bound to protein) vs free ligand concentration (L)	139
38B	Scatchard plot depicting the plot of ν / (L) vs ν	139
39	Resonance energy transfer from HSA to genistein and daidzein	140
40	Quantitation of the interaction of HSA with genistein by fluorescence quenching	
40A	% quench of fluorescence intensity, as a function of constituent genistein concentration	141
40B	Double-reciprocal plot of data	142
40C	Job's plot	142
40D	Mass action plot of data	143
41	Quantitation of the interaction of HSA with daidzein by fluorescence quenching	
41A	% quench of fluorescence intensity	144
41B	Double-reciprocal plot of data	145
41C	Mass action plot of data	145

42	Van't Hoff's plot for HSA	146
43	Effect of ionic Strength on the binding constant of genistein to HSA	152
44	Emission spectra of daidzein showing blue shift on binding to HSA	153
45	Interaction of genistein with HSA, defatted HSA and BSA	
45A	% quench of fluorescence intensity, for HSA, defatted HSA and BSA as a function of constituent genistein concentration	157
45B	Mass action plot of HSA and BSA	158
46	Fluorimetric titration of HSA-ANS complex with genistein	159
47	Fluorimetric titration of HSA-genistein complex with palmitic acid	160
48	Competitive ligand interactions of HSA: warfarin and genistein (CD Measurements)	
48A	Effect of warfarin on the near UV CD of HSA	161
48B	Effect of genistein on near UV CD of warfarin–bound HSA	162
49	Competitive ligand binding interactions of HSA: Genistein and daidzein (Fluorescence measurements)	
49A	Emission spectra of daidzein with increasing micro molar concentration of HSA	163
49B	Emission spectra of daidzein-HSA complex with increasing micro molar concentration of genistein	164
49C	F_{max} / F vs genistein concentration	164
50	Variation in fluorescence anisotropy of daidzein as a function of HSA concentration	165
51	Molecular visualization of binding of genistein with HSA/warfarin complex	175
52	Elution profile of cyanogen bromide fragmented HSA on a sephadex G-100 gel filtration column	178
53	Ion-exchange profile of N+M domain on a SP Sephadex C-25 column	178
54	Non-reducing page of domains of human serum albumin	179
55	Quantitation of the interaction of genistein with the M-domain of HSA by fluorescence quenching	
55A	% quench of fluorescence intensity, as a function of constituent genistein concentration	183
55B	Double-reciprocal plot of data	184
55C	Mass action plot of data	184
56	Fluorescence resonance energy transfer between M-domain and genistein	185
57	Emission spectra of daidzein showing blue shift on binding to M and C domains of serum albumin	186

58	Variation in fluorescence anisotropy of daidzein as a function of M and C domains of serum albumin	187
59	Gel electrophoresis of soy lipoxygenase-1	
59A	SDS-PAGE of LOX-1	191
59B	Native PAGE of LOX-1	191
60A	Time course of lipoxygenase catalyzed reaction	193
60B	Inhibition of lipoxygenase by isoflavones	194
61A	Time course of lipoxygenase catalyzed reaction	
	Lineweaver-Burk plot analysis for inhibition of	196
61B	lipoxygenase by genistein	197
61C	Determination of K_i of genistein	198
61D	Dixon Plot	198
62A	Lineweaver-Burk plot analysis for inhibition of lipoxygenase by daidzein	199
62B	Determination of K_i of daidzein	200
63	Stopped flow inhibition of active ferric lipoxygenase by genistein	202
64	Effect of genistein on the absorption spectra of ferric lipoxygenase	203
65	Effect of genistein on the CD spectrum ferric lipoxygenase	207
66	Effect of daidzein on the CD spectrum ferric lipoxygenase	208
67	Effect of genistein on the EPR spectrum of ferric soybean lipoxygenase	209
68	Effect of daidzein on the EPR spectrum of ferric soybean lipoxygenase	210
69	EPR spectra of genistein due to base-catalyzed auto oxidation	211
70	HPLC profile of genistein in presence of soy LOX-1 and linoleic acid	212
	Gel electrophoresis of soy glycinin and conglycinin	
71A	SDS-PAGE of glycinin	221
71B	SDS-PAGE of conglycinin	
72	HPLC Profile of 11S extract	222
73	HPLC Profile of 7S extract	223

INTRODUCTION

INTRODUCTION

Human diet contains, in addition to essential micro and macronutrients, a complex array of naturally occurring bioactive compounds known as phytochemicals. Phytochemicals are plant-derived compounds of natural origin (Bradbury and White, 1954). More and more phytochemicals that posses biological activity are being discovered as the understanding of associations between diet and disease states is getting better with studies. These phytochemicals may confer significant long-term health benefits when incorporated in the diet either as supplement or as ingredients. This revolutionary concept has promoted the relatively new field of functional foods. Epidemiological studies have demonstrated that a significant difference that exists in the incidence of cancers and heart diseases among different ethnic groups is partly attributable to dietary factors. In recent years, soy isoflavones have acquired greater attention of public and the medical community thanks to evidence from published research about the health benefits of soy-based foods to humans. These soy-based foods are rich in bioactive phytochemicals called isoflavones. Isoflavones are present in varying amounts primarily in members of the leguminosae family. Foods such as soy, lentil, bean and chickpea are sources of isoflavones. Soybeans are the major source of isoflavones. Isoflavones belong to a class of diphenol compounds known as phytoestrogens (Knight & Eden 1994). The isoflavones in soybeans include genistein, daidzein, **(Fig. 1)** and glycitein, each of which exist in four chemical forms, namely aglycone

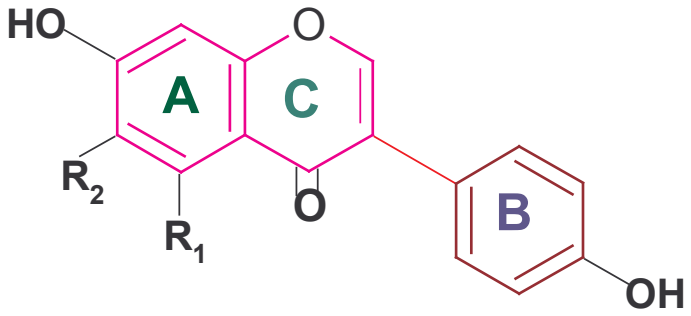

Figure 1. Generic structure of isoflavones.

R1	R2	COMPOUNDS
H	H	Daidzein
OH	H	Genistein
H	OCH3	Glycitein

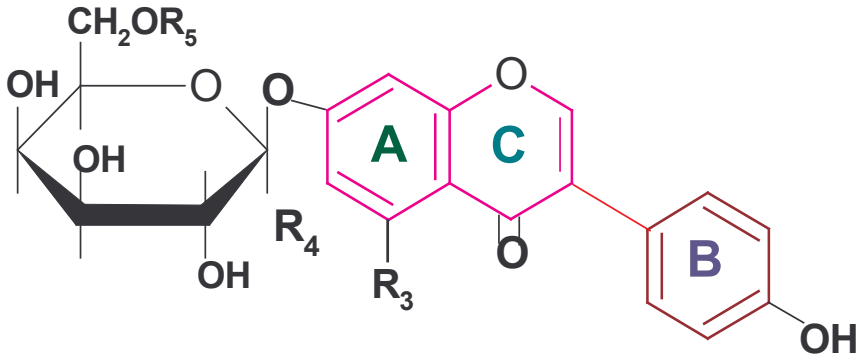

R3	R4	R5	COMPOUNDS
H	H	H	daidzin
OH	H	H	genistin
H	OCH3	H	glycitin
H	H	COCH3	6”-O-Acetyldaidzin
OH	H	COCH3	6”-O-Acetylgenistin
H	OCH3	COCH3	6”-O-Acetylglycitin
H	H	COCH2COOH	6”-O-Malonyldaidzin
OH	H	COCH2COOH	6”-O-Malonylgenistin
H	OCH3	COCH2COOH	6”-O-Malonylglycitin

(genistein, daidzein, and glycitein), β-glycoside (genistin, daidzin, and glycitin), acetylglycoside (6"-*O*-acetylgenistin, 6"-*O*-acetyldaidzin, 6"-*O*-acetylglycitin) and malonylglycoside (6"-*O*-malonylgenistin, 6"-*O*-malonyldaidzin, 6"-*O*-malonylglycitin) (Barnes *et. al.,* 1994). The basic structure of isoflavones comprises two benzyl rings joined by a three-carbon bridge, represented by C_6-C_3-C_6. Isoflavones differ from flavones in that the benzyl ring B is joined at position 3 instead of position 2. Upon ingestion, isoflavone glycosides are hydrolyzed in the intestine by bacterial β-glycosidases and converted to corresponding bioactive aglycones (Coldham *et.al.,* 2002; Coldham and Sauer, 2001). Wang and Murphy (1994) characterized the concentration and distribution of all 12 isoflavone isomers in 29 commercial soybean foods.

Unprocessed soybeans contain 1.2-4.2 mg of isoflavones/g, dry weight, while high-protein soy ingredients such as soy flour and texturized vegetable protein (TVP) contain 1.1-1.4 mg/g dry weight. Soy concentrate, produced by water or alcohol wash of soy flakes to remove soluble carbohydrates and improve functionality, has an extremely low isoflavone concentration. Second-generation soy foods such as tofu, yogurt and tempeh burger contain 6-20% of the isoflavones found in whole soybeans (Wang and Murphy, 1994), since most of the matrices in these foods are nonsoybean constituents. Processing is known to have a bearing on the forms of isoflavones found in soy foods. Minimally processed soy flour contains 6"-*O*-malonylgenistin, 6"-*O*-malonyldaidzin as the major isomers. In contrast, TVP contains appreciable amounts of 6"-*O*-acetylgenistin, 6"-*O*-acetyldaidzin, as a

result of the transformation of the malonyl isoflavones to their acetyl forms by heat treatment during extrusion processing. Nonfermented soy foods (e.g. tofu) contain greater levels of glycoside, while fermented soy foods (e. g. tempeh) contain greater levels of aglycones as a result of enzymatic hydrolysis during fermentation (Wang and Murphy, 1994). Isoflavones undergo degradation and modifications during processing of foods, leading to changes in their bioactivity. Genistein forms conjugates with very high UV absorption when mixed with dextrose, fructose, maltose or sucrose, proportional to the amount of sugar added (Wang *et.al.,* 1990). Genistein undergoes auto-degradation and reacts with lysine forming Maillard browning products (Davies *et.al.,* 1998). Genistein and daidzein are degraded when exposed to high temperature. In alkaline solution the concentration of genistein is reduced by 60%, whereas daidzein is less affected by the thermal treatment and a minor 15% reduction has been observed. Interestingly, in the neutral pH, daidzein is less stable than genistein, and its concentration decreases by 40%, as compared to 22% for genistein (Ungar *et.al.,* 2003).

Heat treatment also appears to affect their antioxidant activity. The antioxidant activity of genistein is reduced by 60% at pH 9.0 as against daidzeins 20% decline in its activity. At pH 7.0, both genistein and daidzein maintain their antioxidant abilities at >70% for at least 30 days (Ungar *et.al.,* 2003). Isoflavones are also called phytoestrogens, as they have nonsteroidal structure and can behave as estrogen mimics. As phytoestrogens are of dietary origin and are extensively biotransformed in

the intestine by the action of bacterial enzymes, isoflavones can be nicknamed as dietary oestrogens. Isoflavones can interact with oestrogen receptors and the similarity of their structure to the 17β-oestradiol molecules is in all probability, the basis of this mimicry. These molecules share several features in common with the oestradiol structure (Fig.2), including a pair of hydroxyl groups separated at a similar distance; one hydroxyl group is a substituent of an aromatic A ring while the second hydroxyl lies at the opposite end of the molecule (Miksicek, 1993). The oestrogen-like structures of the phyto-oestrogens help explain the ability of these molecules to occupy the oestrogen receptor; however, the interaction is not equivalent since both the occupancy time and affinity for the receptor are significantly reduced for phyto-oestrogens (Miksicek, 1994). In addition, small differences in the structures of individual isoflavones dramatically alter their oestrogenicity. Genistein and daidzein share identical structures except for an additional hydroxyl group on the A ring of genistein; this may be the reason for 5-6-fold greater oestrogenic activity of genistein in some assays in comparison to daidzein (Markiewicz *et.al.,* 1993).

The identification and cloning of a second and novel estrogen receptor, named as Erβ (Kuiper *et.al.,* 1996), with its unique anatomical distribution in tissues such as bone, brain, vascular endothelia and bladder and its ligand specificity toward phytoestrogen (Kuiper *et.al.,* 1997) emphasize the need to understand the hormone like functions of isoflavones. The preferential binding of nonsteroidal oestrogens to the Erβ receptor suggests that they

may deliver their actions differently compared to those of classical steroidal oestrogens.

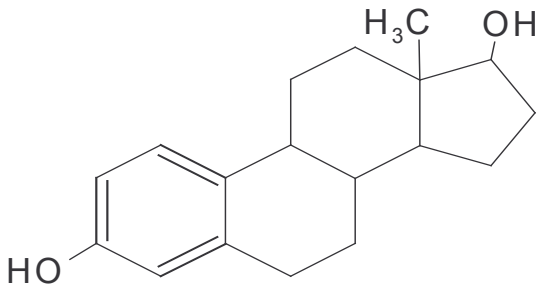

17β- oestradiol

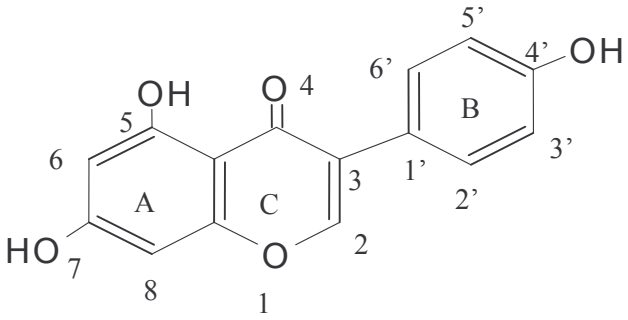

Genistein

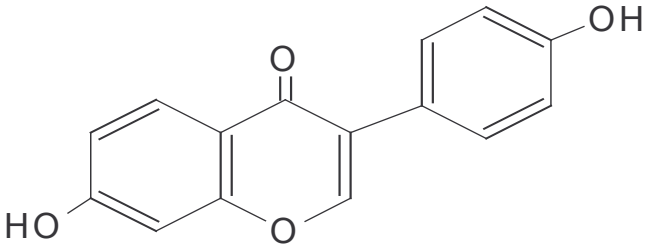

Daidzein

Figure. 2

Physiologic Behavior of Soy Isoflavones

Isoflavones undergo significant metabolism by bacteria in the gastrointestinal tract. Daidzein is metabolized to dihydrodaidzein, which is further metabolized to both equol and O-desmethylangolensin (O-DMA). Genistein is transformed to dihydrogenistein and is further metabolized to 6'-hydroxy-O-DMA (Joannou *et.al.,* 1995). Isoflavone absorption and utilization require a series of deconjugation and conjugation steps. Absorption is facilitated by hydrolysis of the sugar moiety by human gut bacterial β-glucosidases, gastric hydrochloric acid and β-glucosidases in foods (Kelly *et.al.,* 1993). After absorption in the small intestine, isoflavones are conjugated with glucuronic acid and sulfate by hepatic phase II enzymes (UDP-glucoronosyltransferases and sulfotransferases). Like endogenous oestrogens, these conjugates are excreted through both urine and bile and undergo enterohepatic circulation. After excretion into bile, conjugated isoflavones can be deconjugated once again by gut bacteria. Deconjugation may promote reabsorption, further metabolism and degradation in the lower intestine (Setchell and Adlercreutz, 1988; Xu *et. al.,* 1995).

Circulating concentrations of daidzein, genistein, equol and desmethylangolensin are relatively low in plasma <40 nmol/L (10 ng/mL) of humans consuming non-soy diets and are considerably higher in vegetarians consuming soy rich diet (Adlercreutz *et. al.,* 1993). When soy is consumed acutely, plasma daidzein, genistein and equol concentrations increase markedly and values of 0.08-2.4 μmol/L (20-600 ng/ml) are attained (Morton *et.al.,* 1994). The plasma half-life is generally between 6-8 hr after ingestion.

The half-life of plasma disappearance is relatively long at 7-9 h. These are impressive concentrations of isoflavones, when compared with endogenous plasma concentrations of oestradiol, throughout life. Even though isoflavones exhibit weak oestrogenic activity, it is possible that normal dietary concentrations of isoflavones are quite sufficient to account for many *in vivo* and *in vitro* biological effects that have been attributed to isoflavones. Factors that influence the concentrations of isoflavones in plasma are not clear and there are considerable gaps in knowledge of the pharmacokinetics of dietary isoflavones (Adlercreutz *et. al.,* 1993). Metabolites of isoflavones are excreted in the urine in varying concentrations.

Physiological Effects of isoflavones

Hormonal Effects

The oestrogenic activity of isoflavones was first recognized in relation to a syndrome known as clover disease in sheep (Bennetts *et.al.,* 1946; Braden *et. al.,* 1967). After grazing on pastures of subterranean and red clover, Australian ewes suffered from severe reproductive disorder that led to permanent infertility. The cause of infertility was identified as isoflavones genistein and daidzein and their precursor's biochanin A and formononetin. It was further identified that equol, degradation product of daidzein possessed more oestrogenic activity than daidzein and leading to the conclusion that equol was responsible for the estrogenic effects observed in sheep (Shutt and Cox, 1972).

Phytoestrogens bind to the ER, although weakly in comparison with oestradiol. Coumestrol, daidzein, genistein, equol and O-DMA have been

reported to bind the ER in cytosol preparations of sheep uteri with relative binding affinities of 5, 0.1, 0.9, 0.4 and 0.05% of oestradiol, respectively (Shutt and Cox, 1972). This suggests that, in the absence of endogenous oestrogens, isoflavones exert oestrogenic influences. These oestrogenic effects are evidenced by their abilities to stimulate growth of oestrogen-dependent MCF-7 human breast cancer cells (Martin *et. al.,* 1978). Genistein and daidzein enhance cell proliferation at concentrations below 1-10 μM (Welshons *et. al.*, 1990). Genistein stimulates expression of oestrogen-responsive pS2 mRNA at concentrations as low as 0.01 μM and induces proliferation of ER-positive MCF-& cells but not ER-negative MDA-MB-231 cells at concentrations between 0.01 and 1.0 μM (Wang *et. al.*, 1996). Isoflavones also exhibit antiestrogenic effects. A diet rich in isoflavones may prevent oestrogen-stimulated growth in mammals due to high concentration (100-1000 fold) of oestradiol leading to the isoflavones competing with the oestrogens in binding to oestrogen receptor. This may also interfere with the release of gonadotropins and interrupt the feedback-regulating system of the hypothalamus-pituitary-gonadal axis (Adlercreutz *et.al.,* 1995). Cassidy *et. al.*(1994) have reported that six premenopausal women receiving 60 g of soy protein/day (containing 45 mg of isoflavones) for one menstrual cycle had significantly increased follicular phase length, mid-cycle peaks of LH and FSH suppressed and peak progesterone concentrations delayed. Bioactive compounds that promote terminal differentiation of human tumor cells lead to inhibition of cancer cell proliferation. These bioactive compounds function as inducers of cell differentiation by inhibiting the enzymes, which promote

cell proliferation and belong to a variety of chemical classes and modulate numerous cellular processes (Sartorelli, 1985). Protein tyrosine kinases (PTKs) and DNA topoisomerases belong to this class of enzymes. PTKs are oncogene products, which catalyze phosphorylation of their own tyrosine residues and other proteins such as growth factors, involved in tumor cell signal transduction and proliferation (Hunter and Cooper, 1985). *In vitro* experiments with epidermal growth factor receptor from plasma membrane of human epidermoid carcinoma A-431 cells showed that genistein inhibits receptor tyrosine autophosphorylation and tyrosine phosphorylation with IC_{50} values of 2.6-3.7 μM (Akiyama *et.al.,* 1987). PTK inhibition is responsible for growth-inhibiting effects of genistein in different human cancer cells. Genistein induces terminal differentiation and inhibits proliferation of human leukemia and melanoma cells in a dose-dependent manner (Constantinou and Huberman, 1995; Constantinou *et.al.,* 1990).

DNA topoisomerases are enzymes that catalyze topologic changes in DNA during DNA replication. Genistein inhibits both topoisomerase I and II activity. Decatenation activity of purified calf thymus DNA topoisomerase II is completely inhibited by genistein at 80 μM (Markovits *et. al.,* 1989). The major constituents of isoflavones, daidzein (DZ) and genistein (GE) are known to interact with the alpha and beta oestrogen receptors (ERalpha/beta) in several tissues including mammary. DZ and GE prevented chemically induced mutagenesis and carcinogenesis in the mammary glands (Manjanatha *et. al.,* 2006). *In vitro* biological activities of isoflavone and their metabolites (DZ, GTN, dihydrogenistein (DGTN), dihydrodaidzein (DDZ),

tetrahydrodaidzein (TDZ), O-desmethylangolensin (ODMA), and equol (EQL)) have shown that they bind very weakly to both ERs and are less potent in inducing transcriptional activity, gene expression, and mammary cell proliferation than their precursors. EQL has the strongest binding affinities and oestrogenic activities especially for ERbeta among the daidzin metabolites and shows the ability to suppress osteoclast formation at high doses. The isoflavonoids act like estrogen antagonists with the premenopausal dose of E2 and thus inhibit oestrogenic actions by E2, whereas they exert oestrogen agonist activity with the lower dose of oestrogen close to the serum levels of postmenopausal women. Phytoestrogens such as isoflavones may exert their effects as oestrogen antagonists in a high oestrogen environment, or they may act as oestrogen agonists in a low oestrogen environment (Hwang *et. al.* 2006).

Angiogenesis

Isoflavones have the ability to suppress angiogenesis. Genistein, when supplemented with basic fibroblast growth factor, delay the proliferation of endothelial cells derived from bovine brain capillaries. Inhibition of endothelial cell growth by genistein occurs as a consequence of the competitive inhibition of ATP binding to the catalytic domain of tyrosine kinase or as a consequence of the attenuation of activity of S6 kinase, the enzyme stimulated by basic fibroblast growth factor (Fotsis *et. al.,* 1993).

Antioxidant Effects

Isoflavones are known to exhibit antioxidant activity *in vitro* and *in vivo*. Isoflavones inhibit lipoxygenase action and prevent peroxidative hemolysis of

sheep erythrocytes *in vitro* (Naim *et. al.,* 1976). Genistein (IC_{50} = 25 μM) and daidzein (IC_{50} =150 μM) inhibit hydrogen peroxide production in 12-O-tetradecanonylphorbol-13-acetate-activated HL-60 cells (Wei *et. al.,* 1995). Genistein is also a potent inhibitor of the superoxide anion generated by xanthine/xanthine oxidase system (Wei *et. al.,* 1995). In addition to displaying antioxidant effects, genistein is also capable of stimulating activities of antioxidant enzymes. Genistein (250 ppm) fed to 6-7 week-old female CD-1 mice for 30 days significantly enhanced the activities of catalase, superoxide dismutase, glutathione peroxidase and glutathione reductase by 10-30% in skin and small intestine (Wei *et. al.,* 1995). This clearly illustrates soy isoflavones can act as antioxidants directly or indirectly through stimulation of antioxidant enzyme activities. The microglial activation plays an important role in neurodegenerative disorders by producing several proinflammatory cytokines and nitric oxide (NO). Isoflavones and their metabolites, transformed by the human intestinal microflora, act as antioxidants and anti-inflammatory agents by suppressing the LPS-induced release of NO and TNF-alpha in primary cultured microglia and BV2 microglial cell lines. The inhibitory effect of the isoflavone metabolites (aglycone form) was more potent than that of isoflavones (glycoside form). The RNase protection assay showed that the isoflavone metabolites regulated iNOS and the cytokines at either the transcriptional or post-transcriptional level. So isoflavones may have therapeutic potential for various neurodegenerative disorders including ischemic cerebral disease (Park *et. al.,* 2006). Recently genistein has been shown to upregulate the

expression of antioxidant genes such as manganese-superoxide dismutase (MnSOD) (Borras *et. al.,* 2006).

Osteoporosis

In women, the onset of menopause due to the failure of the ovaries to respond to gonadotropins and reduction of gonadal oestrogens, causes a number of physiological changes that contribute to the development of osteoporosis and increased risk of coronary heart disease. Osteoporosis among postmenopausal women leads to the fracture of vertebrae, forearm and hip (Hadley, 1993). The incidence of osteoporosis and the risk of hip fracture are significantly low in postmenopausal Japanese women compared to postmenopausal western women (Cooper *et. al.,* 1992). The discovery of oestrogen receptors in osteoblast cells and the importance of oestrogen in down-regulating the activity of osteoclasts leading to decreased bone resorption is well established (Komm *et. al.,* 1988; Eriksen *et. al.,* 1988).

It is established that oestrogen (a) reduces sensitivity of bone tissue to the resorptive effects of parathyroid hormone, (b) blocks the release of interleukin-1, a potent bone resorption agent or (c) directly modulates osteoblast activity (Aurbach *et. al.,* 1992). Isoflavones exhibit oestrogenic effects, by preventing bone resorption and promoting increase in bone density. Genistein behaves like an oestrogen with bone retaining properties in maintaining trabecular bone tissue in rats (Anderson *et. al.,* 1995). Osteoporosis, due to ovariectomy, is responsible for reduced bone mineral content, femoral weight, femoral density, mechanical strength of the tibia and increased levels of bone specific alkaline phosphatase in the serum and

the number of osteoclasts in the femur. Treatment with isoflavones significantly increases bone mineral content, mechanical strength of the tibia, femoral weight, femoral density and prevents the rise of serum alkaline phosphatase levels. In addition, they significantly reduce the number of osteoclasts compared with the ovariectomized control rats (Occhiuto *et. al.,* 2006).

Cancer

A number of epidemiological studies have examined the relationship between soy food consumption and cancer risk. Japanese men who consumed tofu more than five times a week had half the risk of prostate cancer compared with those who consumed tofu less than once a week. Hence tofu consumption is associated with a reduced risk of prostate cancer (Severson *et. al.,* 1989). Tofu consumption is also negatively correlated with gastric cancer in Japanese men and women (Nagai *et. al.,* 1982). *In vitro* studies have shown the numerous biochemical ways by which isoflavones inhibit the growth of cancer cells. Genistein inhibits the growth of both estrogen receptor-negative and –positive human breast cancer cell lines (IC_{50} = 24-44 μM) (Peterson and Barnes, 1991). Genistein inhibits the autophosphorylation of the epidermal growth factor receptor in A431 human epidermoid carcinoma cells (IC_{50} = 2.6 μM) (Akiyama *et. al.,* 1987). It also inhibits DNA topoisomerase II in human leukemic MOLT-4 and HL-60 cells (IC_{50} = 31.5 μM and 48μM respectively) but not in normal human proliferating lymphocytes (Traganos *et. al.,* 1992).

Angiogenesis is an essential process involved in the development and progression of prostate cancer. Vascular endothelial growth factor (VEGF) is hypothesized to be a critical regulator of angiogenesis during prostate carcinogenesis. Genistein is a potential antiangiogenic agent and a critical regulator of angiogenesis during prostate carcinogenesis. Genistein (10-50 μM) cause significant inhibition of basal VEGF expression and hypoxia-stimulated VEGF expression in both human prostate cancer PC-3 cells and HUVECs. Furthermore, genistein (10-50 μM) significantly reduces PC-3 nuclear accumulation of hypoxia-inducible factor-1alpha, the principle transcription factor that regulates VEGF expression in response to hypoxia. These observations support the hypothesis that genistein may inhibit prostate tumor angiogenesis through the suppression of VEGF-mediated autocrine and paracrine-signaling pathways between tumor cells and vascular endothelial cells (Guo *et. al.,* 2006). The cellular actions of genistein are responsible for the decreased risk of breast cancer associated with high soy consumption. Genistein is selectively taken up into T47D cells and subjected to metabolism by CYP450 enzymes leading to the formation of both 5, 7, 3', 4'-tetrahydroxyisoflavone (THIF) and two glutathionyl conjugates of THIF. THIF is found to inhibit cdc2 activation via the phosphorylation of p38 MAP kinase, suggesting that this species may mediate genistein's cellular actions. THIF exposure activated p38 and caused subsequent inhibition of cyclin B1 (Ser 147) and cdc2 (Thr 161) phosphorylation, two events critical for the correct functioning of the cdc2-cyclin B1 complex. Formation of THIF, the intracellular metabolite of genistein may mediate the cellular actions of

genistein in tumorigenic breast epithelial cells via the activation of signaling through p38 (Nguyen *et. al.,* 2006). Daidzin has been shown to exhibit anticancer activity by inhibiting telomerase. Isoflavones exhibit anti-cancer effects by complexing with DNA (Li *et. al.,* 2006).

Heart Disease

Postmenopausal women experience deficiency of gonadal steroid production. In general, they experience decreased plasma concentration of high-density lipoprotein (HDL, good cholesterol) and increased plasma concentration of low-density lipoprotein (LDL, bad cholesterol) as result of downregulation of oestrogen production (Bierman and Glomset, 1992). Normally, oestrogen replacement therapy is advised as it has been shown that oestrogens decrease LDL cholesterol and increase HDL cholesterol. Isoflavones act as oestrogen agonists, thereby simulating the effects of oestrogen. This is supported by epidemiological data showing that incidence of coronary heart disease and hypercholesterolemia is high in populations that consume diets rich in animal protein than in those that consume diets rich in vegetable protein (Stamler, 1979). A controlled clinical trial has shown that consumption of soy protein rather than animal protein significantly decreases blood cholesterol, LDL cholesterol and triglycerides (Anderson *et.al.,* 1995).

The role of isoflavones in reducing LDL+VLDL cholesterol is made clear by a recent study with rhesus monkeys. Compared with an alcohol-extracted soy protein, isoflavones-soy proteins significantly reduce LDL+VLDL cholesterol concentrations in both males and females (30-40 % lower) dramatically increase HDL cholesterol concentration. These experiments clearly evidence

the contribution of isoflavones towards the hypolipidemic effects of soy isoflavones consumption (Anthony *et. al.,* 1996). Retinoic acid receptors (RAR) belong to the same nuclear receptor superfamily as thyroid hormone receptors (TR) and induce hypertriglyceridemia. Dietary soy proteins containing isoflavones affect hepatic RARbeta2 protein content and RARbeta DNA binding activity, which may contribute to the suppression of retinoid-induced hypertriglyceridemia (Xiao *et. al.,* 2007). Isoflavones reduce the formation of nitric oxide derivatives, cholesterol oxides and inhibit low-density lipoprotein oxidation more efficiently than hormone therapy in hypercholesterolemic postmenopausal women (Pereira *et. al.,* 2006).

Obesity and diabetes

Obesity and type II diabetes is a major public health concern of the modern world. Diabetes is a complex metabolic disorder involving abnormalities of insulin, glucose and lipid metabolism. As isoflavones have been shown to improve plasma lipid profile, they may help control obesity and type II diabetes. An isoflavone rich diet has shown to reduce body fat in both rats and genetically obese mice (Aoyama *et. al.,* 2000). Isoflavones may provide anti-diabetic and hypolipidemic effect by activating peroxisome-proliferator activated receptor (PPAR), which is a ubiquitous nuclear receptor that regulates the transcription of genes involved in lipid and glucose metabolism (Mezei *et. al.,* 2003). Genistein, with carnitine, transcriptionally up-regulates expressions of acyl-coenzyme A synthetase (ACS) and carnitine palmitoyltransferase-I (CPT-I). Hence, genistein, with carnitine, delivers anti-

obesity effects, probably by modulating peroxisome proliferator-activated receptor-associated genes (Yang *et. al.,* 2006).

Isoflavones have been shown to be potent inhibitors of aldose reductase, which is an important rate-limiting enzyme in the process of cataract induction in the metabolic disease galactosemia. It is found that genistein delays the progression of cataracts induced by dietary galactose by increased expression of connexin (Cx) 43 in the lens but does not affect the expression of soluble guanylyl cyclase (sGC) subunits. This finding suggests that the protective effect of genistein on cataract induction appears to bear no relation to sGC but may be mediated by enhanced expression of Cx43 and changed metabolic state (Huang *et. al.,* 2007).

Isoflavones present in human diet exhibit many biological effects, which are beneficial in the prevention and/ or treatment of cancer, cardiovascular disease, hormone-related disorders, obesity and type II diabetes. The nature of the effects depend on a multitude of factors, which include age at exposure, exposure dose, differences among compounds, presence of other dietary components. Research on isoflavones has led to tremendous increase in publications in the areas of isoflavone pharmacokinetics, tissue distribution, and physiological effects in humans.

Bovine Serum Albumin:

The protein chemist has a long-standing affinity to serum albumin, and often selects this protein as a model for physical or chemical studies. The word albumin derives from the Latin *albus,* meaning white. In the earliest separation of plasma proteins, the fraction, which remained soluble upon dialysis against water, has been called albumin and the precipitated proteins globulins (Schultze and Heremans, 1966). Bovine serum albumin's chief features are those of an acidic, very soluble, stable protein. Its isoelectric point is pH 4.8. Solutions of 30% (W/V) at neutrality are readily prepared and used in serology. Bovine serum albumin is characterized by a low content of tryptophan and methionine and a high content of cystine and charged aminoacids, aspartic and glutamic acids, lysine and arginine. The high total charge of about 185 ions per molecule at pH 7, aids its solubility and the many disulfide bonds contribute to its stability (Feldhoff and Peters, 1976). Bovine serum albumin has two tryptophans at positions 212 and 134. Sequence alignment of bovine serum albumin and human serum albumin reveals about 80% homology. Important residues such as cys-34, Trp-$_{212}$ or 214, sequence 143-155 in loop 3 and sequence 244-263 in the small arm of loop 4 are conserved (Peters Jr, 1985). The difference between HSA and BSA with reference to fluorescence is an additional tryptophan at position 134 in site IB (Carter and Ho, 1994).

Human Serum Abumin:

Human serum albumin is the most extensively studied and applied proteins in biochemistry. Serum albumin is the main component of blood with blood

concentrations of 5g/100ml. It is albumin, which contributes 80% to colloid osmotic blood pressure also responsible for maintaining physiological pH. It is the major extracellular protein distributed in every tissue comprising 60% of total protein. The most outstanding property of albumin, which makes it the most thoroughly investigated protein, is its ability to bind reversibly and selectively an incredible variety of insoluble bioactive endogenous and exogenous ligands. Albumin is the principal carrier of fatty acids, otherwise like bilirubin. The other most vital function is transport of drug molecules to target organs. Human Serum Albumin is a 585 amino acid molecule characterized unusually by high percentages of Cys (35%) and charged amino acids and low percentages of tryptophan, glycine and methionine. The primary structure possesses a single free sulfhydryl group (Cys-34) and is not glycosylated. Albumin exhibits a high degree of conformational flexibility and several isomeric forms of albumin can be induced reversibly as a function of pH. In spite of its conformational flexibility, it is not readily denatured and survives heat pasteurization at temperatures of 60°C for 10 h (Carter and Ho, 1994).

Crystal structure of albumin resolved at 2.8 Å and 2.5 Å reveals that it is a heart shaped molecule, with approximate dimensions of 80 x 80 x 30 Å. It consists of three repeating homologous domains (labeled domain I, II and III). The domains are topologically identical, having similar three-dimensional structure. Each domain in turn is the product of two domains (A and B), which are helical and extensively cross-linked by 17 disulfide bridges.

Domains I and II are almost perpendicular to each other to form a T-shaped assembly in which the tail of sub domain IIA is attached to the interface region between subdomain IA and IB by hydrophobic interactions and hydrogen bonds. Domain III protrudes from sub domain IIB at an angle of about 45^0 to form a Y-shaped assembly for domains II and domains III. Domain III interacts only with sub domain IIB. All these topological features impart HSA a heart shaped structure (Sugio *et. al.,* 1999). The protein has a high α-helical content (67%) and a β-sheet and β-turn percentages of 10% and 19%, respectively. Albumin has asymmetric surface charge distribution within the primary structure and is negatively charged at neutral pH. Surface charge contributes to its high solubility, making albumin ideally suited for its role as a major plasma protein. Albumin exhibits conformational flexibility and can assume different forms in response to pH. Foster classified the pH dependent forms as "N" for normal form, which predominantly occurs at neutral pH, "B" for the basic form occurring above pH 8.0, "F" for the fast migrating form produced at pH values less than 4.0, "E" for expanded form at pH less than 3.5 and "A" for aged form occurring with time at pH values greater than 8.0 (Foster, 1977). These forms of albumin can undergo transitions and N-F transition results in abrupt opening of the molecule facilitating ligand off-loading at various tissue interfaces. Apart from this transition, albumin also undergoes F-E and N-B transition.

Nature of Ligand Binding in Human Serum Albumin

The most active area of investigation of albumin biochemistry is its incredible ability to bind wide variety of ligands reversibly, with typical association

constants ranging from 10^4 to 10^6 M^{-1}. The binding sites on albumin have been identified and studied primarily by biophysical techniques like equilibrium dialysis or spectroscopic methods. There is a lot of controversy about the exact number of binding sites on albumin, but based on experimental studies, a general consensus has been arrived at. There are at least seven binding sites for medium-chain and long-chain fatty acids as analyzed by X-ray crystallography (Bhattacharya *et.al.,* 2000). There are two prinicipal binding locations for small heterocyclic compounds also named as Sudlow' s site 1 and site 2 (Sudlow *et. al.,* 1976). There are two distinct metal binding sites, one involving Cys-34 and the other N terminus. At normal physiological concentrations albumin has six dominant areas of ligand association.

X-ray structure of Human Serum Albumin

The three dimensional structure of human serum albumin has been determined crystallographically to a resolution of 2.8 Å and 2.5 Å (Fig.3). It comprises three homologous domains that repeat in the molecule (denoted as I, II and III). Each domain is a product of two sub domains A and B that possess common structural motifs. The six sub domains form a heart shaped molecule that can be approximated to a solid equilateral triangle with sides of 80 Å and averaged depth of 30 Å. Each domain has 10 principal helices (h1-h10). Sub domain A and B share a common motif that includes h1, h2, h3 and h4 for sub domain A, and h7, h8, h9 and h10 for sub domain B. In sub domain IA a disulphide bridge connecting h1 and h3 does not exist. Sub

domain A consists of two additional short antiparallel helices, h5 and h6, which are tied together by a pair of disulphide bridges forming a smaller disulphide double loop (loops 2, 5 and 8). Due to these structural features sub domain A forms a virtually continuous helical globin like fold extensively cross-linked by a total of four interhelical disulphide bridges. The B sub domains supplement the helical motif with an N-terminal portion of extended polypeptide, in a folding topology closely resembling up-down helical bundle. The intradomain connections between sub domains IA-IB, IIA-IIB and IIIA-IIIB consist of extended polypeptide from residues Lys_{106} to Glu_{119}, Glu_{119} to Val_{315} and Glu_{492} to Ala_{511} in domains I, II and III respectively. HSA has a unique disulfide bond topology. There are 35 cysteine residues in HSA, 34 of which form 17 disulfide bridges. Sixteen disulfide bridges participate in the formation of eight double disulfide bridges. The 17 cystines form disulphide linkages between α-helices distorting the local helical conformation (He and Carter, 1992; Sugio *et. al.,* 1999). Cys-34 is located in a loop between helices IA-h2 and IA-h3 and does not participate in any disulfide bridges. Its sulfahydryl group is oxidized by cysteine or glutathione in 30-40 % of HSA molecules in bloodstream to form an intermolecular disulfide linkage (Peters, 1985). The secondary structure scheme of HSA is depicted in Fig. 4.

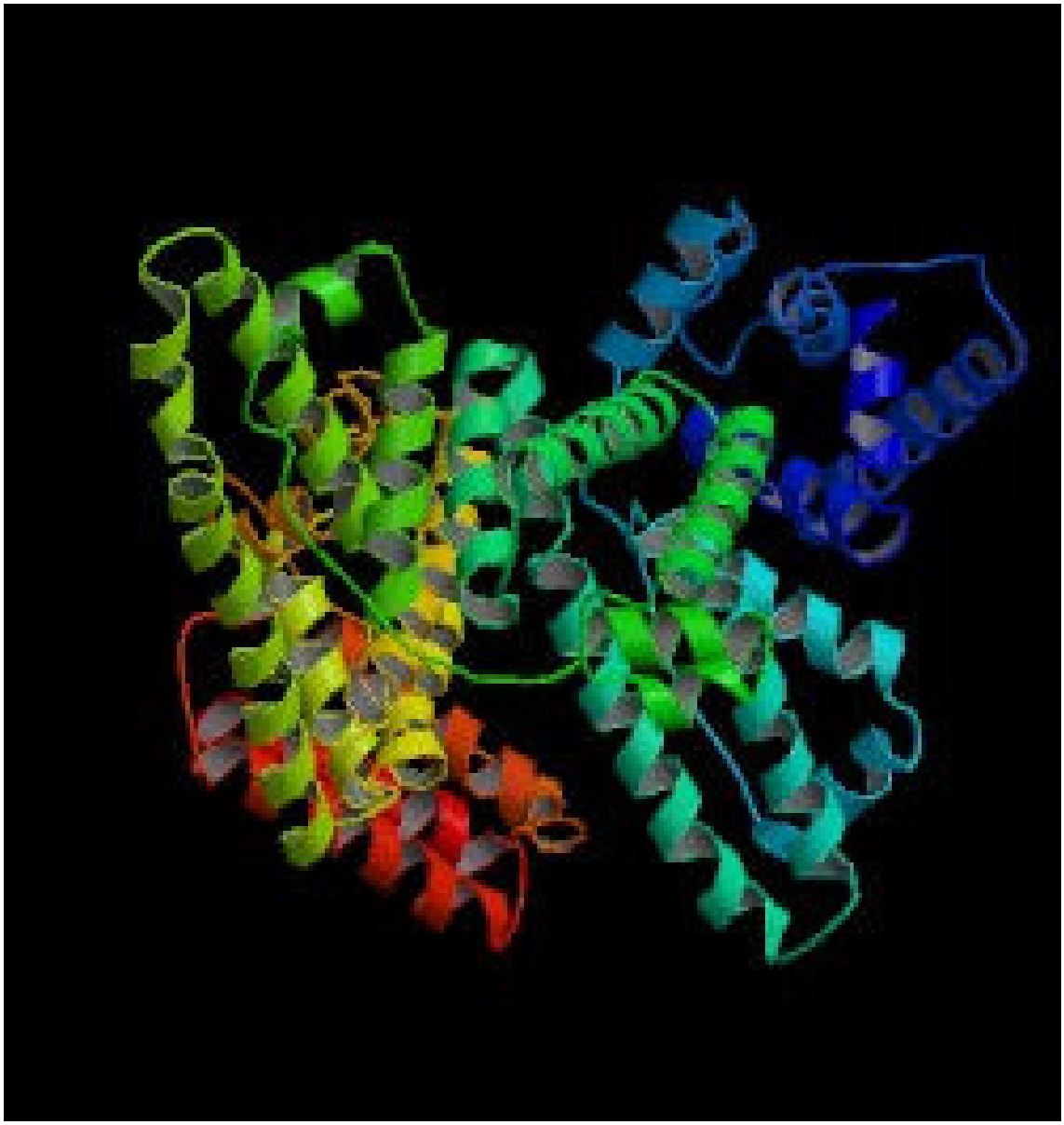

Figure. 3 Crystal structure of human serum albumin at 2.5 Å (PDB No. 1BMO) Sugio *et. al.,* (1999).

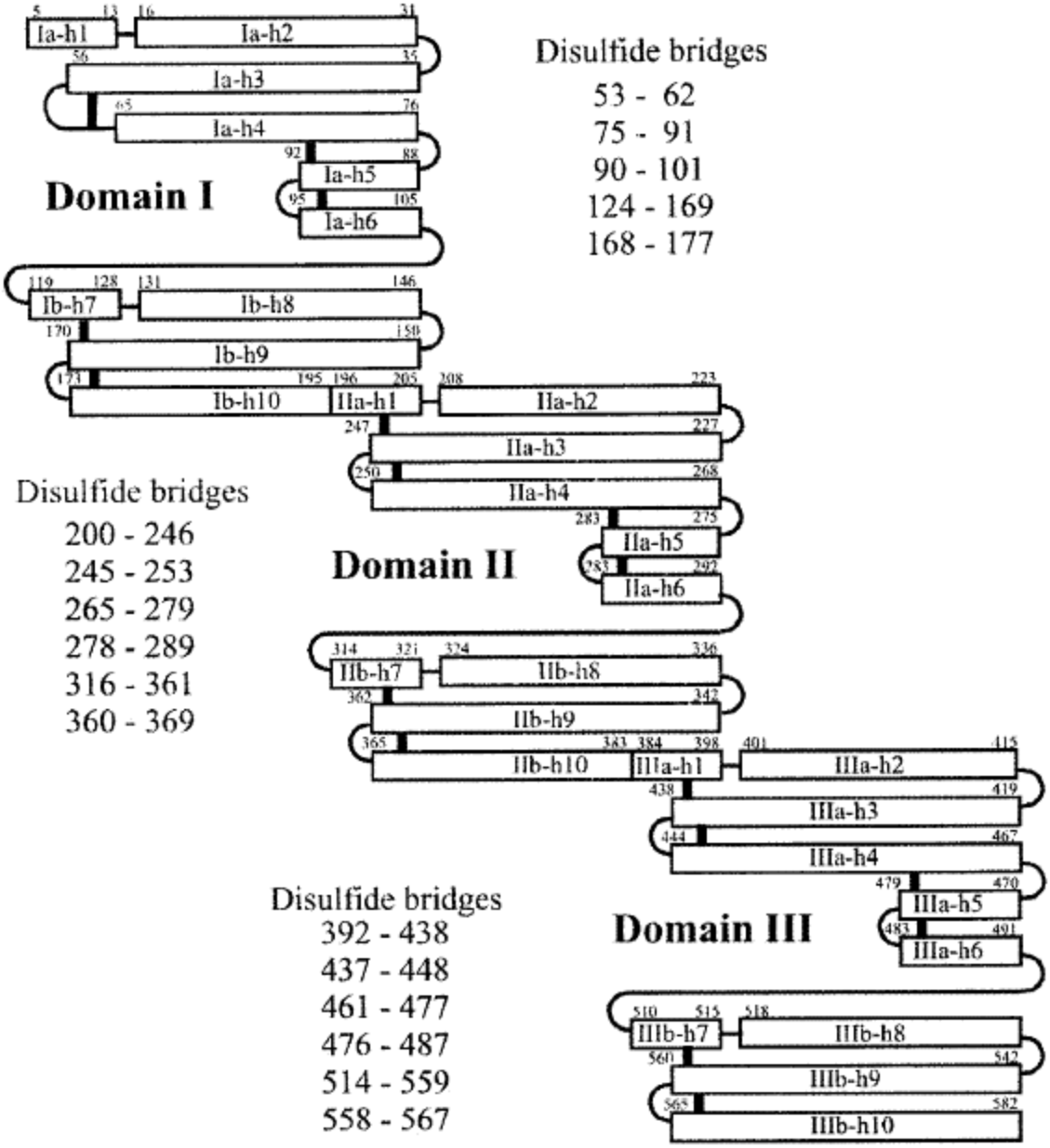

Figure 4. Secondary structure scheme of HSA, after Sugio *et al.,* (1999). Vertical thick lines denote disulphide bridges.

Ligand binding: Site 1 and Site 2

Site 1 and site 2 are the main drug binding sites mapped on albumin using various fluorescent marker ligands. Site 1 corresponds to hydrophobic pocket in sub domain IIA, which contains the lone tryptophan at position 214 and site 2 corresponds to the sub domain IIIA, which is the primary binding site for fatty acids. In each of the sub domains there is an asymmetric distribution leading to a hydrophobic surface on one side and a basic or positively charged surface on the other. Domain IIIA is elongated sock-shaped pocket wherein the foot region is primarily hydrophobic and the leg is primarily hydrophilic. In sub domain IIA binding pocket, amino acid residues Leu_{219}, Phe_{223}, Leu_{234}, Leu_{260}, Ala_{261}, Ile_{264}, Ile_{290}, Ala_{291} and the hydrocarbon chain of Glu_{292} contribute to hydrophobic interactions. Amino acid residues Arg_{257}, Arg_{222}, Lys_{199} and His_{242} contribute to hydrophilic interactions. Similarly in sub domain IIIA binding pocket, amino acid residues Pro_{384}, Leu_{387}, Ile388, Phe_{395}, Leu_{407}, Leu_{430}, Val_{433}, Ala_{449}, Leu_{453} and the hydrocarbon chains of Arg_{485} and Glu_{450} contribute to hydrophobic interactions. Amino acid residues Arg_{410} and Tyr_{411} contribute to hydrophilic interaction.

Site 1 consists of two overlapping regions, the warfarin and azapropazone binding regions. Chemical modification of the lone tryphtophan residue of albumin affected the binding of warfarin (Fehske *et. al.,* 1982). Warfarin, phenprocoumon and acenocoumarol bind to single high-affinity binding site (Tillement *et. al.,* 1974; Husted and Andreasen, 1979). Azapropazone, phenylbutazone and glibenclamide bind to region different from warfarin

binding region called azapropazone binding site, where tryptophan is not affected by the binding (Fehske *et. al.,* 1982). Competitive ligand binding measurements, to identify exact binding site of acenocoumarol, DNSA and n-butyl p-ABE, suggest the presence of an additional binding region in the vicinity of the warfarin binding region. This new region overlaps warfarin binding region but is located far off from azapropazone region. So warfarin may play a bridge between the azapropazone region and new binding site. Site 1 has three-ligand binding sites classified as regions 1a, 1b and 1c, which correspond to the warfarin, azapropazone and novel binding region (Yamasaki *et. al.,* 1996). Crystallographic study of HSA-fatty acid complexes reinforced by NMR drug competition analysis has revealed that there are seven fatty acid binding sites on serum albumin molecule. These consist of a single site in sub-domain IB, one at the interface between sub-domain IA and IIA, two sites in IIIA (sudlow's drug-binding site 2), fifth in IIIB, sixth site is positioned at the interface between sub-domain IIA and IIB. A seventh site is drug-binding cavity IIA (Sudlow's drug-binding site 1) (Bhattacharya *et.al.,* 2000; Simard *et. al.,* 2006). Albumin has high affinity sites for Cu (II), Ni (II), Hg (II), Au (I) and Ag (II) and weak affinity for calcium and zinc. The metal binding site is located in domain I which has free reactive sulfahydryl (Cys-34) group. Cys-34 has unusually low pK_{SH} of 5 and is highly reactive. Cys-34 binds many metal ions such as Au, Ag, HG, Cd and Cu. Drugs such as antiarthritic auranofin or gold (I)-containing thiolates (Shaw, 1989) have affinity for Cys-34.

X-ray Crystallographic Analysis of Ligand binding sites on albumin molecule

Drug site 1 contains a binding pocket within the core of sub domain IIA that comprises all six helices of the sub domain and a loop-helix feature (residues 148–154) contributed by IB. The interior of the pocket is rich in hydrophobic amino acids but also contains two clusters of polar residues, an inner one towards the bottom of the pocket (Y_{150}, H_{242}, R_{257}) and an outer one at the pocket entrance (K_{195}, K_{199}, R_{218}, R_{222}). The large binding pocket consists of a central zone that extends into three distinct compartments. The back end of the pocket is divided by I_{264} into left and right hydrophobic sub-chambers, whereas a third sub chamber protrudes from the front of the pocket, delineated by F_{211}, W_{214}, A_{215}, L_{238} and aliphatic portions of K_{199} and R_{218}. CMPF, oxyphenbutazone, phenylbutazone and warfarin cluster in the centre of the site 1 pocket. The marker ligands of site 1 invariably have a planar group pinned snugly between the apolar side-chains of L_{238} and A_{291}; in contrast, there is much greater variation in the drug position within the plane perpendicular to the line between these two residues. The mouth of the binding pocket in site 1 has a wide opening and presence of flexible side-chains provides significant room for movement. The drugs bind to the apolar compartments of site 1 to different extents. All compounds can access the right-hand sub-chamber to a greater (oxyphenbutazone, phenylbutazone, warfarin) or lesser (CMPF, thyroxine) degree but only phenylbutazone and CMPF project their hydrophobic moieties into the left-hand sub-chamber. The front, lower sub-chamber is occupied by phenyl groups of oxyphenbutazone

and warfarin, and one of the iodine atoms projecting from the outer phenyl ring of thyroxine. Drug site 1 is bestowed with the ability of making a number of specific interactions with residues belonging to the inner and outer polar clusters, apart from making hydrophobic contacts. All of the compounds are positioned to make a hydrogen bond interaction with the hydroxyl group of Y_{150}, as found previously for thyroxine, and this residue, therefore, assumes a central role in drug interactions. Site 1 is rich in basic residues and the complete absence of acidic residues establishes the specificity of the pocket. The structural data suggest that the pocket appears to be specific for molecules with two anionic or electronegative features on opposite sides of the ligand that can simultaneously interact with the two polar patches. The distance between these basic patches accounts for the finding that the presence of two electronegative groups separated by five to six bonds. The size of the binding pocket allows more adaptability and does not place steric constraints on the binding of small drugs and allows co-binding of water molecules that can flexibly mediate protein-ligand interactions (Ghuman *et. al.,* 2005).

Drug site 1 in HSA-myristate complex

Fatty acid binding has a profound influence on the tertiary structure and induces the movement of Y_{150} from sub domain IB to interact with the carboxylate moiety of the lipid bound to the site that straddles domains I and II (fatty acid site FA_{23}). This helps to drive the relative rotation of domains II and I, affecting the ligand binding capabilities of drug site 1. There is an extensive rearrangement of the H-bond network involving Y_{150}, E_{153}, Q_{196},

H_{242}, R_{257} and H_{288}, which results in the opening of the solvent channel between Y_{150} and Q_{196}, thereby increasing the volume of the pocket and altering its polarity distribution. Fatty acid binding partially neutralizes and disrupts the inner polar cluster; only, H_{242} is relatively unaffected. The helix containing L_{198} is also displaced outwards. This appears to impact an adjacent helix from sub domain IIIA (residues 442–466) and its disulphide-bonded neighbor. In spite of the structural changes brought by fatty acid binding, comparison of the structural features of fatty acid free and bound albumin reveals that site 1 is not drastically affected in terms of its ligand binding capabilities. Y_{150} is removed from the pocket to interact with fatty acid, so it is no longer available to make the central contribution to drug binding that is observed in complexes with defatted HSA. In the absence of Y_{150}, different drugs make use of the various basic and polar ligands on both sides of the binding pocket. Most interactions are made with the side-chains of K_{199} and R_{222} on one side of the pocket and H_{242} on the other, though R_{218} and R_{257}. Addition of fatty acids to HSA reportedly increases the affinity of site 1 for warfarin but it is difficult to give a precise molecular explanation for this effect from the structural data alone. One interesting observation is that the electron density for the coumarin ring of the drug at the back end of the pocket is significantly stronger in the HSA-myristate complex than defatted HSA, suggesting that this moiety is more stably associated with the pocket in the presence of fatty acid. The simultaneous accommodation of indomethacin and either azapropazone or phenylbutazone in drug site 1 of the crystal structure is supported by binding data, which show that these drugs do not

displace one another from HSA. These results were obtained using defatted HSA, indicating that co-binding also happens in the absence of fatty acid as expected from modeling experiments (Ghuman *et. al.,* 2005).

Drug site 2

Drug site 2 comprises of all six helices of sub domain IIIA and is topologically similar to site 1 (sub domain IIA), comprising a largely pre-formed hydrophobic cavity with distinct polar features. Yet, there are significant differences between the two drug pockets. Drug site 2 is smaller than site 1. The principal binding region of drug site 2 is equivalent to the central portion of the drug site 1 pocket and possess, the rear right-hand hydrophobic sub-chamber, which can only be accessed following ligand induced side-chain movements. The left-hand sub-chamber is eliminated by the presence of Y_{411}, which occurs in sub domain IIIA at the position corresponding to L_{219} in IIA. Although the two drug sites have structurally similar sub domains, these are packed in different contexts with respect to the remainder of the protein. The entrance to drug site 1 is enclosed by sub domains IIB and IIIA. However, the entrance to site 2 is not similar to site I, although IIIA is followed by IIIB, this sub domain is rotated further away from the drug site entrance (in comparison to drug site 1, domain II) and leaves the pocket entrance more exposed to solvent. In contrast to site 1, drug site 2 has a single polar patch, located close to one side of the entrance of the binding pocket and centered on Y_{411} including R_{410}, K_{414} and S_{489}. Thus, in terms of shape, size and polarity, drug sites 1 and 2 are clearly distinguishable and

this helps to account for the different binding specificities of the two pockets. Diflunisal, diazepam, ibuprofen and indoxyl sulphate all cluster in the centre of the binding pocket of sub domain IIIA, oriented with at least one oxygen atom in the vicinity of the polar patch. In each case, there is an interaction of drugs with the hydroxyl group of Y_{410}, whereas none of the drugs are found to interact with K_{414}. R_{410} and S_{489} contribute to salt-bridge and hydrogen bond interactions to drug binding, except in the case of diazepam. Thus, the observation that site 2 is generally selective for drugs with a peripherally located electronegative group is due to the presence of a basic polar patch located at one end of a generally apolar pocket in sub domain IIIA (Ghuman *et. al.,* 2005).

Drug site 2 in sub domain IIIA can bind two molecules of long-chain fatty acid (in fatty acid sites FA_3 and FA_4) or one of thyroxine. Comparison of drug and fatty acid binding reveals the very different ways in which these classes of ligand bind to a common locus on the protein. Drug site 2 is composed of the apolar region that is occupied by the methylene tails of fatty acids bound to FA_3 and the polar patch that interacts with the carboxylate moiety of fatty acids bound to FA_4. None of the drugs, examined to date is observed to access the long, narrow hydrophobic tunnel of FA_4 that accommodates the methylene tails of lipids bound to this site. Moreover, fatty acids bound to FA_3 do not interact with the polar patch centered on Y_{411}. Instead, binding of the fatty acid opens access to a different polar patch by inducing the same rotations of L_{387} and L_{453} that are observed upon diazepam binding and the lipid carboxylate group supplants E_{450} in a salt-bridge interaction with R_{348} in

sub domain IIB. These observations suggest possible ways in which drugs could be modified in order to take advantage of this flexible binding facility in the pocket. Fatty acid binding produces a large conformational change in HSA, involving rotations of domains III and I relative to domain II, which suggests a possible molecular mechanism for allosteric interactions between fatty acid binding sites. In contrast, the conformational changes observed for drug binding at sites 1 and 2 are more local and there is no proof of global conformational changes on the scale observed with fatty acid binding. The observed instances of allosteric interactions between drug sites 1 and 2 may possibly be due to more subtle structural effects or to the presence of additional binding sites (Ghuman *et. al.,* 2005).

Structural data reveal that the two primary drug sites on HSA are highly adaptable binding cavities containing distinct sub-compartments, some of which are only accessed by local drug induced conformational changes, and reveal a range of secondary binding sites distributed widely across the protein. In each case, the drug sites overlap with endogenous ligand-binding sites. The binding specificities of the pockets are determined by their shapes and the particular distributions of basic and polar residues on the largely hydrophobic interior walls that are involved in charge neutralization and hydrogen bonding interactions with acidic or electronegative small molecule ligands (Ghuman *et. al.,* 2005). The detailed insights into HSA–drug interactions provide an invaluable structural framework for the interpretation of drug binding data and will facilitate efforts to modify new therapeutic

compounds to control their interaction with HSA and therefore optimize their distribution within the human body.

Albumin is an extraordinary molecule designed to perform vital biochemical functions. The principal role of albumin is to aid in the transport, metabolism and distribution of endogenous and exogenous bioactive ligands. The ligand binding capacity of albumin is aptly summarized in the Fig.5. Binding to albumin can alter the distribution, metabolism and the potency of many drugs. It is essential to study albumin-drug interaction so that essential parameters of interaction become clear. These parameters may help to design efficient drug delivery process. Fig. 5 summarizes the various ligand-binding sites of different bioactive compounds determined by X-ray crystallographic analysis.

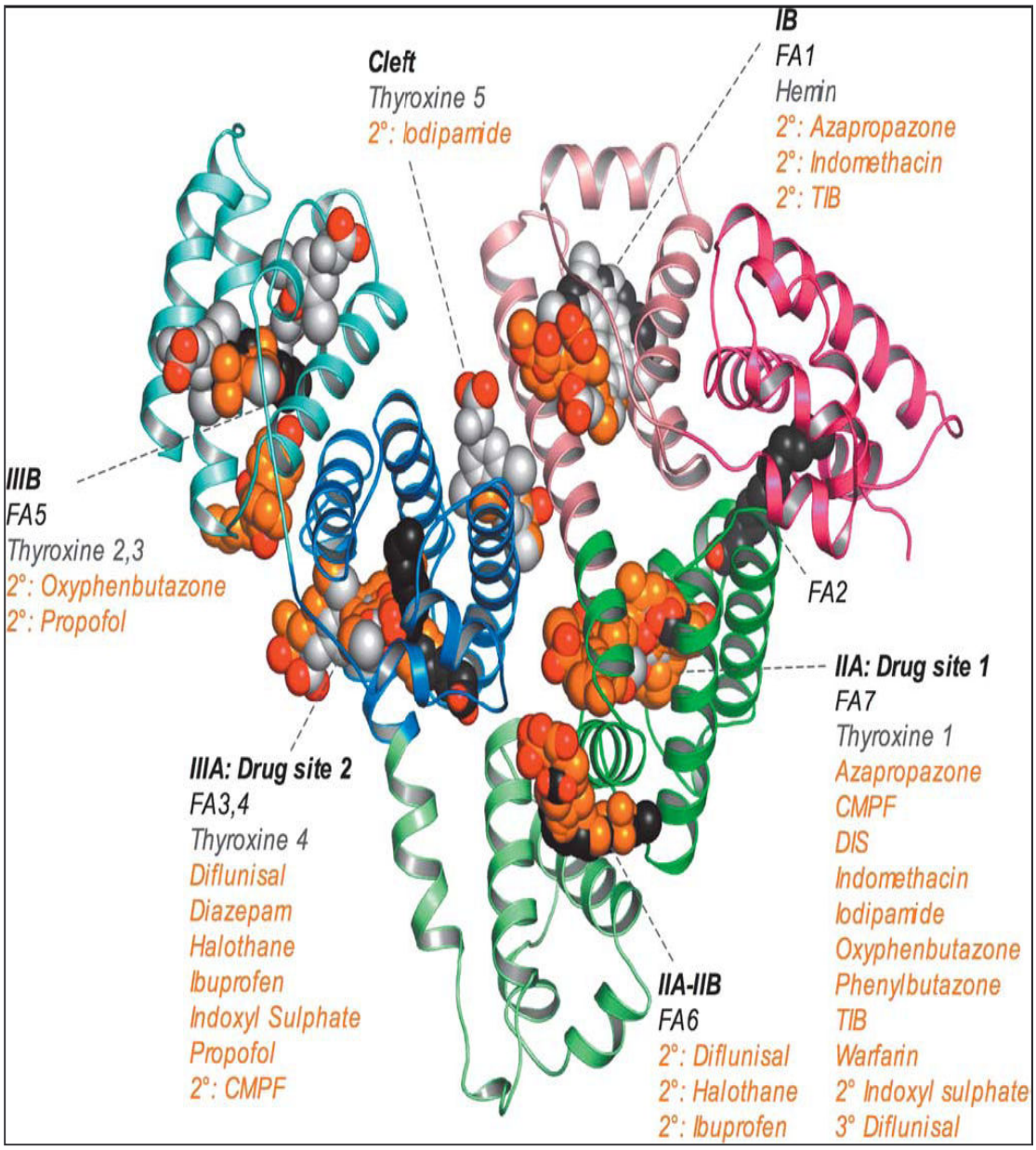

Figure. 5. Summary of the ligand binding capacity of HSA as defined by crystallographic studies to date. Ligands are depicted in space-filling representation; oxygen atoms are coloured red; all other atoms in fatty acids (myristic acid), other endogenous ligands (hemin, thyroxin) and drugs are colored dark-grey, light grey and orange, respectively (Ghuman *et. al.,* 2005).

Lipoxygenase: Structure and Function

Lipoxygenases (LOX)-linoleate oxygen oxidoreductase, (EC 1.13.11.12) are enzymes ubiquitous in nature. These nonheme, nonsulfur dioxygenases catalyze the dioxygenation of polyunsaturated fatty acids (Fig. 6) possessing a *cis, cis*-1, 4-pentadiene unit to yield *cis, trans* conjugated diene hydroperoxides (Gardner, 1991). LOXs from mammals, plants and microorganisms differ from one another in their substrates as well as products formed as a result of catalysis.

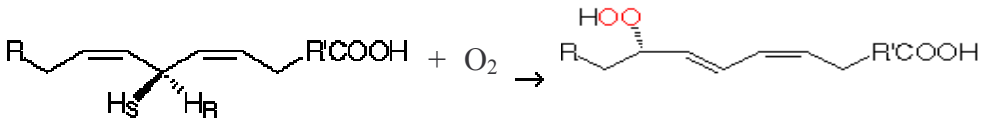

Fatty acid (1,4 diene)

Fatty acid hydroperoxide
(1hydroperoxy 2, 4diene)

Figure 6. Schematic representation of the reaction catalyzed by SLO-1.

(http:/metallo.scripps.edu/promise/)

Occurrence

LOXs are widely expressed in animal and plant cells. Plant and animal LOXs have evolved separately as shown by the phylogenetic tree, each forming different subgroups (Brash, 1999, Feussner and Wasternack, 2002).

Nomenclature and Biochemical Classification

In plants, linoleic acid (LA) is the main substrate and plant LOXs are classified based on their positional specificity for linoleic acid (LA) dioxygenation. LA is oxygenated at either the C-9 or C-13 of the hydrocarbon backbone of the fatty acid, resulting in the formation of either 9-hydroperoxy or 13- hydroperoxy derivatives of LA (Feussner and Wasternack, 2002). Based on product formation, soy LOX-1 is a 13-LOX, while potato LOX is a 9-LOX. In case of animals, LOX enzymes can add a hydroperoxy group at carbons 5, 8, 12 or 15, when arachidonic acid (C20: 4) is the substrate. These isoenzymes are designated as 5-, 8-, 12- or 15-lipoxygenases (Fig. 7) (Maccarone *et. al.,* 2001).

EC 1.13.11.12 lipoxygenase (linoleate: oxygen 13-oxidoreductase)
linoleate + O_2 = (9*Z*, 11E, 13S)-13-hydroperoxyoctadeca-9,11-dienoate

EC 1.13.11.31 arachidonate 12-lipoxygenase (arachidonate: oxygen 12-oxidoreductase) arachidonate + O_2 = (5*Z*, 8Z, 10E, 12S, 14Z)-12-hydroperoxyicosa-5, 8, 10, 14-tetraenoate

EC 1.13.11.33 arachidonate 15-lipoxygenase (arachidonate: oxygen 15-oxidoreductase) arachidonate + O_2 = (5*Z*, 8Z, 11Z, 13E, 15S)-15-hydroperoxyicosa-5, 8, 11, 13-tetraenoate

EC 1.13.11.34 arachidonate 5-lipoxygenase (arachidonate: oxygen 5-oxidoreductase) arachidonate + O_2 = leukotriene A_4 + H_2

EC 1.13.11.40 arachidonate 8-lipoxygenase (arachidonate: oxygen 8-oxidoreductase) arachidonate + O_2 = (5*Z*, 8R, 9E, 11Z, 14Z)-8-hydroperoxyicosa-5, 9, 11, 14-tetraenoate

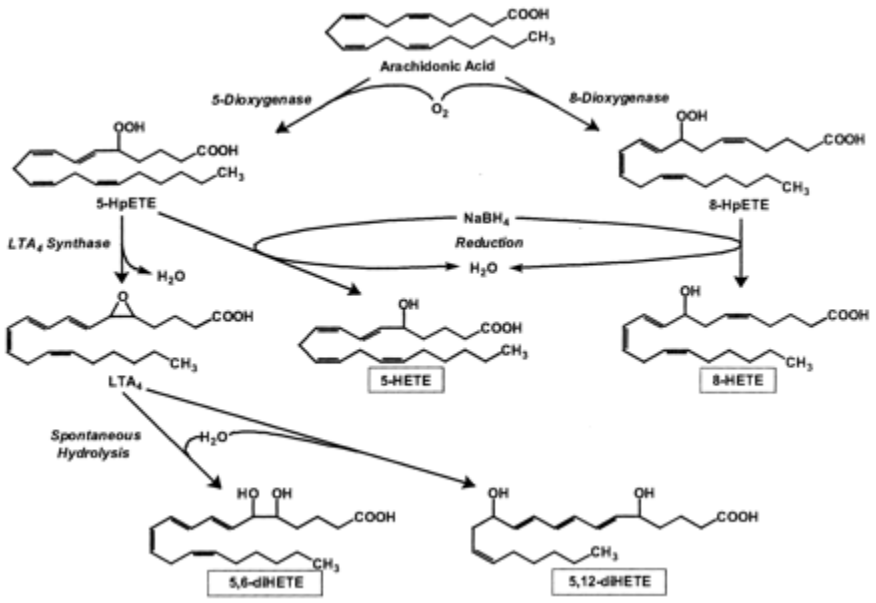

Figure. 7 Reactions catalyzed by mammalian lipoxygenase. (Schewe *et. al.,* 2002)

Structure of Lipoxygenases

Lipoxygenases are purified and characterized from both plant and animal tissues. The sequences of over 50 lipoxygenases have been reported and many have been expressed as active proteins (Kuhn and Thiele, 1999). They range in length from 923 residues (rice LOX-2) to 661 residues (rabbit 15-LOX); the plant LOX sequences are longer than the mammalian LOX sequences. Pair-wise sequence identity between plant and mammalian lipoxygenases is 21-27%, while the identity among pairs of plant sequences is 43-86%. The sequence identity between plant and animal lipoxygenases is

highest in the region of the catalytic domain near the iron atom (Prigge *et.al.,* 1996). Although the catalytic mechanism of all lipoxygenases may be similar, there are significant differences in the properties of the plant and animal enzymes. Soy LOX is a soluble cytosolic protein, whereas mammalian 5-LOX is membrane bound and requires membrane associated activating protein (FLAP) (Ford-Hutchinson *et. al.,* 1994).

The most exhaustively studied plant LOX from soy exists in the form of several isozymes sharing 70% of sequence homology (Siedow, 1991). Soy LOX isozymes LOX1, LOX2 and LOX3 have significantly different properties. LOX1 contains 839 amino acid residues with a molecular weight of 94,262 daltons. The corresponding values for LOX2 and LOX3 are 865 (97,053) and 857 (96,541), respectively (Boyington *et. al.,* 1993). These isozymes further differ with respect to their isoelectric points, with values of 5.68, 6.25 and 6.15 for LOX1, LOX2 and LOX3, respectively (Siedow, 1991).

Assay and Purification of Soy Lipoxygenase

Assay of Lipoxygenase

The enzyme assay is based on the dioxygenation of polyenoic fatty acids containing atleast one *cis, cis,* 1-4 pentadiene system. Three methods are commonly used.

(1) The polarographic method of assay, by which the uptake of oxygen, which is one of the reactants is measured polarographically using Clark electrode (Schewe *et. al.,* 1986).

(2) The spectroscopic method by which the increase in absorbance at 234nm due to the formation of product conjugated diene is measured (Axelrod *et. al.,* 1981). This method is more sensitive and convenient for the routine assay of lipoxygenase.

(3) In the third method, products of the reaction are quantified using either 14C or 3H labeled substrate. This method, though more sensitive, requires an additional step of separation of products by thin layer chromatography or high performance liquid chromatography (Schewe *et. al.,* 1986).

Purification of Lipoxygenase

The various isolation and purification methods are based on the physical and chemical properties of the enzyme. Purification of LOX-1 is done according to the method of Axelrod *et. al.,*(1981). In this method, the enzyme is extracted at pH 4.5, the isoelectric point for other proteins from defatted soy flour. Further purification is achieved by precipitating the enzyme between 30-60% saturation of ammonium sulphate. The precipitated protein is further resolved on anion exchange column using DEAE-Sephadex A-50 with a phosphate gradient. Grossman *et. al.,* (1972) reported the purification of lipoxygenase by affinity chromatography using linoleyl aminoethyl agarose column. This method results in better yields of the enzyme, but suffers from the disadvantage of being unable to separate the isoenzymes. Based on the net charge differences, various isoenzymes are normally resolved by either ion exchange chromatography or hydroxyapatite columns (Grossman *et. al.,*

1974; Borthakur *et. al.,* 1988). All three isozymes have been resolved using isoelectric focusing and chromatofocussing (Funk *et. al.,* 1986).

Three Dimensional Structures of Lipoxygenases

X-ray crystallographic structures of soybean and rabbit lipoxygenases have been resolved. (Boyington *et.al.,* 1993; Minor *et. al.,* 1996; Skrzypczak-Jankun *et. al.,* 1997; Gillmor *et. al.,* 1997). All these enzymes consist of a small N-terminal domain and a major C-terminal domain, which contain the active site. The proteins share an overall folding pattern and contain similar non-heme iron sites. The only significant difference is with respect to the catalytic center, where iron is co-ordinated to different amino acid ligands. In the case of rabbit lipoxygenase, one of the iron coordination positions is occupied by histidine, while the structures of the soybean lipoxygenase contain asparagine in the same location, just beyond the bonding distance. The structures of all of the complexes of these two enzymes, determined to date, identify the same site for ligand binding adjacent to the non-heme iron.

Structure of Lipoxygenase

X-ray crystal structure of LOX-1 was resolved at 1.4 Å and 2.3 Å by two different research groups (Boyington *et. al.,* 1993; Minor *et. al.,* 1996; Gaffney, 1996). LOX-1 is an ellipsoid molecule of dimensions 90 Å x 65 Å x 60 Å (Fig.8). It consists of two domains, a smaller N-terminal domain comprising of residues 1-146 and a larger C-terminal domain comprising of 693 residues. The three-dimensional structure of LOX-1 shows a α- helical content of 38% and β-sheet content of 14%. The N-terminal domain is an

eight-stranded antiparallel β-barrel. The interior of the barrel is densely clustered with hydrophobic side chains. The N-terminal domain is independent from the rest of the molecule and is linked to the C-terminal domain, on one side of helix 17. The C-terminal domain consists of two distinct stretches of π-helix. π-helix, with hydrogen bonding between residues i and i+5 instead of i and i+4 are quite unusual. This π-helices are present in the middle of the two longest helices in the molecule and both contain residues serving as ligands to the iron. The first π-helix present in helix 9 is the longest π-helix reported so far, for a globular protein (65 Å long). It has 13-residues extending from His_{494} to Ala_{506}. Two of these residues His_{499} and His_{504} are iron ligands. The second π-helix (six residues long Ile_{685} to His_{690}) is found in helix 18 and contains His_{690}, third histidine iron ligand. Two antiparallel β-sheets, with three and 5 strands are also present in the C-terminal domain. Both sheets lie at or near the surface of the domain and are separated from the active site by the bundle of helices. The structure of LOX can be divided into five domains (Minor *et. al.,* 1996) such that four smaller domains of 90-170 residues associate on the surface of one longer C-terminal domain. The first domain spans residues 1-170 so that it includes the N-terminal and helix 1. The second domain consists of residues 117-250, which form a contiguous but loosely organized unit, domain three, residues 251-340, is organized into a three β-stranded antiparallel β-sheet and three well defined helices (2, 3 and 4). Domain four starts and ends approximately at residues 341 to 470 and comprises the five-stranded β-sheet and two associated helices (7 and 8). The fifth and final domain starts approximately

at residues 471 near the N-terminal of core helix 9 and includes the remainder of polypeptide chain (368 residues) and also holds the catalytic site. It is exclusively α-helical and encompasses more than ten helices organized into two long core helices (9 and 18). The motions of the domains could facilitate binding, transport and release of substrates and products. The likely entrances/exists to the internal cavities implicated in substrate binding and passage of the substrate to the binding site is located at interfaces between the catalytic domain 5 and peripheral domains 3 and 4.

Recently, the X-ray structure of Soy LOX-1 was refined using X-PLOR 3.1. A significant change in Fe-ligand bond lengths for LOX-1 is the contraction of the Fe-H_2O bond length, from 2.56 to 2.11 Å. Hydrogen bonded network consisting of Asn_{694}-Gln_{697}-Gln_{495} extends to include His_{499}. The hydrogen-bonded network plays an important role in the enzymatic mechanism as mutation of these residues had decreased solvent isotope effect compared to wild type LOX-1 (Tomchick *et. al.,* 2001).

Based on the structural studies, a model of linoleic acid was docked into the substrate-binding cavity (Fig 10). The substrate was positioned with the hydrophobic end buried into the binding cavity and the carboxylate end near the surface of the protein. The carbons (C-9 & C-13) involved in the formation of pentadienyl radical were modeled as planar unit. This result in the placing of *pro*-S hydrogen of C-11 of the substrate near the Fe (II)-OH2 species ready for abstraction, with a 3.3 Å distance between the water position and C-11.

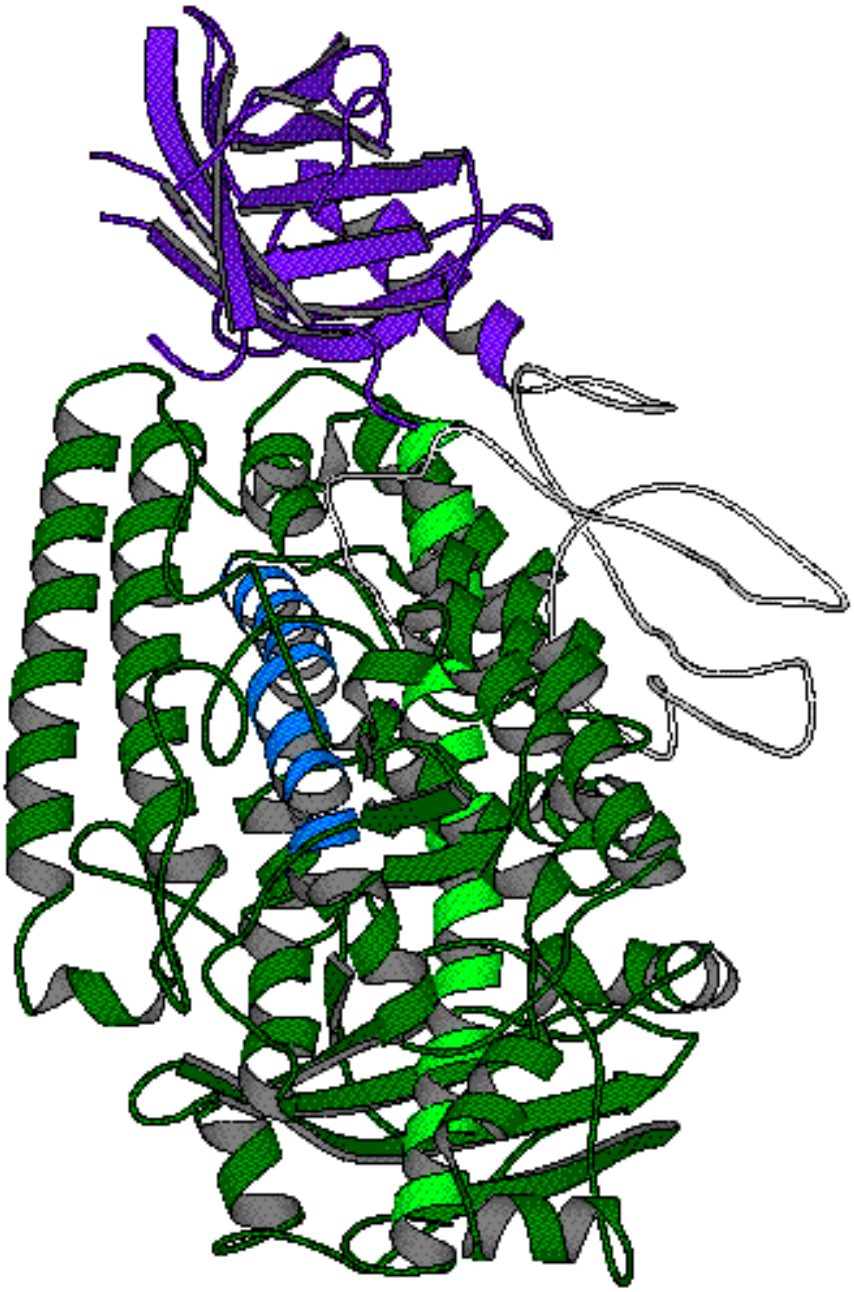

Figure. 8 Ribbon representation of the soybean lipoxygenase-1 (PDB code 2SBL). Color codes: N terminal domain (7-170) = violet; C terminal domain (255-839) = dark green; helix 9 (474-516) = light green; helix 18 (672-701) = light blue (Boyington *et. al.,* 1993).

But this distance is much longer than would be required for hydrogen abstraction by the Fe (III)-OH- species, suggesting a rearrangement of substrate binding cavity upon oxidation or substrate binding. The site of oxygenation is C-13 and is near Gln_{495}, Leu_{546} and the alternate conformation of His_{499}. The C-14 to C-18 hydrocarbon tail is flanked by the hydrophobic portion of the Gln_{495} side chain, while C-2 to C-8 are positioned in a hydrophobic channel past Leu_{538}. The proper positioning of Gln_{495} and His_{499}, in addition to the hydrophobic residues that flank the pentadiene (Leu546, Leu_{745}, Trp_{500} and Leu_{538}) provides suitable binding pocket for the substrate, facilitating catalysis (Tomchick *et. al.,* 2001). Efficient C-H bond cleavage is achieved by the correct positioning of the substrate through steric interaction with the side chain of Gln_{496} and the hydrogen bond network of Gln_{496}, Gln_{697} and Asn_{694} is responsible for the hydrogen bond rearrangement step after the substrate binding. Fe (III)-OH- species is the active site base for hydrogen atom abstraction and (Tomchick *et. al.,* 2001).

Iron Coordination in Lipoxygenase

The iron is situated at the center of the major domain coordinated to four protein ligands: three histidines and C-terminal carboxylate. The three histidines (His_{499}, His_{504} and His_{690}) are coordinated through the Nε and the fourth position is occupied by oxygen of the carboxy terminal (Ile_{839}) (Fig. 9 & 10). The terminal carboxylate provides the only negative charge in the immediate vicinity of the iron. The ligands are arranged as distorted octahedron with two adjacent (unoccupied) positions. The three Fe-Nε distances are all similar to each other, ranging from 2.07 to 2.28 Å. The Fe-O

distance is 2.08-2.12 Å. The C-Nε-Fe angles formed by the ligands are all close to 120°. Two of the Fe- Nε bonds are in the plane of their immidazole rings. The third Fe- Nε bond (His_{499}) on the other hand makes a 33° angle with plane of the immidazole ring. The unique orientation of the three-histidine ligands in LOX1 is a consequence of their presence in the regions of π-helices. In addition, the three imidazole rings are held in position by a network of hydrogen bonds formed by the both main chain and side chain atoms. Asn_{694} is a part of this network. The Oδ or Nδ of Asn_{694} is 3.3 Å from the iron. Both the water molecule and Asn_{694} are too far to be iron ligands. It has been suggested that these groups could become iron ligands during the catalytic cycle of the enzyme (Minor *et. al.,* 1996; Gaffney, 1996). Residue Gln_{495} lines the substrate cavity wall and begins an extensive hydrogen network that stretches towards the catalytic iron and may provide structural link between substrate binding and iron coordination (Minor *et. al.,* 1996). Gln_{495} hydrogen bonds to Gln_{697}, which in turn hydrogen bonds to Asn_{694}, a weak first-coordination ligand sphere. Spectroscopic data of SLO-1 indicate that the iron center exists as a mixture of five- and six-coordinate species (40% and 60%, respectively) in solution with possible detachment of the asparagine-derived ligand from the iron center. Though not observed in the crystal structures, an exogenous water molecule in all likelihood completes the octahedral coordination of the Fe (II) center.

Unlike many of the mononuclear non-heme iron enzymes, the ferrous form, Fe (II), of LOX is in resting state, and the iron center must be oxidized to the ferric state, Fe (III), for catalytic activity. Auto activation of SLO occurs in the

presence of the hydroperoxy product of linoleic acid. Extended X-ray absorption fine structure (EXAFS) and magnetic circular dichroism studies on the Fe (III) form of SLO-1 indicate a six-coordinate metal center. EXAFS studies reveal the presence of a short iron-ligand bond distance of 1.88 Å that is attributed to a single hydroxide ligand (Scarrow *et. al.,* 1994).

Internal cavities of LOX1

Two cavities (Cavity I and Cavity II) in the major domain of LOX1 extend from the surface to the active site. Cavity I is funnel shaped and functions as a dioxygen channel; the long narrow cavity II is the substrate pocket. Cavity I interacts with all three histidines and forms a tunnel that connects the position opposite to the Nε of His_{504} to the surface of the protein. The sides of the funnel are lined by the side chains of 29 residues most of which are hydrophobic. When using this path, the oxygen will reach the correct location to bind to one of the 2 unoccupied coordination sites of the iron. Cavity II is the locus of the catalytic events of the enzyme, which connect to the outside solvent through a small entrance (Minor *et. al.,* 1996; Gaffney, 1996).

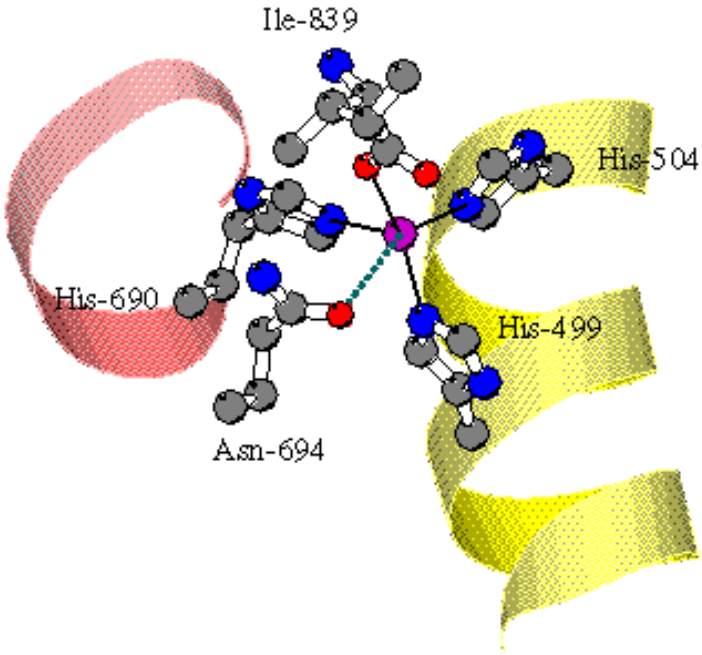

Fig.9 Active site structure: πhelices 494-506 (yellow) and 685-690 (pink) and iron ligands His_{499}, His_{504}, His_{690}, Ile_{839} and Asn_{694} (Boyington *et. al.,* 1993). (http:/metallo.scripps.edu/promise/)

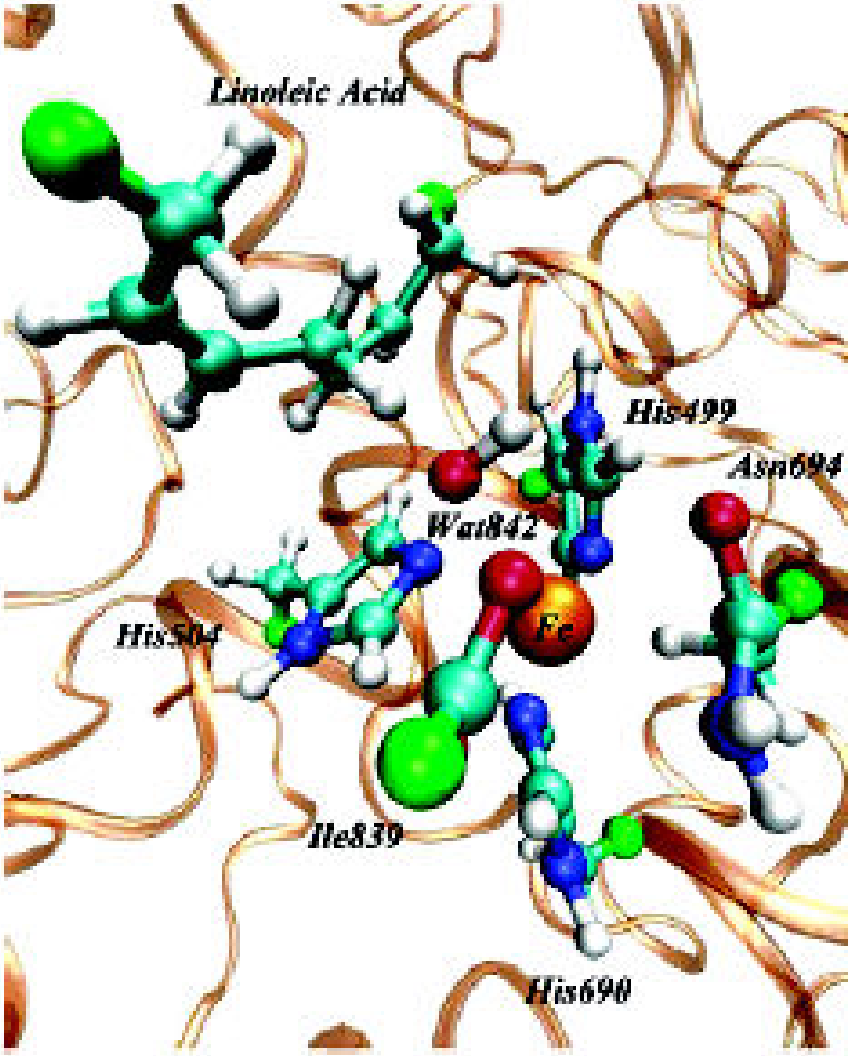

Figure. 10 Active center in SLO-1. The QM atoms are represented in a ball-and-stick model (link atoms in green) (Tejero *et. al.,* 2006).

Three Dimensional Structure of Mammalian Lipoxygenase

X-ray crystallographic structure of rabbit 15-lipoxygenase with its bound inhibitor, aryl carboxylate (RS75091) was solved by Gillmor *et. al.,*1997) (Fig. 11). The structure comprises two β-barrel domains and a larger C-terminal domain. The existence of the N-terminal 115 amino acid β-barrel domain in the mammalian lipoxygenase was not predicted based on the structure of the soybean enzyme. The first 250 amino acid residues between mammalian and plant LOXS are unidentical including the β-barrel domain (Prigge *et. al.,* 1996). The overall architecture of the mammalian lipoxygenase is similar to the soybean isozymes. Seventeen of eighteen helices of the mammalian lipoxygenase correspond to a structurally similar helix in the soybean enzyme, which has a total of twenty-three helices.

The β-barrel domain of mammalian lipoxygenase, in comparison with the plant lipoxygenase structure, shows that the mammalian lipoxygenase β-barrel is shifted and rotated across the surface of the helical domain with respect to the orientation of domains in the soybean structure. The β-barrel has densely packed interior and is the catalytic domain. β-barrel domain make rigid body motions with respect to the catalytic domain. The β-barrel domain is eight stranded and is similar in size and structure to an analogous C-terminal β-barrel domain in the mammalian lipases in comparison to homologous domain in plant lipoxygenases (Funk and Loll, 1997). The C-terminal domain is connected to the N-terminal domain by several helices that lead to a small 5-stranded β-sheet region at the opposite end of the catalytic domain. The catalytic domain contains eighteen helices that are

interrupted once by the small β-sheet sub-domain. The core of the catalytic domain contains two long central helices, one of which adopts π-helix conformation for the length of several residues (360-366 and 534-543). The π-helical section of these two helices contains four of the protein ligands (His_{361}, His_{366}, His_{541} and His_{545}) that coordinate the non-heme catalytic iron. The fifth protein-iron ligand is the carboxylate of the C-terminal residue Ile_{663}. These five ligands coordinate the iron with excellent octahedral geometry. Based on X-ray structure of mammalian 15-lipoxygenases, a unifying hypothesis has been proposed for the positional specificity of mammalian lipoxygenases with a single orientation of arachidonic acid bound toward the center of the enzyme with the carboxylic acid tethered near the surface of the enzyme by a polar residue arginine or lysine (Gillmor *et. al.,* 1997; Funk and Loll, 1997).

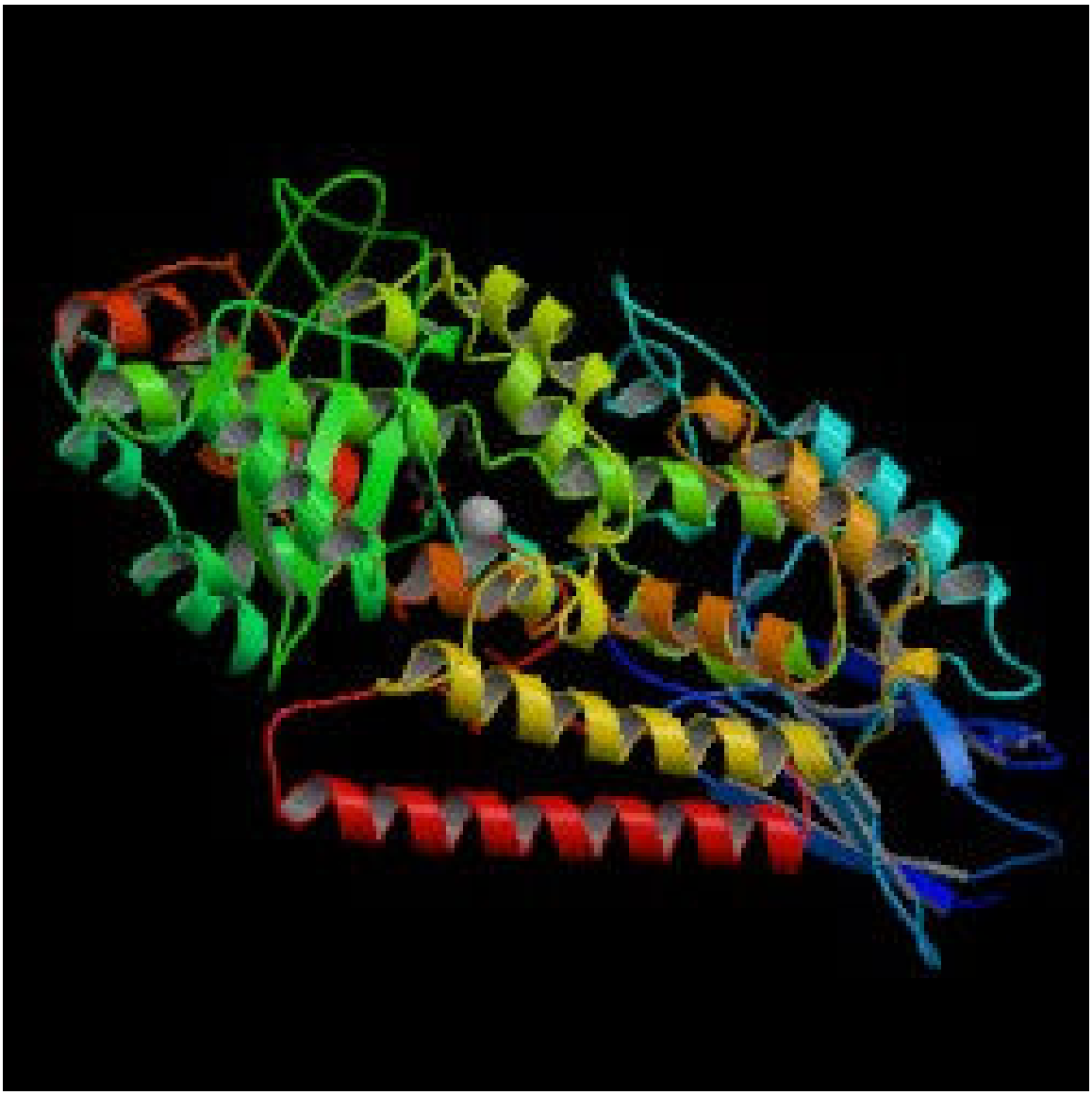

Figure. 11 Structure of rabbit reticulocyte 15-LOX
(PDB No. 1-LOX, Gillmor et. al., 1997)

Catalytic mechanism of lipoxygenases

Lipoxygenases contain non-heme iron, which is covalently bound to the protein as the co-factor. Iron exists in one of the two oxidation states; Fe^{2+} (resting enzyme) and Fe^{3+} (active form). In most of the mechanisms proposed, iron oscillates between the Fe^{2+} and Fe^{3+} forms during catalysis. Two hypotheses exist to explain this (Nelson and Seitz, 1994).

(1) *Product activation model:* This model suggests that the hydroperoxide produced is required to activate the enzyme by oxidizing the ferrous ion to ferric ion. In this hypothesis only the ferric enzyme is active.

(2) *Substrate inhibition model:* In this model, both ferric form and ferrous form are active and are inhibited by the substrate to a non-catalytic site. Here the lag period reflects the displacement of substrate in the regulatory sites by products they accumulate.

As regards the catalytic mechanism of LOX, three different mechanisms have been proposed in the literature and they are depicted in Fig.12. Each of them is discussed below with experimental findings in their support (Borowski & Broclawik, 2003). The radical mechanism, which involves steps 1a-c shown in Fig. 12. The first step (1a) is the hydrogen atom abstraction from the substrate-taking place simultaneously with the active site iron ion reduction. Hydrogen abstraction requires the ferric form of the enzyme and leading to the formation of hydrocarbon radical formation, which is well documented. Schilstra *et. al.,* (1994) have demonstrated that only the ferric form of LO is catalytically active, while Glickman and Klinman (1995) have established that

the hydrogen atom abstraction precedes dioxygen binding. The formation of carbon-centered radicals in the absence of oxygen has been confirmed (De Groot *et. al.,* 1973). Nelson and coworkers have proved the identity of the carbon-centered radical, present in the purple form solution, by EPR spectroscopy (Nelson *et. al.,* 1990). The EPR data have been interpreted in favor of the pentadiene radical that might be slightly twisted around the C10-C11 bond. Since there are no groups capable of abstracting either hydrogen atom or proton from the substrate in the vicinity of the iron site, both the electron and the proton, i.e., the whole hydrogen atom, is accepted by the iron site. Therefore, it has been suggested by Scarrow *et. al.,* (1994) that the hydroxide group bound to the ferric ion in the active form of LO constitutes a perfect candidate for the hydrogen-abstracting moiety.

In the second step of the radical mechanism (step 1b in Fig. 12), molecular oxygen reacts with the pentadiene radical and forms the peroxy radical. The presence of the latter radical bound to the enzyme has been proved by EPR experiments, (Nelson *et. al.,* 1990) and the direct radical molecular oxygen reaction is consistent with the very high rate for the reaction between molecular oxygen and SLO-1 with a bound carbon-centered radical (Glickman *et. al.,* 1997). On the basis of regio and stereochemistry of the products obtained with some point mutants of SLO-1, Knapp *et. al.* (2001) have proposed that the stereo- and regioselectivities of SLO-1 are tuned by the enzyme's steric control of the oxygen approach to the radical. In the last step of the radical mechanism (step 1c in Fig. 12), the peroxy radical is reduced by the ferrous form of the active site, which indicates the product formation

and the ferric active site regeneration. In the radical mechanism the purple form of lipoxygenase is a catalytically irrelevant byproduct. In addition, all of the oxygen dependent steps in the catalytic reaction are reversible (Glickman and Klinman, 1996).

The organo-iron mechanism (steps 2a-c in Fig. 12) proposed by Corey and Nagata (1987) presumes that close to the iron site there is a basic group that serves as a proton acceptor site. Thus, the first step of this mechanism (step 2a in Fig. 12) comprises the proton shift from the substrate to this basic site and the simultaneous ferric site attack on the forming carbanion. In the second step (step 2b in Fig. 12), molecular oxygen reacts with the organo-iron intermediate leading to formation of the peroxy radical-iron site complex. In the last step (step 2c in Fig. 12), this complex reacts with the acid, which is coupled with the before-mentioned bases, and forms the product. This organo-iron mechanism very elegantly explains the regio- and stereoselectivities of LO, and the purple form of lipoxygenase turns out to be the catalytic reaction intermediate formed by oxygen insertion into a single organo-iron bond (step 2b in Fig. 12). However, in the X-ray crystal structure, there are no candidates for the basic site proposed in the mechanism. Moreover, there is no experimental evidence supporting the organoiron complex formation. On the other hand, the chemical character of the purple form of lipoxygenase, i.e., the peroxy radical complex with the ferrous site, is confirmed by spectroscopic and crystallographic experiments.

The ene-radical mechanism, proposed by Nelson and co-workers, (1990) is a variation of the radical mechanism. The first step (step 3a in Fig. 12), is the hydrogen atom abstraction by the ferric site, ending with a vinyl-allyl radical formation. The substrate channel bends in the proximity of the iron site and causes the twist of the radical formed in this step. Next, the molecular oxygen binds to the ferrous site and thus activated oxygen molecule attacks the vinyl fragment of the radical (step 3b in Fig. 12). The vinyl fragment of the radical has a closed-shell character, which suggests that the activated molecule should have properties of the singlet oxygen. Magnetic susceptibility measurements have indicated that oxygen does not bind to the ferrous active site of LO (Petersson *et. al.,* 1985) and the twist of the substrate channel has been evidenced by the X-ray structural data. Moreover, the epoxy-like complex formed in the second step of this mechanism (step 3b in Fig. 12) explains the EPR spectra observed for the purple form solution. It has been suggested that this complex rearranges into the purple form and the latter is the catalytic reaction intermediate. The epoxy-like complex and/or purple form decomposition (steps 3c and 2c in Fig. 12) completes the catalytic cycle. Thus, three distinctive mechanisms have been proposed in the literature, as depicted in Fig. 12.

Some of the catalytic steps have been explained based on the X-ray structure of LOX1 (Gaffney, 1996; Minor *et. al.,* 1996). In the catalytic cycle of LOX1, the Fe^{3+} form of the enzyme abstracts one electron from the 1, 4-diene moiety of the fatty acid and a base abstracts a proton producing the

free radical form of the 1, 4-diene system and Fe^{2+} form of enzyme. The rate-limiting step is hydrogen abstraction.

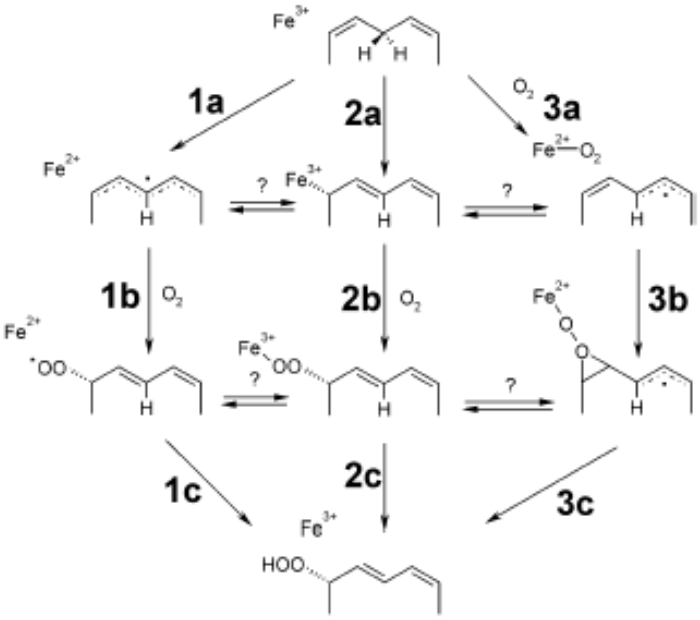

Figure. 12 Catalytic mechanism of LOX-1
(Borowski & Broclawik, 2003)

Molecular oxygen reacts with the substrate radical to form a peroxyl radical, which then abstracts an electron from the metal, regenerating Fe^{3+} and producing a peroxide anion. The peroxidate receives a proton from the base yielding the hydroperoxide product. A fatty acid molecule can enter cavity II following a small movement of the side chains of leu_{480} and Met_{341}. In the cavity, it can approach the iron in such a way that the site from which the electron will be abstracted is close to the oxygen ligand. The water molecule found close to the iron, probably a hydroxyl in the Fe^{3+} form of the enzyme,

is the most suitable candidate for the abstraction of the proton from the base. The second oxygen of the carboxy terminus may have a role in orienting this hydroxyl group through a hydrogen bonding interaction. Molecular oxygen can enter the molecule with the iron in the other unoccupied position to the Nε of His_{504}. The side chain of Asn_{694} is close to position where it may hydrogen bond to the bound oxygen. If the oxygen and fatty acid are both coordinated to the iron, the molecular oxygen and the reactive radical position of the fatty acid are in adjacent positions of the iron coordination sphere. This arrangement is well suited for carrying out necessary electron transfers. After the hydroperoxide is produced and released, the coordination of iron will return to an arrangement similar to the one observed in the X-ray structure.

The catalytic mechanism of mammalian 15-LOX has been explained through a scheme (Gillmor *et. al.,* 1997). The catalytic iron Fe^{3+} with a bound hydroxide ion serves as the general base for abstraction of hydrogen from arachidonic acid. There is no second cavity near the active site, which normally serves either as an oxygen-binding site or as a channel for controlling oxygen access to the active site. The enzyme does not position oxygen, but the positional and stereo-specificity of the lipoxygenase action is determined by the bound substrate. The mechanism generally involves the abstraction of the pro-R-hydrogen atom at the C-13 position of the substrate, followed by insertion of dioxygen in the opposite face of the molecule at C-15 to form 15-hydroperoxy eicosatetraenoic acid (15 HPETE). The catalytic iron is in EPR silent mode in resting state. It is oxidized to ferric state by small

amounts of oxidized substrate. Based on the substrate binding model (Gillmor *et. al.,* 1997) arachidonic acid adopts an extended conformation when bound the active site. The methyl end of the substrate would be buried in the toe of the boot-shaped active site pocket that is lined by hydrophobic residues. The carboxylate end would make a salt bridge interaction with Arg_{403}, which lies at the opening of the channel on the surface on the protein.

Role of Iron in kinetic mechanism of lipoxygenase

The cofactor iron present in lipoxygenase plays an active role in the reaction mechanism. (Pistorius and Axelrod, 1974). The iron exists in Fe^{2+} state during resting. During catalysis, the Fe^{2+} (ferrous state) is converted to Fe^{3+} (ferric form) by the action of product, hydroperoxide. Iron is maintained in the Fe^{3+} form during the steady-state turnover of the enzyme (Veldink *et. al.,* 1977).

The transition in the oxidation state of the iron co-factor is marked by changes in the spectroscopic properties of both the protein and co-factor species (Degroot *et. al.,* 1975; Pistorius *et. al.,* 1976; Edmond *et. al.,* 1977; Slappendel *et. al.,* 1981). The changes associated with the protein *(i)* appearance of an absorption band at 330nm, yellow form of the enzyme which gets converted to purple form upon interaction with excess hydroperoxide, *(ii)* about 30% decrease in the fluorescence intensity in the tryptophan fluorescence emission, *(iii)* appearance of positive dichroic band at 425 nm. The change associated with cofactor iron is the appearance of EPR signal at g= 6.1, due to the transition in the high-spin Fe^{2+} to the high-

spin Fe^{3+}. Due to this transition, there exists a finite induction period (lag period) before the onset of steady state kinetics (Veldink *et. al.,* 1977).

Substrate specificity of LOXs

The substrate for LOX should contain a *cis cis* 1, 4-pentadiene moiety, with an activated methylene group between the double bonds. Majority of LOXs prefer free fatty acids as substrates. However, two 13-LOXs- soy LOX-1 and cucumber lipoxygenase oxygenate the PUFA moieties esterified to phospholipids in biomembranes (Kuhn and Theile, 1999). Among mammalian LOXs rabbit reticulocyte is known to act on biomembranes (Kuhn *et. al.,* 2005). Hence, LOXs play a role in membrane permeabilization. LOXs from other sources act on neutral lipids (triglycerides) suggesting their involvement in triglyceride catabolism (Gardner, 1991).

Physiological effects of lipoxygenase and its products.

Hydroperoxides, products of LOX reaction with unsaturated fatty acids, are the key molecules responsible for the initiation of many diseases and disorders. In animals, LOXs carry out the first step in arachidonic acid cascade, which is the source of numerous powerful bioregulators that include prostaglandins, thrombaxanes, leukotrienes, lipoxins, hepoxilins and others in a variety of cellular responses (Samuelsson *et. al.,* 1987; Parker, 1987; Yamamoto, 1997; Funk, 1996). Lipoxygenase products such as dihydroxy fatty acid leukotriene B4 (LTB4) and 9S-hydroxyeicosatetraenoic acid (9S-HETE) are ligands for G-protein coupled receptors and nuclear hormone receptors, which regulate pathways involved in inflammation and lipid

homeostasis (Yokomizo *et. al.,* 1997; Devachand *et. al.,* 1996; Forman *et. al.,* 1997). The activities and products of the LOX enzymes influence atherosclerosis, inflammatory bowel disease, psoriasis, asthma and other immune system disorders, 12-lipoxygenase is over-expressed in the pathological lesions of inflammatory bowel disease and psoriasis (Shannon *et. al.,* 1993). The ability of 15-LOX (but not other lipoxygenenases) to oxidize low-density lipoproteins (LDL) is suggestive of an important role for this enzyme in the pathogenesis of atherosclerosis (Steinberg *et. al.,* 1989). Inhibition of 5-LOX has been shown to have therapeutic value in the treatment of asthma (Israel *et. al.,* 1996). Mounting evidence suggests that lipoxygenase (LO)-catalyzed products have a profound influence on the development and progression of human cancers.

Compared with normal tissues, significantly elevated levels of LO metabolites have been found in lung, prostate, breast, colon, and skin cancer cells, as well as in cells from patients with both acute and chronicleukemias. LO-mediated products elicit diverse biological activities needed for neoplastic cell growth, influencing growth factor and transcription factor activation, oncogene induction, stimulation of tumor cell adhesion, and regulation of apoptotic cell death. Agents that block LO-catalyzed activity may be effective in preventing Cancer by interfering with signaling events needed for tumor growth. In fact, in a few studies, LO inhibitors have prevented carcinogen-induced lung adenomas and rat mammary gland cancers.

LO Metabolites in Carcinogenesis

Evidence from studies in human cancer cells shows that the LO pathways are involved in carcinogenesis in several major tissues. More importantly, a few studies in animal carcinogenesis models show that inhibition of the LO pathways also may inhibit carcinogenesis.

Lung. Two recent studies found that LO inhibitors have chemopreventive activity in animal lung carcinogenesis. Moody *et al.* (1998) and Rioux and Castonguay (1998) showed that the FLAP inhibitor MK 886 (25mg/kg diet) and 5-LO inhibitor A 79175 (75 mg/kg diet) reduced the multiplicity of NNK-induced tumors in strain A/J mice; Aspirin (294 mg/kg diet) reduced tumor multiplicity and the combination of aspirin and A 79175 synergistically lowered tumor incidence and multiplicity. These results convincingly suggested that 5-LO pathway inhibitors might have chemo preventive activity in lung.

Prostrate Cancer. Eicosanoid biosynthesis in relation to prostate cancer development has been thoroughly investigated. Initial studies revealed reduced levels of arachidonic acid. 10-fold greater turnover in malignant *versus* benign prostatic tissue suggested a possible increase in metabolism via the LO and COX pathways in this tissue (Chaudry *et al.,* 1991; Chaudry *et. al.,* 1994). Linoleic acid stimulated cell growth in experiments conducted in human prostate cancer cells, whereas indomethacin, esculetin, and piroxicam inhibited it, proving the involvement of eicosanoids in prostate cancer cell proliferation (Rose and Connolly, 1991).

Breast. Studies published over the past two decades strengthen the regulatory role for fatty acid metabolites, especially for the arachidonic acid-derived eicosanoids in the etiology of mammary carcinogenesis (Karmali, 1987). Feeding studies conducted in rodent models of mammary tumorigenesis showed that diets rich in linoleic acid, n-6 polyunsaturated fatty acid, and arachidonic acid precursor, stimulate mammary tumor growth induced by either MNU or DMBA (Fischer *et. al.,* 1992; Welsch, 1992; Cohen *et. al.,* 1986). Linoleic acid enhances the invasive capacity of breast cancer cells; this effect could be completely blocked by adding esculetin (20 mM), an inhibitor of 5- and 12-LO, but not by adding the COX-specific inhibitor piroxicam. Interestingly, adding 0.1 mM 12-HETE mimics the stimulatory effect of linoleic acid on cell invasion, whereas PGE2 and 5-HETE are found to have no effect. Collectively, these data support the concept that enhanced 12-HETE, not PG, is involved in the etiology of breast cancer cell metastasis. Besides overwhelming data linking PGs to the etiology of colon carcinogenesis (Rigas *et. al.,* 1993), several recent lines of study suggest that LO products may also be involved in this process. Platelet-type 12-LO mRNA has been recovered from a human colon carcinoma cell line, treatment of these cells with 12(*S*)-HETE resulted in up-regulation of 12-LO mRNA and protein (Gao and Honn, 1995). Collectively, these data strongly suggest that LO metabolism may play a role in colon tumor proliferation.

Skin. Biochemical evidence suggests that LOXs are responsible for epidermal tumor development. Compared with normal epidermis, large quantities of 12(*S*)-HETE (50–60-fold greater) are found in papillomas and carcinomas

induced by DMBA and TPA in a mouse skin tumor model (Takahashi *et. al.,* 1993). 12-LO enzyme activity was elevated 6-fold in papillomas and 3-fold in carcinomas compared with normal tissue. Moreover, expression of platelet-type 12-LO has been confirmed in both normal human epidermis (Liu *et. al.,* 1994) and human epidermoid A431 carcinoma cells (Chang *et. al.,* 1993). 12(*S*)-HETE overproduction in papillomas may be a mechanism for progression to malignant carcinoma. Inhibition of lipoxygenases enzymes results directly in reducing the production of fatty acid metabolites with concomitant damping of the associated inflammatory, proliferative and metastatic activities that contributes to carcinogenesis.

Inhibitors of Lipoxygenase

The interest in the inhibitors of lipoxygenase is due to deleterious effects of the products of lipoxygenase reaction on health. Broadly there are three classes of inhibitors (1) substrate analogs, (2) redox inhibitors, those that affect the catalytic iron center and (3) radical trappers, which function by reacting with free radical intermediates of lipoxygenase reaction. The redox inhibitors are very potent but of little pharmaceutical value as they have the tendency to produce toxic side effects. The nonredox inhibitors are more relevant as therapeutic drugs, but their mode of action is difficult to establish, because of the multiple oxidation states of the enzymatic cycle. The design and mechanistic characterization of specific inhibitors becomes more complicated when one considers the possibility of an allosteric site that is separate from the active site. At high substrate concentration, two

independent sites are occupied by the substrate. It has been suggested that there exists a regulatory site near the catalytic site (Aharony and Stein, 1986). This hypothesis has been proposed by kinetic analysis of lipoxygenase-catalyzed reaction. It has been suggested that monomeric lipoxygenase-1 possesses at least two classes of binding sites, a catalytic site and a regulatory site. The binding sites are designed such that the catalytic site can bind either the substrate or product, whereas the regulatory site can bind either two molecules of substrate or one molecule of product. Mammalian lipoxygenases are a target for drug design. Since mammalian enzymes are difficult to purify, design of inhibitors rely heavily on structural and mechanistic studies on soybean lipoxygenase, whose three-dimensional structure and catalytic mechanism have been explored in detail (Minor *et. al.,* 1996; Siedow, 1991). Soy LOX-1 is used as *in vitro* biochemical models as it resembles human lipoxygenases, in its substrate specificity and inhibition characteristics (Borgeat *et. al.,* 1983; Kingston, 1991). The quest for new as well as natural inhibitors of lipoxygenase poses a challenge. A number of monoenoic fatty acids, which resemble fatty acid substrates but structurally differ in *cis, cis,* 1-4 pentadiene system are shown to be competitive inhibitors of LOX1 (St Angelo and Ory, 1984). The inhibitors like 4-nitrocatechol, N-alkylhydroxylamine and disulfiram are redox inhibitors inhibiting LOX1 activity by reduction of active yellow form (Fe^{3+}) to its resting Fe^{2+} form (Galpini *et. al.,* 1976; Clapp *et. al.,* 1985; Hausknecht and Funk, 1984). Inhibitors such as nordihydroguiaretic acid (NDGA), n-propylgallate and butyl hydroxytoluene are antioxidants that function by reacting with free

radical intermediates of lipoxygenase catalyzed reaction thereby acting as free radical scavengers (Tappel *et. al.,* 1952; Yasumato *et. al.,* 1970). NDGA has been shown to inhibit lipoxygenase by reducing the catalytically active ferric enzyme to the catalytically inactive ferrous form thereby acting as an efficient redox inhibitor (Kemal *et. al.,* 1987). α-tocopherol and chlorophyll form an enzyme inhibitor complex, thereby inhibiting LOX activity (Grossman and Walksman, 1984; Cohen *et. al.,* 1984). Esculetin, a coumarin derivative extracted from the bark of *Aesculus hippocastanum*, is a competitive inhibitor of both the LO and COX metabolic pathways (Sekiya *et. al.,* 1982; Panossian *et. al.,* 1984; Kimura *et. al.,* 1985). At concentrations of 0.1–1 mM, esculetin exerts LO inhibitory activity, where as levels of 10 mM are required for COX inhibition (Sekiya *et. al.,* 1982; Kimura *et. al.,* 1985). The antiproliferative action of esculetin has been shown in several *in vitro* biochemical models. Concentrations of 3–30 mg/ml significantly reduce LTB4 secretion and produce growth suppression in the MDA-MB-231 human breast cancer cell line (Earashi *et. al.,* 1995). Esculetin at 20 mM completely suppresses production of 12-HETE in estrogen-independent human MDA-MB-435 breast cancer cells stimulated with linoleic acid (Liu *et. al.,* 1996), 2 or 20 mM of esculetin totally blocked the invasiveness of cells stimulated by linoleic acid while totally suppressing type IV collagenase (metalloproteinase-9) mRNA expression. Thus, esculetin is a effective natural chemopreventive agent capable of inhibiting lipoxygenases. Baicalein, a low molecular weight flavonoid isolated from *Scutellaria baicalensis* Georgy roots, is a key component of Japanese herbal medicine Sho-saiko-to, commonly used to

treat chronic liver diseases in Japan. Studies conducted in rat platelets showed that nanomolar concentrations of baicalein exert potent 12-LO inhibitory activity, whereas much higher levels are required for COX inhibition (Butenko *et. al.,* 1993). So baicalein is also a natural inhibitor of lipoxygenase. Flavonoids, in general, are potent inhibitors of lipoxygenase.

Soybean Proteins. Soybeans contain a broad range of proteins, which are classified in different terms (*Liu 1997*). On the basis of their solubility they are classified as globulins or albumins. Glycinin is the most abundant protein found in soybeans. It represents ≈25-35% of total seed protein and accounts for >40% of the total soybean globulin. It is widely used in the food industry as a filling agent due to its favorable gelatinous properties in aqueous solutions (Lakemond *et. al.,* 2003), as well as for its emulsifying and foaming activities (Lakemond *et. al.,* 2002).

Glycinin is a hexameric protein comprising of five subunits with molecular masses reported between 320-375 kDa (Zhang *et. al.,* 2003). Each hexamer is composed of two trimers that are rotated 60° with respect to each other to form a triagonal antiprism. The trimers consist of three monomers. Each subunit comprises an acidic (molecular mass 40 kDa) and a basic (molecular mass 20 kDa) polypeptide, linked by a single disulfide bridge (Staswick *et. al.,* 1984). These polypeptides are highly heterogeneous (Lalles *et. al.,* 1999). Different glycinin subunits and corresponding glycinin genes have been identified and reported by various authors (Lakemond *et. al.,* 2002). Furthermore, different soybean cultivars appear to differ in content of the polypeptides constituting glycinin molecules (Zhang *et. al.,* 2003). Glycinin molecules from different origins have been proved to posses' different properties with respect to amino acid composition, molecular weight, and isoelectric point (Riblett *et. al.,* 2003). It is also reported that glycinin from the same origin exhibited different compositions and properties. The secondary structure of glycinin has been predicted to be 25% α-helices, 25%

,β-sheet, 42% turns and 8% unordered forms on the basis of its amino acid sequence by modeling (Argos *et. al.,* 1985).

Another abundant globulin protein found in soybeans is β-conglycinin, which represents ≈35% of soluble soy proteins. β-Conglycinin consists of three subunits, α', α and β with molecular masses of 76, 72, and 53 kDa, respectively. The subunits associate randomly into trimers of molecular masses of 150-220 kDa (Lalles *et. al.,* 1999). All three major subunits are rich in aspartate/asparagines, glutamate/glutamine, leucine and arginine. The two subunits,α' andα, are very similar in amino acid composition. Both are devoid of cysteine and have low levels of methionine. In contrast, β subunit contains no methionine (Coates *et. al.,* 1985). Both glycinin and β-conglycinin are acid precipitable. Glycinin has an isoelectric point in the pH range from 5.2 to 4.9, while that of β-conglycinin is in the pH range of 5.0-4.7. However, it has been observed by many authors and confirmed that both proteins precipitate readily and abundantly as soon as the pH of the solution decreases below 6.5.

SCOPE AND OBJECTIVES OF THE PRESENT INVESTIGATION

Understanding protein-ligand or enzyme-inhibitor interaction is central to drug design and the discovery of new medicines benefit human health. The discovery of novel drugs to treat important diseases is still a major challenge in pharmaceutical research. Structure-based design plays an increasingly important role in this endeavor and is now an integral part of medicinal chemistry. It has been shown for a large number of targets that the 3-D structure of the protein can be used to design small molecules binding tightly to the protein. A key to success and further progress in this field is a detailed understanding of the protein-ligand interaction. A number of biophysical methods are employed to predict protein-ligand interactions.

Isoflavones are the major bioactive (natural) phytochemicals present in soybean. There pronounced influence on human health has been a subject of numerous studies. To correlate between the beneficial effects of isoflavones and health requires a deeper understanding of the interactions of isoflavones with biomolecules present in the body. One of the ways isoflavones achieve this objective is by interacting with proteins/enzymes, responsible for many physiological/biochemical actions observed in the body. The main objective is to study the interaction of isoflavones with proteins of biochemical/physiological interest by biophysical and enzyme kinetic measurements. To obtain the benefits of their action, isoflavones must be transported to different parts of the body. The transport of isoflavones is not

clear. Serum albumin is the major carrier protein for insoluble bioactive ligands such as isoflavones. One of the main objectives is to study the interaction of isoflavones with serum albumin to elucidate its mechanism of transport at the molecular level. The other objective is to study the isoflavones-lipoxygenase interaction to asses the antioxidant capability of isoflavones. Isoflavones always go along with meal and they are completely absent in the oil phase. This shows that they have high affinity for proteins. The last objective is to study the interaction of isoflavones with major soybean storage proteins-glycinin and conglycinin. This study is likely to help in understanding the partitioning of isoflavones.

OBJECTIVES

[1] To isolate and purify major isoflavones genistein and daidzein and their glycosylated forms from defatted flour.

[2] To understand the nature of interaction and relative *in vitro* affinities of isoflavones with bovine and human serum albumin by spectroscopic and direct binding measurements.

To understand the relative *in vitro* affinities of isoflavones with bovine and human serum albumin in the presence of other ligands like fatty acids and ANS by competitive ligand measurements.

[3] To understand the nature and mechanism of *in vitro* inhibition of oxygenase using soy LOX-1 (plant LOX) and a mammalian LOX as models.

[4] To understand the nature of interaction and relative affinities of isoflavones with soybean storage proteins-glycinin and conglycinin.

MATERIALS AND METHODS

MATERIALS AND METHODS

MATERIALS

Human serum albumin (A-1653) (HSA), Bovine serum albumin (A-7638) (BSA) warfarin (A-2250), diazepam, triiodobenzoic acid N-acetyltryptophanamide, N-acetyltyrosine ester, Trizma base, Palmitic acid and N-bromosuccinimide, Linoleic acid, arachidonic acid, and Tween-20 were from Sigma Aldrich (St. Louis, MO). 8–Anilino-1- naphthalene sulfonic acid (ANS) was from Aldrich Chemical Co. USA. All other reagents were of analytical grade.

Soybean seed (Hardy variety) was procured from GKVK, University of Agricultural Sciences, Bangalore, Karnataka, India. Soybean seeds were finely ground in a hand mill and then exhaustively extracted with hexane. The defatted meal was stored in an airtight container at 4 °C.

METHODS

Purification of isoflavones: Isoflavones, genistein and daidzein (aglycones), genistin and daidzin (glycosylated) were purified from defatted soy flour (Ohta *et. al.,* 1979). Finely defatted soy flour (50gm) was extracted with 500ml of 80% methanol three times at 80°C for 3 hours. The extract was filtered and the supernatant concentrated under atmospheric pressure first and then under vacuum. A brownish syrupy liquid was obtained. This was subjected to extraction with two volumes of acetone. The acetone extract was concentrated by vacuum drying. The solid obtained was

dissolved in water and subjected to solvent partition using ethylacetate. The extract was partitioned into three layers, uppermost ethylacetate layer, middle solid mass and lower aqueous layer. The ethylacetate extract was subjected to adsorption chromatography on silica gel. The column (30 cm x 2.5) was eluted with 50% water saturated ethylacetate and 50% water saturated ethylacetate containing 2% ethanol with a flow rate of 1ml/min. Fraction F_1 is rich genistein and daidzein, F_5 is rich in genistin and F_6 is rich in daidzin. Each fraction obtained was rechromatographed on silica gel using the same procedure. All the fractions (F_1, F_5 & F_6) were further purified on a sephadex LH-20 column. The column (140 cm X 2) was eluted with 100% ethanol with a flow rate of 30ml/hr. Fraction F_1 was resolved into two fractions, genistein and daidzein. Fraction F_5 was genistin and fraction F_6 was daidzin. The purity of isoflavones was determined by HPLC employing a C_{18} column (Wang and Murphy, 1994) with gradient elution using acetonitrile water (15 – 35%, in 50 min, flow rate: 1ml /min and detection at 262 nm). The concentration of isoflavones was determined by the molar absorption coefficients (Coward *et. al.,* 1993) (genistein = 37.3 x 10^3 M^{-1} cm^{-1}; daidzein = 26 x 10^3 M^{-1} cm^{-1}; genistin = 41.7 x 10^3 M^{-1} cm^{-1} and daidzin = 29 x 10^3 M^{-1} cm^{-1}).

Defatting of serum albumin: Bovine serum albumin and human serum albumin was defatted using the method described by Chen (1967). 50 mg of HSA and BSA was dissolved in 0.5 ml of water. To this 25 mg of activated charcoal was added and the pH of the solution was brought to 3.0 with the addition of 0.2 N HCl. The solution was then placed in an ice-bath and stirred

for 1 hr. Charcoal was then removed by centrifugation. The clarified solution was then brought to pH 7.0 by the addition of 0.2 N NaOH. The serum albumin solution was lyophilized.

Purification of bovine and human serum albumin: The higher molecular weight aggregates associated with commercial preparations of bovine and human serum albumin were removed by size exclusion chromatography on a G-100 Sephadex column (120 x 1 cm) pre-equilibrated with 50 mM Tris- HCl buffer (pH 7.4). Fractions of 1 ml were collected at a flow rate of 10-ml/ h and the purity was ascertained by SDS–PAGE (Laemmli, 1970). Protein concentration of the HSA fractions was determined using a value of 5.30 for $E_{1\%}^{1cm}$ at 278 nm. (Clark *et. al.,* 1962). BSA concentration was estimated using a value of 6.67 for $E_{1\%}^{1cm}$ at 279 nm (Föster and Sternman, 1956).

Modification of tryptophan residue on serum albumin: The tryptophan residue on BSA & HSA was modified using N-bromosuccinimide according to the method of Spande and Witkop (1967). A 3-mg/ml solution of serum albumin in 50 mM acetate buffer (pH 4.0) was titrated with 10 mM aqueous solution of N-bromosuccinimide. Initially the absorbance decreases and the titration was stopped when absorbance increased with the addition of N-bromosuccinimide. The albumin solution was dialyzed against 50 mM Tris-HCl buffer (pH 7.4).

Preparation of cyanogen bromide albumin fragments: The high molecular aggregates of commercial human serum albumin were removed by size exclusion chromatography on a G-100 Sephadex column (120 x 2.5 cm)

pre-equilibrated with 50 mM Tris- HCl buffer (pH 7.4). Fractions of 2.5 ml were collected at a flow rate of 10 ml/ h. Protein concentration of the HSA fractions was determined using a value of 5.30 for $E_{1\%}$ at 278 nm (Clark *et. al.,* 1962). The CNBr fragments were prepared according to the procedure of Meloun *et. al.* (1977). A solution of 100mg of albumin (monomeric form) in 2ml of water was treated with 600μg of iodoacetamide (2-3 fold molar excess in terms of the SH-group). The solution was adjusted to pH 7.5 and was maintained at 25°C for 1hr. The albumin was freed from its low-molecular components by gel filtration on a (1 x 30cm) column of Sephadex G-25 equilibrated in water. The monoS- (aminoethyl) cysteinyl derivative of human serum albumin was lyophilized. A solution of 94mg of modified albumin in 1ml of water was treated 100mg of cyanogen bromide in 4ml of formic acid. The reaction mixture was incubated for 48hr at 5°C. The reaction mixture was freed of excess formic acid and CNBr by gel filtration on a (1 x 30cm) column of Sephadex G-25 equilibrated in formate buffer (2ml of 26% NH_4OH, 8ml of 99% formic acid and 990ml of water, pH 2.9). The protein digest was concentrated on an Amicon ultrafiltration unit with 10 Kda cutoff membrane. The CNBr digest was fractionated on a (1 x 120cm) column of Sephadex G-100 column equilibrated in formate buffer. Fractions designated as N+M and C fragments were obtained. Fraction N+M was concentrated and diluted with water and loaded on to a SP-Sephadex C-25 equilibrated in 50mM acetate buffer pH 5.0 containing 8M urea. The ion-exchange column was eluted by a linear concentration gradient of NaCl (0-0.3M) in the same buffer. Fragments N and M were obtained. All three fragments were

subjected to Sephadex G-25 gel filtration equilibrated with 50mM Tris-HCl buffer pH 7.4. The purity of albumin and isolated N, M and C fragments was ascertained by non-reducing SDS–PAGE (Laemmli, 1970). The concentration of domains is determined by their molar absorbtion coefficient value (ε) at 280 nm based on their aromatic amino acid content (Gill and von Hippel, 1989). The ε of N fragment is 3855M^{-1} cm^{-1}, ε of M fragment is 15940 M^{-1} cm^{-1} and ε of C fragment is 16900 M^{-1} cm^{-1}.

Equilibrium dialysis: Aliquots (1 ml) of protein solutions human serum albumin (63.64 μM) and bovine serum albumin (75 μM) in 50 mM Tris- HCl, pH 7.4 containing 20 mM KCl was dialyzed for a period of 24 h at 27°C against 3.0 ml buffer solution containing varying concentrations of genistein (10-100 μM). Corresponding "Blanks" containing only buffer solutions were run. At the end of equilibration, the concentration of genistein in the outside solutions was estimated by measuring the absorbance of solution and using a molar absorption coefficient of 37.3 x 10^3 M^{-1} cm^{-1} for genistein. Inside solutions could not be used since protein interfered in the estimation. From the observed difference in genistein concentration between "blank" and experimental, the number of genistein molecules bound per mole of protein was calculated.

Absorbance measurements: All the absorbance measurements were made at 27°C using a 1601 Shimadzu double beam UV spectrophotometer in a 10 mm path length cell.

Fluorescence measurements: Fluorescence measurements were carried out using a Shimadzu RF 5000 spectrofluorimeter attached with a thermostated circulating water bath. The spectrofluorimeter was calibrated for wavelength accuracy and S/N ratio as suggested by the manufacturer. The solution in the cuvette was stirred using a Hellma cuv-o-stir®. Excitation and emission slit widths were set at 5 nm and 10 nm, respectively. Measurements were made using a 10 mm path length cuvette with the sample in 0.05 M Tris-HCl buffer (pH 7.4).

The efficiency of energy transfer as well as distances between isoflavones and tryptophan in serum albumin in the binding pocket was measured according to the Förster non-radiation energy transfer theory (Förster, 1967). The non-radiation energy transfer would occur between the donor and the acceptor of the fluorescence energy because of the proper overlap of the emission spectrum of the donor with the absorption spectrum of the acceptor. The energy transfer efficiency E is related to the distance (r_0) between acceptor and donor, and also to the critical energy transfer distance (R_0), by the equation,

$$E= R_0^6/ (R_0^6 + r_0^6),$$

where R_0 is a characteristic distance, called the Förster distance or critical distance, at which the efficiency of transfer is 50%, computed from the relation,

$$R_0^6 = 8.8 \times 10^{-25} \kappa^2 N^{-4} \Phi J,$$

where κ^2 is the spatial orientation factor describing the relative orientation in space of the transition dipoles of the donor and acceptor, N is the refractive

index of the medium, Φ is the fluorescence quantum yield of the donor in the absence of the acceptor and J is the overlap integral between the donor fluorescence emission spectrum and the acceptor absorption spectrum. J is given by,

$$J = \sum F(\lambda)\, \varepsilon(\lambda)\, \lambda^4 \Delta\lambda / \sum F(\lambda) \Delta\lambda,$$

where $F(\lambda)$ is the fluorescence intensity of the donor at wavelength λ, $\varepsilon(\lambda)$ is the molar absorption coefficient of the acceptor at wavelength λ and its unit is $cm^{-1}\ mol^{-1}$. The energy transfer efficiency E is,

$$E = 1 - F/F_0,$$

where F_0 = Fluorescence intensity of HSA/BSA alone and F = Fluorescence intensity of HSA/BSA with ligand.

All the samples were centrifuged at 26,000 x g for 30 min to remove any aggregates. Fluorescence quenching of HSA and BSA by genistein and daidzein were followed at 27 ± 0.2°C. Stock solutions (1.25 mM) of genistein or daidzein were added in increments of 2 μl in 80% methanol to 1μM HSA and 1μM BSA in 0.05 M Tris-HCl (pH 7.4). The excitation and emission wavelengths were set at 295 nm and 333 nm, respectively. Slit widths for excitation and emission were 5 and 10 nm, respectively. Blank titrations, with 80% methanol, were carried out to correct the quenching. Percentage quenching of the fluorescence intensity of the protein by genistein was corrected empirically for internal absorption and filtration by subtracting the percentage quenching by the same concentration of genistein (used in HSA and BSA titration) in a solution of N-acetyl tryptophanamide, equivalent in absorption to HSA and BSA at 280 nm. The fluorescence intensity of

HSA/BSA in the absence of genistein and daidzein did not change during the course of the experiment. Fluorescence quenching of the N, M and C fragments of HSA by genistein were followed at 27 ± 0.2°C. Stock solutions (1.25 mM) of genistein were added in increments of 2 μl in 80% methanol to 3μM of N, M and C domain in 0.05 M Tris-HCl (pH 7.4). The excitation and emission wavelengths were set at 295 nm and 333 nm, respectively for M domain. Slit widths for excitation and emission were 5 and 10 nm, respectively. Percentage quenching of the fluorescence intensity of the protein by genistein was corrected empirically for internal absorption and filtration by subtracting the percentage quenching by the same concentration of genistein (used in domain M titration) in a solution of N-acetyl tryptophanamide, equivalent in absorption to of domain M at 280 nm. The fluorescence intensity of domain M in the absence of genistein did not change during the course of the experiment. Fluorescence quenching of the N and C domain were followed by setting the exciting and emission wavelength at 280 and 307 nm. The correction due to inner filter effect was given by using N-acetyl tyrosine ester.

Quenching, as a function of genistein concentration, has been analyzed in terms of binding of the isoflavones by HSA, BSA and domains of human serum albumin using established procedures (Rao and Cann, 1981). Thus, if it is assumed that the binding of each isoflavone molecule causes the same degree of quenching and that binding is statistical, the intrinsic genistein – binding constant, K, is given by the equation,

$$K = \beta/ (1-\beta). 1/ C_f,$$

where $\beta = Q / Q_{max}$ and $C_f = C_T - n\beta T$, in which Q is the corrected percentage quenching; Q_{max}, the maximal quenching; C_f, the molar equilibrium concentration of unbound genistein; C_T, the molar constituent concentration of genistein; T, the molar constituent concentration of serum albumin; and n is the binding stoichiometry (Lee *et. al.,* 1975). The value of K is given by the slope of a plot of $\beta/ 1-\beta$ against C_f. Q_{max} has been determined by extrapolation of a double reciprocal plot of 1/ Q vs. 1/C, to 1/C = 0. In both cases, the data are fitted to a straight line by the method of least squares. The value of n for genistein has been estimated by Job's method (Jaffé and Orchin, 1962). Fluorescence quenching of HSA/BSA by genistin and daidzin, the glycosylated forms have been followed at 27 ± 0.2°C on similar lines.

Effect of temperature: The effect of temperature in the range 17 - 47°C on the binding constant of genistein with bovine serum albumin, human serum albumin, and M-domain of human serum albumin was determined by fluorescence quenching studies using a Shimadzu RF 5000 spectrofluorimeter and appropriate blanks. The concentrations of BSA, HSA, M-domain of HSA and the quencher (genistein) were the same as given above.

Effect of ionic strength: The effect of ionic strength on the binding constant of genistein with HSA/BSA was determined by increasing concentrations of potassium chloride (0–200 mM) in buffer by fluorescence titration at 27 ± 0.2°C as given above. Protein (HSA/BSA) and genistein were

used in the same concentrations as in the quenching studies and using appropriate blanks.

Stokes radius measurements. For the determination of Stokes radius, gel filtration measurements were carried out using an TSK Super SW 2000 (300 x 4.6 mm), with the manufacturer's exclusion limit of 5 – 150 x 10^3 for proteins, on a Waters HPLC system, equipped with a 1525 binary pump and Waters 2996-photodiode array detector. The column was equilibrated with 50 mM Tris-HCl (pH 7.4), containing the desired salt concentrations, at 27°C. HSA/BSA solution (20 μl of 4-5 μM) equilibrated in the desired salt concentration (0 – 200 mM KCl in 50 mM Tris-HCl (pH 7.4) was injected into the column and eluted in the same buffer at 0.2 ml/min flow rate. The absorbance was detected at 280 nm. Standard proteins from a molecular weight marker kit for gel filtration (Sigma) including alcohol dehydrogenase (150,000), bovine serum albumin (66,000), carbonic anhydrase (29,000), cytochrome c (12,400) with known Stokes radius were used for calibrating the column. Blue dextran, at a 1 mg·ml^{-1} concentration, was used for determining the void volume.

Effect of palmitic acid on binding of genistein: Human serum albumin and bovine serum albumin was saturated with genistein in the molar ratio of 1: 10. To this solution, 1 μM palmitic acid in ethanol was added in increments of 2.5 μl. The increase in protein fluorescence was recorded by excitation at 295 nm and emission at 333 nm. Blank titrations were carried out by

addition of palmitic acid to genistein saturated N-Acetyltryptophanamide in 50 mM Tris–HCl (pH 7.4).

Effect of ANS on binding of genistein: HSA (1μM) was complexed with ANS (3 μM), BSA (1μM) complexed with ANS (6μM) in 50 mM Tris-HCl (pH 7.4) and 5 μl increments of 1μM methanolic (80%) solution of genistein added to this solution. Concentration of ANS was determined by its molar absorption coefficient of 4.95 x 10^3 M^{-1} cm^{-1}, at 350 nm (Weber and Young, 1964). The decrease in fluorescence of ANS bound HSA/BSA was recorded. Blank titrations with 80% methanol were carried out and corrected for dilution. The excitation and emission wavelengths for ANS bound HSA/BSA were set at 375 and 467 nm respectively. Dissociation constant of the competing ligand was determined (Aceto *et. al.,* 1995).

Fluorescence anisotropy measurements: Fluorescence anisotropy measurements were recorded at 27 ± 0.2°C on a Shimadzu RF 5000 spectrofluorimeter attached with UV polarizers (POLACOAT Co., USA). The temperature was maintained using a circulating water bath. The data were obtained by setting the excitation and emission wavelengths at 340 and 465 nm, respectively. The excitation and emission slit widths were 5 and 10 nm, respectively. Daidzein concentration was 2.5 μM and 10 μl of 0.6 mM HSA/BSA was added in increments.

Anisotropy of the daidzein bound HSA/BSA was measured in the presence of warfarin and triiodobenzoic acid (TIB) (bind to domain IIA) and diazepam (marker to domain IIIA, primary fatty acid binding site). Daidzein and

HSA/BSA, 10 μM each, were complexed and titrated with 2 μl increments of the marker ligands (warfarin- 17 mM, triiodobenzoic acid –19 mM and diazepam – 20 mM). All the stock solutions of marker ligands were prepared in DMSO. The excitation and emission wavelengths were the same as for daidzein alone.

Fluorescence anisotropy measurements with warfarin: Warfarin (5 μM) and HSA/BSA (10 μM) complex was titrated with 2μl increments of Genistein (20mM) dissolved in DMSO. The data were obtained by setting the excitation and emission wavelengths at 310 and 385nm, respectively. The excitation and emission slit widths were 5 and 10 nm, respectively.

For anisotropy measurements, intensities of horizontal and vertical components of the emitted light ($I_{||}$ and $I_{\perp)}$ were corrected for the contribution of scattered light. G, the grating factor that corrects for wavelength dependent distortions of the polarizing system was obtained using

$$G = F_{hv} / F_{hh} \quad \text{and}$$

$$I_{||} / I_{\perp} = (F_{vv})/ (F_{vh}) (F_{hh}/ F_{hv}),$$

Where, $F_{vv,}$ F_{vh}, F_{hv} and F_{hh} are the fluorescence intensity components, in which the subscripts refer to the horizontal (h) or vertical (v) positions of the excitation and emission polarizers separately. Anisotropy was calculated using the equation

$$A = (I_{||} / I_{\perp}) - 1/ (I_{||} / I_{\perp}) + 2$$

Effect of daidzein on binding of genistein: Daidzein (2.75 μM) was titrated against increasing concentrations of HSA/BSA to a final concentration of 14.75 μM in 50 mM Tris–HCl buffer (pH 7.4). The excitation wavelength was 340nm and emission range was 400-550 nm. Excitation slit width was 5 nm and emission slit width was 10 nm. To the above daidzein-HSA complex, 5 μl of stock genistein in 80% methanol (1.4 mM) was added in aliquots and the spectra recorded at 27°C. The final concentration of genistein was 27 μM. Blank titrations were carried out for the daidzein-HSA/BSA complex with 80% methanol alone.

Circular dichroism measurements: CD spectra in the near UV region of 250 – 350 nm were recorded on a Jasco J – 810 spectropolarimeter and calibrated with d-10-camphor sulfonic acid. Dry nitrogen gas was purged before and during the course of measurements. All measurements were obtained using a 10 mm path length quartz cell. An average of 3 scans at a speed of 10-nm/ min with a bandwidth of 1 nm and a response time of 1s were recorded. The HSA and BSA concentration was 15 μM; warfarin concentration was in the range of 0–50 μM. The concentration of warfarin was estimated by its molar absorption coefficient at 310 nm (13610 $M^{-1}cm^{-1}$) (Twine *et. al.,* 2003). Genistein concentration was varied between 0 – 50 μM.

CD spectra in the far UV region of 200 – 250 nm were recorded on a Jasco J – 810 spectropolarimeter. All measurements were obtained using a 10 mm path length quartz cell. An average of 3 scans at a speed of 10-nm/ min with a bandwidth of 1 nm and a response time of 1s were recorded. The concentration of albumin was 2 μM and genistein concentration was varied

(0-20 μM). The concentration of HSA, N, M and C domains were 3.2, 3.7, 2.63 and 3.7 μM. All measurements were made in 0.05 M Tris-HCl (pH 7.4). The secondary structure was analyzed by using the software of Yang *et. al.* (1986).

Molecular visualization: In order to generate a ternary complex of HSA-warfarin – genistein we used the crystal structure of the binary complex HSA-warfarin that is available at 2.5 Å resolution. We used Sybyl software (Tripos Inc., St. Louis) for this purpose. The DOCK option in Sybyl was employed in order to accommodate genistein in the binding site of HSA. The presence of wafarin in the crystal structure provided a concrete indication of the binding site in HSA. The binding site was located within one of the domains, near the domain-domain interface in the structure. The residues in and around this site have been provided as indicators of approximate binding location for genistein in the DOCK option of Sybyl. The positioning of genistein was further optimized in Sybyl and analyzed using the Setor software (Evans, 1993).

Lipoxygenase

Purification of Soy Lipoxygenase: Soybean LOX-1 was isolated according to the method of Axelrod *et al.* (1981) with some modifications (Sudharshan and Appu Rao, 1997).

Extraction

All steps were performed at 4° C. The defatted soy meal (60g) was extracted with 600ml of ice-cold 0.2M sodium acetate buffer (pH 4.5) for 1 hour. The suspension was centrifuged at 6000 rpm for 30 min. The pH of the supernatant solution was adjusted to 6.8 with 10M NaoH and centrifuged for 30 min at 6000 rpm.

Ammonium sulphate precipitation

To the above-clarified supernatant solution, ammonium sulphate was added (with constant stirring) to 30% saturation. The resultant precipate was removed after centrifugation at 6000 rpm. To the clarified supernatant ammonium sulphate was added to raise the saturation to 60%. The protein fraction that precipitates at this stage was dissolved in 20mM sodium phosphate buffer (pH 6.8). This solution was dialyzed against the same buffer with three changes of 3 liters.

Anion exchange chromatography

The dialyzed protein was centrifuged at 6000 rpm and the supernatant was chromatographed on DEAE-Sephadex A-50 column (25 × 4 cm), which was pre-equilibrated with 20mM sodium phosphate buffer (pH 6.8). The column was developed with a linear gradient formed from 20mM to 170mM of

phosphate buffer (pH 6.8) and the enzyme was eluted with a linear gradient of 170mM to 240mM phosphate buffer (pH 6.8). The fraction containing maximum lipoxygenase activity was pooled and the solution was made to 70% saturation by slow addition of ammonium sulphate. After 1 hour, the precipitate was centrifuged, dissolved in 20mM phosphate buffer pH 6.8 and was dialyzed against three changes of the same buffer.

Molecular sieve chromatography

The dialyzed protein solution was loaded on a sephadex G100 column (90 × 2.5 cm), which was pre-equilibrated with 20mM phosphate buffer pH 6.8. The enzyme was eluted with the same buffer. The protein fractions, which showed maximum activity were pooled, concentrated using an Amicon ultrafiltration cell with a 30kD cut-off membrane. The specific activity was 180-200 μmoles/min/mg of protein. The concentration of LOX-1 was calculated using the value $E^{1cm}_{1\%}$ at 280nm = 14.0 (Axelrod *et. al.,* 1981).

Isolation of 5-lipoxygenase enzyme from polymorpho nuclear leukocytes (PMNLs) of human blood:

Human peripheral venous blood from healthy individuals, who had not received any medication, was collected in tubes containing sodium citrate as anticoagulant. PMNLs were isolated from blood by Ficoll-Histopaque density gradient and hypotonic lysis of erythrocytes (Boyum, 1976). PMNL cells were resuspended in phosphate buffered saline and sonicated for 20-30 s at 20 kHz to release the cytosolic 5-lipoxygenase into the solution. The solution was centrifuged at 10,000 g for 30 min at 4°C and the supernatant was

directly used as a source of enzyme. Protein concentration was estimated by the method of Lowry (Lowry *et. al.,* 1951) using BSA as standard.

Enzyme assays:

Assay of soy LOX-1:

LOX-1 activity was determined by following the increase in absorbance at 234 nm due to the formation of hydroperoxide (product, ε = 25000 $M^{-1}cm^{-1}$). The substrate was prepared according the method of Axelrod *et al.* (1981). The reaction was followed at pH 9.0 using 0.2 M borate buffer. The amount of enzyme required to form 1 μM of hydroperoxide per min under the conditions of the assay, was taken to be one unit of activity.

5-Lipoxygenase-enzyme assay:

5-LOX was assayed according to the method of Aharony and Stein (1986) by following the increase in absorbance at 236 nm due to the formation of 5-HETE (ε = 28000 $M^{-1}cm^{-1}$) at 27°C for 3 min. The substrate, arachidonic acid (AA), was prepared according the method of Axelrod *et al.* (1981). The standard reaction mixture contained 100 mM phosphate buffer (pH 7.4) 50 μM of DTT, 200 μM of ATP, 300 μM $CaCl_2$, 150 μM of arachidonic acid and 5 μg of protein. One unit of activity is defined as the amount of enzyme required to form 1 μM of product per min under the conditions of assay.

Inhibition of Lipoxygenase Activity:

For inhibition experiments, lipoxygenase was incubated with inhibitor for 5 min (in case of soy LOX-1) and 2 min (for 5-LOX) in a 10 mm pathlength cuvette. The reaction was started by the addition of substrate. Since the

inhibitor was in DMSO, control was run in presence of DMSO. For the determination of IC_{50}, the inhibitor was varied at constant substrate concentration of 100 μM linoleic acid and 150 μM arachidonic acid. The % inhibition of LOX activity by isoflavones was calculated from the ΔO.D. values at 234 nm at the end of 3 min. K_i was determined by varying the inhibitor and substrate both by Dixon and L-B plot. The data obtained were fitted to a straight line by the method of least squares. For checking the reversibility, the enzyme was incubated with the inhibitor and the mixture was dialyzed at 4°C to remove inhibitor. The residual activity was assayed. All measurements are an average of at least 3 sets of measurements.

Stopped-flow inhibition kinetics:

Sodium borate buffer (0.2M, pH 9.0) was used in all stopped flow measurements. The fast reaction kinetics of interaction of lipoxygenase with genistein was followed at 234 nm using a stopped-flow spectrophotometer model SX-18MV version 4.4 (Applied Photophysics, Leatherhead U.K.) at 25 ± 1°C with a pathlength of 2 mm and pressure of 125 psi (8 bar) compressed nitrogen. The inhibitor and protein were mixed in equal volumes. The solutions of enzyme, substrate and genistein were prepared immediately before the kinetic experiments. The inhibitor was allowed to equilibrate with the enzyme (active Fe^{3+}) for 15 min and was used within 30 min of preparation. The Fe^{3+} form of the enzyme was freshly prepared by the addition of 2 fold molar excess of linoleic acid to the resting enzyme at pH 9.0. The Fe^{3+} enzyme was separated from the reaction products by repeated

centrifugation through Centricon®-30 device. The Fe^{3+} form of the enzyme was stored at 0°C during the entire course of the experiment. The final syringe concentrations for the active Fe^{3+} form were 2.4 μM lipoxygenase and 20 μM linoleate giving 1.2 μM lipoxygenase and 10μM linoleate after stopped–flow mixing. All the experiments were average of six determinations. The data scan was recorded on an Acorn Risc computer interfaced with the instrument. The dead time of the instrument is $<$ 1 ms.

Spectroscopic studies:

Absorbance measurements:

The active (Fe^{3+}, yellow) state or resting state of iron (Fe^{2+}) in the catalytic center of LOX could be followed by spectral changes in the region 300 – 600 nm. Absorbance measurements were made at 27°C, using a Shimadzu double beam UV spectrophotometer (model 1601), equipped with a 10 mm path length cell. Lipoxygenase (160 μM) in 0.1 M borate buffer (pH 9.0) was mixed with of linoleic acid (160 μM) to convert the resting enzyme (Fe^{2+}) completely to yellow active lipoxygenase (Fe^{3+}). Aliquots of isoflavones (160 and 320 μM), solubilized in DMSO, were added (both to the sample cuvette and the reference cuvette) and the spectra recorded. The reference cuvette did not have the enzyme (LOX-1). Results are average of 3 experiments.

Circular dichroism measurements:

Circular Dichroism measurements were made with a Jasco J – 810 spectropolarimeter and calibrated with ammonium salt of d-10-camphor

sulfonic acid. Dry nitrogen gas was purged before and during the course of measurements. The state of iron (Fe^{2+} or Fe^{3+}) in soy LOX-1 was followed in the visible region of 350 – 550 nm using a 10 mm path length quartz cell at 27°C. An average of 3 scans at a speed of 10-nm/ min with a bandwidth of 1 nm and a response time of 1 s was recorded. Soy LOX-1 concentration used was 150 μM in 0.1 M borate buffer (pH 9.0) with an equal concentration of linoleic acid (150 μM) to convert resting (Fe^{2+}) to yellow lipoxygenase (Fe^{3+}) state. Genistein (300 μM) or daidzein (300 μM), in DMSO, were added to the above and the change in the spectra recorded. Blanks containing buffer and isoflavones were run to correct baselines. The mean residue ellipticity $[\theta]_{MRW}$ was calculated using a value of 115 for mean residue weight.

EPR measurements:

EPR measurements were performed on a Bruker EMX X-band spectrometer with a continuous helium cryostat (Oxford Instruments, UK) at 20 ± 0.5 K. Spectra were recorded at 9.39 GHz, 100 KHz modulation frequency, 10.0G modulation amplitude and 66 mW microwave power. Resting lipoxygenase (200 μM) in 0.1 M borate buffer (pH 9.0) containing 3% methanol was treated with linoleic acid (200 μM) to convert to its active form (iron in Fe^{3+} state). Small aliquots (2 and 4 μL) of genistein (400 and 800 μM) were added to the active form of lipoxygenase and incubated at 27°C for 5 min before recording the spectra. To record the reversibility of effects of isoflavones on lipoxygenase, an excess of linoleic acid (800 μM) was added to sample containing 400 μM genistein. Volumes of samples were 300 μL. EPR spectra of genistein was recorded at 100 ± 0.5 K, 9.389 GHz frequency, 100 KHz

modulation frequency, 0.5G modulation amplitude, 2mW microwave power and sweep width of 40G. Genistein (1mM) was dissolved in 0.1 M borate buffer (pH 9.0) containing 120mM $MgCl_2$.

HPLC Measurements:

To study the nature of interaction of genistein with LOX, enzyme assay was carried out in the presence of genistein (100 μM). Linoleic acid (100 μM) in 0.2 M borate buffer (pH 9.0) was used as the substrate. At the end of 5 min, ether was added to the reaction mixture. The reaction mixture was vortexed to extract genistein and flushed with nitrogen (to evaporate ether). The residue was dissolved in a small amount of methanol, filtered and injected into a Waters® HPLC system fitted with a C_{18} (300 x 4.6 mm, 5 μM) column (Wang and Murphy, 1994). A gradient elution using acetonitrile - water (15 – 35%) was run over a period of 50 min at a flow rate: 1 mL /min. The genistein peak was detected at 262 nm. LOX with genistein (100 μM) was also run as control.

Mass Spectrometry:

The genistein peak was collected after HPLC and passed into the electrospray ionization source in the negative ion mode of a Waters Corporation Mass spectrometer (Model Q-TOF Ultima). The voltage of the electrospray capillary was –3000 V, source temperature 120°C and resolution temperature 300°C. Negative ion spectra was recorded over an m/z range of 20-400. Data was analyzed using Mass Lynx version 4.4 software provided by the manufacturer.

Soy glycinin and conglycinin

Purification of glycinin and conglycinin:

Glycinin (11S) was purified according to method of Thanh *et. al.,* (1975). 2 gm of defatted soy flour was extracted with 40ml of 30mM Tris-HCl buffer (pH 8.0) containing 10mM mercaptoethanol. The extract was centrifuged at 10,000 rpm for 30 minutes at room temperature. The supernatant's pH was raised to 6.4 with 2N HCl. The extract was centrifuged and the precipitate was washed with 30mM Tris-HCl buffer (pH 6.4) and dissolved 30mM Tris-HCl buffer (pH 8.0). The supernatant obtained was used to isolate conglycinin (7S). The dissolved protein solution was kept at 3-5 °C overnight. A trace of precipitate was removed by centrifugation. The crude glycinin obtained was fractionated on sepharose CL-6B gel filtration column equilibriated with 30mM Tris-HCl buffer (pH 8.0) containing 0.4M NaCl and 10mM mercaptoethanol. The pure glycinin fraction was pooled and concentrated. It was immediately used for interaction studies. The purity was ascertained by SDS-PAGE.

Conglycinin (7S) was purified according to the method of Koshiyama, (1972). The pH of the supernatant obtained during the purification of glycinin was raised to 4.50 with 2N HCl. The extract was centrifuged at 6000 rpm at room temperature. The precipitate obtained was suspended in 50ml of 0.01N HCl containing 0.6M NaCl and stirred for 30 minutes. The suspension was centrifuged at 15,000 rpm and the supernatant rich crude conglycinin was dialyzed against 30mM Tris-HCl buffer (pH 8.0) containing 10mM mercaptoethanol. The crude conglycinin contained 2S as impurity. The

protein solution was fractionated on sepharose CL-6B gel filtration column equilibrated with 30mM Tris-HCl buffer (pH 8.0) containing 0.4M NaCl and 10mM mercaptoethanol. The pure conglycinin fraction was pooled and concentrated. It was immediately used for interaction studies. The purity was ascertained by SDS-PAGE.

Preparation of Polyphenol free fraction glycinin and conglycinin:

The purified proteins were freed of intrinsically bound polyphenols by different methods.

- **Treatment with activated charcoal:** The protein solutions were treated with 1% activated charcoal and the resulting solution was clarified by centrifugation.
- **Ammonium sulfate precipitation:** The purified protein solutions were subjected to ammonium sulphate precipitation (70%). The precipitate was dissolved in 30mM Tris-HCl buffer (pH 8.0) containing 0.4M NaCl and 10mM mercaptoethanol and dialyzed against the same buffer to remove ammonium sulphate.
- **Fractionation on Sephadex LH-20 Column:** The purified protein solutions were fractionated on Sephadex LH-20 Column equilibrated with 30mM Tris-HCl buffer (pH 8.0). The protein fraction was pooled and used for interaction studies.
- **Treatment with Polyvinylpyrrolidine:** The protein solutions were treated with 1% Polyvinylpyrrolidine and the mixture was incubated at room temperature. The mixture was fractionated on a sepharose CL-6B column equilibrated with 30 mM Tris-HCl buffer (pH 8.0).

Interaction of glycinin and conglycinin with Isoflavones:

Fluorescence quenching of glycinin and conglycinin by genistein, daidzein, genistin and daidzin were followed at 27 ± 0.2°C. All the samples were centrifuged at 26,000-x g for 30 min to remove any aggregates. Stock solutions (1.25 mM) of genistein, daidzein, genistin and daidzin were added in increments of 2 μl in 80% methanol to 0.5 μM glycinin and conglycinin of in 50 mM Tris-HCl (pH 7.4). The excitation and emission wavelengths were set at 295 nm and 333 nm for glycinin, 295 nm and 344 nm for conglycinin, respectively. Slit widths for excitation and emission were 5 and 10 nm, respectively. Blank titrations, with 80% methanol, were carried out to correct the quenching. Percentage quenching of the fluorescence intensity of the protein by genistein was corrected empirically for internal absorption and filtration by subtracting the percentage quenching by the same concentration of genistein (used in glycinin and conglycinin titration) in a solution of N-acetyl tryptophanamide, equivalent in absorption to glycinin and conglycinin at 280 nm.

Effect of glycinin and conglycinin on daidzein fluorescence:

Daidzein (2.75 μM) was titrated against increasing concentrations of glycinin and conglycinin to a final concentration of 30 μM in 50 mM Tris – HCl buffer (pH 7.4). The excitation wavelength was 340nm and emission range was 400-550 nm. Excitation slit width was 5 nm and emission slit width was 10 nm.

Equilibrium dialysis: Aliquots (1 ml) of protein solutions glycinin (10 mg/ml) and conglycinin (10 mg/ml) in 50 mM Tris- HCl (pH 7.4) containing

20 mM KCl was dialyzed for a period of 24 h at 27°C against 3.0 ml buffer solution containing varying concentrations of genistein (10-100 μM). Corresponding "Blanks" containing only buffer solutions were run. At the end of equilibration, the concentration of genistein in the outside solutions was estimated by measuring the absorbance of solution and using a molar absorption coefficient of 37.3 x 10^3 M^{-1} cm^{-1} for genistein. Inside solutions could not be used since protein interfered in the estimation. From the observed difference in genistein concentration between "blank" and experimental, the number of genistein molecules bound per mole of protein was calculated.

Extraction and Quantification of bound isoflavones from glycinin and conglycinin: Purified glycinin (650 mg) and conglycinin (400 mg) was extracted with 20 ml of 80% methanol for 3 hrs at 60 °C. The extract was centrifuged at 6000 rpm at room temperature. The methanolic extract was concentrated under vaccum to dryness. To this a known volume of 80% methanol was added to extract isoflavones. The methanolic solution was centrifuged and passed through a syringe filter. A suitable aliquot was injected into RP-HPLC C_{18} column and quantified as mentioned in the previous procedure using standard isoflavones.

RESULTS

AND

DISCUSSION

RESULTS AND DISCUSSION

Isolation and purification of isoflavones: The ethyl acetate extract on a silica gel column was resolved into three fractions F_1, F_5 and F_6 (Fig.13). F_1 fraction which was eluted with 50% water saturated ethyl acetate contained genistein and daidzein. F_5 and F_6 fractions which were eluted with 50% water saturated ethyl acetate containing 2% ethanol contained genistin and daidzin respectively. Each fraction obtained was rechromatographed on a silica gel using similar conditions (Fig. 14 & Fig. 15). The fractions obtained were further purified on a sephadex LH-20 column. F_1 fraction was resolved into daidzein and genistein (Fig. 16). F_5 and F_6 fractions yielded pure genistin and lated isoflavones, genistin, daidzin, genistein, and daidzein purified from defatted soy flour, had a purity of >95% (confirmed by HPLC) (Fig. 19, 20, 21 & 22).

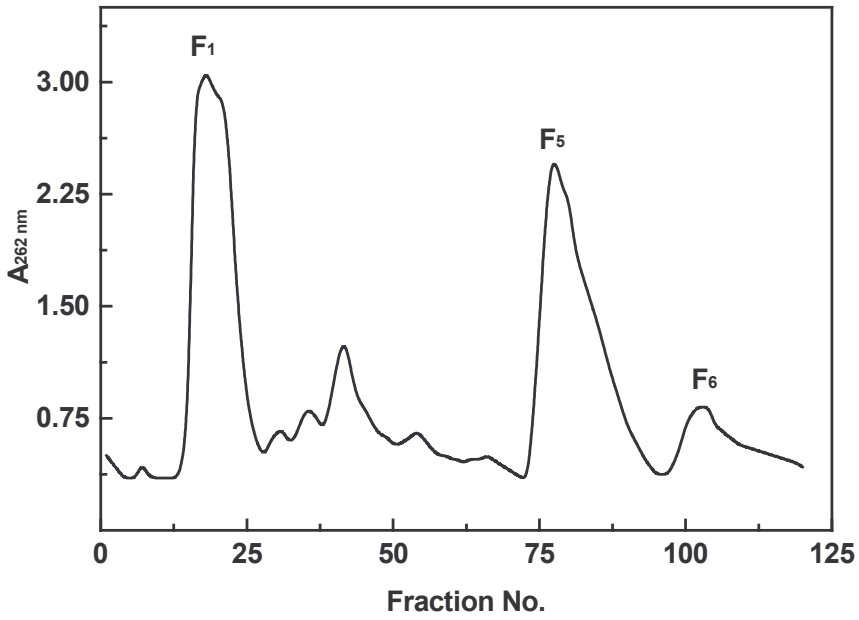

Figure 13. Elution profile of ethyl acetate extract on silica gel column: F_1 fraction is a mixture of genistein and daidzein, F_5 and F_6 fraction are rich in genistin and daidzin.10ml fractions were collected at a flow rate of 1ml/min

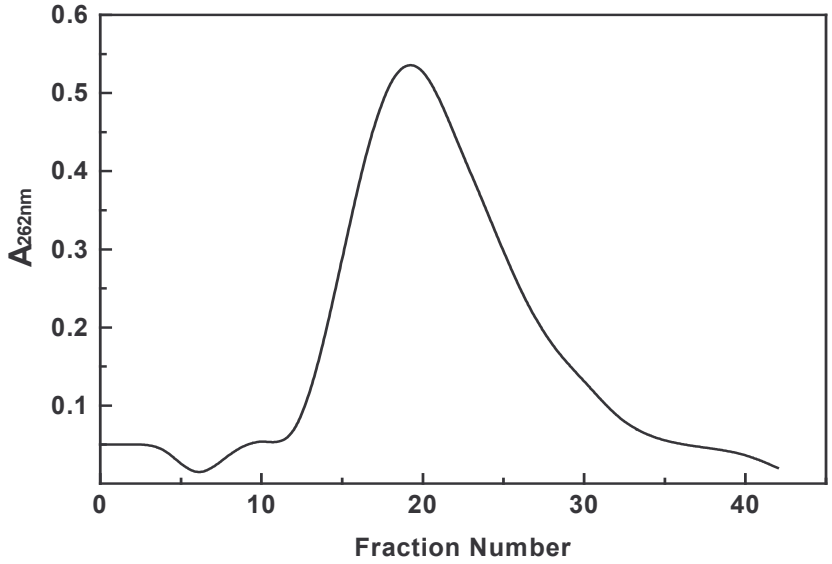

Figure 14. Rechromatography of F_1 fraction: The F_1 fraction was rechromatographed on a silica gel column. 10ml fractions were collected at a flow rate of 1ml/min.

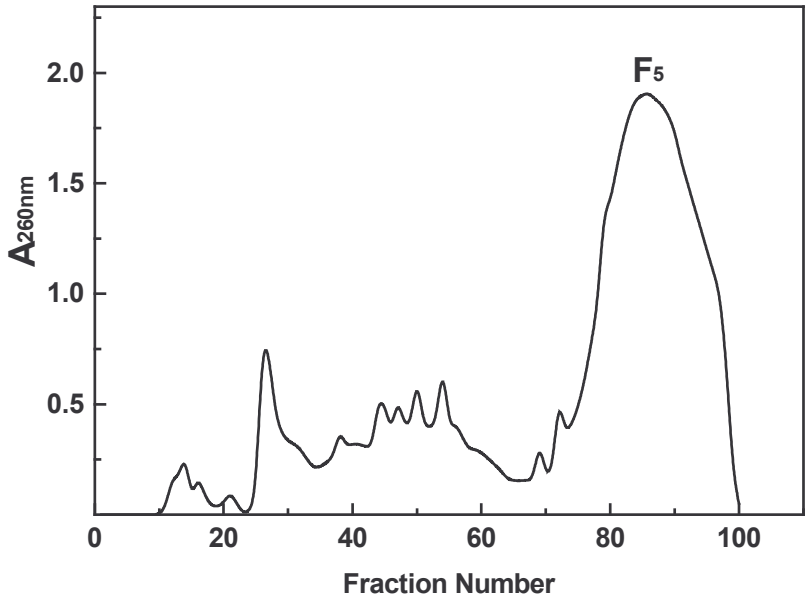

Figure 15. Rechromatography of F_5 fraction: The F_5 fraction was rechromatographed on a silica gel column. 10ml fractions were collected at a flow rate of 1ml/min.

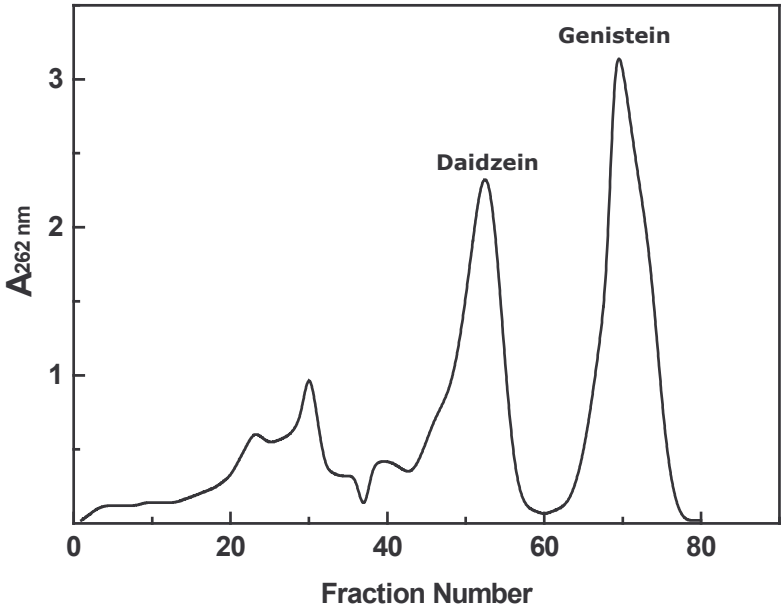

Figure 16. Adsorption chromatography of F_1 fraction: The F_1 fraction was chromatographed on a sephadex LH-20 column. 5ml fractions were collected at a flow rate of 30ml/hr.

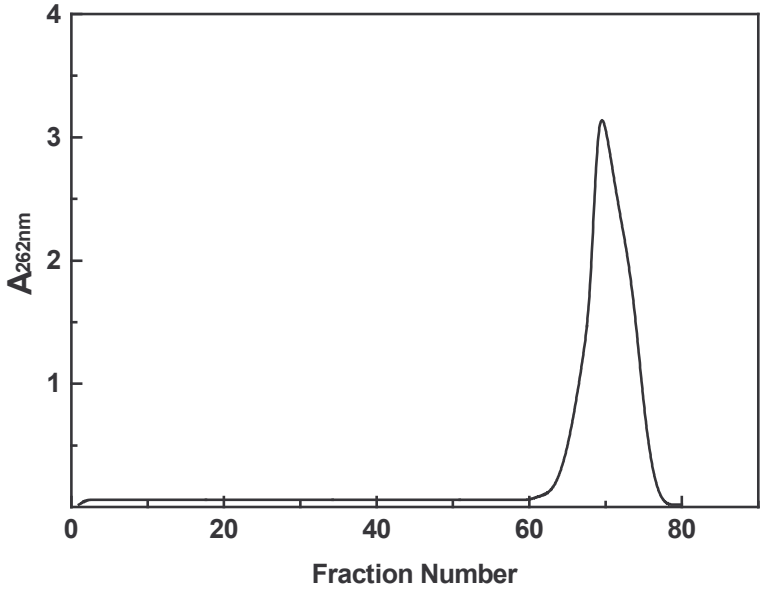

Figure 17. Adsorption chromatography of F_5 fraction: The F_5 fraction was chromatographed on a sephadex LH-20 column. 5ml fractions were collected at a flow rate of 30ml/hr.

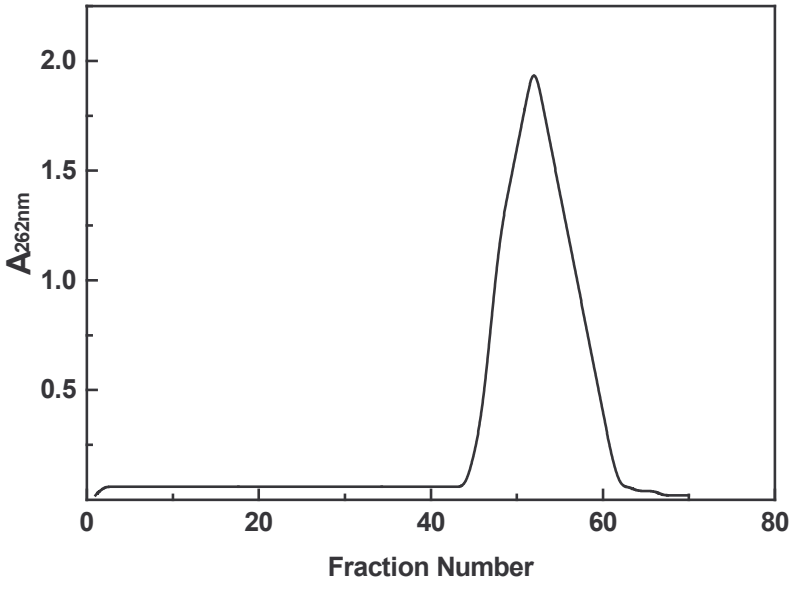

Figure 18. Adsorption chromatography of F_6 fraction: The F_6 fraction was chromatographed on a sephadex LH-20 column. 5ml fractions were collected at a flow rate of 30ml/hr.

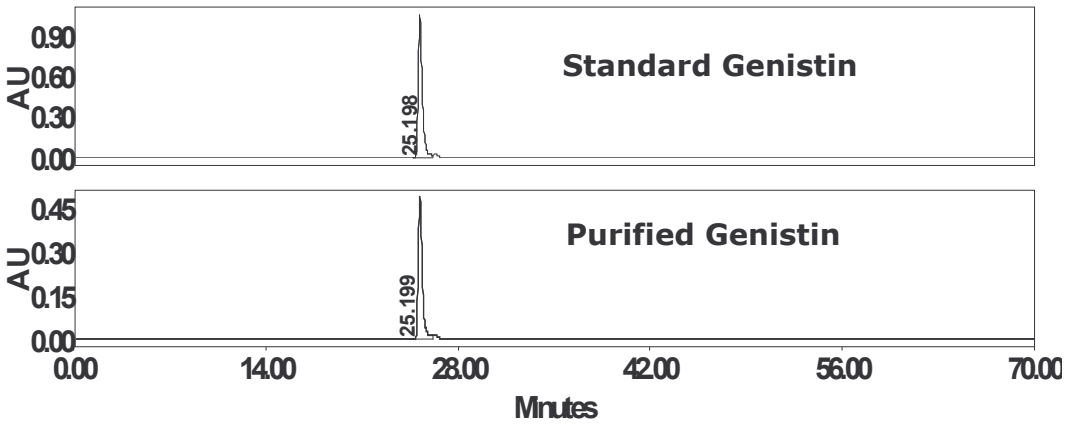

Figure 19. HPLC profile of genistin. A gradient elution using acetonitrile-water (15-35%) was run over a period of 50 min at a flow rate of 1ml/min.

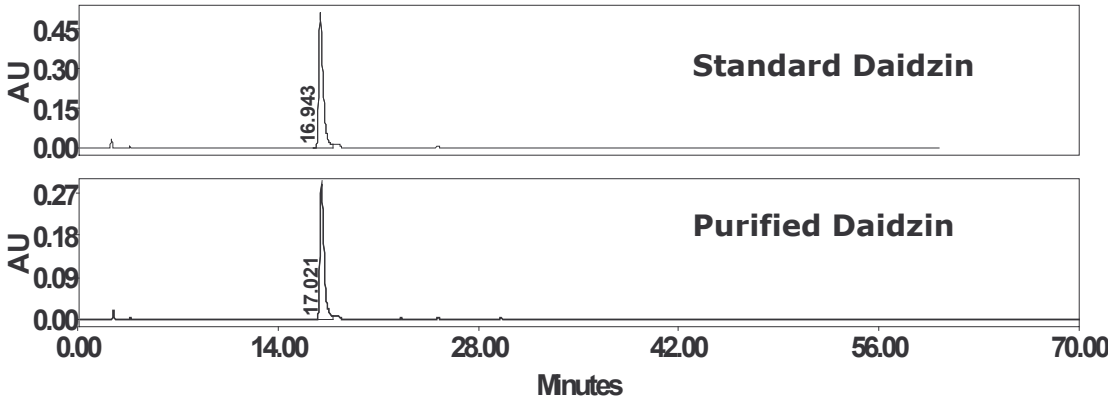

Figure 20. HPLC profile of daidzin. Conditions used are similar as mentioned in Fig. 19.

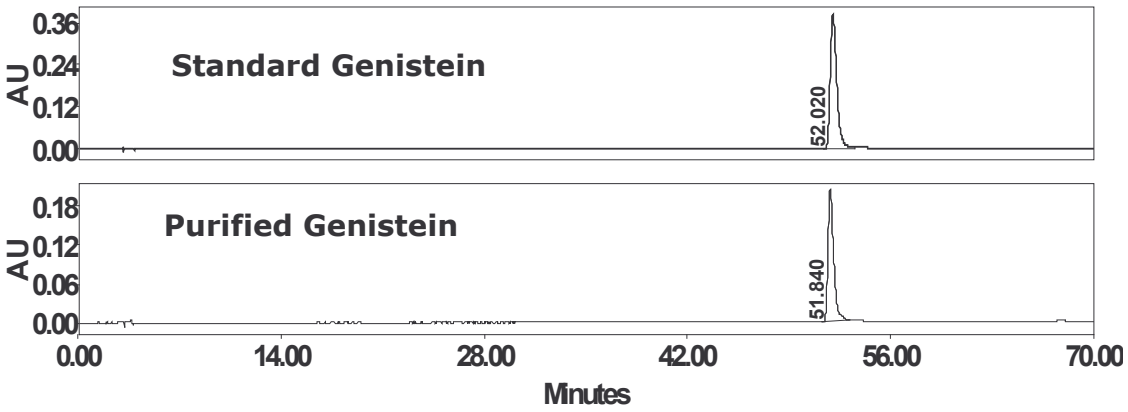

Figure 21. HPLC profile of genistein. Conditions used are similar as mentioned in Fig. 19.

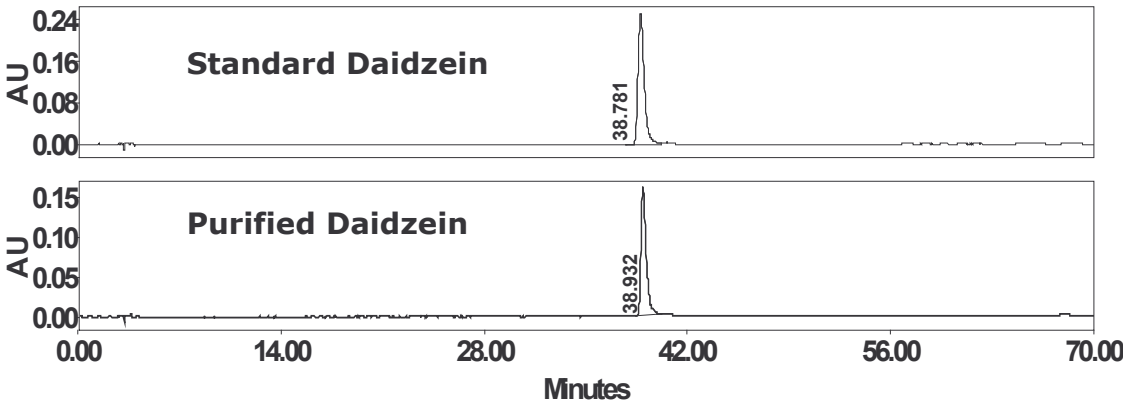

Figure 22. HPLC profile of daidzein. Conditions used are similar as mentioned in Fig. 19.

Section A: Interaction of isoflavones with serum albumin: Identification and molecular visualization of the binding site on serum albumin

Interaction of isoflavones with bovine serum albumin

SDS-PAGE of bovine serum albumin:

The purity of bovine serum albumin was checked by running SDS-PAGE under reducing conditions. The purity of BSA is > 95% as shown in Fig. 23.

Equilibrium dialysis: To determine the classes and number of genistein binding sites, saturation of these sites on BSA is required. The binding data are given in Fig. 24. The number of genistein molecules bound by a mole of protein (ν) is plotted against free genistein concentration [L]. BSA was saturated at 60 μM. Scatchard plot (1949) of the above data shows only one high affinity-binding site for genistein on BSA with a binding constant of 1.78 x 10^5 M^{-1} (Fig.24B). Non-linear fitting algorithms for the data given in Fig. 24A (ν vs [L]) have been fitted to obtain number of binding sites and binding constant for single occupancy.

Fluorescence measurements: BSA, when excited at 295 nm, has an emission maximum at 343 nm. The absorption spectra of isoflavones overlap in the emission region of serum albumin. Genistein and daidzein have absorption peaks at 325 and 340 nm, respectively (Fig25 & 26). With the

addition of genistein & daidzein there is a quenching of fluorescence intensity, indicating efficient Förster type energy transfer (FRET). The overlap integral J has been calculated by integrating the spectra in the wavelength range 310-400 nm to be 2.5 x 10^{-15} and 4.28 x 10^{-15} cm^3 l mol^{-1} for genistein and daidzein respectively (Fig 25 & 26). The energy transfer efficiency E (κ^2 = 2/3, N = 1.45 (Berde *et. al.,* 1979), Φ = 0.118 (Wu and Brand, 1994) for genistein and daidzein are 0.06 and 0.033 respectively. The Förster distance $R_{0,}$ were 1.84 and 2.01 nm for genistein and daidzein respectively. So, the distance between the compounds studied and tryptophan residue was obtained and the r_0, distance between acceptor and donor are 2.91 and 3.53 nm respectively for these compounds. The maximal critical distance for R_0 is from 5 to 10 nm (Chen *et. al.,* 1990) and the maximum distance between donor and acceptor for r_0 is in the range 7 – 10 nm (Chen *et. al.,* 1990a). The values of R_0 and r_0 for genistein and daidzein suggested that non-radiation transfer occurred between these isoflavones and BSA.

Fluorescence quenching studies with genistein and daidzein: Interaction of genistein with BSA has been monitored following the quenching of relative fluorescence intensity of serum albumin. Quenching of fluorescence by genistein does not lead to detectable changes in wavelength of maximum emission or the band shape. Quantitation of genistein-BSA interaction is displayed in Fig. 27A. A maximum quench of 35% has been observed at 12 μM of genistein, representing 70% completion of the reaction as deduced from the linear double reciprocal plot of Q vs genistein

concentration to be 51 ± 3 (Fig. 27B) for BSA. The stoichiometry of genistein-BSA has been estimated from the Job's plot (Jaffé and Orchin, 1962) (Fig. 27C) to be 1:1 ± 0.2. The mass action plot, presented in Fig. 27D has been constructed (using the value of n=1 and the extent of reaction reckoned from Fig. 27B). The binding constant given by the slope of this plot is 1.5 ± 0.2 x 10^5 M^{-1}. It is found that, tryptophan modified BSA did not interact with genistein in the concentration range studied. Quantitation of daidzein-BSA interaction is displayed in Fig. 28A maximum quench of 12% has been observed at 12 μM of daidzein, representing 39% completion of the reaction as deduced from the linear double reciprocal plot of Q vs daidzein concentration to be 18 ± 3 (Fig. 28B) for BSA. The mass action plot, presented in Fig. 28C. The binding constant given by the slope of this plot is 1.2 ± 0.2 x 10^5 M^{-1}. It is also found that genistin and daidzin–the glycosylated forms of genistein and daidzein- did not interact with bovine serum albumin as evidenced from fluorescence quenching measurements.

Binding energetics:

The effect of temperature on the interaction of genistein to serum albumin has been followed in the range 17 to 47°C. The binding constant, *K* decreased with increase in temperature range studied and its dependence on temperature is graphically presented in Fig. 29. Thus, van't Hoff enthalpy, ΔH° =-11.5 kcal mol^{-1} and the binding reaction is entropy driven; ΔS° = -15.5 cal mol^{-1} K^{-1} at 27°C with activation free energy of ΔG° = -RTlnK_{eq} =-6.9 kcal mol^{-1}.

Figure 23. SDS-PAGE of monomeric bovine serum albumin on 12% separating and 5% stacking gels. Electrophoresis was run according to Laemmelli (1970).

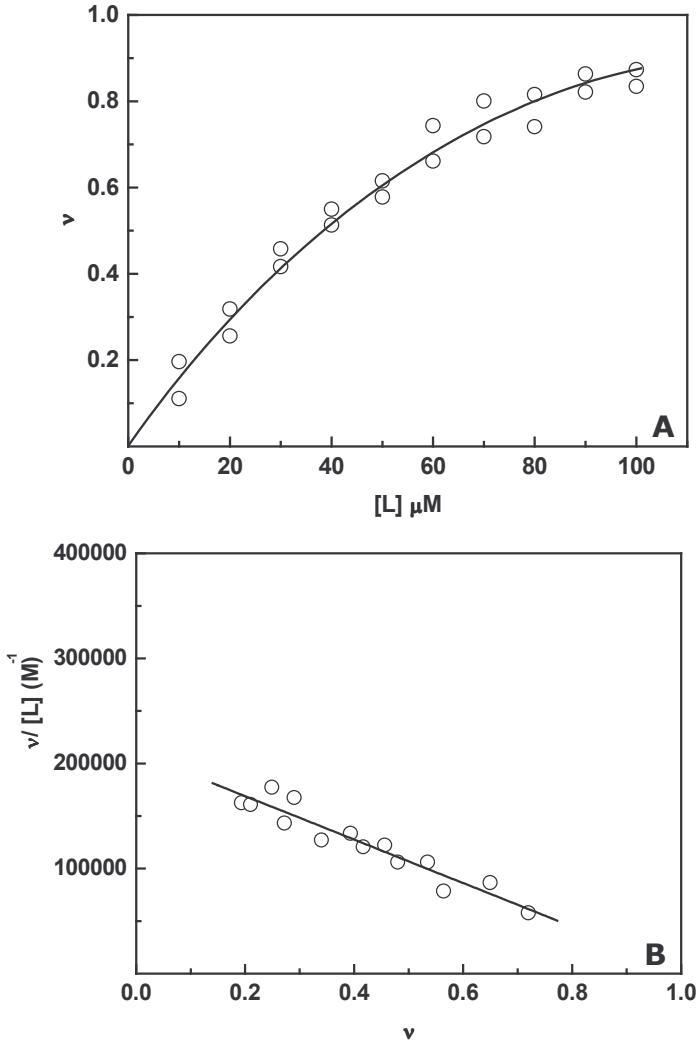

Figure 24. Bovine serum albumin interaction with genistein: equilibrium dialysis:

1ml of bovine serum albumin (75 μm) was dialyzed against 3ml of genistein (10-100 μM) in 50mM Tris-HCl buffer (pH 7.4) for 24 h at 27°C. Corresponding blanks containing 1ml of the above buffer were dialyzed against 3 ml of 10 – 100 μM genistein. The tubes were kept in a water bath at 27°C with shaking at 100 rpm for the entire period. The concentrations of free genistein in equilibrium were determined by molar absorption coefficient 37.3 x 10^3 $M^{-1}cm^{-1}$. A: A plot of ν (moles of ligand bound to protein) vs free ligand concentration (L) B: Scatchard plot depicting the plot of ν / (L) vs ν

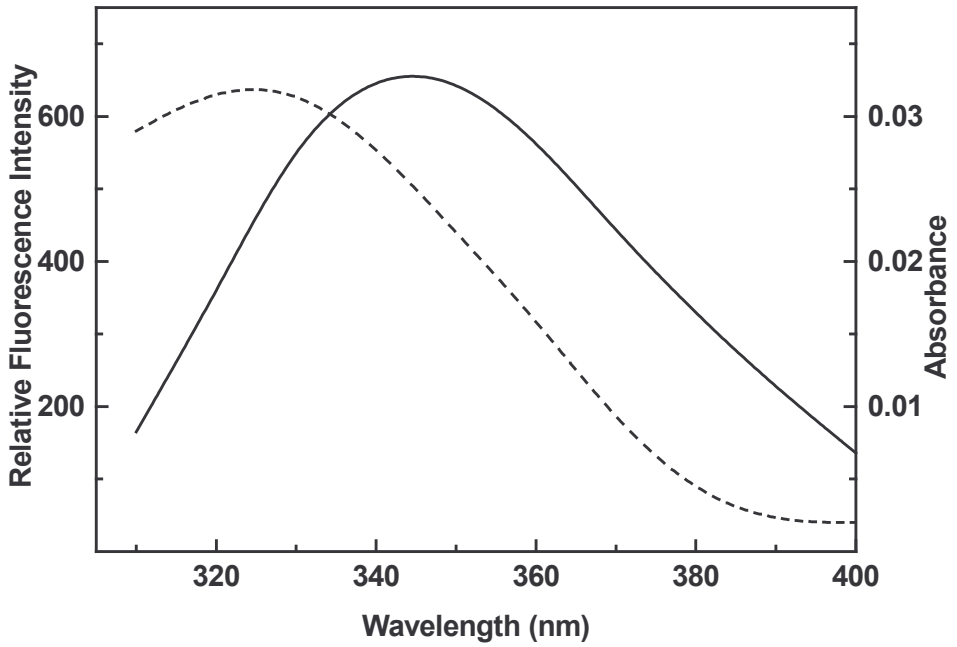

Figure 25. Förster energy transfer: Overlap of emission spectra of BSA with genistein

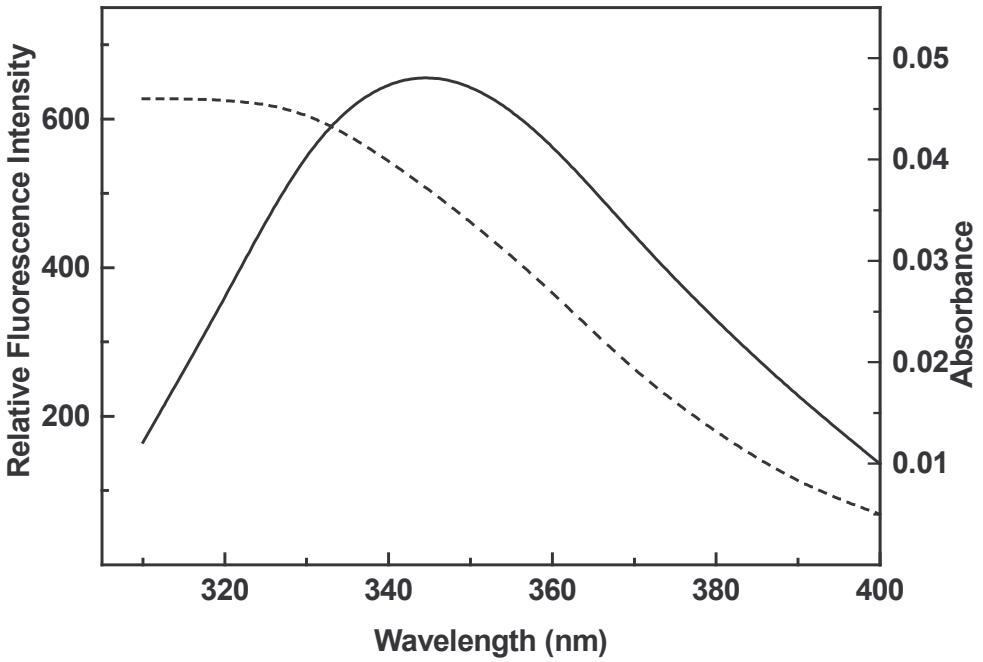

Figure 26. Förster energy transfer: Overlap of emission spectra of BSA with daidzein.

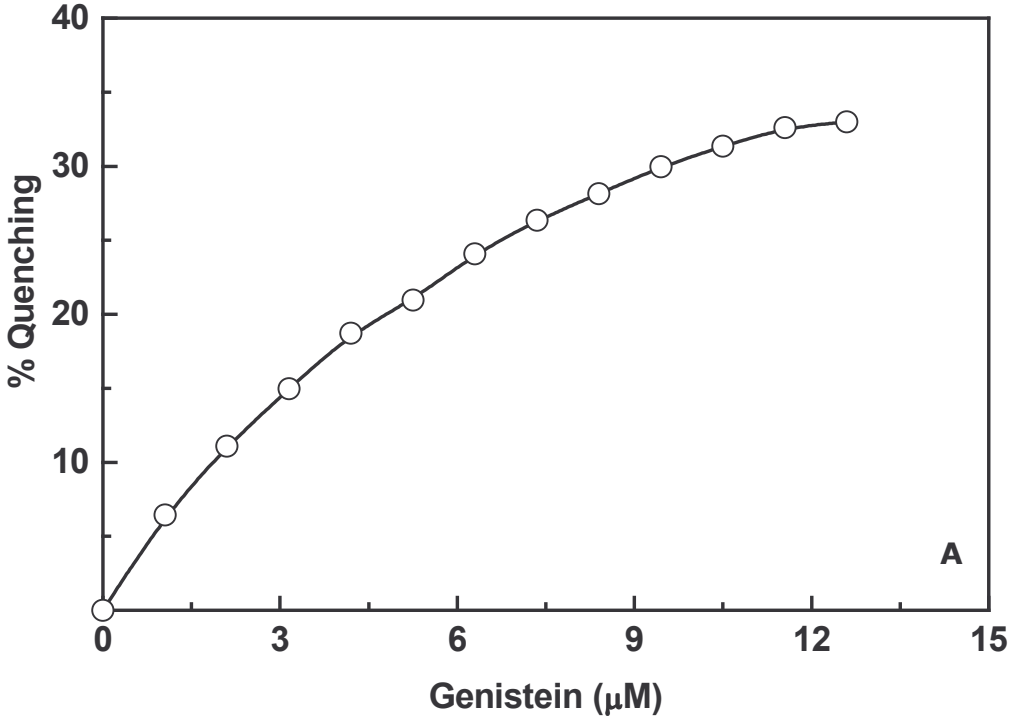

Figure 27. Quantitation of the interaction of BSA with genistein by fluorescence quenching:

BSA (1μM) in 50 mM Tris-HCl buffer (pH 7.4) was titrated with increasing aliquots of stock genistein solution (2 μl equivalent to 1 μM genistein per aliquot) in 80% methanol and the % quench was recorded. Blank titrations with N-acetyl tryptophanamide of equivalent absorbance at 280 nm as BSA in presence of varying concentration of genistein were carried out.

A: % quench of fluorescence intensity, as a function of constituent genistein concentration.

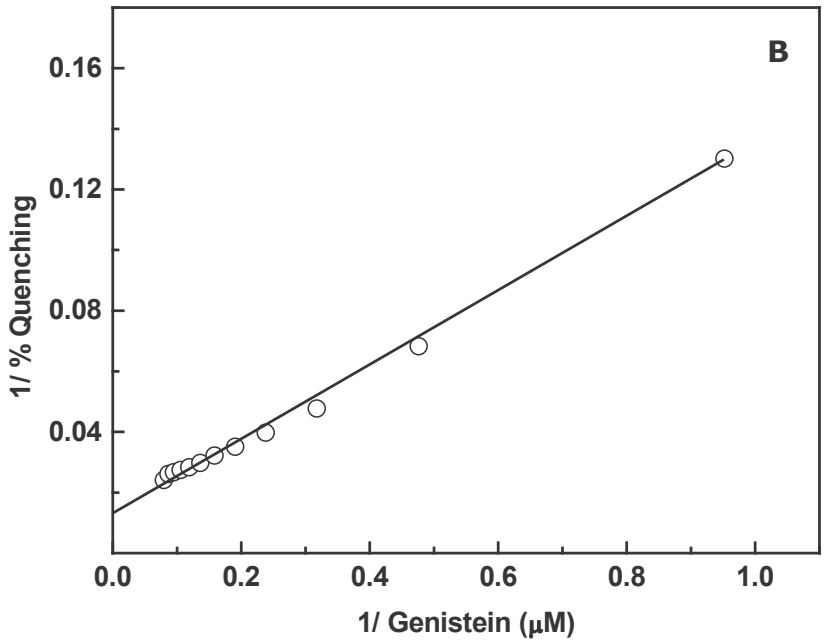

Figure 27 B. Double-reciprocal plot of data in A: Q_{max} = 51±3 (± indicates probable error in all cases).

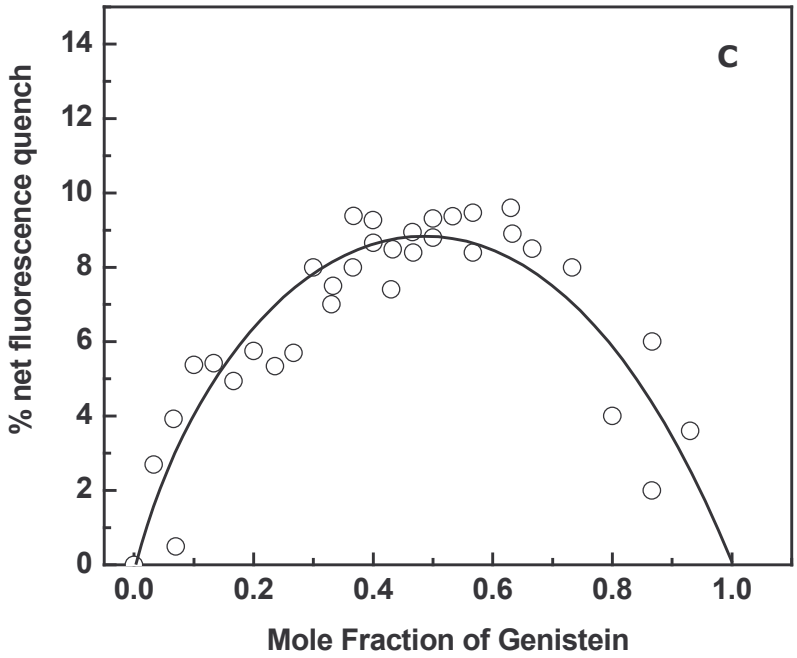

Figure 27C. Job's plot: C_{BSA} + $C_{genistein}$ = 10 μM showing the stoichiometry of 1: 1.

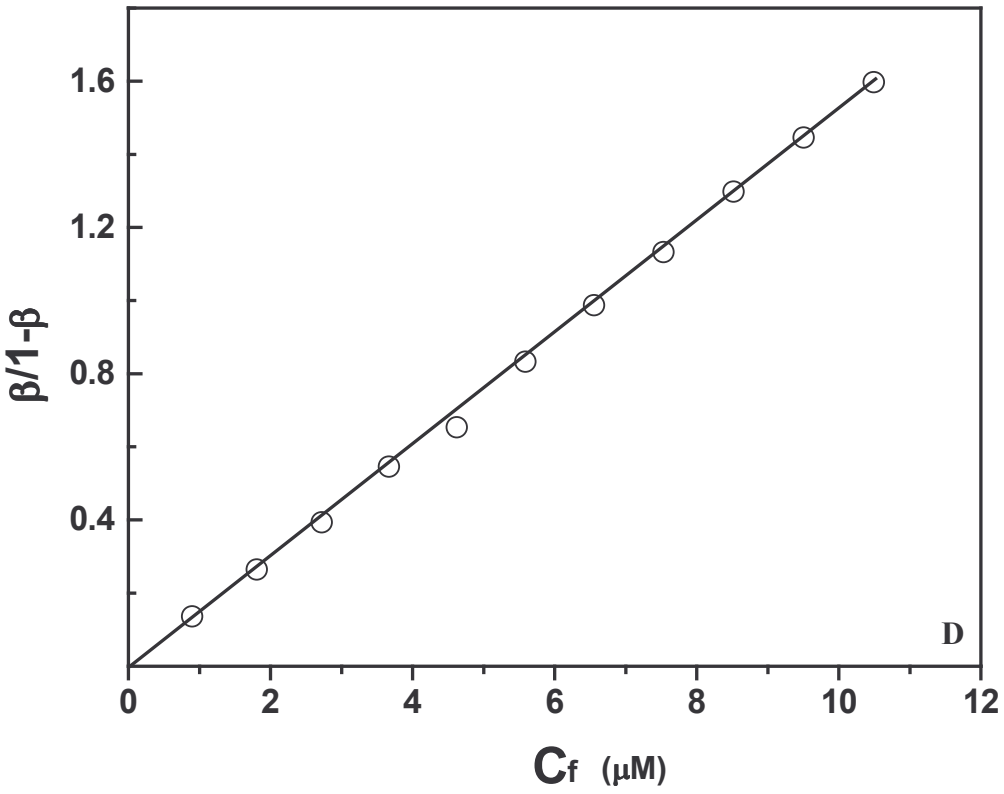

Figure 27 D. Mass action plot of data.

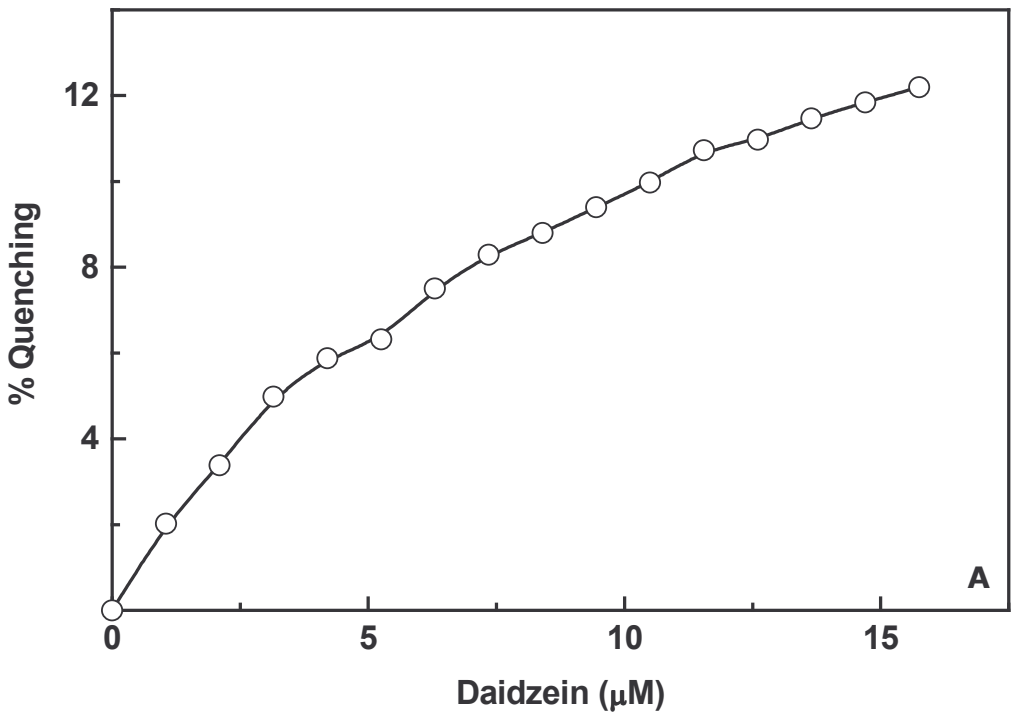

Figure 28. Quantitation of the interaction of BSA with daidzein by fluorescence quenching:

BSA (1μM) in 50 mM Tris-HCl buffer (pH 7.4) was titrated with increasing aliquots of stock daidzein solution (2 μl equivalent to 1 μM daidzein per aliquot) in 80% methanol and the % quench was recorded. Blank titrations with N-acetyl tryptophanamide of equivalent absorbance at 280 nm as BSA in presence of varying concentration of daidzein were carried out.

A: % quench of fluorescence intensity, as a function of constituent daidzein concentration.

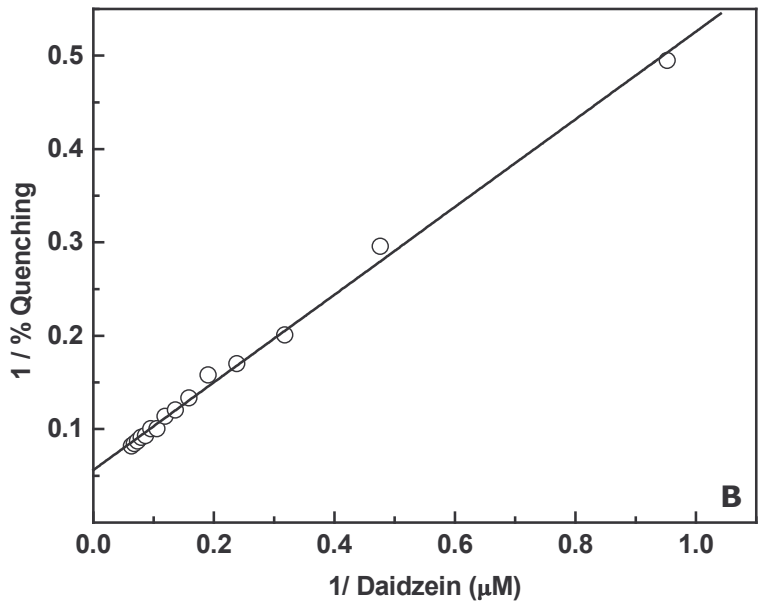

Figure 28 B. Double-reciprocal plot of data in A: Q_{max} = 18±3 (± indicates probable error in all cases).

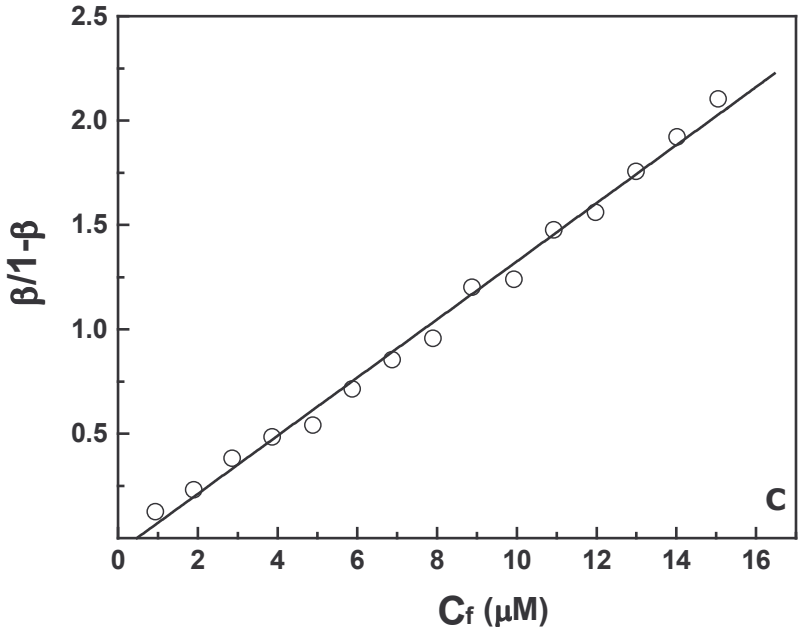

Figure 28C. Mass action plot of data.

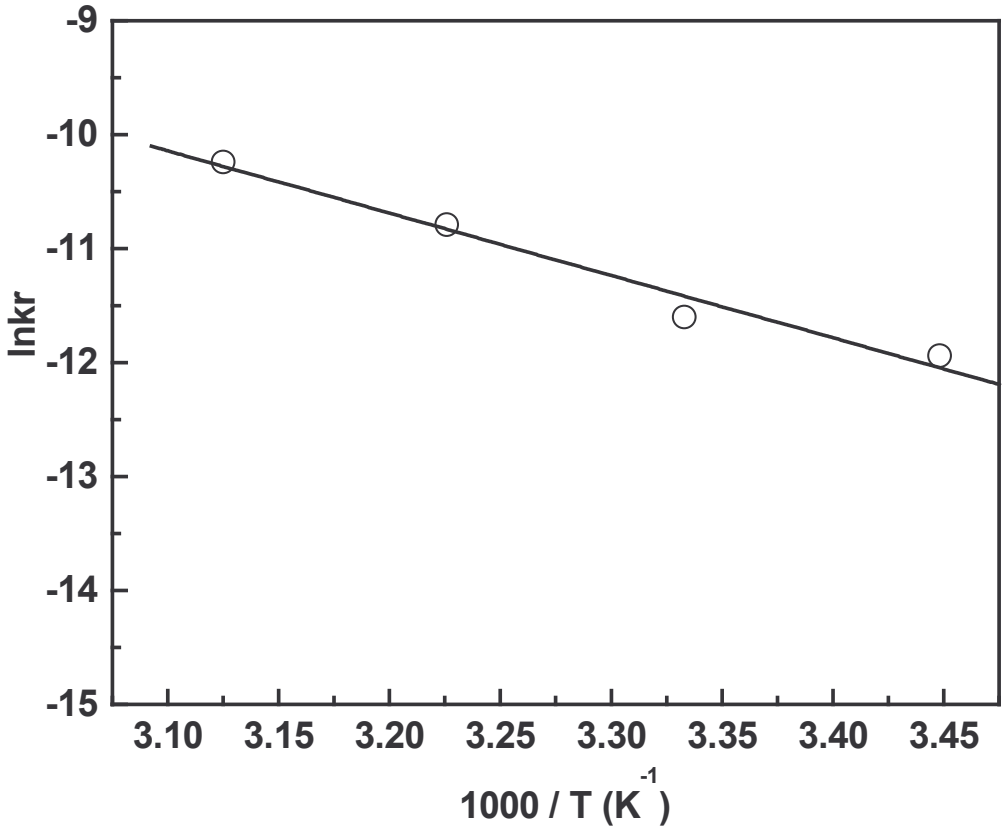

Figure 29. Effect of temperature on the binding constant of genistein to BSA: van't Hoff's plot:

BSA (1μM) in 50 mM Tris- HCl buffer (pH 7.4) was titrated with increasing aliquots of stock genistein solution (2 μl equivalent to 1 μM genistein per aliquot) in 80% methanol at different temperatures (17^{o}C, 27 ^{o}C, 37 ^{o}C and 47 ^{o}C) and the % quench was recorded. Blank titrations were carried out as described for Fig. 27. van't Hoff's plot was constructed to obtain the thermodynamic parameters.

Effect of ionic strength on binding of genistein–BSA interaction: To determine the role of ionic interactions in genistein – BSA interaction, the ionic strength of the buffer was increased by the addition of potassium chloride (0 –200 mM). It was observed that Q_{max} remained unaltered on increasing the ionic strength of the buffer implying no change in the binding geometry. The binding constant decreased with increasing ionic strength (Fig. 30), establishing the role of ionic interaction in the binding.

The Stokes radius of BSA, in presence of increasing concentrations of potassium chloride in buffer, was measured by size exclusion chromatography. The elution volume of the protein increased with ionic strength, indicating a decrease in Stokes radius (Fig. 30 inset). The decreased Stokes radius of the molecule may also have contributed to the observed decrease in affinity.

Fluorescence of albumin bound daidzein: Daidzein is the only intrinsically fluorescent isoflavone among those studied. This property has been exploited to study the nature of binding to BSA. There is a shift of the emission maxima of the daidzein bound albumin towards shorter wavelengths (from 465 to 457nm) compared to unbound daidzein (Fig.31). This indicates that daidzein is binding on the hydrophobic pocket in BSA.

ANS binding studies: ANS, known to bind to hydrophobic pockets of the proteins, is a much-utilized fluorescent 'hydrophobic probe' for examining the non-polar character of proteins and membranes (Matulis and Lovrien, 1998).

To examine systematically the role of hydrophobic interactions in the binding of genistein to serum albumin, ANS–bound BSA has been titrated with genistein. The replacement of ANS by genistein in the protein indicates that ANS and genistein bind to the same site. This is corroborated by the decrease in ANS-bound BSA fluorescence with increasing concentrations of genistein. The binding constant, estimated by the competitive ligand binding measurements is ($1.4 \pm 0.2 \times 10^5$ M^{-1}), very similar to genistein-BSA interaction (Fig 32).

Studies with Fatty acid: Among the various ligands, fatty acids alone can attach to the primary binding site of BSA. Experiments have been conducted using palmitic acid and defatted BSA to understand the affinity characteristics of genistein bound BSA. The increase in the fluorescence of genistein bound protein with the rise in fatty acid concentration evidences the displacement of genistein by palmitic acid (Fig.33).

Effect of genistein on tertiary and secondary structure of BSA: The effect of increasing genistein concentration on the tertiary and secondary structure of BSA has been studied by measuring CD spectra in near and far UV region, respectively. The characteristic patterns in the near UV region, caused by the asymmetric environment of tryptophan, tyrosine and phenylalanine residues in the native structure, are not affected in presence of genistein, upto a concentration of 50 μM. This indicates that genistein has no effect on the tertiary structure of BSA (Fig. 34A). There are no changes in

the far UV CD bands up to a concentration of 20 μM genistein, indicating that genistein had no effect on the secondary structure of BSA. These results helped to establish that the genistein does not affect the conformation of serum albumin. BSA did not induce any CD band for genistein (0 to 50 μM). However, the addition of warfarin to BSA induced a CD band at 310 nm and 255 nm (Fig. 34B). There was no decrease in the CD signal on adding genistein to the warfarin bound BSA; there was an additional CD band at 270 nm (Fig. 34B).

Binding of genistein in the presence of daidzein: The fluorescence of daidzein was found to increase on binding to BSA as mentioned in an earlier section. The saturation was reached at 14.75 μM BSA (Fig. 35A). Quenching of fluorescence was observed on adding genistein to the daidzein bound BSA, (Fig. 35B) indicating the replacement of daidzein by genistein. The quench was maximum at 27 μM of genistein. The binding constant of the competing ligand (Fig. 35C) was evaluated from a plot of F_{max} / F vs molarity of genistein (Aceto *et. al.,* 1995); the binding constant of genistein was calculated to be 6.02 x 10^5 M^{-1}.

Fluorescence anisotropy measurements: Fluorescence anisotropy measurements were made for the daidzein–BSA system by exciting at 340 nm (maxima for daidzein) and emission at 465 nm. There was an increase in fluorescence anisotropy of daidzein on binding to BSA. Anisotropy of daidzein increased from 0.01 to 0.25 on binding (Fig. 36). The increase in anisotropy

could be due to the restriction imposed by the binding on the rotation around the daidzein molecule.

The anisotropy of daidzein bound to BSA remained constant in the presence of diazepam. Diazepam is known to bind to the domain IIIA of BSA, which is the primary binding site for fatty acids. Warfarin also did not affect the anisotropy of daidzein bound to BSA. TIB decreased the anisotropy of daidzein from 0.186 to 0.09. The anisotropy of free daidzein was 0.025. Hence, TIB partially displaced the daidzein in BSA (Table 1).

The anisotropy of warfarin bound to BSA was measured in the presence of genistein. The anisotropy of warfarin bound to BSA (5 μM bound to 10 μM BSA) was found to be 0.58. This was unaltered with the addition of genistein even up to 100 μM revealing that warfarin was not displaced by genistein (Table 2).

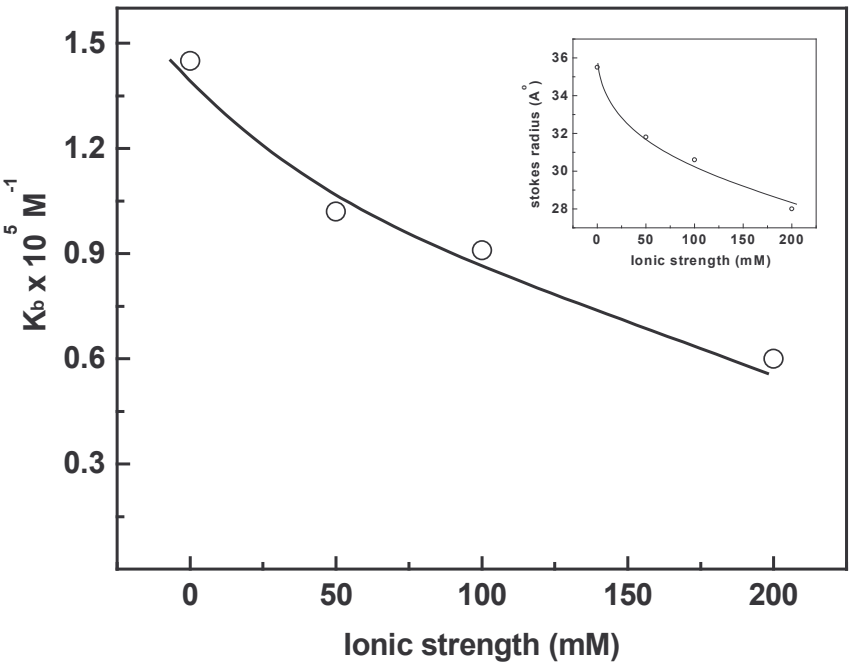

Figure 30. Effect of ionic strength on the binding constant of genistein to BSA:

A plot of the binding constant as a function of ionic strength to show the effect of ionic strength on the binding constant of genistein. BSA (1μM) in 50 mM Tris-HCl buffer (pH 7.4) was titrated at different ionic strengths adjusted by using potassium chloride (0 mM, 50 mM, 100 mM and 200 mM) with increasing aliquots of stock genistein solution (2 μl equivalent to 1 μM genistein per aliquot) in 80% methanol. The % quench of the intrinsic fluorescence of BSA was recorded. Blank titrations were carried out as described for Fig. 4.

Inset: Stokes radius of BSA at different molarities of KCl (0 – 200 mM) was determined by size exclusion chromatography on HPLC using an TSK SW 2000 column (300 x 4.6 mm, 4μ). The column was pre-equilibrated at the required ionic strength attained using KCl of buffer 50 mM Tris-HCl (pH 7.4). Equilibrated samples (20 μl) of the protein (1 mg/ ml) were injected at 27°C at a flow rate of 0.2-ml/ min. The protein was eluted isocratically using the same buffer and detected at 280 nm.

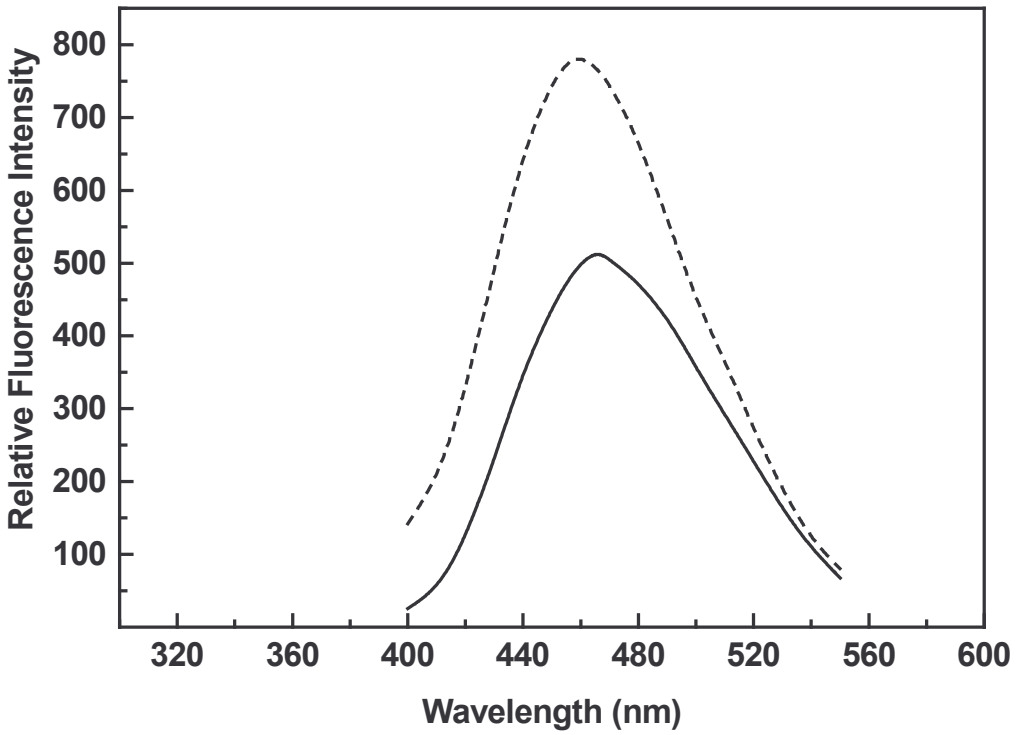

Figure 31. Emission spectra of daidzein showing blue shift on binding to BSA:

Daidzein (2.75 μM) in 50 mM Tris–HCl (pH 7.4) was titrated against increasing concentrations of BSA in the same buffer. The final concentration of BSA was 14.75 μM. Stock BSA (835 μM) was added in 5 μl aliquots and the spectra recorded between 400 – 550 nm after excitation at 340 nm, the excitation maxima for daidzein. Excitation slit width was 5 nm and emission slit width was 10 nm. *Solid Line*- Daidzein; *Dashed Line*- Daidzein bound BSA

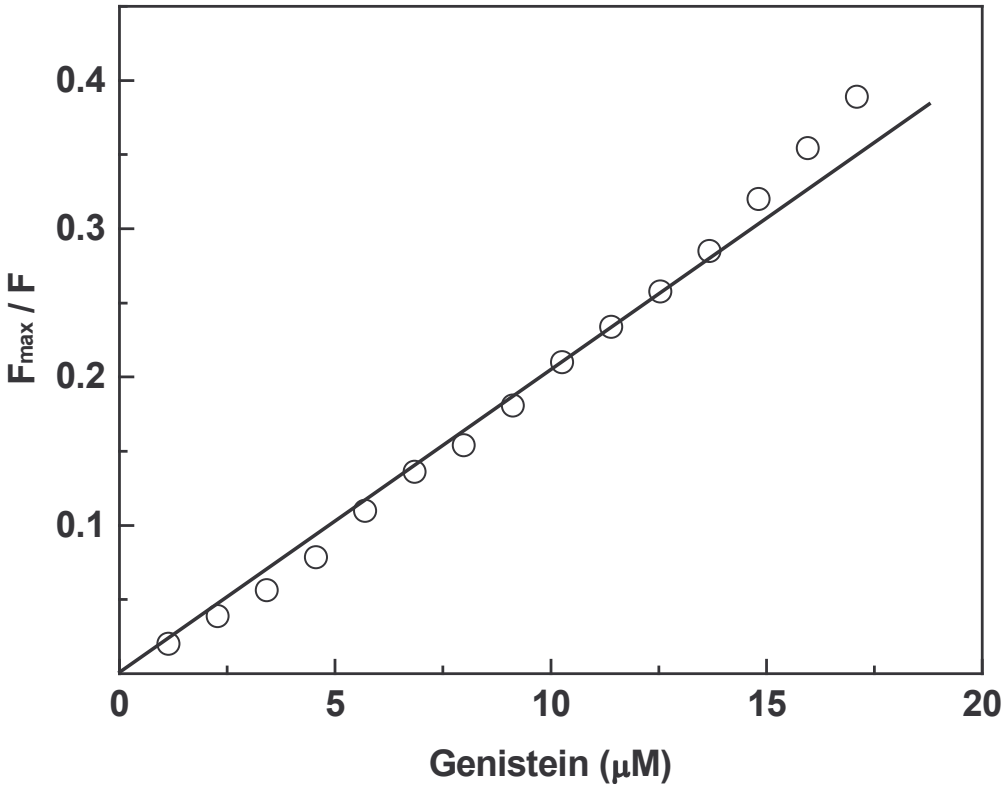

Figure 32. Fluorimetric titration of BSA-ANS complex with genistein: The concentration of ANS is 6 μM and BSA is 1μM. The excitation and emission wavelength for BSA-ANS complex is 375 nm and 465 nm. Excitation and emission slit widths were 5 nm and 10 nm respectively.

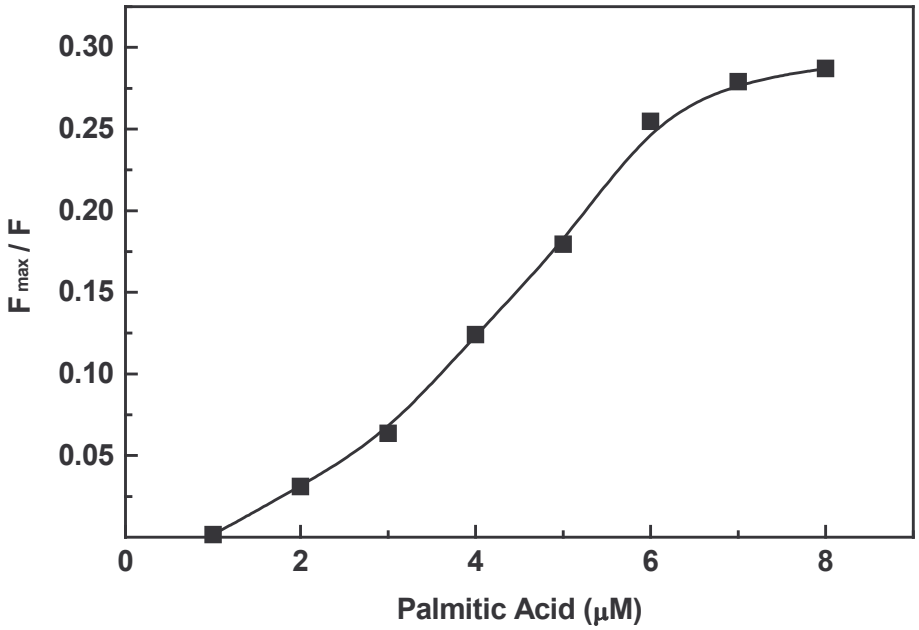

Figure 33. Fluorimetric titration of BSA-genistein acid complex with palmitic acid: The concentration of genistein is 10 μM and BSA is 1μM. The excitation and emission wavelength for BSA-genistein complex is 295 nm and 343 nm. Excitation and emission slit widths were 5 nm and 10 nm respectively.

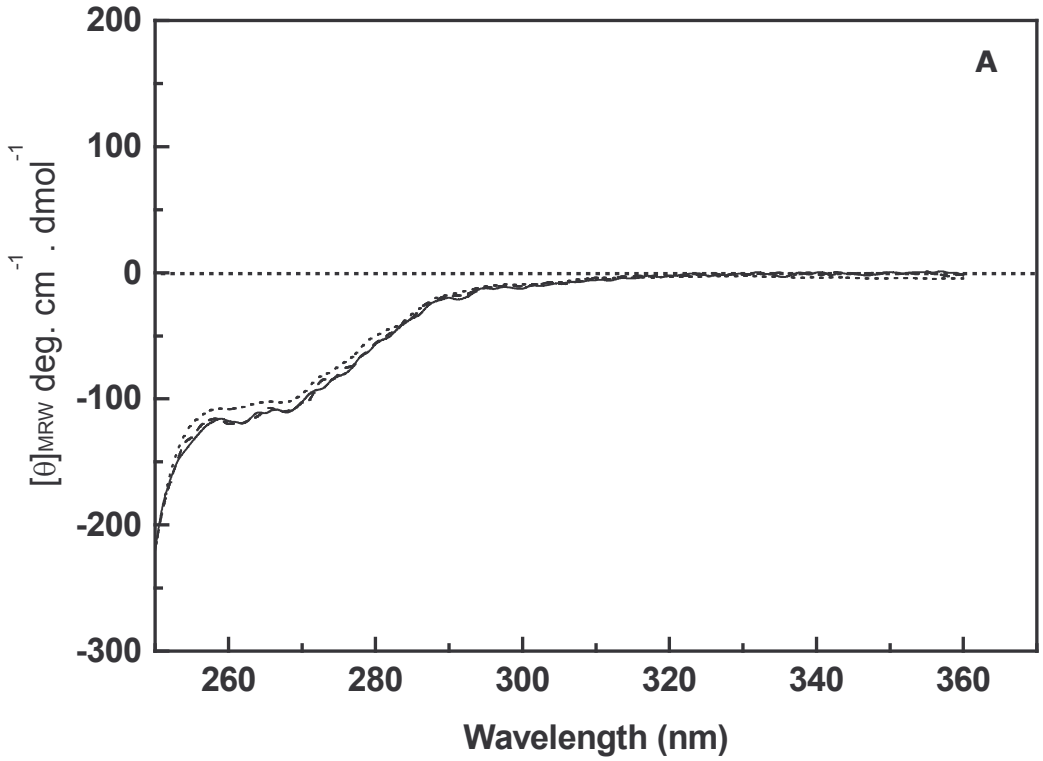

Figure 34A. Effect of genistein on the tertiary structure of BSA:

CD measurements were carried out in the near UV region of 250 – 360 nm in 50 mM Tris-HCl buffer (pH 7.4). The cell path length was 1 cm and spectra were recorded at a speed of 10 nm min^{-1}. All scans are an average of 3 runs. A mean residue weight of 115 was used for calculating the molar ellipticity values. The concentration of BSA used was 15 μM and genistein (0 – 50 μM). *Solid line*: BSA in buffer; *Dashed line*: BSA with 25 μM genistein; *Dotted line*: BSA with 50 μM genistein.

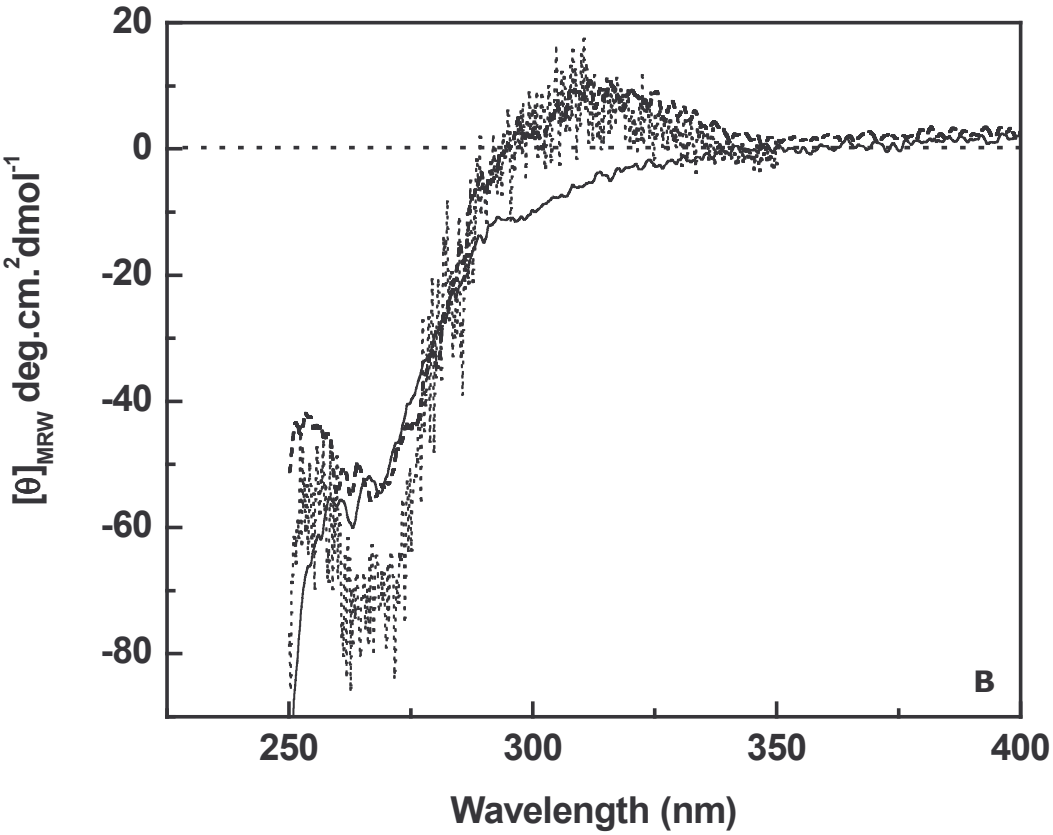

Figure 34B. Effect of genistein on near UV CD of warfarin–bound BSA: Spectra were recorded after genistein (50 μM) was added to BSA with 50 μM warfarin. *Solid line*: BSA (15 μM) *Dashed line*: BSA in presence of warfarin (50 μM); *Dotted line*: 50 μM genistein in presence of warfarin-bound BSA (50 μM).

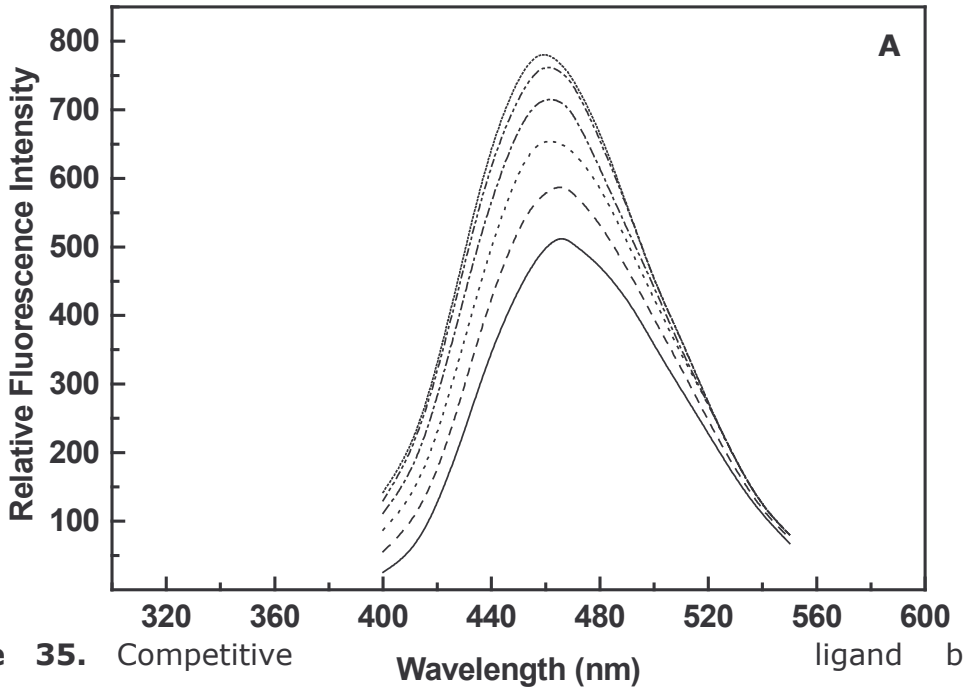

Figure 35. Competitive ligand binding interactions of BSA: Genistein and daidzein (Fluorescence measurements): Daidzein (2.75 μM) was titrated against increasing concentrations of BSA to a final concentration of 14.75 μM) in 50 mM Tris–HCl buffer (pH 7.4). The excitation wavelength was 340 nm and emission range was 400-550 nm. Excitation slit width was 5 nm and emission slit width was 10 nm. To the above solution, 5 μl of stock genistein in 80% methanol (1.4 mM) was added in aliquots and the spectra recorded at 27°C. The final concentration of genistein was 27 μM.

A. Emission spectra of daidzein with increasing micro molar concentration of BSA (*Solid Line* 0; *dashed line* 1.66; *dotted line* 4.98; *dashed and dotted line* 8.26; dash two dotted line 11.52; *short dash and dotted line* 14.75)

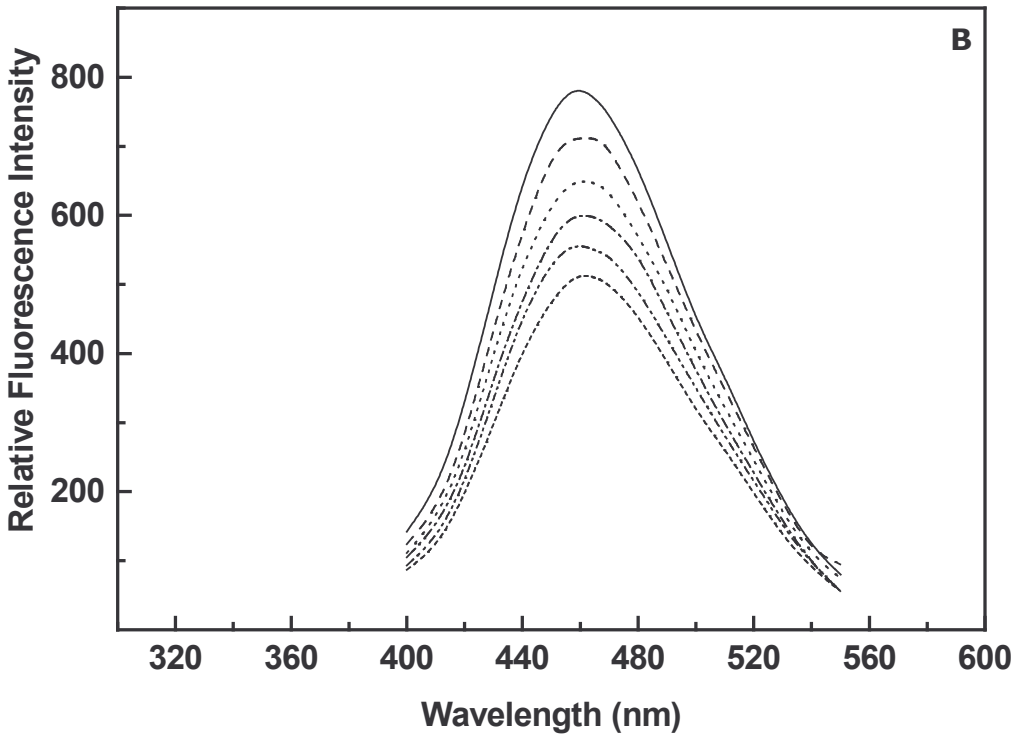

Figure 35B. Emission spectra of daidzein-BSA complex with increasing micro molar concentration of genistein (*Solid Line* 0; *dashed line* 5.48; *dotted line* 10.92; *dashed and dotted line* 16.29; dash two dotted line 21.64; short dash line 26.94).

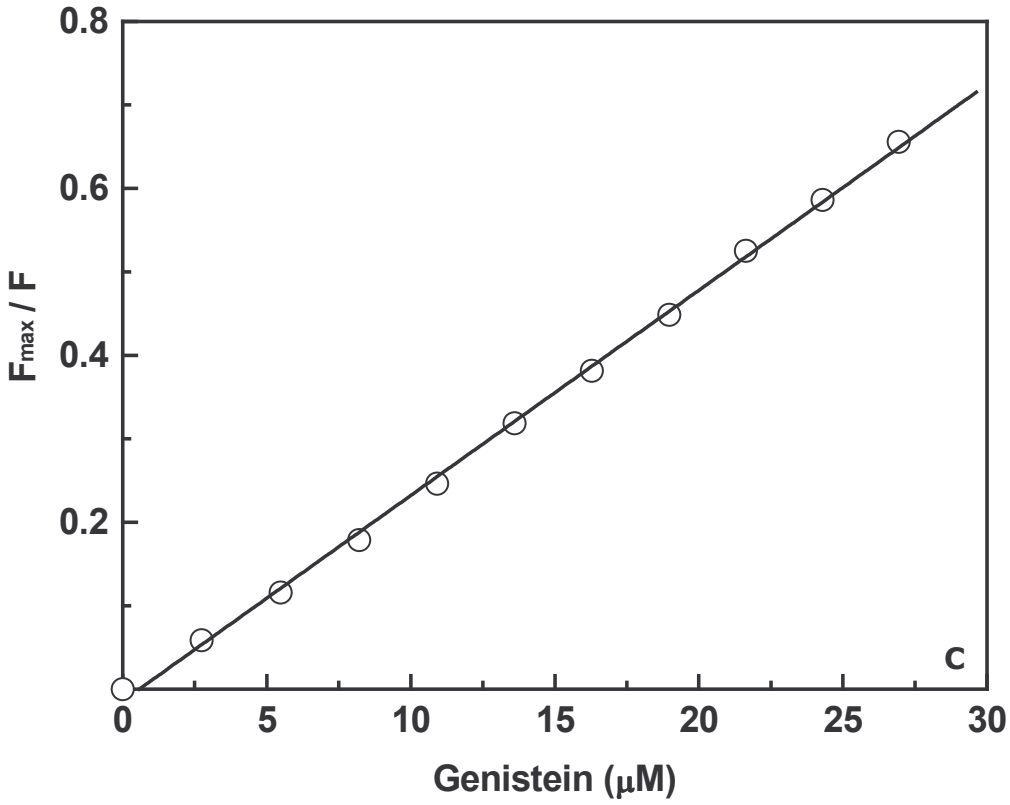

Figure 35C. F_{max} / F vs genistein concentration to obtain the binding constant of the competing ligand–genistein.

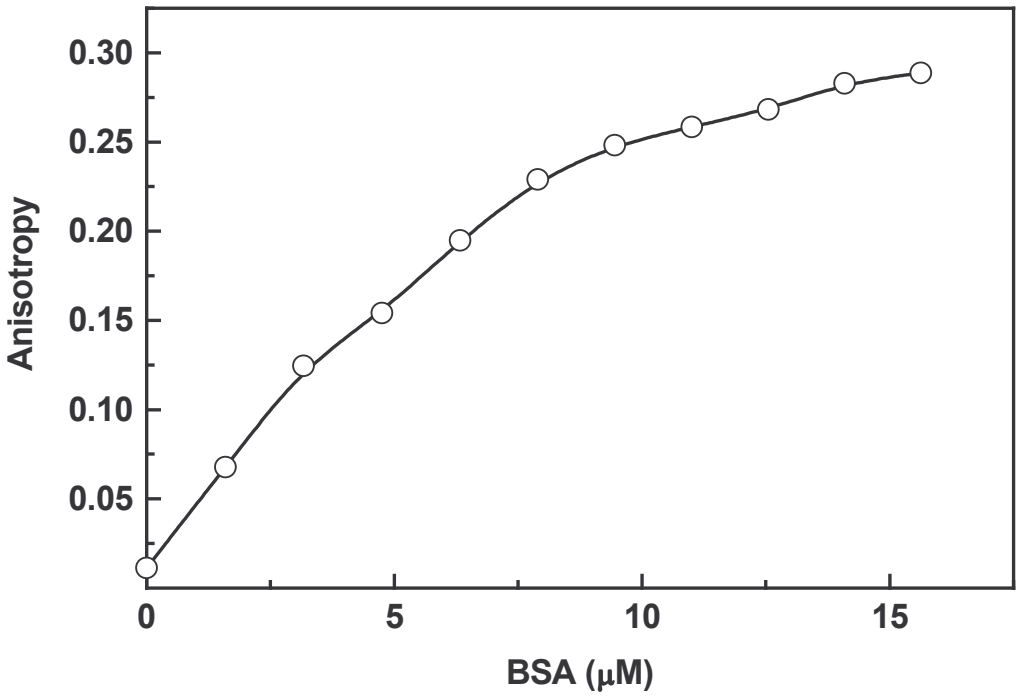

Figure 36. Variation in fluorescence anisotropy of daidzein as a function of BSA concentration: Daidzein (2.75μM) was titrated against increasing concentrations of BSA. The excitation and emission wavelengths were 340 and 465 nm respectively. Slit widths were at 5 and 10 nm for excitation and emission respectively.

Table 1. Corrected fluorescence anisotropy values of the daidzein-BSA complex, when different aliquots of warfarin, diazepam and triiodobenzoic acid were added.

Concentration (μM)	Anisotropy values
Warfarin	
0	0.186
16	0.189
32	0.183
48	0.184
64	0.184
80	0.179
96	0.177
Daizepam	
0	0.186
20	0.189
40	0.184
60	0.183
80	0.185
100	0.183
Triiodobenzoic acid	
0	0.186
11	0.174
23	0.165
35	0.158
46	0.148
57	0.140
69	0.135
92	0.127
115	0.113
137	0.107
160	0.09

Table 2. Corrected fluorescence anisotropy values of the warfarin-BSA complex, when different aliquots of genistein were added.

Concentration (μM)	Anisotropy values
0	0.583
20	0.586
40	0.585
60	0.586
80	0.584
100	0.586

Interaction of isoflavones with human serum albumin

SDS-PAGE of human serum albumin:

The purity of human serum albumin has been checked by running SDS-PAGE under reducing conditions. The purity of HSA is > 95% as shown in Fig. 37.

Equilibrium dialysis: To determine the classes and number of genistein binding sites, saturation of these sites on HSA is required. The binding data are given in Fig. 38. The number of genistein molecules bound by a mole of protein (ν) is plotted against free genistein concentration [L]. HSA has been saturated at 50 μM genistein (Fig. 38A). Scatchard plot (1949) of the above data shows only one high affinity-binding site for genistein with a binding constant of 1 x 10^5 M^{-1} (Fig. 38B). Non- linear fitting algorithms for the data given in Fig. 38A (ν vs [L]) have been fitted to obtain number of binding sites and binding constant for single occupancy.

Fluorescence measurements: HSA, when excited at 295 nm, has an emission maximum at 333 nm (Fig. 39). The absorption spectra of isoflavones overlap in the emission region of serum albumin. Genistein and daidzein have absorption peaks at 325 and 340 nm, respectively (Fig. 39 inset). With the addition of genistein, there is a quenching of fluorescence intensity, indicating efficient Förster type energy transfer (FRET). The overlap

integral J has been calculated by integrating the spectra in the wavelength range 310-400 nm to be 8.5 x 10^{-15} and 9.28 x 10^{-15} cm^3 l mol^{-1} for genistein and daidzein, respectively. The energy transfer efficiency E (κ^2 = 2/3, N = 1.45 (Berde *et. al.,* 1979), Φ = 0.118 (Wu and Brand, 1994) for the genistein and daidzein are 0.05 and 0.022 respectively. The Förster distance $R_{0,}$ is 2.25 and 2.29 nm, respectively for genistein and daidzein. The distance between the compounds studied and tryptophan residue has been obtained and the r_0, distance between acceptor and donor are 3.69 and 4.35 nm, respectively for these compounds. The maximal critical distance for R_0 is from 5 to 10 nm (Chen *et. al.,* 1990) and the maximum distance between donor and acceptor for r_0 is in the range 7 – 10 nm (Chen *et. al.,* 1990a). The values of R_0 and r_0 for genistein and daidzein suggest that non-radiation transfer occurred between these isoflavones and HSA. A comparison of the J, Ro and r values of different ligands bound to HSA is given in Table 3.

Fluorescence quenching studies with genistein and daidzein: Interaction of genistein with HSA has been monitored following the quenching of relative fluorescence intensity of serum albumin. Quenching of fluorescence by genistein does not lead to detectable changes in wavelength of maximum emission or the band shape. Quantitation of genistein–HSA interaction is displayed in Fig. 40A. A maximum quench of 17% has been observed at 12 μM of genistein, representing 59% completion of the reaction as deduced from the linear double reciprocal plot of Q vs genistein concentration to be 28 ± 3 (Fig. 40B). The stoichiometry of genistein–HSA

complex has been estimated from the Job's plot (Fig. 40C) to be 1:1 ± 0.2. The mass action plot, presented in Fig. 40D has been constructed (using the value of n=1 and the extent of reaction reckoned from Fig. 40B). The binding constant given by the slope of this plot is 1.5 ± 0.2 x 10^5 M^{-1}. However, tryptophan modified HSA does not interact with genistein in the concentration range studied. Quantitation of daidzein-HSA interaction is displayed in Fig. 41A maximum quench of 12% has been observed at 12 μM of genistein, representing 39% completion of the reaction as deduced from the linear double reciprocal plot of Q vs daidzein concentration to be 12 ± 3 (Fig. 41B) for HSA. The mass action plot, presented in Fig. 41C. The binding constant given by the slope of this plot is 1.4 ± 0.2 x 10^5 M^{-1}. Genistin and daidzin– the glycosylated forms of genistein and daidzein do not interact with serum albumin as evidenced from fluorescence quenching measurements.

Binding energetics: Effect of temperature on the interaction of genistein with serum albumin has been followed in the range 17 to 47°C. The binding constant, K, exhibits a reciprocal relationship with temperature (Fig. 42). Thus, van't Hoff enthalpy, ΔH°, is determined to be -13.16 kcal mol^{-1}. The binding reaction is entropy driven. ΔS° has been determined as –21.0 cal mol^{-1} K^{-1} and ΔG° is found to be -6.86 kcal mol^{-1} at 27°C.

Figure 37. SDS-PAGE of monomeric HSA. A 5% stacking gel and 12% resolving gel was used and electrophoresis was run according to Laemmelli (1970).

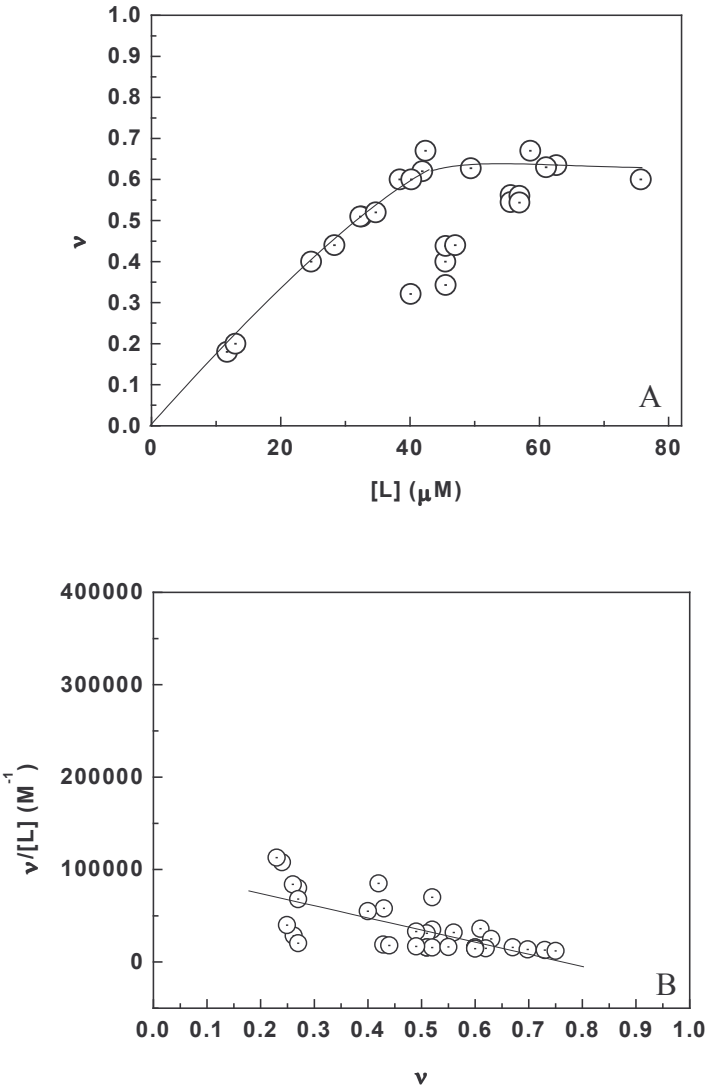

Figure 38. Human serum albumin interaction with genistein: equilibrium dialysis

1ml of Human serum albumin (63.64 μm) was dialyzed against 3ml of genistein (10-100 μM) in 50mM Tris-HCl buffer (pH 7.4) for 24 h at 27°C. Corresponding blanks containing 1ml of the above buffer were dialyzed against 3 ml of 10 – 100 μM genistein. The tubes were kept in a water bath at 27°C with shaking at 100 rpm for the entire period. The concentrations of free genistein in equilibrium were determined by molar absorption coefficient 37.3 x 10^3 $M^{-1}cm^{-1}$.

A: A plot of ν (moles of ligand bound to protein) vs free ligand concentration (L)

B: Scatchard plot depicting the plot of ν / (L) vs ν

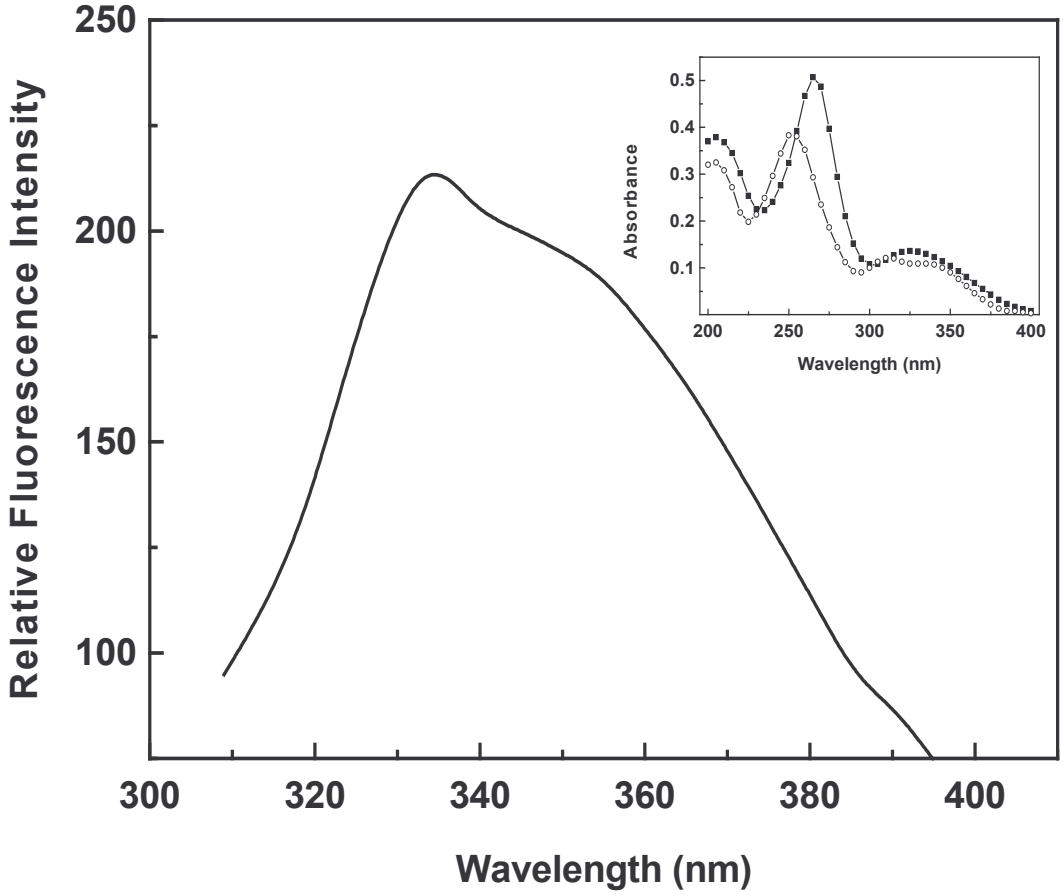

Figure 39. Resonance energy transfer from HSA to genistein and daidzein: Emission spectra of HSA in 50 mM Tris-HCl (pH 7.4). Excitation wavelength was 295nm. Emission range was 300-400nm with slit widths of 5nm for excitation and 10 nm for emission. Protein concentrations used was 1 μM. Temperature was maintained at 27°C using a water bath.

Inset: Absorption spectra of genistein (-■-) and daidzein (-○-) showing peak at 325 - 340 nm for daidzein and genistein, overlapping the emission maxima of 333 nm for HSA.

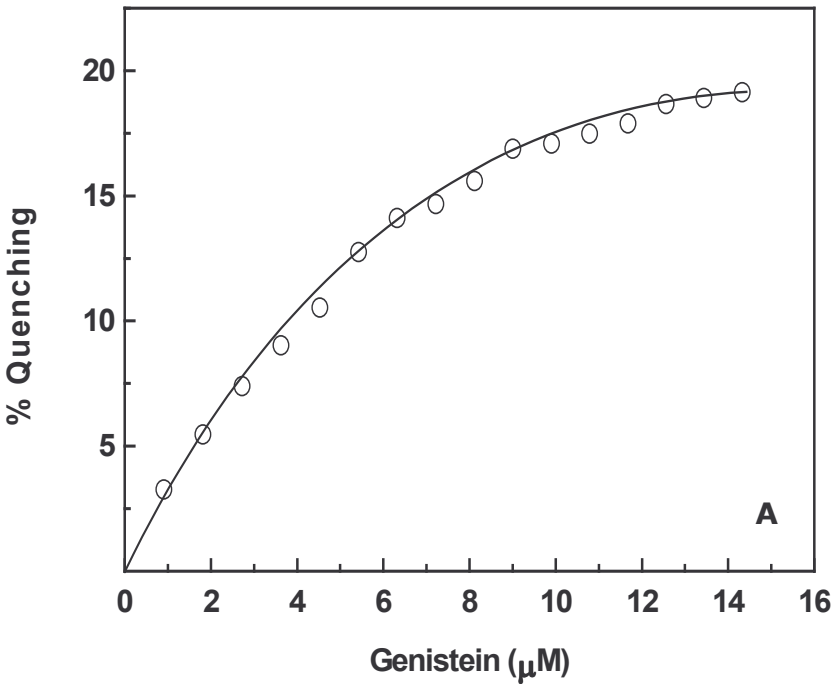

Figure 40. Quantitation of the interaction of HSA with genistein by fluorescence quenching:

HSA (1μM) in 50 mM Tris-HCl buffer (pH 7.4) was titrated with increasing aliquots of stock genistein solution (2 μl equivalent to 1 μM genistein per aliquot) in 80% methanol and the % quench was recorded. Blank titrations with N-acetyl tryptophanamide of equivalent absorbance at 280 nm as HSA in presence of varying concentration of genistein were carried out.

A: % quench of fluorescence intensity, as a function of constituent genistein concentration.

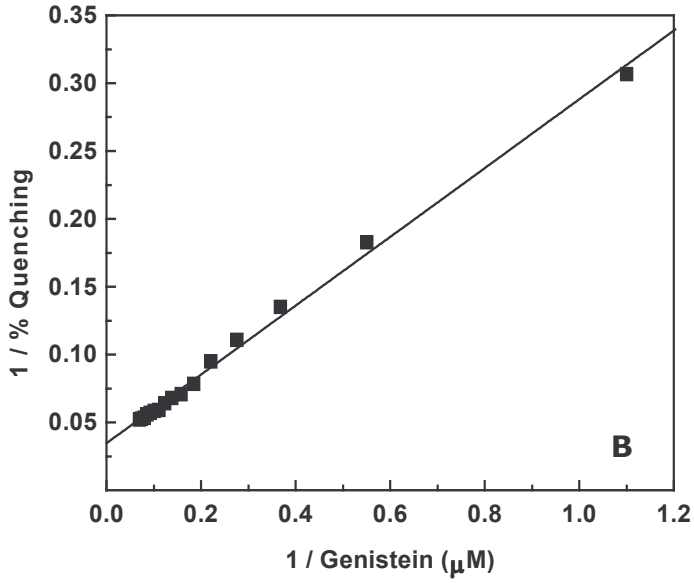

Figure 40B. Double-reciprocal plot of data in A; Q_{max} = 28±3 (± indicates probable error in all cases).

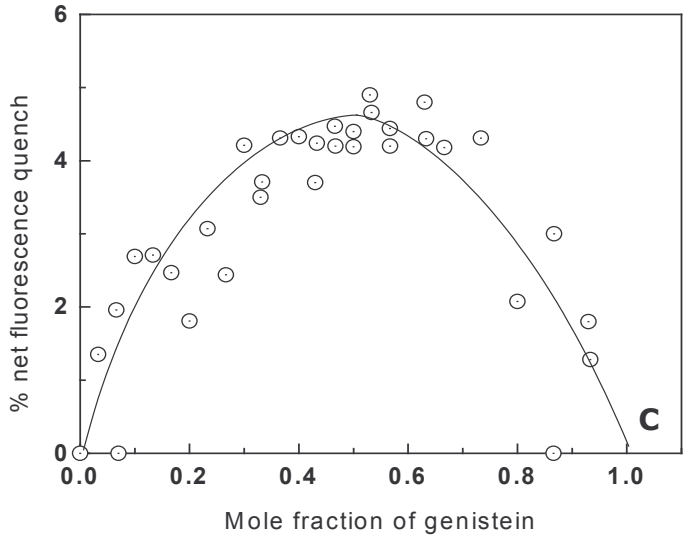

Figure 40C. Job's plot, C_{HSA} + $C_{genistein}$ = 10 μM showing the stoichiometry of 1: 1.

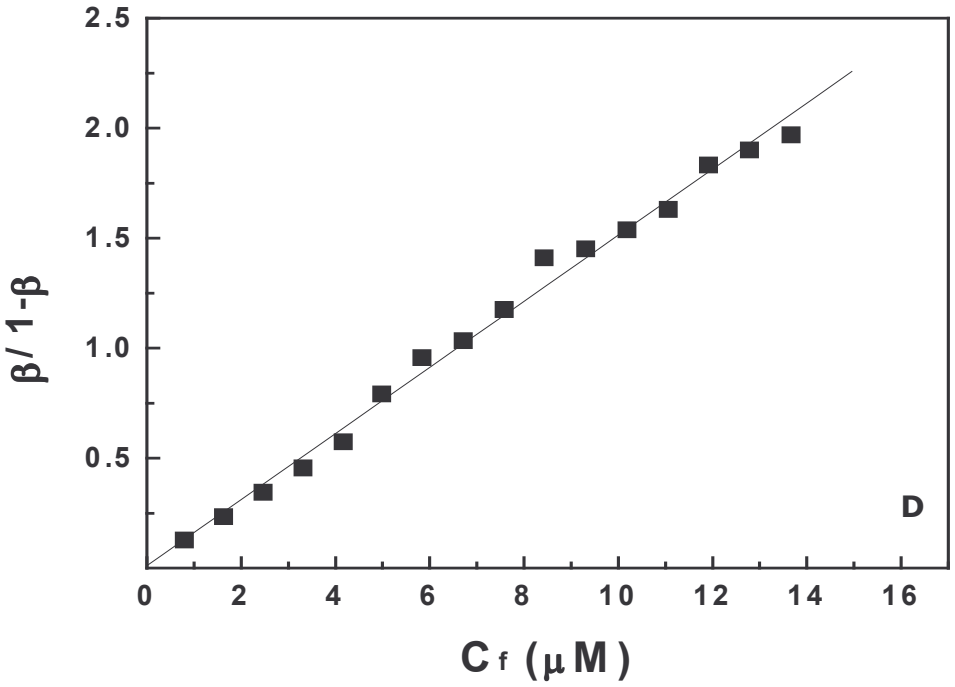

Figure 40D. Mass action plot of data.

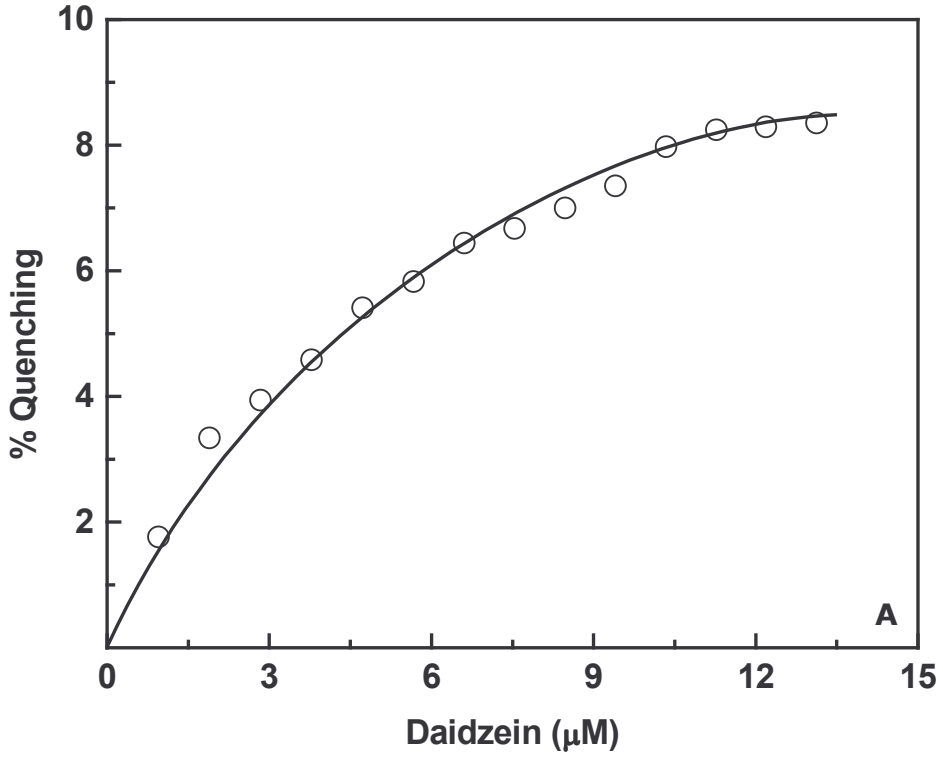

Figure 41. Quantitation of the interaction of HSA with daidzein by fluorescence quenching:

HSA (1μM) in 50 mM Tris-HCl buffer (pH 7.4) was titrated with increasing aliquots of stock daidzein solution (2 μl equivalent to 1 μM genistein per aliquot) in 80% methanol and the % quench was recorded. Blank titrations with N-acetyl tryptophanamide of equivalent absorbance at 280 nm as HSA in presence of varying concentration of daidzein were carried out.

A: % quench of fluorescence intensity, as a function of constituent daidzein concentration.

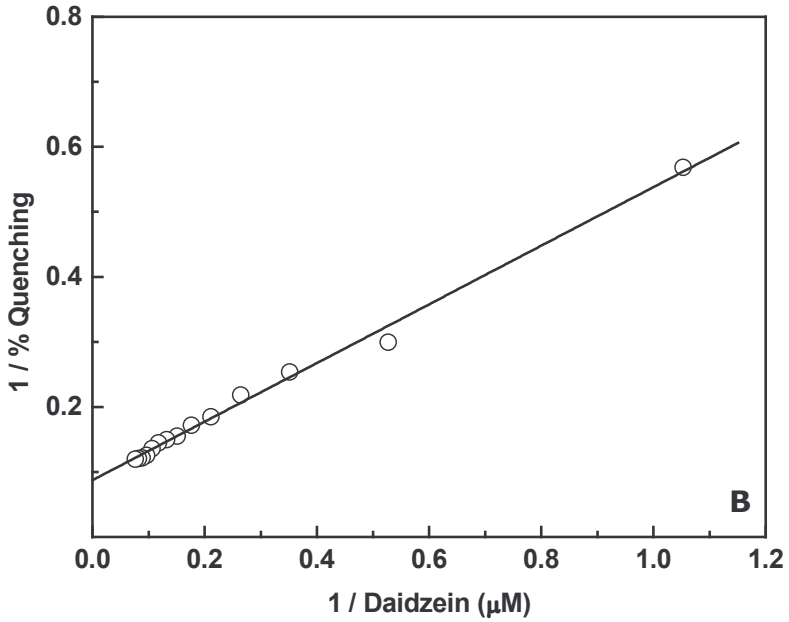

Figure 41B. Double-reciprocal plot of data in A; Q_{max} = 12±3 (± indicates probable error in all cases).

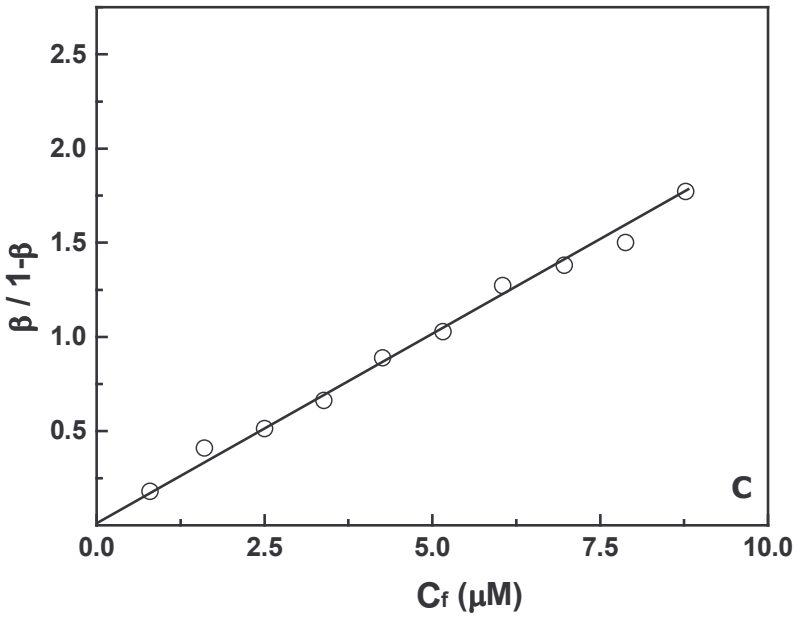

Figure 41C. Mass action plot of data.

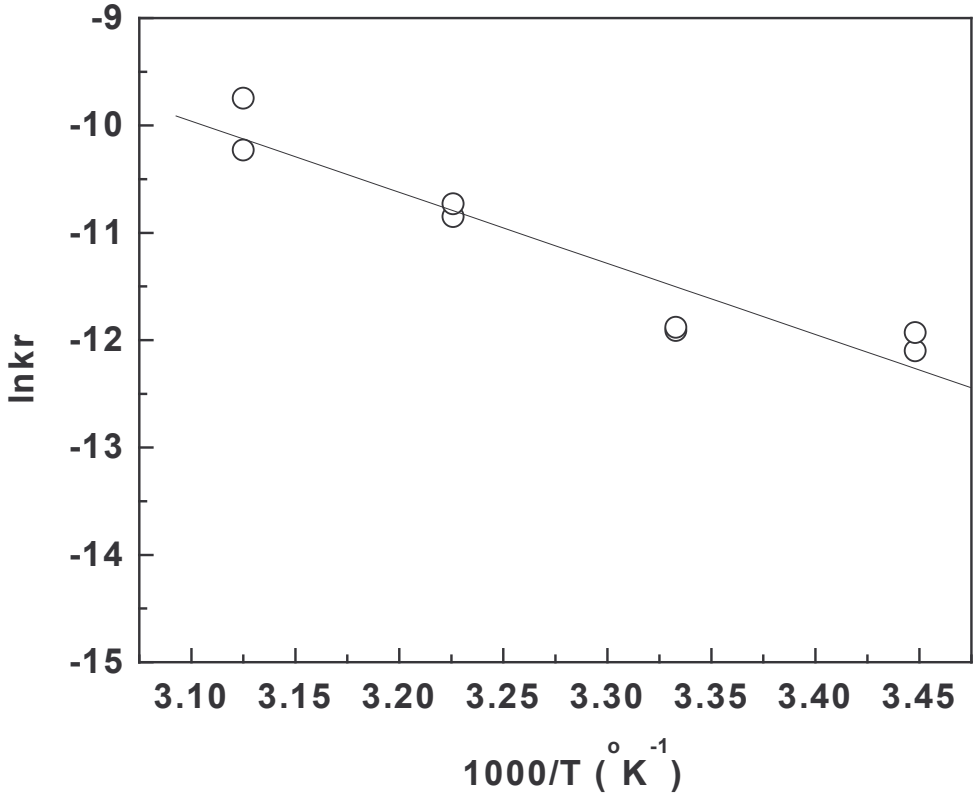

Figure 42. Effect of temperature on the binding constant of genistein to HSA: van't Hoff's plot.

HSA (1μM) in 50 mM Tris-HCl buffer (pH 7.4) was titrated with increasing aliquots of stock genistein solution (2 μl equivalent to 1 μM genistein per aliquot) in 80% methanol at different temperatures (17°C, 27 °C, 37 °C and 47 °C) and the % quench was recorded. Blank titrations were carried out as described for Fig. 40**.** van't Hoff's plot was constructed to obtain the thermodynamic parameters.

Effect of ionic strength on binding of genistein–HSA interaction: To determine whether ionic interactions played a role in genistein–HSA interaction, the ionic strength of the buffer was increased by the addition of potassium chloride (0 –200 mM). It was observed that Q_{max} remained unaltered on increasing the ionic strength of the buffer implying no change in the binding geometry. The binding constant decreased with increasing ionic strength (Fig. 43), establishing the role of ionic interaction in the binding.

The Stokes radius of HSA in presence of increasing concentrations of potassium chloride in buffer was measured by size exclusion chromatography. The elution volume of the protein increased with ionic strength indicating a decrease in Stokes radius (Fig. 43 inset). The decreased Stokes radius of the molecule could also contribute to the observed decrease in affinity.

Fluorescence of albumin bound daidzein: Daidzein is the only intrinsically fluorescent isoflavone among those studied. This property has been exploited to study the nature of binding to HSA. There is a shift of the emission maxima of the daidzein bound albumin towards shorter wavelengths (from 465 to 457nm) compared to unbound daidzein (Fig. 44). This indicates that daidzein is binding on the hydrophobic pocket in HSA.

Fluorescence quenching studies with defatted HSA and BSA: HSA and BSA have similar folding with a well- known primary structure. The important difference is that BSA has two tryptophan residues (W_{134} and W_{212}) located in domain I and domain II, respectively, while HSA has only one tryptophan at

position 214 in domain II. This property is employed to identify the binding pocket for isoflavones in serum albumin. Primary quenching curves of both HSA and BSA and the defatted HSA are plotted (Fig. 45A). The different intercepts of the double reciprocal plots (data not shown) correspond to different Q_{max} values. The overlap of the mass action plots (Fig. 45B), indicates that the binding constant for genistein is the same for both HSA and BSA, both of which are known to contain bound fatty acid. The quenching curve for genistein with fatty acid free HSA (Fig. 45A) shows that fatty acid free HSA binds genistein with a lower affinity (1.25×10^5 M^{-1}), compared to control. Bound fatty acid may enhance the affinity of genistein to serum albumin.

ANS binding studies: ANS, known to bind to hydrophobic pockets of the proteins, is a much-utilized fluorescent 'hydrophobic probe' for examining the non-polar character of proteins and membranes (Matulis and Lovrien, 1998). To examine systematically the role of hydrophobic interactions in the binding of genistein to serum albumin, ANS–bound HSA has been titrated with genistein. The replacement of ANS by genistein in the protein indicates that ANS and genistein bind to the same site. This is corroborated by the decrease in ANS- bound HSA fluorescence with increasing concentrations of genistein (Fig. 46). The binding constant, estimated by the competitive ligand binding measurements is ($1.27 \pm 0.2 \times 10^5$ M^{-1}), very similar to genistein-HSA interaction. The hydrophobic amino acid residues in HSA that form hydrophobic cavities in each domain interact with the alkyl chain of

fatty acids whereas two to three basic amino acid residues at the entrance of the hydrophobic pocket interact with the carboxy group of fatty acids (Spector, 1975).

Studies with Fatty acid: Among the various ligands, fatty acids alone can attach to the primary binding site of HSA. Experiments have been conducted using palmitic acid and defatted HSA to understand the affinity characteristics of genistein bound HSA. The increase in the fluorescence of genistein bound protein with the rise in fatty acid concentration evidences the displacement of genistein by palmitic acid (Fig. 47). It has been suggested that hydrophobic interactions are the dominant contributing factors for the affinity of fatty acid to HSA apart from electrostatic interactions (Bhattacharya *et. al.,* 2000).

Effect of genistein on tertiary and secondary structure of HSA: The effect of increasing genistein concentration on the tertiary and secondary structure of HSA has been studied by measuring CD spectra in near and far UV region, respectively. The characteristic patterns in the near UV region, caused by the asymmetric environment of tryptophan, tyrosine and phenyl alanine residues in the native structure, are not affected in presence of genistein, upto a concentration of 50 μM. This indicates that genistein has no effect on the tertiary structure of HSA. There are no changes in the far UV CD bands upto a concentration of 50 μM genistein, indicating that genistein had no effect on the secondary structure of HSA. These results helped to

establish that the genistein does not affect the conformation of serum albumin.

Warfarin binding using induced CD measurements: CD spectra in the near UV region (250 – 350 nm) were recorded for genistein (0 to 50 μM), HSA in presence of varying concentrations of genistein (0 to 50 μM), HSA (15 μM) in the presence or absence of warfarin (50 μM), with the concentration of genistein varying from 0 to 50 μM. Genistein did not exhibit any CD bands in the above wavelength region. HSA did not induce any CD band for genistein (0 to50 μM). However, the addition of warfarin to HSA induced a CD band at 310 nm and 255 nm (Fig. 48A). There was no decrease in the CD signal on adding genistein to the warfarin bound HSA; there was an additional CD band at 270 nm (Fig. 48B), which is not observed in the absence of warfarin. Warfarin, reportedly, binds to subdomain IIA (Petitpas *et. al.,* 2001). These results made it clear that genistein did not replace warfarin but binds alongside warfarin to HSA.

Binding of genistein in the presence of daidzein: The fluorescence of daidzein was found to increase on binding to HSA as mentioned in an earlier section. The saturation was reached at 14.75 μM HSA (Fig. 49A). Quenching of fluorescence was observed on adding genistein to the daidzein bound HSA, (Fig. 49B) indicating the replacement of daidzein by genistein. The quench was maximum at 27 μM of genistein. The binding constant of the competing ligand (Fig. 49C) was evaluated from a plot of F_{max} / F vs molarity of

genistein (Aceto et. al., 1995), the binding constant of genistein was calculated to be 5.63 x 10^5 M^{-1}.

Fluorescence anisotropy measurements: Fluorescence anisotropy measurements were made for the daidzein–HSA system by exciting at 340 nm (maxima for daidzein) and emission at 465 nm. There was an increase in fluorescence anisotropy of daidzein on binding to HSA. Anisotropy of daidzein increased from 0.01 to 0.25 on binding (Fig. 50). The increase in anisotropy could be due to the restriction imposed by the binding on the rotation around the daidzein molecule.

The anisotropy of daidzein bound to HSA is found to remain constant in the presence of diazepam. Diazepam is known to bind to the domain IIIA of HSA, which is the primary binding site for fatty acids. Warfarin also does not affect the anisotropy of daidzein bound to HSA. TIB decrease the anisotropy of daidzein from 0.16 to 0.08. The anisotropy of free daidzein is 0.02. Hence, TIB partially displace the daidzein in HSA (Table 4).

The anisotropy of warfarin bound to HSA was measured in the presence of genistein. The anisotropy of warfarin bound to HSA (5 μM bound to 10 μM HSA) was found to be 0.5. This was unaltered with the addition of genistein even up to 100 μM revealing that warfarin was not displaced by genistein (Table 5).

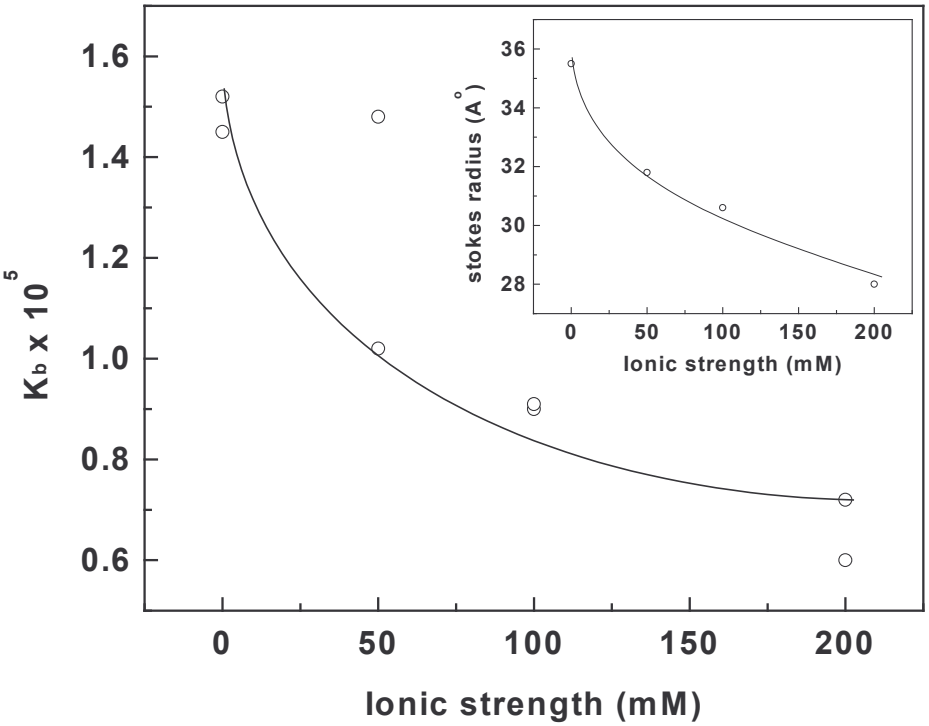

Figure 43. Effect of ionic strength on the binding constant of genistein to HSA:

A plot of the binding constant as a function of ionic strength to show the effect of ionic strength on the binding constant of genistein. HSA (1μM) in 50 mM Tris-HCl buffer (pH 7.4) was titrated at different ionic strengths adjusted by using potassium chloride (0 mM, 50 mM, 100 mM and 200 mM) with increasing aliquots of stock genistein solution (2 μl equivalent to 1 μM genistein per aliquot) in 80% methanol. The % quench of the intrinsic fluorescence of HSA was recorded. Blank titrations were carried out as described for Fig. 40.

Inset: Stokes radius of HSA at different molarities of KCl (0 – 200 mM) was determined by size exclusion chromatography on HPLC using a TSK SW 2000 column (300 x 4.6 mm, 4μ). The column was preequilibrated at the required ionic strength attained using KCl of buffer 50 mM Tris-HCl (pH 7.4). Equilibrated samples (20 μl) of the protein (1 mg/ ml) were injected at 27°C at a flow rate of 0.2-ml/ min. The protein was eluted isocratically using the same buffer and detected at 280 nm.

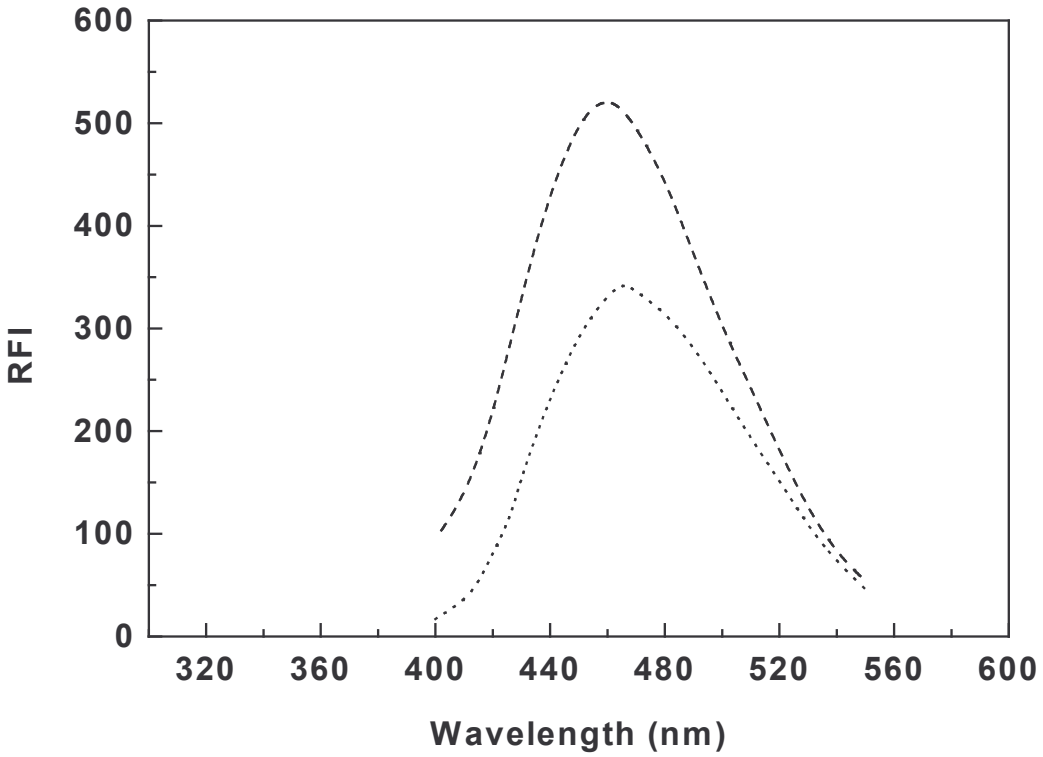

Figure 44. Emission spectra of daidzein showing blue shift on binding to HSA.

Daidzein (2.75 μM) in 50 mM Tris–HCl (pH 7.4) was titrated against increasing concentrations of HSA in the same buffer. The final concentration of HSA was 14.75 μM. Stock HSA (835 μM) was added in 5 μl aliquots and the spectra recorded between 400 – 550 nm after excitation at 340 nm, the excitation maxima for daidzein. Excitation slit width was 5nm and emission slit width was 10nm.

Dotted line: free daidzein*; dashed line*: daidzein bound to HSA, concentration of HSA is 14.75 μM.

Table 3. Comparison of the genistein (ligand) distance to tryptophan (HSA) measured by Forster non-radiative energy transfer with other ligands bound to HSA.

Ligand	J ($cm^3.L.M^{-1}$)	R_o (nm)	r (nm)
Shikonin [99]	3.76×10^{-14}	2.08	2.12
Bendroflumethiazide [162]	5.86×10^{-16}	1.55	1.47
3-hydroxy flavone [213]	1.64×10^{-14}	2.54	2.55
Quercetin* [20]	1.35×10^{-13}	3.35	3.78
Rutin*	1.56×10^{-13}	3.43	5.61
Hyperin*	1.57×10^{-13}	3.44	5.05
Baicalin*	6.58×10^{-14}	2.97	4.46
Ferulic acid[$] [110]	1.26×10^{-14}	2.53	3.57
Chlorogenic acid[$] [110]	2.53×10^{-14}	1.95	2.45
Genistein (present study)	8.35×10^{-15}	2.25	3.68
Daidzein (present study)	9.28×10^{-15}	2.29	4.35

Table 4. Corrected fluorescence anisotropy values of the daidzein-HSA complex, when different aliquots of warfarin, diazepam and triiodobenzoic acid were added.

Concentration (μM)	Anisotropy values
Warfarin	
0	0.160
16	0.162
32	0.157
48	0.158
64	0.158
80	0.154
96	0.152
Daizepam	
0	0.160
20	0.162
40	0.158
60	0.157
80	0.159
100	0.157
Triiodobenzoic acid	
0	0.160
11	0.149
23	0.142
35	0.136
46	0.127
57	0.120
69	0.116
92	0.109
115	0.097
137	0.092
160	0.080

Table 5. Corrected fluorescence anisotropy values of the warfarin-HSA complex, when different aliquots of genistein were added.

Concentration (μM)	Anisotropy values
0	0.500
20	0.503
40	0.502
60	0.503
80	0.501
100	0.503

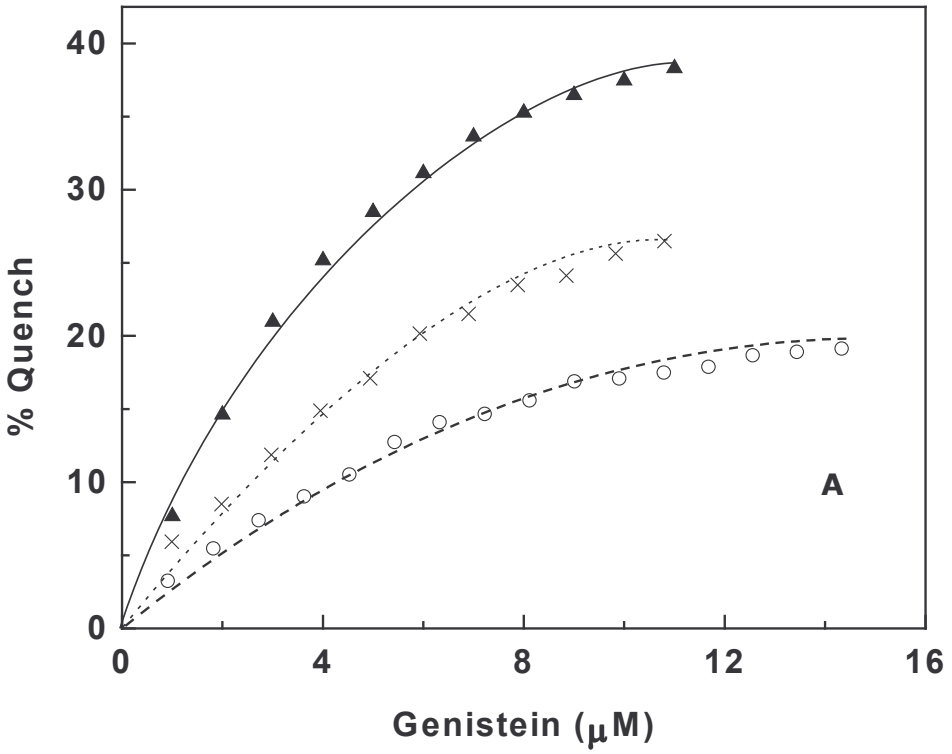

Figure 45A. Interaction of genistein with HSA, defatted HSA and BSA: HSA (1μM) was titrated with increasing aliquots of genistein and the % quench was recorded. HSA was defatted by the procedure described previously and the effect of fatty acid removal on genistein binding was followed by fluorescence quenching measurements. HSA (-O-) defatted HSA (-x-), BSA (-▲-). The excitation and emission slit widths were at 5 and 10 nm respectively. Conditions were same as described for Fig. 40.

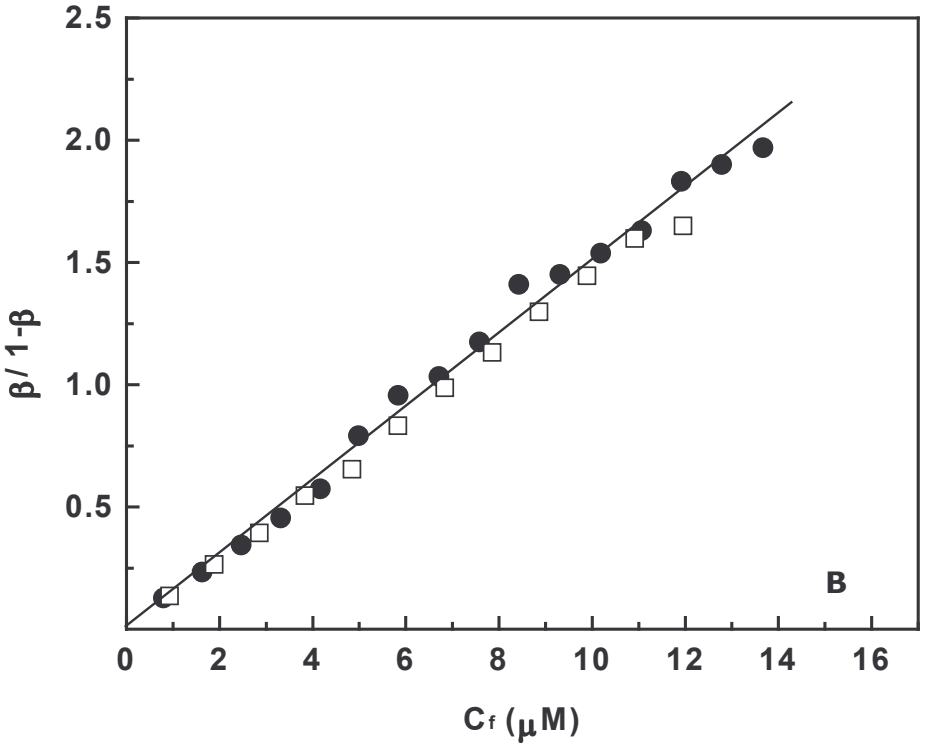

Figure 45B. Mass action plot of HSA and BSA:

HSA (1μM) or BSA in 50 mM Tris-HCl buffer (pH 7.4) was titrated with increasing aliquots of genistein and the % quench in fluorescence was recorded as described for Fig. 40. The mass action plot was constructed from the double reciprocal data to obtain the binding constant. ●-HSA; □-BSA

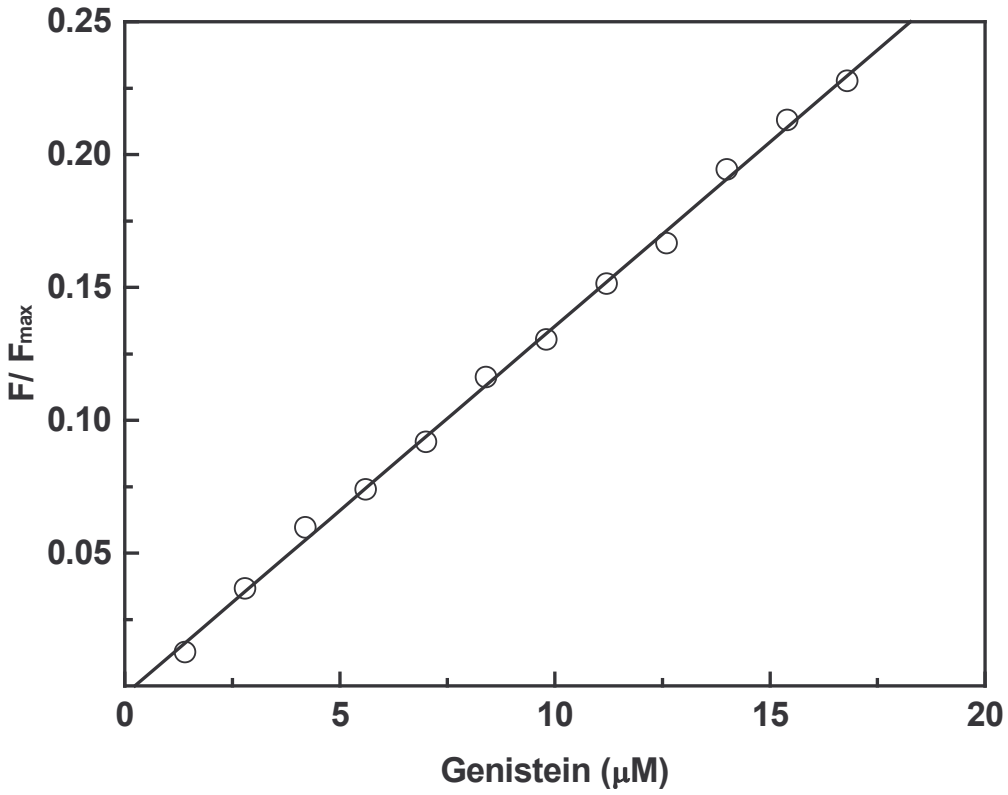

Figure 46. Fluorimetric titration of HSA-ANS complex with genistein:

The concentration of ANS is 3 μM and HSA is 1μM. The excitation and emission wavelength for HSA-ANS complex is 375 nm and 465 nm. Excitation and emission slit widths were 5 nm and 10 nm respectively.

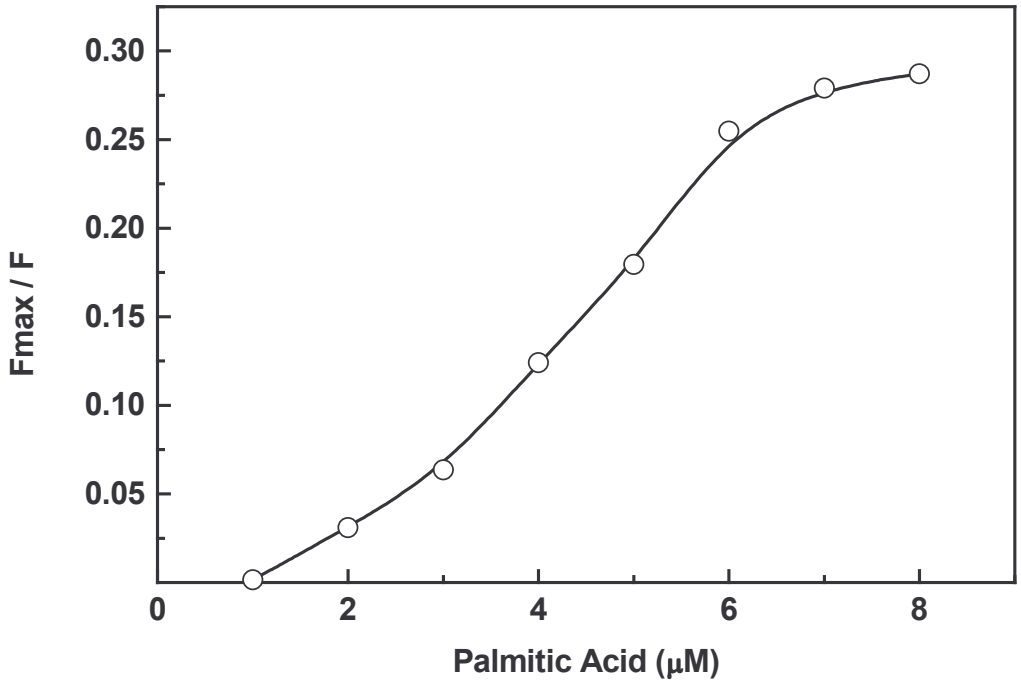

Figure 47. Fluorimetric titration of HSA-genistein complex with palmitic acid: The concentration of genistein is 10 μM and HSA is 1μM. The excitation and emission wavelength for HSA-genistein complex is 295 nm and 342 nm. Excitation and emission slit widths were 5 nm and 10 nm respectively.

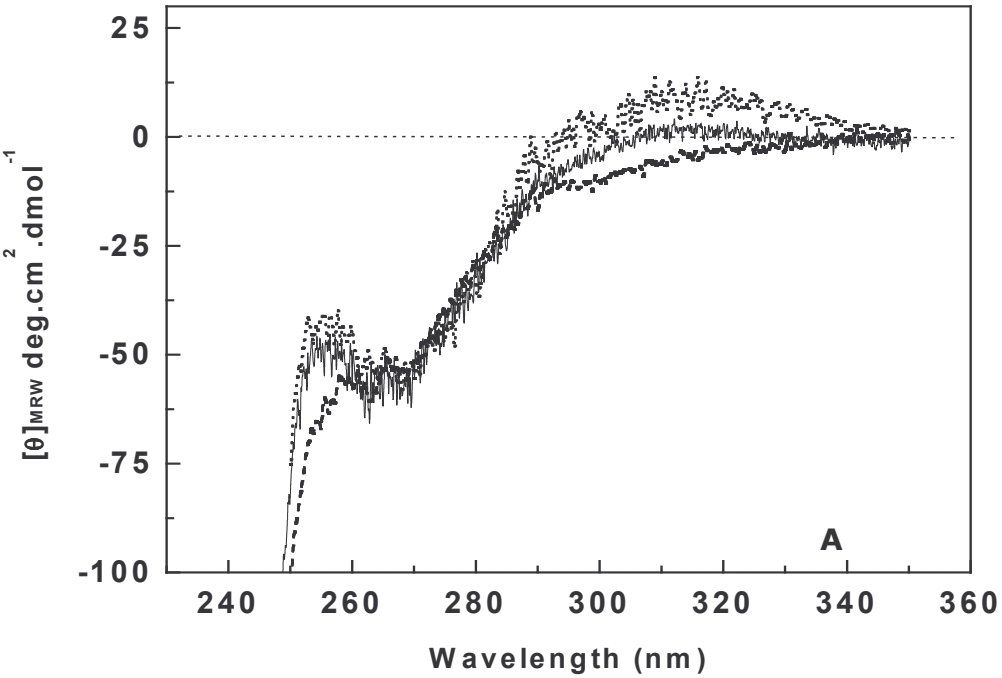

Figure 48. Competitive ligand interactions of HSA: warfarin and genistein: CD measurements were carried out in the near UV region of 250 – 350 nm in 50 mM Tris-HCl buffer (pH 7.4). The cell path length was 1 cm and spectra were recorded at a speed of 10 nm min^{-1}. All scans are an average of 3 runs. A mean residue weight of 115 was used for calculating the molar ellipticity values.

A. Effect of warfarin on the near UV CD of HSA**:**

The concentration of HSA used was 15 μM and warfarin at concentrations of 0 – 50 μM. *Dashed line*: HSA in buffer; *Solid line*: HSA with 10 μM warfarin; *Dotted line*: HSA with 50 μM warfarin.

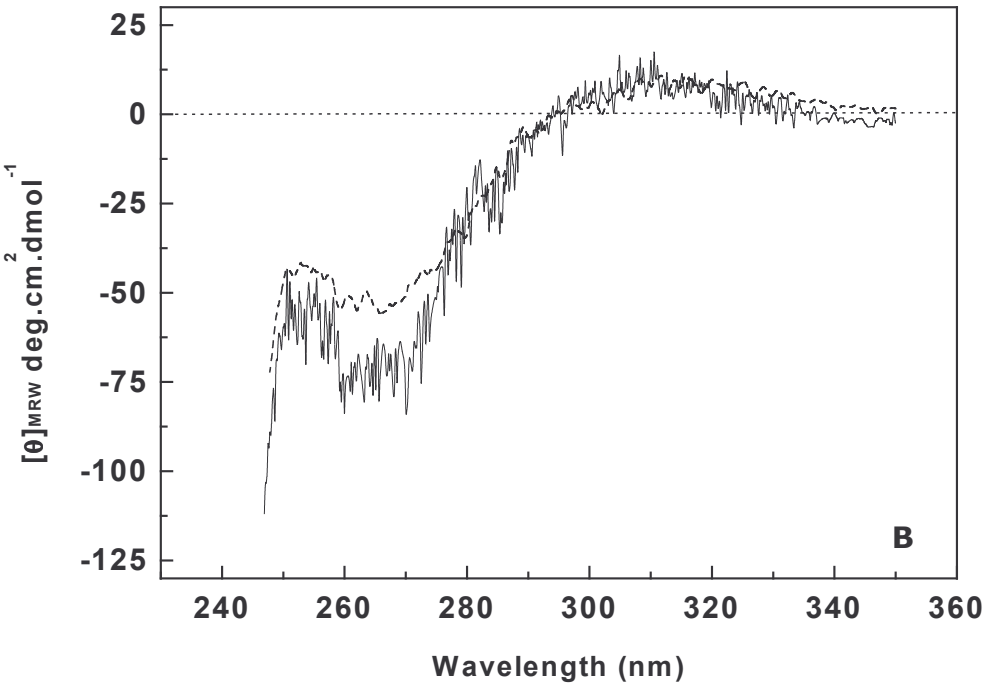

Figure 48B. Effect of genistein on near UV CD of warfarin–bound HSA: Spectra were recorded after genistein (50 μM) was added to HSA with 50 μM warfarin. *Dashed line*: HSA in presence of warfarin (50 μM); *Solid line*: 50 μM genistein in presence of warfarin-bound HSA (50 μM).

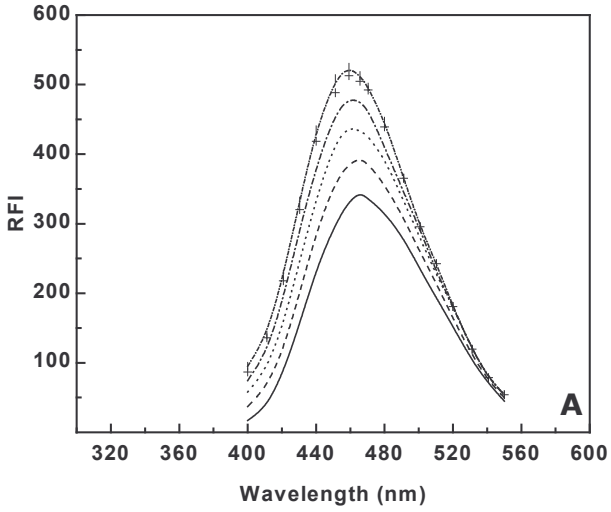

Figure 49A. Competitive ligand binding interactions of HSA: Genistein and daidzein (Fluorescence measurements).

Daidzein (2.75 μM) was titrated against increasing concentrations of HSA to a final concentration of 14.75 μM) in 50 mM Tris–HCl buffer (pH 7.4). The excitation wavelength was 340 nm and emission range was 400-550 nm. Excitation slit width was 5 nm and emission slit width was 10 nm. To the above solution, 5 μl of stock genistein in 80% methanol (1.4 mM) was added in aliquots and the spectra recorded at 27°C. The final concentration of genistein was 27 μM.

A. Emission spectra of daidzein with increasing micro molar concentration of HSA (*Solid Line* 0; *dashed line* 1.66; *dotted line* 4.98; *dashed and dotted line* 8.26; ++++ 11.52; *short dash and dotted line* 14.75)

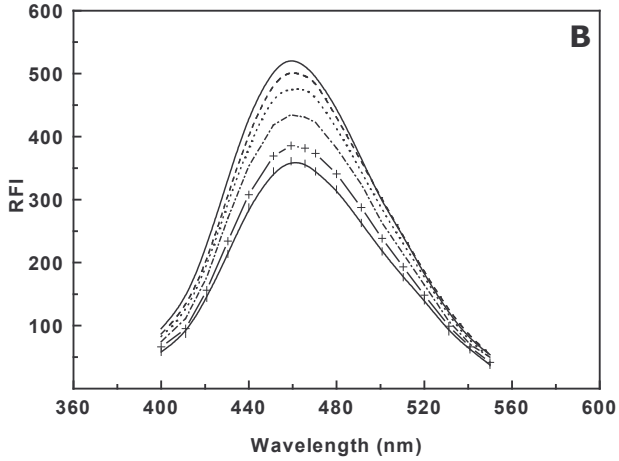

Figure 49B. Emission spectra of daidzein-HSA complex with increasing micro molar concentration of genistein (*Solid Line* 0; *dashed line* 5.48; *dotted line* 10.92; *dashed and dotted line* 16.29; -+-+- 21.64; —|—|— 26.94).

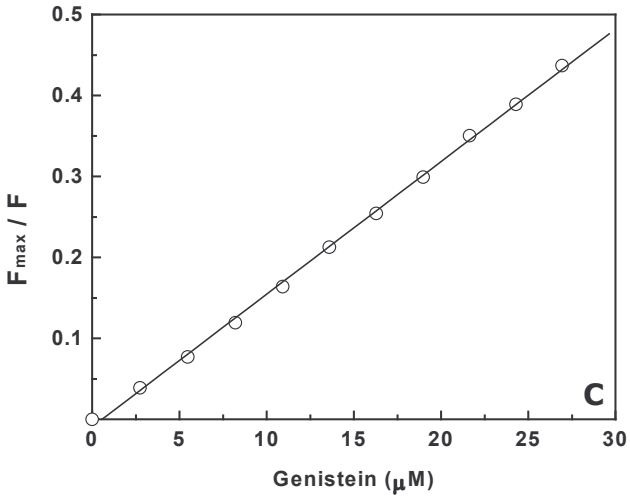

Figure 49C. F_{max} / F vs genistein concentration to obtain the binding constant of the competing ligand–genistein

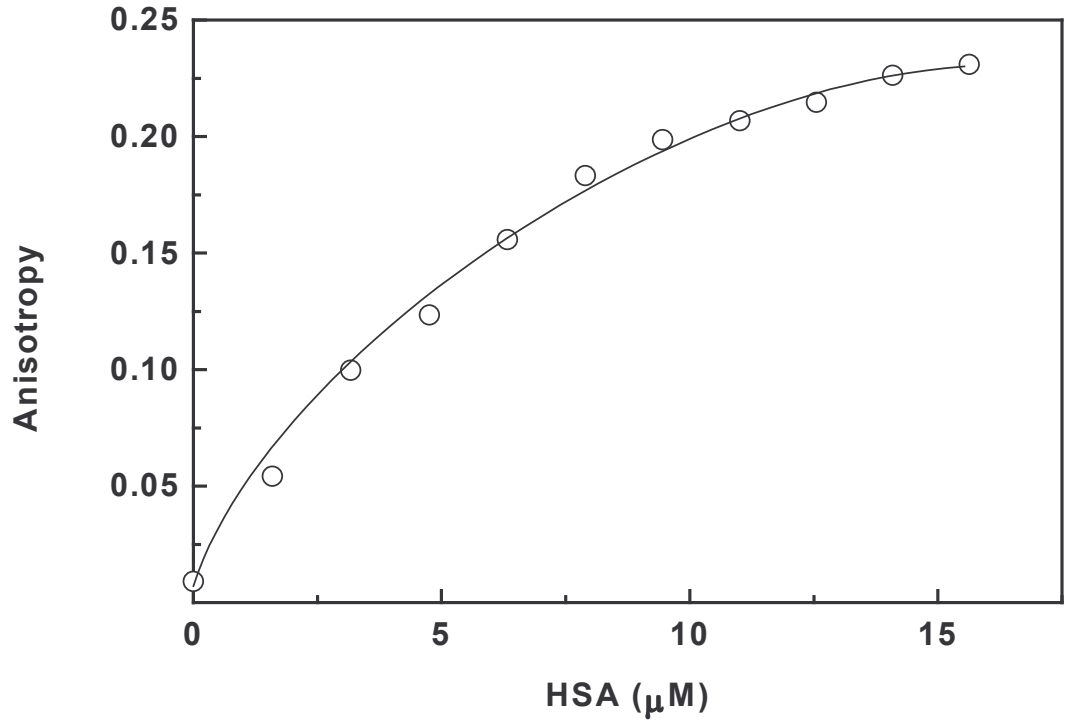

Figure 50. Variation in fluorescence anisotropy of daidzein as a function of HSA concentration:

Daidzein (2.75μM) was titrated against increasing concentrations of HSA. The excitation and emission wavelengths were 340 and 465 nm respectively. Slit widths were at 5 and 10 nm for excitation and emission respectively.

DISCUSSION

The characteristic of albumin to allow a variety of ligands to bind to it is amazing. Albumin is the principal carrier of fatty acids that are otherwise insoluble in the circulating plasma. Serum albumin is composed of three homologous domains (I, II and III). Each domain, in turn, is the product of 2 subdomains, which are predominantly helical and extensively cross-linked by several disulfide bridges (Carter and Ho, 1994). The typical binding constants for various ligands range from 10^4 to 10^6 M^{-1}. The vast majority of ligands bind reversibly on one or both sites within specialized cavities of sub domains IIA and IIIA of albumin. The binding property of the subdomain IIIA of albumin is general, whereas that of subdomain IIA is more specific. The amino acid residues that line the cavities are quite similar in charge distribution for both the subdomains IIA and IIIA. Yet, they impart desired selectivity. In each of the two subdomains, there is an asymmetric charge distribution, leading to a hydrophobic surface on one side and a basic or positively charged surface on the other. This explains the discriminatory affinity of albumin for small anionic compounds. The van der Waals surface of the binding pocket in IIA appears like an elongated sock wherein the foot region is primarily hydrophobic and the leg is primarily hydrophilic. The opening to the pocket is clearly accessible to the solvent. The affinity of flavonoids for serum albumin is in line with its general ability to bind small negatively charged ligands (He and Carter, 1992; Carter and Ho, 1994; Peters Jr, 1985).

Results of the present study indicate that the binding of genistein to HSA and BSA by equilibrium dialysis is characterized by the equilibrium constant 1.0 ± 0.2 x 10^5 M^{-1} (Fig. 38) and 1.78 ± 0.2 x 10^5 M^{-1} (Fig. 24). The binding constants obtained by fluorescence quenching measurements for genistein and daidzein to HSA are 1.5 ± 0.2 x 10^5 M^{-1} and 1.4 ± 0.2 x 10^5 M^{-1}; genistein and daidzein to BSA are 1.5 ± 0.2 x 10^5 M^{-1} and 1.2 ± 0.2 x 10^5 M^{-1} respectively. Thus, there is good agreement in the binding constants obtained for genistein-HSA interaction and genistein-BSA interaction by both direct and indirect methods. The binding of the isoflavones to HSA is similar and the R_2 group at position 5 of the aromatic A-ring does not play a significant role in the binding of either genistein or daidzein (Fig.1). The B-ring of the flavonoids is electron richer than the A-ring, rendering it more susceptible to ionization at physiological pH (Jovanovic *et. al.,* 1994). The reported plasma concentrations of daidzein and genistein are in the range of 50–800 μg/liter (Setchell and Cassidy, 1999). Thus, the concentrations used to determine the equilibrium constant are physiologically relevant. The interaction of genistein and daidzein with HSA is difficult to be followed by isothermal calorimetry due to the limited solubility of the above in aqueous buffers employed in the study.

The decrease in the binding constant with increase in temperature (Fig 29 & 42), suggests the involvement of non-covalent interactions and a major role for ionic interactions in the binding of genistein to HSA and BSA, which is further corroborated by the observed decrease in the binding constant on the addition of potassium chloride. The negative free energy values indicate that

the binding is spontaneous and that it is energetically more favorable for genistein or daidzein to link to serum albumin. Negative entropy indicates a loss in the degree of freedom of genistein when embedded in the HSA cavity. The effect of KCl and temperature point to the presence of electrostatic interactions apart from the hydrophobic interactions.

The blue shift of daidzein bound protein fluorescence (Fig. 44) is indicative of the role of hydrophobic interactions in the binding of this aglycone to HSA and BSA (Fig. 31) with the emission maxima shifting from 465 to 457 nm. The binding of daidzein to a hydrophobic pocket in HSA may be a cause for this phenomenon. Further, fluorescence of the albumin bound ANS is found to be quenched by the addition of either genistein or daidzein. The observed concentration dependence of quenching of fluorescence indicates that the binding sites of ANS and genistein are the same apparently leading to possible replacement of ANS by the isoflavones. These experiments suggest the involvement of hydrophobic interactions in the binding of genistein or daidzein to HSA and BSA. Isoflavones, genistein and daidzein (Fig.2), have a flavone nucleus made up of two benzene rings (A and B) linked through a heterocyclic pyrane C ring. These aromatic rings may be involved in hydrophobic interactions with hydrophobic pockets of domain IIA of HSA. The complete three-dimensional structure of human serum albumin has recently been determined by X-ray crystallography, and the binding sites for several drugs have been identified. ANS reportedly binds to two sites on HSA – IIA and IIIA, with a binding constant of 7.9 x $10^4 M^{-1}$ and 8.7 x $10^5 M^{-1}$

respectively. Subdomain IIIA is the site where ANS binds to HSA with a higher affinity (Bagatolli *et. al.,* 1996).

The intrinsic fluorescence of albumin is due to the tryptophan residue (W_{214}) (Carter and Ho, 1994), conserved in all mammalian albumins and located strategically in the domain IIA for developing van der Waals interactions with ligands bound at that site (Dangles *et. al.,* 2001). Domain IIA has five lysine residues (positions 203, 210, 220, 231 and 241) and one arginine residue at position 218. These residues are positively charged at the pH used in the present study and could contribute to ionic interactions with genistein or daidzein. Genistein and daidzein have a phenolic structure with conjugated double bonds. Albumin is known to reversibly complex with phenols via hydrogen bonding and hydrophobic interactions (Maliwal, *et. al.,* 1985).

The increase in anisotropy of daidzein bound HSA and BSA with increase in protein concentration, (Fig. 36 & 50), indicates the reduction of freedom of rotation of daidzein bound HSA and BSA. Increase in anisotropy may be due to decreased Brownian motion or energy transfer between identical chromophores. The high value of anisotropy (0.25) indicates that daidzein is binding at a motionally restricted site on HSA and BSA.

Identification of the binding pocket for isoflavones on HSA. The binding pocket on HSA for isoflavones was identified through (i) Förster energy transfer measurements; (ii) binding of genistein with HSA and BSA; and (iii) competitive ligand binding measurements using warfarin.

Förster distance (R_0) and the distance between acceptor and donor (r_0) for the genistein and daidzein were in the range known to prove that non-radiation transfer occurred between these isoflavones and HSA.

The quenching of intrinsic fluorescence measurements of HSA and BSA by genistein (Fig. 45A & B) assist in identification of the binding site on the albumin molecule. The Q_{max} for HSA is 28% compared to 53% with BSA. The difference between HSA and BSA is the presence of an additional tryptophan in BSA at position 134. This is at site II, the interface of domain IA and IIA of HSA (Peters Jr, 1985). The conserved tryptophan is at position 214. The binding constants for genistein with BSA and HSA are same, the stoichiometry for binding being 1:1. The isoflavone has an identical binding site on both the molecules. Hence, the binding site on both the albumins for genistein is the same.

Our extrinsic CD measurements of genistein binding in presence of warfarin suggest that the binding is inclusive. There is enough conformational flexibility in domain IIA of HSA to accommodate both warfarin and genistein. The binding of warfarin and its crystal structure with HSA-myristic acid is reported (Petitpas *et. al.,* 2001). Warfarin has only one binding site in domain IIA having tryptophan at 214. The structure and binding constant of genistein with warfarin are similar. Tryptophan residue (W_{214}) is in domain IIA, which explains the quenching of protein fluorescence due to genistein binding. In the case of BSA, the additional tryptophan W_{134} is very near to W_{214} (Peters Jr, 1985). The accommodation of genistein at site I may, therefore, quench the fluorescence due to both tryptophans in BSA,

corroborating the higher quenching observed in case of BSA. The modification of tryptophan residues on HSA has resulted in the loss of interaction of genistein with albumin. Quercetin (3, 5, 7, 3, '4' –pentahydroxy flavone, a plant derived flavonoid compound) binds to HSA with an association constant of 1.46 x 10^4 M^{-1} at 37°C in the large hydrophobic cavity of subdomain IIA and the protein micro environment of this site is rich in polar (basic) amino acid residues which are of help in stabilizing the negatively charged ligand bound in non planar conformation. The position of Quercetin within the binding pocket similarly allows simultaneous binding of other ligands such as warfarin or sodium salicylate [Kragh-Hansen, 1988; Zsila *et. al.,* 2003). However, the binding of daidzein in HSA excluded genistein. This has a ramification in the transport of these isoflavones. Both daidzein and genistein are present in soy-based foods in the ratio 1:3.

The binding of 17β-oestradiol to domain II of human serum albumin is already reported (André *et. al.,* 2003). Binding constant of this ligand to HSA is 1.11 $\pm$ 0.28 x 10^5 M^{-1} (Daughaday, 1959). Structures of both genistein and daidzein being very similar to 17β-oestradiol (Fig. 2), they can be expected to bind to the same domain in HSA as 17β-oestradiol.

Fluorescence anisotropy measurements

Our experiments show that anisotropy of daidzein-HSA and daidzein-BSA complex does not change in the presence of either warfarin or diazepam indicating that they are not displacing daidzein from the complex. There is a decrease in anisotropy from 0.16 to 0.08 (in presence of 160 μM TIB)

observed when the daidzein- HSA complex and daidzein-BSA complex is titrated with TIB (Table 1 & 4).

TIB is shown to bind to two well- separated binding sites, one distinctly more occupied than the other. The well – occupied site (total occupancy 0.74) is located in sub-domain IIA (Curry *et. al.,* 1998). A second site occurs in sub-domain 1B and only occurs in the presence of significant amounts of bound fatty acid. This strengthens our observation that daidzein and genistein are binding to sub domain IIA. Warfarin can bind alongside the isoflavone and hence there is no change observed in the anisotropy. Titration of the warfarin-HSA complex and warfarin-BSA complex with genistein also does not result in any change in anisotropy (Table 2 & 5) further strengthening our argument that warfarin and genistein bind simultaneously and in the near vicinity of one another. Diazepam, a characteristic marker ligand for sub domain IIIA (primary fatty acid binding site) (Maruyana *et. al.,* 1993) also does not displace the daidzein in the daidzein–HSA and daidzein–BSA complex ruling out the binding of isoflavones to sub domain IIIA.

Binding site details – outlining potential residues and cavities within sub domain IIA. Based on the experimental work the possibility of simultaneous binding of warfarin and genistein has been raised. It is important to check if the binding site of HSA has space and appropriate shape and residues to accommodate both warfarin and genistein. The main purpose of the computational analysis of 3-D structure and modeling is to ensure that the space and suitable residues for interaction are available at the binding site of HSA in order to accommodate genistein in addition to

accommodating warfarin. Results obtained from the interaction of genistein and warfarin to HSA by CD measurements indicate that both ligands bind simultaneously to sub domain IIA of HSA. Stoichiometric analysis indicates that genistein binds to HSA and BSA in 1:1 ratio as warfarin, suggesting that genistein occupies a unique binding site in domain II distinct from the binding site of warfarin. However, daidzein bound to HSA and BSA can be easily displaced by genistein despite the presence of additional hydroxyl group in ring A of genistein. Therefore, the recognition of unique binding sites in HSA by genistein and warfarin is due to significant structural differences in ring B and such characteristic binding mode could be explained using the crystal structure of HSA/warfarin complex (Petitpas *et. al.,* 2001). The phenyl group of warfarin binds in a sub-pocket formed by Phe_{211}, Trp_{214}, Leu_{219} and Leu_{238} with additional aliphatic contacts from Arg_{218} and His_{242}.

The docking search in and around the warfarin bound site of HSA-warfarin complex structure readily resulted in the identification of a site suitable for accommodating genistein. The predicted genistein binding site is located approximately at a distance of 7Å from warfarin. A number of residues at the binding site have the possibility of their interaction with the –OH groups in genistein. The sidechains include a few optimally charged residues such as His_{440}, His_{288}, Lys_{195}, Lys_{199} and Arg_{160}. Optimization of the positions of these polar side chains can result in favorable hydrogen bonding interactions depending upon the precise position and orientation of genistein, which are difficult to predict accurately with high reliability. Figure 51 shows the close-up of the binding site with a number of possible polar and other residues

capable of interacting with genistein. The ring systems in genistein are potentially accommodated by a network of aromatic residues at the binding site (Fig. 51). These residues include Trp_{214}, Phe_{211}, Tyr_{452}, Phe_{157}, Phe_{149} and Tyr_{150}. While all these aromatic residues may not interact with genistein, some of these residues are likely to interact depending upon the precise orientation and positioning of the genistein within a broader predicted binding site. The interactions of both ligands with albumin are dominated by hydrophobic and electrostatic interactions (supported by thermodynamic analysis).

The binding of genistein and daidzein to serum albumin has been investigated through experimental methods as well as molecular visualization. Experimental results, including the thermodynamic parameters of binding, are in consonance with the indications from the molecular visualisation. The various parameters that have a bearing on the binding of the isoflavones to albumin have been derived from the measurements of protein fluorescence, binding constants and fluorescence anisotropy.

It is extremely difficult to predict the accurate 3-D structure of the ternary complex with precise details of interactions between protein residues and genistein. However, the current analysis clearly shows that space and optimal residues congenial for interaction with genistein exist in HSA structure even when it is bound to warfarin. Thus the modeling studies are consistent with the experimental findings and support the idea of simultaneous binding of warfarin and genistein in HSA.

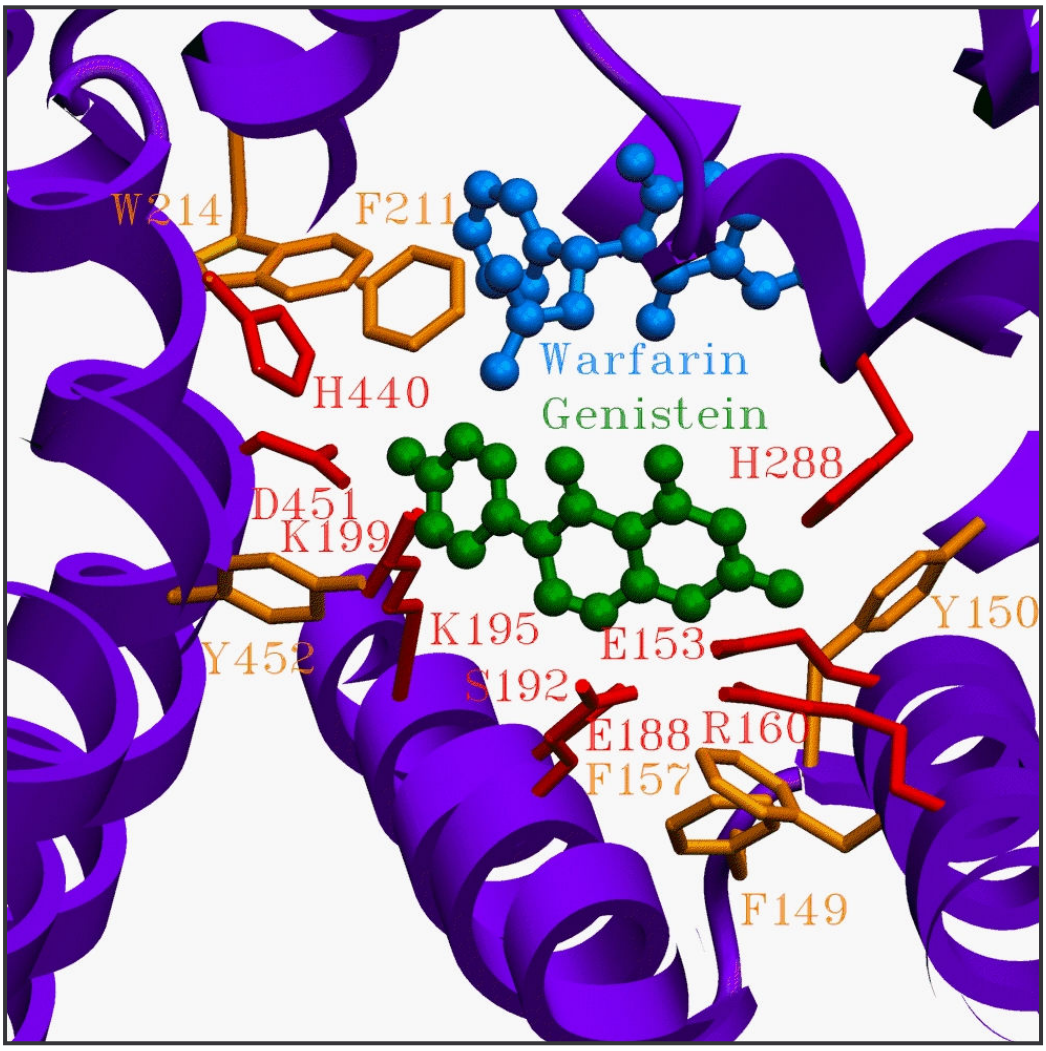

Figure 51. Molecular visualization of binding of genistein with HSA/warfarin complex**.**

The crystal structure of HSA/warfarin complex (PDB ID: 1h9z) was used to understand the possible binding mode of genistein with HSA.

Close-up of the binding site of the modeled structure of HSA-warfarin-genistein ternary complex. The violet ribbons correspond to the backbone of HSA. Warfarin in the crystal structure and modeled genistein are shown in ball and stick representation in blue and green respectively. A set of sidechains of polar residues and aromatic residues that is congenial for interaction with genistein depending on its precise positioning and orientation are also shown. This figure has been produced using Setor program.

Section B: Interaction of isoflavones with domains of human serum albumin

Results and Discussion

Human serum albumin molecule is made up of three homologous regions representing the domains [domain I (residues 1-195), II (196-383) and III (384-585)] of the protein tertiary structure. Each domain consists of three disulfide linked double-loops. According to domain theory fragment N represents the domain 1 shorter by one disulfide double-loop. The fragment M representing the domain 2 includes the middle part of the molecule longer by a double loop of fragment N and shorter by a double loop, which is linked to domain C. Fragment M is the only domain with uninterrupted polypeptide chain. The fragment C includes the complete domain 3, which is longer by a double loop coming from M fragment. But fragment C is interrupted at three positions, but its integrity is preserved due to its disulfide bonds joining the double loops (Brown, 1975; Saber *et. al.,* 1977).

Purification of domains: Fig. 52 shows the gel filtration profile of CNBr cleaved human serum albumin fragments. Fragment C and N+M are obtained. Fig. 53 shows the ion exchange profile of N and M fragments.

Non-reducing SDS-PAGE of purified domains: The purity of isolated domains has been checked by running SDS-PAGE under non-reducing conditions. The purity of domains is > 95% as shown in Fig. 54.

Circular Dichroic analysis of CNBr fragments:

The isolated domains have been purified under denaturing conditions. Their secondary structure has been analyzed to check the integrity of the purified domains and compared with native human serum albumin molecule (Table 6) gives the secondary structural analysis of the native and purified domains of human serum albumin. There is a slight decrease in the α-helix content of isolated domains when compared to the native molecule. This may be due to the disruption of bonds stabilizing the tertiary structure of albumin, as they are subjected to denaturing conditions during isolation of the domains. So analysis of secondary structure reveals that there is no major change in the secondary structure. The interaction of isoflavones with domains of serum albumin is justified.

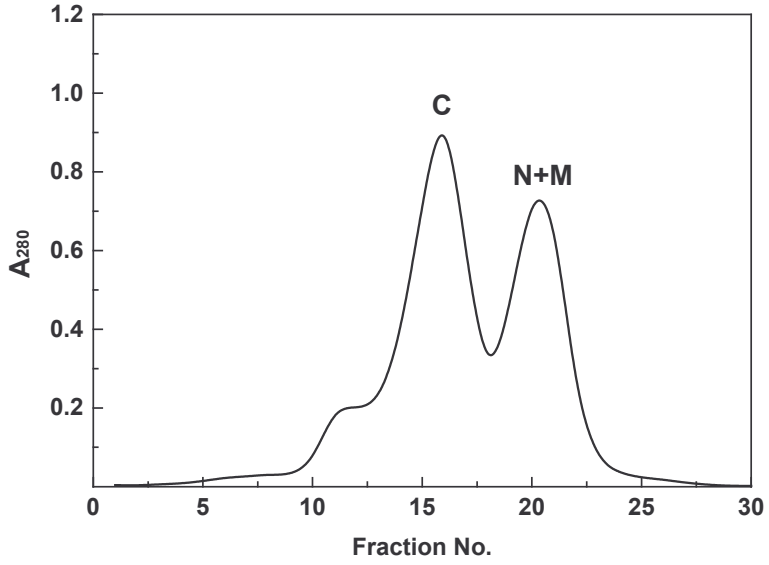

Figure 52. Elution profile of cyanogen bromide fragmented HSA on a sephadex G-100 gel filtration column:

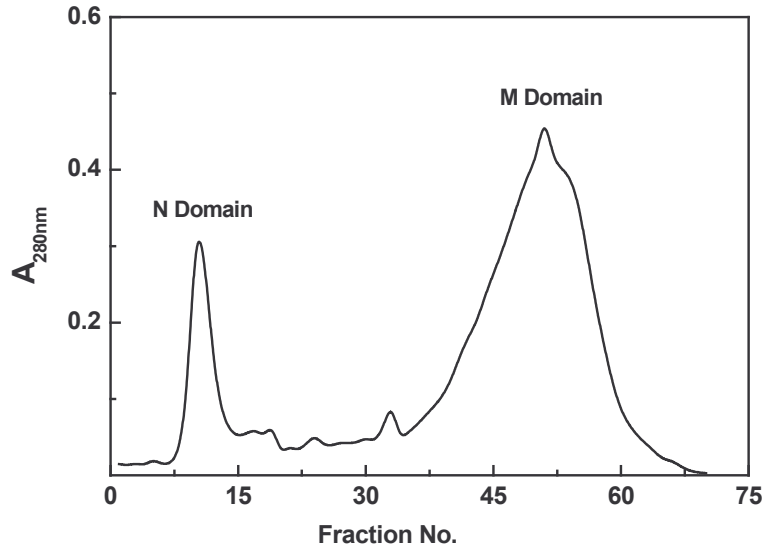

Figure 53. Ion-exchange profile of N+M domain on a SP Sephadex C-25 column: The column was eluted with 50 mM (pH 5.0) acetate buffer containing 8M urea at a flow rate of 30 ml/hr. A linear gradient of 0-0.3 M NaCl in the same buffer was used.

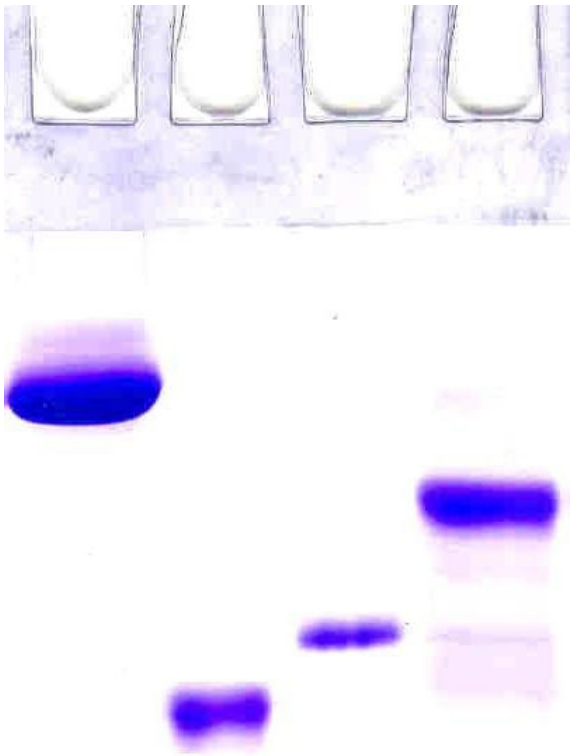

Figure 54. Non-reducing page of domains of human serum albumin on 15% separating and 5% stacking gels: 20 μg of isolated domains was loaded. Lane -1: HSA, Lane - 2: N domain, Lane - 3: M domain and Lane - 4: C domain.

Table 6.

Secondary structure analysis of the intact human serum albumin and isolated N, M and C fragments

	α-helix (%)	β-sheet (%)	β-turn (%)	Random Coil (%)
HSA	57.6	15.2	0	27.2
N-fragment	27.4	21.2	14.7	36.6
M-fragment	41.5	19.1	2.4	37
C-fragment	38.6	22	0	39.4

Fluorescence Quenching Measurements:

Interaction of genistein with the domains of HSA has been monitored following the quenching of relative fluorescence intensity of the domains. Quenching of fluorescence by genistein does not lead to detectable changes in wavelength of maximum emission or the band shape. It is found that genistein, which could quench the tryptophan fluorescence of M domain, failed to quench the tyrosine fluorescence of C and N domains. M domain corresponds to domain 2A of serum albumin where isoflavones bind. Quantitation of genistein–M domain interaction is displayed in Fig. 55A. A maximum quench of 27% has been observed at 12 μM of genistein, representing 59% completion of the reaction as deduced from the linear double reciprocal plot of Q vs genistein concentration to be 28 $\pm$ 3 (Fig. 55B). The mass action plot, presented in Fig. 55C has been constructed (using the value of n=1 and the extent of reaction reckoned from Fig. 55B). The binding constant given by the slope of this plot is 0.45 $\pm$ 0.2 x 10^5 M^{-1}. The binding constant is found to be invariant of temperature, suggesting a dominant role played by hydrophobic interaction in the binding. Thus, van't Hoff's enthalpy $\triangle H \approx 0$ kcal/mol and the binding reaction was entropy driven; $\triangle S$ = -21.28 cal/mol/K at 27°C with activation free energy of $\triangle G$ = -6.36 kcal/mol. With the addition of genistein, there is a quenching of fluorescence intensity, indicating efficient Förster type energy transfer (FRET). The overlap integral J (Fig. 56) has been calculated by integrating the spectra in the wavelength range 310-400 nm to be 5.7688 x 10^{-15} cm^3 l mol^{-1} for genistein. The energy transfer efficiency E for genistein is 0.08. The Förster distance $R_{0,}$ is 2.1 nm

for genistein. The distance between genistein and tryptophan residue, $r_{0,}$ (the distance between acceptor and donor) is 3.6 nm.

Fluorescence of daidzein bound to albumin fragments:

Daidzein is the only intrinsically fluorescent isoflavone among those studied. This property has been exploited to study the nature of binding to domains of HSA. There is a shift of the emission maxima of the daidzein bound albumin towards shorter wavelengths (from 465 to 457 nm) compared to unbound daidzein (Fig. 57) in presence of M and C domain. The interaction of daidzein with C domain is less compared to M domain, which suggests that it has more affinity towards domain 2A compared to domain 3A. Fluorescence quenching measurements revealed that genistein is unable to quench the tyrosine fluorescence of C domain, but it showed interaction with daidzein by an increase in the fluorescence of daidzein in presence of C domain. So probably daidzein is binding to some hydrophobic regions of domain C, exposed due denaturing conditions employed during purification. Daidzein did not interact with N domain, thereby ruling its possibility of binding with domain 1.

Fluorescence anisotropy measurements:

Fluorescence anisotropy measurements were made for the daidzein–domains of HSA system by exciting at 340 nm (maxima for daidzein) and emission at 465 nm. There was an increase in fluorescence anisotropy of daidzein on binding to M and C domains of HSA. There was no increase in the

anisotropy of daidzein in presence of N domain, confirming that isoflavones do not bind to domain 1. Anisotropy of daidzein increased from 0.01 to 0.14 on binding to M and C domains. Anisotropy increase was more in the presence of M domain compared to C domain, suggesting that daidzein has more affinity towards M domain compared to C domain (Fig.58). The increase in anisotropy could be due to the restriction imposed by the binding on the rotation around the daidzein molecule.

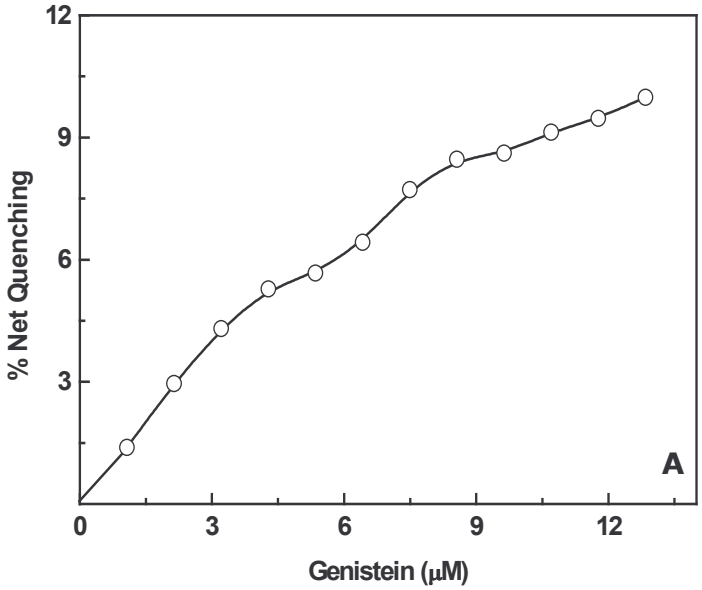

Figure 55A. Quantitation of the interaction of genistein with M-domain of HAS by fluorescence quenching.N, M and C domains of HSA (3 μM) in 50 mM Tris- HCl buffer (pH 7.4) were titrated with increasing aliquots of stock genistein solution (2 μl equivalent to 1 μM genistein per aliquot) in 80% methanol and the % quench was recorded. Blank titrations with N-acetyl tryptophanamide of equivalent absorbance at 280 nm for M domain of HSA in presence of varying concentration of genistein were carried out.

A: % quench of fluorescence intensity, as a function of constituent genistein concentration.

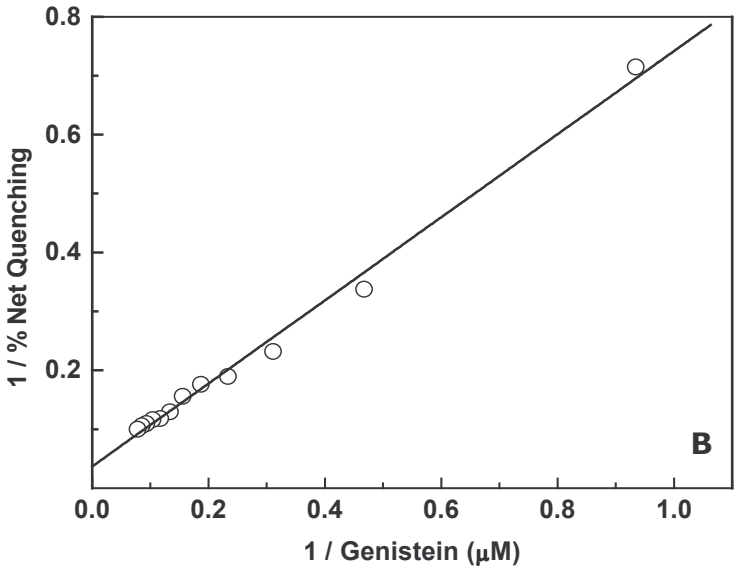

Figure 55B. Double-reciprocal plot of data in A; Q_{max} = 28 ± 3 (± indicates probable error in all cases).

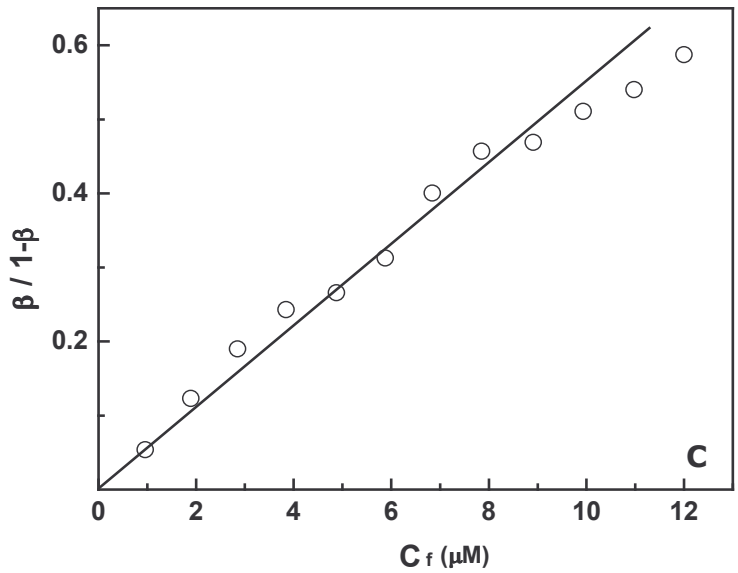

Figure 55C: Mass action plot of the above data:

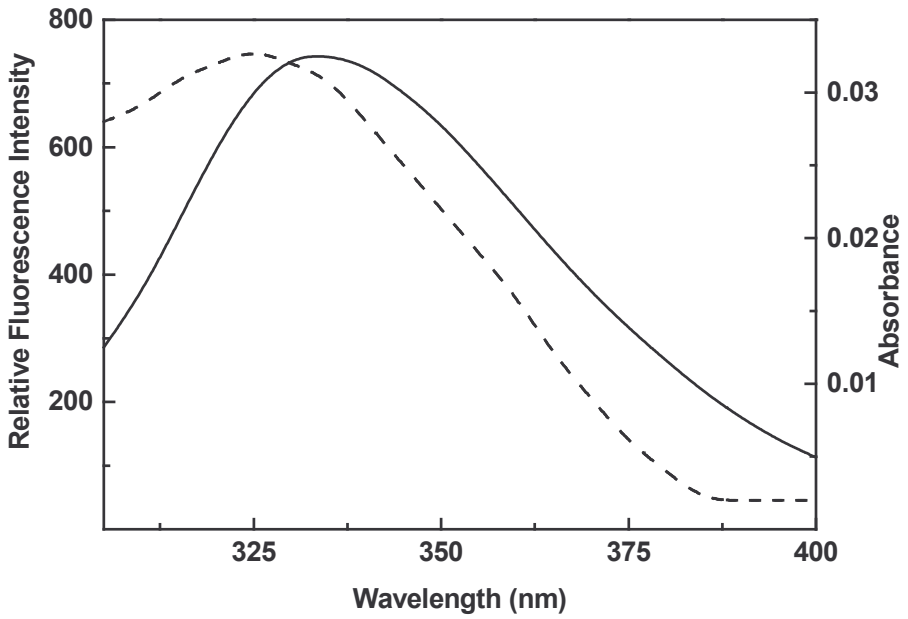

Figure 56. Fluorescence resonance energy transfer between M-domain and genistein: Fluorescence emission spectrum of M-domain overlaps with the absorption spectra of genistein. Solid line: Fluorescence emission spectra of M-domain, Dashed line: absorption spectra of genistein.

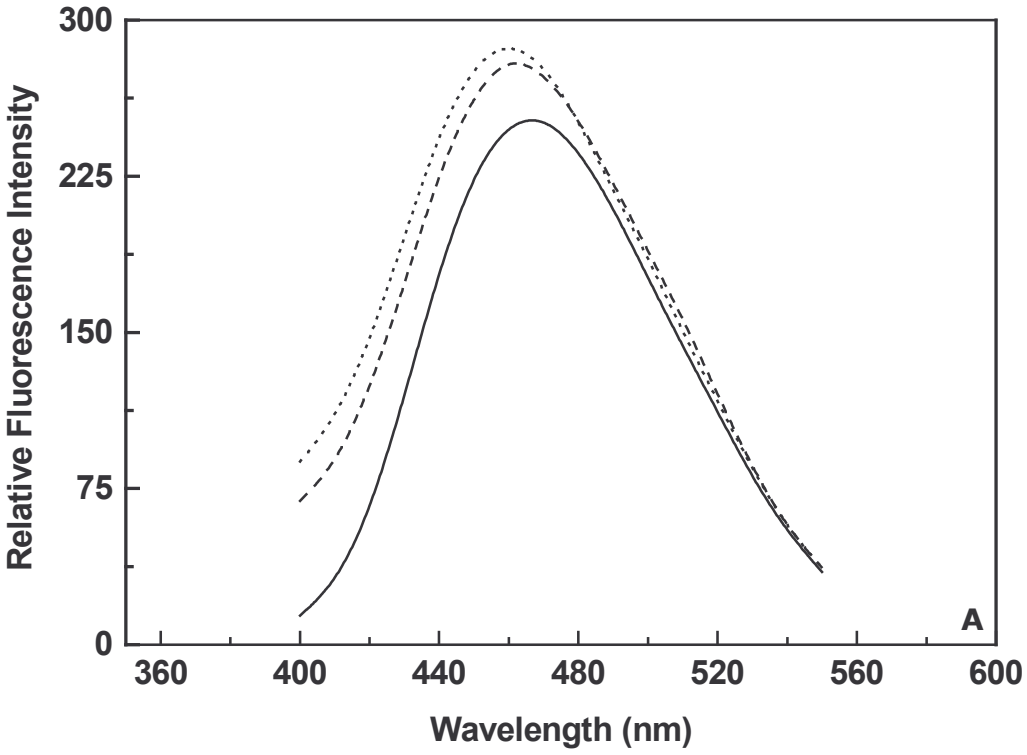

Figure 57. Emission spectra of daidzein showing blue shift on binding to M and C domains:

Daidzein (2.75 μM) in 50 mM Tris–HCl (pH 7.4) was titrated against increasing concentrations of M and C domains in the same buffer. The final concentration of M and C domains was 27 μM. The spectra, recorded between 400–550 nm after excitation at 340 nm, the excitation maxima for daidzein. Excitation slit width was 5 nm and emission slit width was 10 nm.

Solid line: free daidzein*;* dashed line: daidzein bound to C domain of HSA; dotted line: daidzein bound to M domain of HSA.

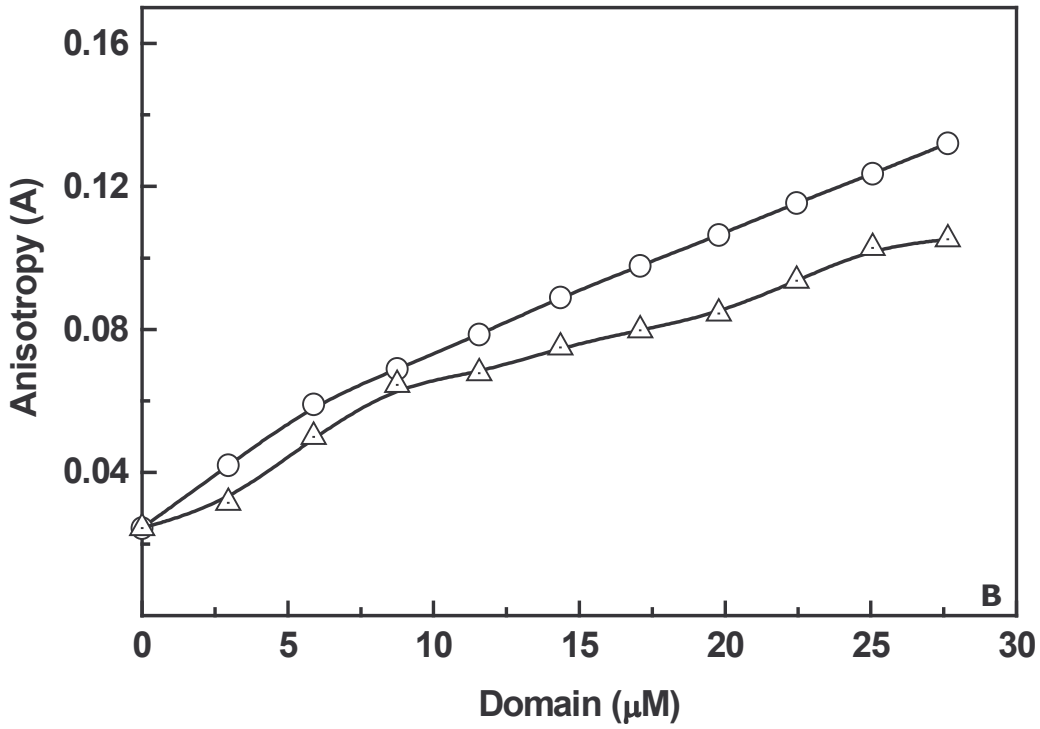

Figure 58. Variation in fluorescence anisotropy of daidzein as a function of M and C domains of serum albumin concentration:

Daidzein (2.75 μM) was titrated against increasing concentrations of M and C domains. (-○-) daidzein bound to M domain of HSA, (-△-) daidzein bound to C domain of HSA. The final concentration of M and C domains was 27 μM. The excitation and emission wavelengths were 340 and 465 nm respectively. Slit widths were at 5 and 10 nm for excitation and emission respectively.

Discussion

The present study of the binding of isoflavones to albumin fragments by spectrofluorimetric methods reveals that isoflavones interact with the domain fragments, with decreased binding affinity, compared to the intact molecule. Genistein is able to quench the lone tryptophan fluorescence of M domain with a binding constant of $0.45 \pm 0.2 \times 10^5$ M^{-1} thereby suggesting that it binds in the vicinity of tryptophan. The estimated binding constant between genistein and intact HSA is $1.5 \pm 0.2 \times 10^5$ M^{-1} (Mahesha *et. al.,* 2006). The weak binding of genistein to fragment M compared to the intact serum albumin molecule stresses the need for a proper tertiary structure for the ligand binding. The CNBr cleavage results in the disruption of the tertiary structure leading to the breakdown of the binding crevice for isoflavones on serum albumin molecule.

The distance between tryptophan of M-domain and genistein is 3.6 nm. The distance between genistein and tryptophan in intact human serum albumin (domain 2A) reported in our previous paper (Mahesha *et. al.,* 2006) is 3.69 nm, which is similar to the distance obtained in the present study. This strengthens our theory that the binding crevice for isoflavones is located in the vicinity of tryptophan of domain 2A (of intact human serum albumin). Daidzein fluorescence and anisotropy is increased in presence of M domain.

Genistein is unable to quench the tyrosine fluorescence of N domain and daidzein fluorescence also remains unaffected in the presence of N domain.

This observation clearly shows that binding crevice of isoflavones is not located in N domain.

Genistein is unable to quench the tyrosine fluorescence of C domain, but daidzein fluorescence and anisotropy is increased in the presence of C domain. This suggests that isoflavones may bind to exposed hydrophobic areas due to denaturing conditions employed during purification of the domains. Fragment C corresponds to the domain 3, which is the primary fatty acid binding domain (Curry *et. al.,* 1998). During physiological conditions, this site is occupied by 0.1-2 moles of fatty acids, which have high affinity for serum albumin (Curry *et. al.,* 1998). Thus, genistein cannot displace fatty acids and hence their binding crevice should be located elsewhere on the serum albumin molecule.

From the current study, it is clear that isoflavones bind to domain 2A of human serum albumin, which contains the lone tryptophan.

Section C: Inhibition of lipoxygenase by isoflavones: Evidence of isoflavones as redox inhibitors

Results

The current interest in inhibition studies of LOX have been spurred by the role played by the products of LOX reaction with unsaturated fatty acids, in inflammation and immediate hypersensitivity. In the recent years, a number of compounds isolated from plants, including isoflavones, have been shown to inhibit LOXs. However, the mechanism of inhibition is not clearly elucidated. In order to understand the interaction as well as the nature of inhibition, we have chosen soy LOX-1, with its known crystal structure, as the model in our experiments.

SDS-PAGE analysis of lipoxygenase:

The purity of lipoxygenase was determined by reducing SDS-PAGE electrophoresis and native PAGE (Fig. 59 A & B). A resolving gel of 12% and stacking gel of 5% was used. The purity of isolated lipoxygenase was >95%.

Enzyme Kinetic Measurements: Inhibition of lipoxygenase by isoflavones:

Time course for the inhibition of LOX activity in presence of 0-136 μM genistein is shown in Fig. 60A. Genistein, daidzein and their glycosylated forms (genistin and daidzin); inhibit soy LOX-1 in a concentration dependent manner (Fig. 60B).

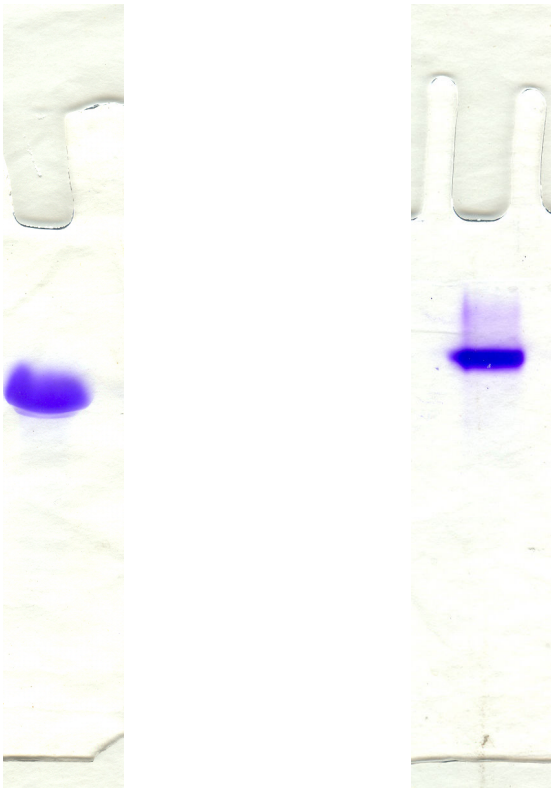

A B

Figure 59. Gel electrophoresis of soy lipoxygenase-1. A SDS-PAGE of LOX-1; **B.** Native PAGE of LOX-1. A 5% stacking gel and 12% resolving gel was used and electrophoresis was run according to Laemmelli (1970).

Glycosylation did not have any effect on the inhibitory potential of isoflavones (Table 7). Genistein and genistin had IC_{50} values of 107 and 109 μM, respectively. Daidzein and daidzin also had similar values (136 and 140 μM, respectively). Genistein and daidzein also inhibited the activity of human PMNL 5-Lipoxygenase (Table 8) in a concentration dependent manner.

The time course for inhibition of lipoxygenase with varying substrate concentration (linoleic acid 10 – 100 μM) in presence of 106 μM genistein is shown in Fig. 61A. Genistein inhibits the ferric form of the enzyme as decrease in the rate of the reaction is observed. The Lineweaver-Burk plots at fixed concentration of genistein and daidzein have revealed that K_m remained constant (16 μM) while V_{max} of soy LOX-1 decreased. This suggests genistein and daidzein to be a noncompetitive inhibitor of LOX-1 (Fig. 61B & 62A) (regression coefficient > 0.99). The inhibitor interacted with the free enzyme as well as substrate bound enzyme. The K_i for genistein and daidzein have been determined to be 60 μM and 80 μM for the resting ferrous form of enzyme (Fe^{2+}) respectively (Fig. 61C & 62B). The inhibition of lipoxygenase is reversible in nature as complete activity could be recovered after checking the residual activity of the dialyzed enzyme, which was free from the inhibitor. Steady state kinetics data has been analyzed by Dixon plot (Fig. 61D). The *Ki* values, obtained from the Dixon plot for genistein and daidzein, are found to be 60 and 80 μM, respectively.

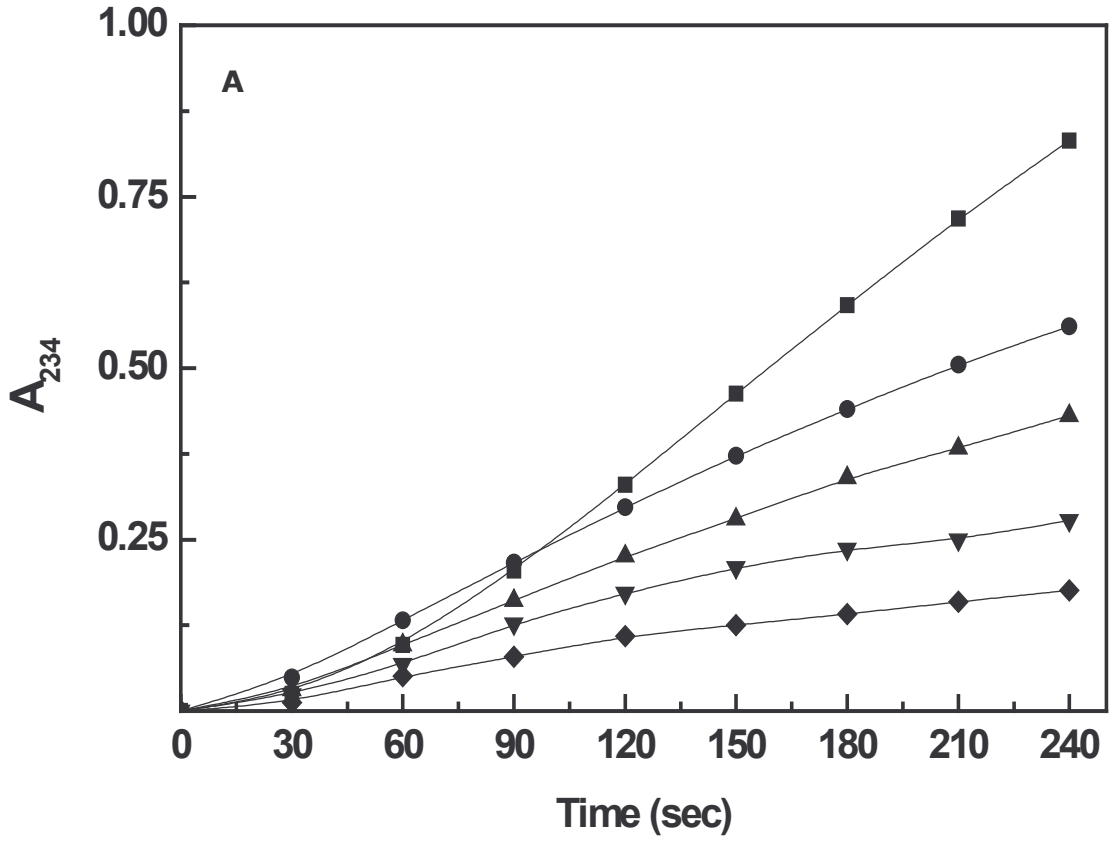

Figure 60A. Time course of lipoxygenase catalyzed reaction:
Genistein was incubated with lipoxygenase for 5 min in 0.2 M borate buffer (pH 9.0) before assaying for LOX activity with linoleic acid as substrate. Formation of the hydroperoxide products of LOX assay was followed at 234 nm. The concentration of genistein were 0 (—■—), 54 (—•—), 84 (—▲—), 106 (—▼—) and 136 μM (—◆—).

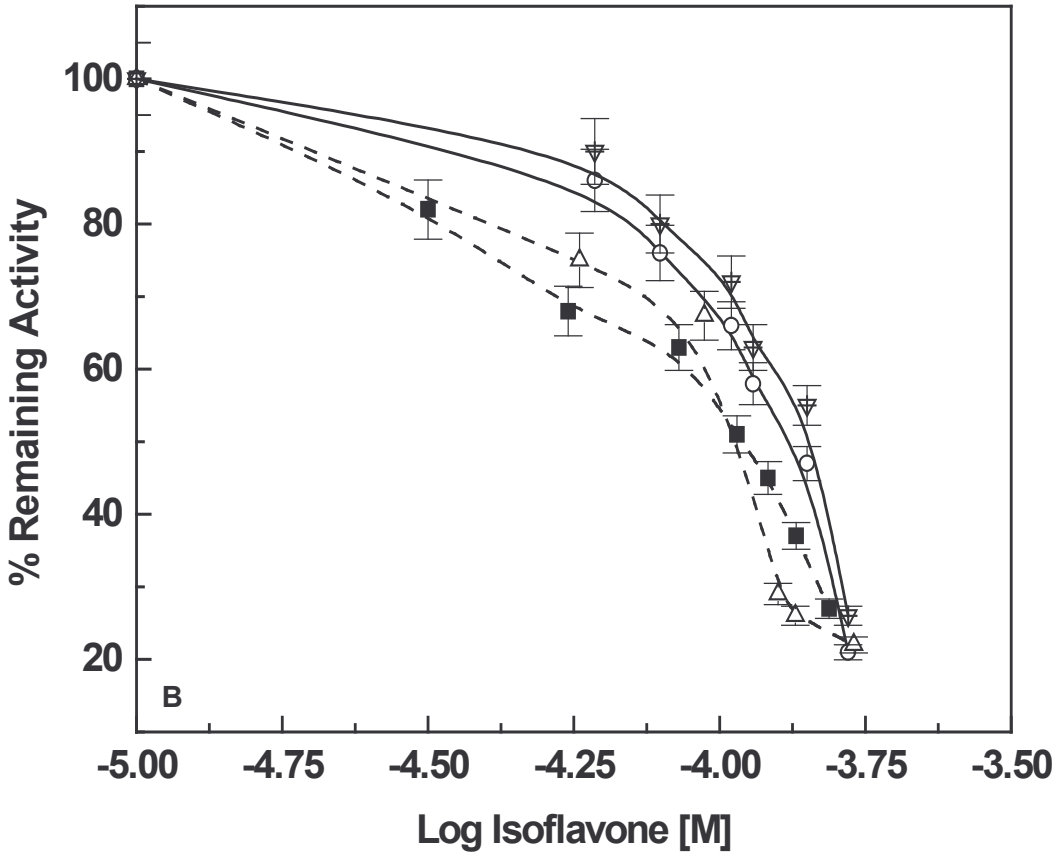

Figure 60B. Inhibition of lipoxygenase by isoflavones:

Genistein (---□---), daidzein (—△—), genistin (---■---) and daidzin (—▼—) were incubated with lipoxygenase for 5 min in 0.2 M borate buffer, pH 9.0. The reaction was started by the addition of 100 μM linoleic acid and enzyme activity was followed spectrophotometrically at 234 nm. All the isoflavones inhibited lipoxygenase in a concentration dependent manner.

Table 7

IC_{50} values for the inhibition of soy lipoxygenase by isoflavones

Isoflavones	IC_{50} (μM)
Genistein	107 ± 5
Daidzein	136 ± 5
Genistin	109 ± 5
Daidzin	140 ± 5

***** Results are average of three experiments

Table 8

IC_{50} values for the inhibition of human PMNL 5- lipoxygenase by isoflavones

Isoflavones	IC_{50} (μM)
Genistein	125 ± 5
Daidzein	157 ± 5

* **Results are average of three experiments**

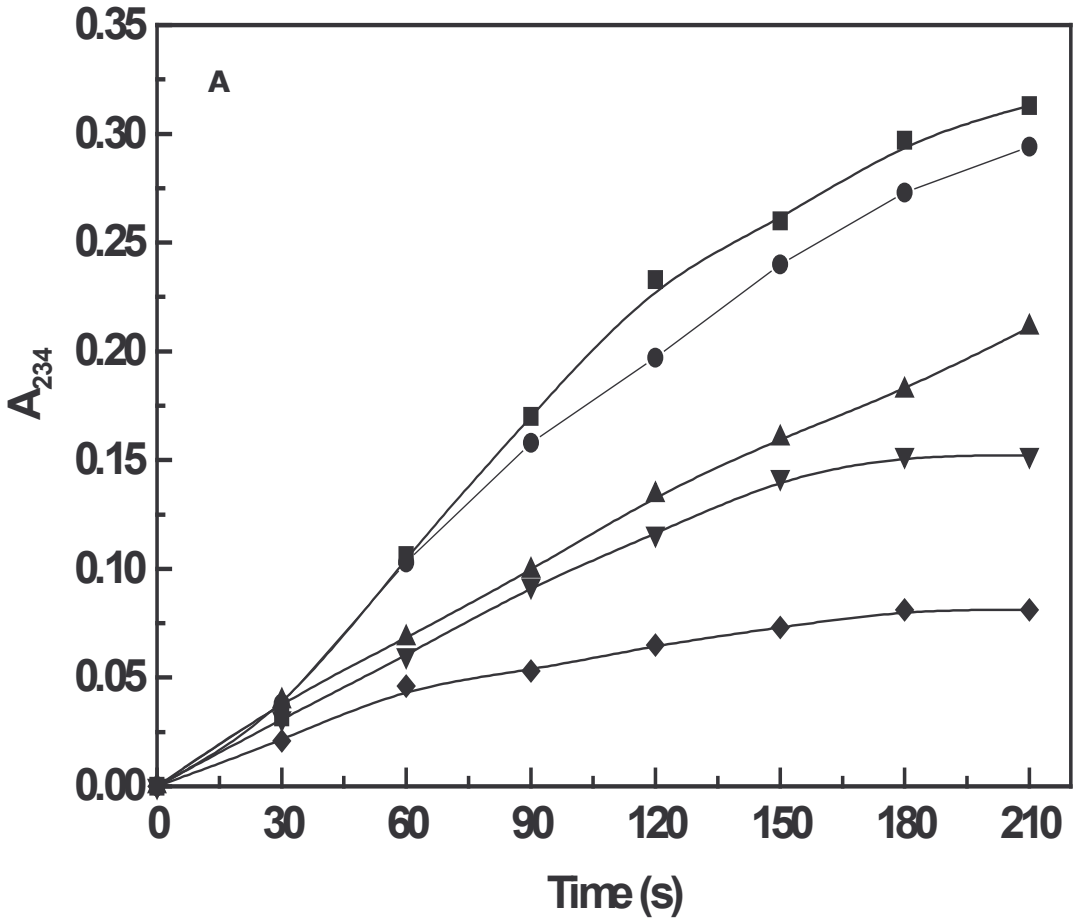

Figure 61A. Time course of lipoxygenase catalyzed reaction:

Genistein (106μM) was incubated with lipoxygenase for 5 min in 0.2 M borate buffer (pH 9.0) before assaying for LOX activity with linoleic acid as substrate. Formation of the hydroperoxide products of LOX assay was followed at 234 nm. The concentration of linoleic acid was 100 (—■—), 75 (—•—), 40 (—▲—), 25 (—▼—) and 10 μM (—◆—).

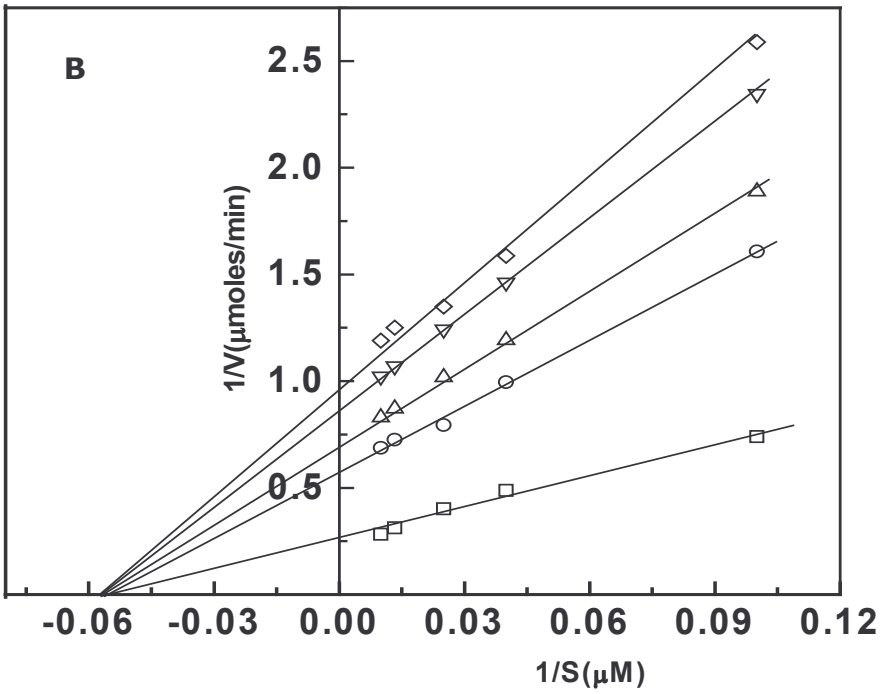

Figure 61B. Lineweaver-Burk plot analysis for inhibition of lipoxygenase by genistein:

Genistein was incubated with lipoxygenase for 5 min in 0.2 M borate buffer (pH 9.0) before assaying for LOX activity with linoleic acid as substrate. Formation of the hydroperoxide products of LOX assay was followed at 234 nm. The concentration of genistein were 0 (—□—), 84 (—○—), 106 (—△—), 136 (—▽—) and 154 μM (—◊—). The substrate concentration was varied from 10-100 μM. All values are average of three experiments.

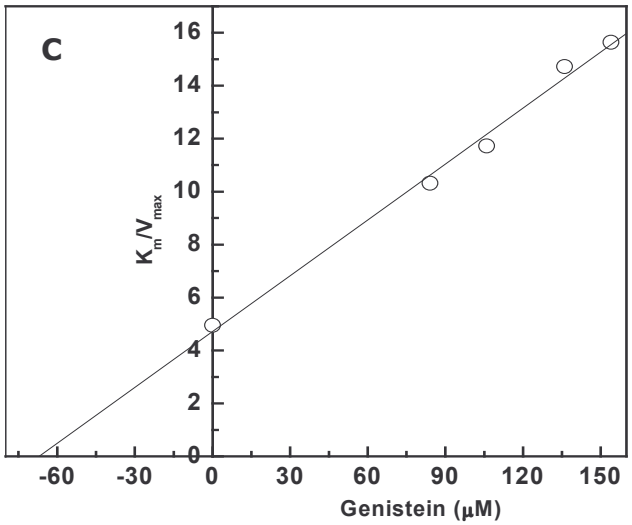

Figure 61C. Determination of K_i of genistein: The slope (K_m / V_{max}) of the lines described from the double reciprocal plot is plotted against the genistein concentration in order to determine the K_i value of genistein. All values are average of three experiments.

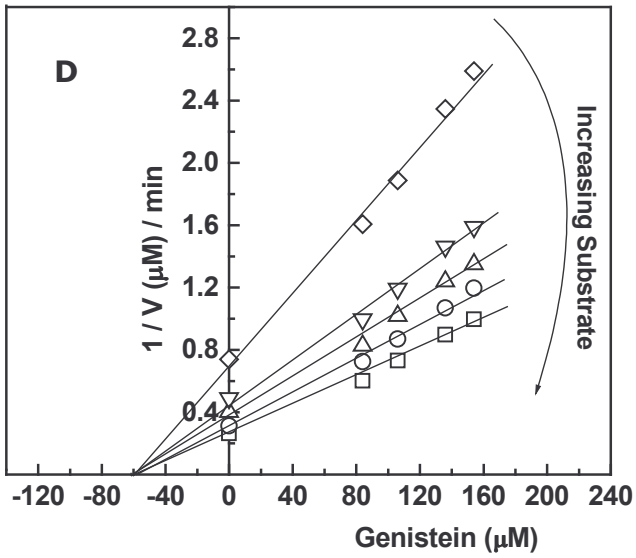

Figure 61D. Dixon Plot: Ki was also determined by Dixon plot. The concentration of genistein and linoleic acid are similar to values used to deduce the L-B plot. The concentration of linoleic acid was 100 (—□—), 75 (—○—), 40 (—△—), 25 (—▽—) and 10 μM (—◊—).

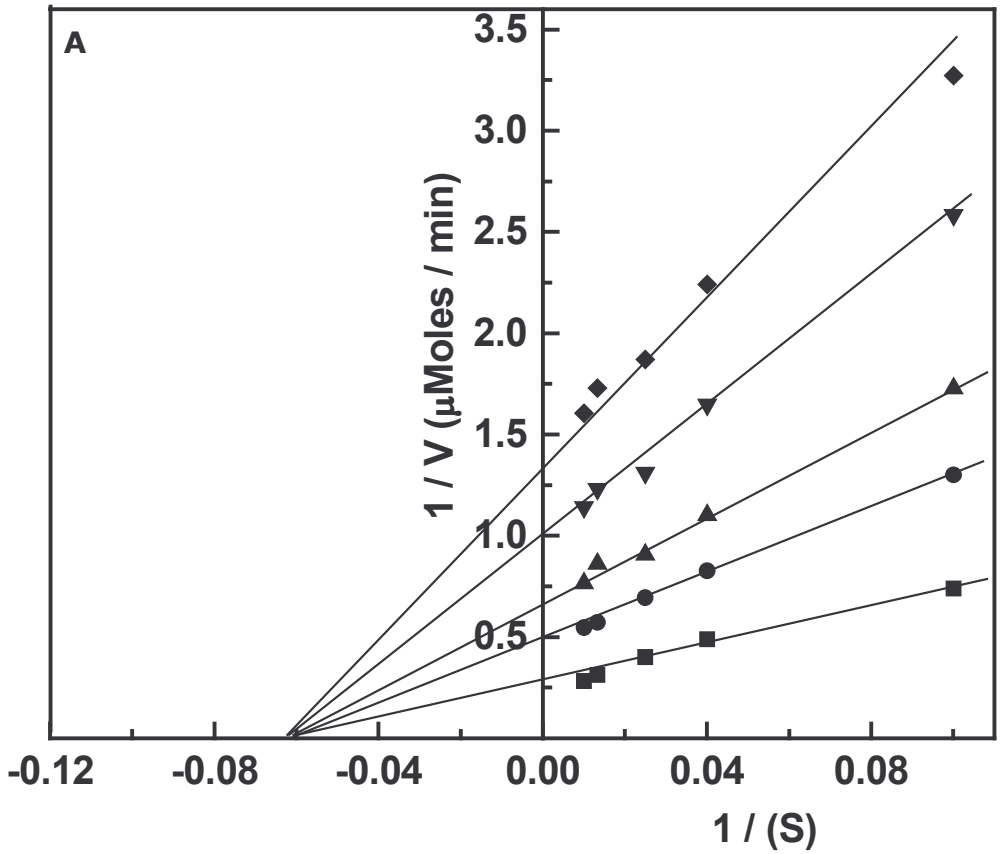

Figure 62A. Lineweaver-Burk plot analysis for inhibition of lipoxygenase by daidzein:

Daidzein was incubated with lipoxygenase for 5 min in 0.2 M borate buffer (pH 9.0) before assaying for LOX activity with linoleic acid as substrate. Formation of the hydroperoxide products of LOX assay was followed at 234 nm. The concentration of genistein were 0 (—■—), 78 (—●—), 104 (—▲—), 141 (—▼—) and 164 μM (—◆—). The substrate concentration was varied from 10-100 μM. All values are average of three experiments.

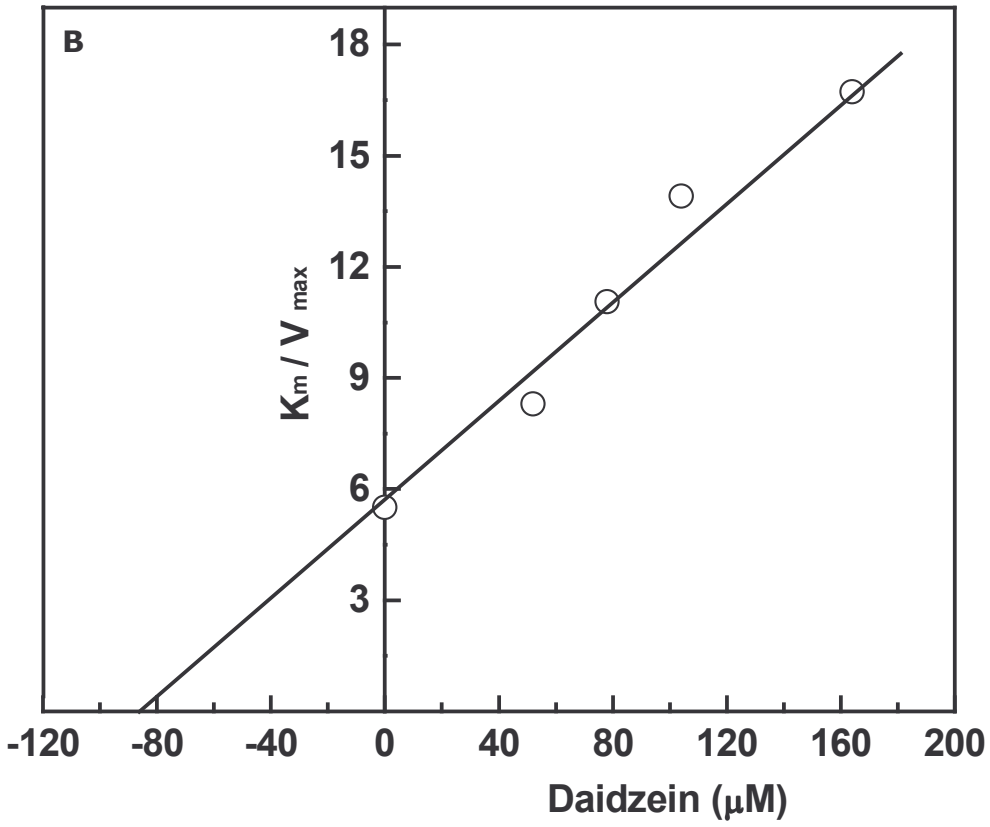

Figure 62B. Determination of K_i of daidzein: The slope (K_m / V_{max}) of the lines described from the double reciprocal plot is plotted against the daidzein concentration in order to determine the K_i value of daidzein. All values are average of three experiments.

Stopped flow inhibition kinetics:

Resting lipoxygenase has iron in its ferrous form. The active enzyme is obtained by the action of hydroperoxide (HPOD), generated as a result of air oxidation of linoleic acid or produced by Fe^{3+} contamination in the resting enzyme. When active lipoxygenase is used, there is no lag phase (Fig. 63a) and only the burst phase is observed. Fig. 63b, c and d represent active Fe^{3+} enzyme, incubated for 15 min, with different concentrations of genistein (0–87 μM). The figure represents the lag observed due to reduction of Fe^{3+} to Fe^{2+} by the inhibitor. The reaction, in presence of inhibitor, not only resembles the reaction of LOX in its resting Fe^{2+} form, but also exhibits a lag phase.

Absorbance measurements:

The absorption spectrum of soy LOX-1 (resting) showed a single peak at 280 nm. Addition of an equimolar amount of linoleic acid to soy LOX-1 (iron in Fe^{2+} state) resulted in the solution turning yellow (iron in Fe^{3+} state) and the appearance of the shoulder at 350 nm (Fig. 64). Addition of genistein to yellow LOX resulted in a decrease in the absorption at 350 nm, pointing to the reduction of iron from the active ferric to the resting ferrous state (Fig. 64).

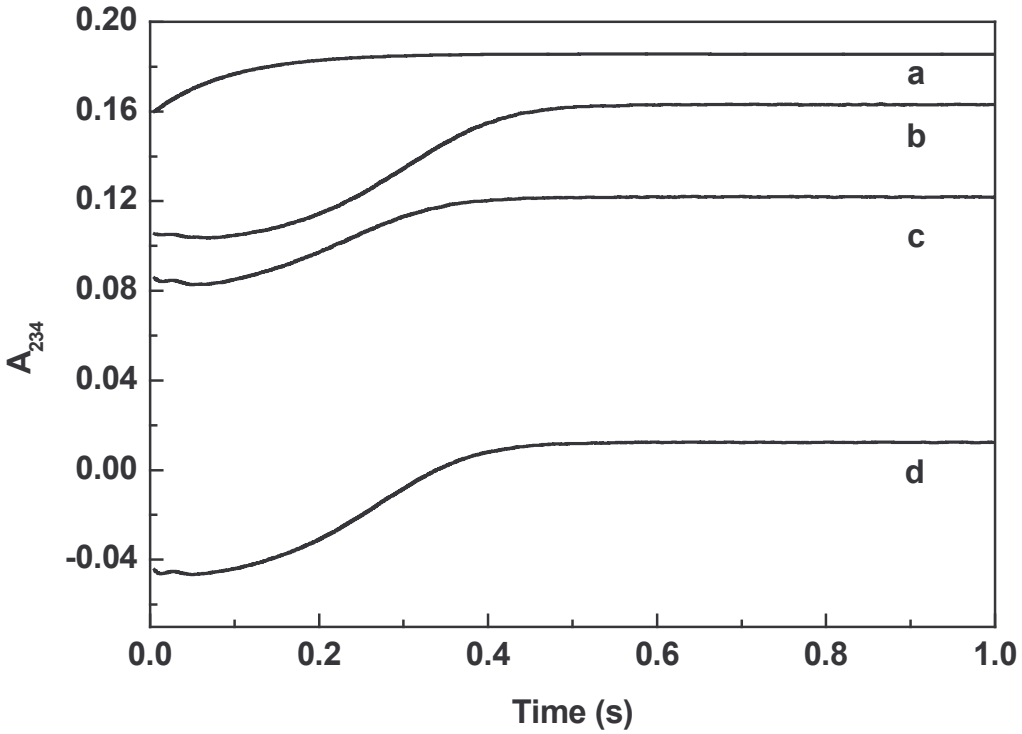

Figure 63. Stopped flow inhibition of active ferric lipoxygenase by genistein: Stopped flow traces for the time dependent conversion of linoleic acid to HPOD. Various concentrations genistein was incubated with active ferric lipoxygenase (1.2 μM) for 15 min in 0.2 M borate buffer (pH 9.0) before assaying for LOX activity with linoleic acid as substrate. Formation of the hydroperoxide products of LOX assay was followed at 234 nm by 1:1 mixing of enzyme-genistein complex and substrate. The reaction was followed for 2 s. The solid lines represent the rate of formation of HPOD and the dotted lines represent the fits. The concentration of genistein was (a) 0 μM, (b) 35 μM, (c) 70 μM and (d) 87 μM.

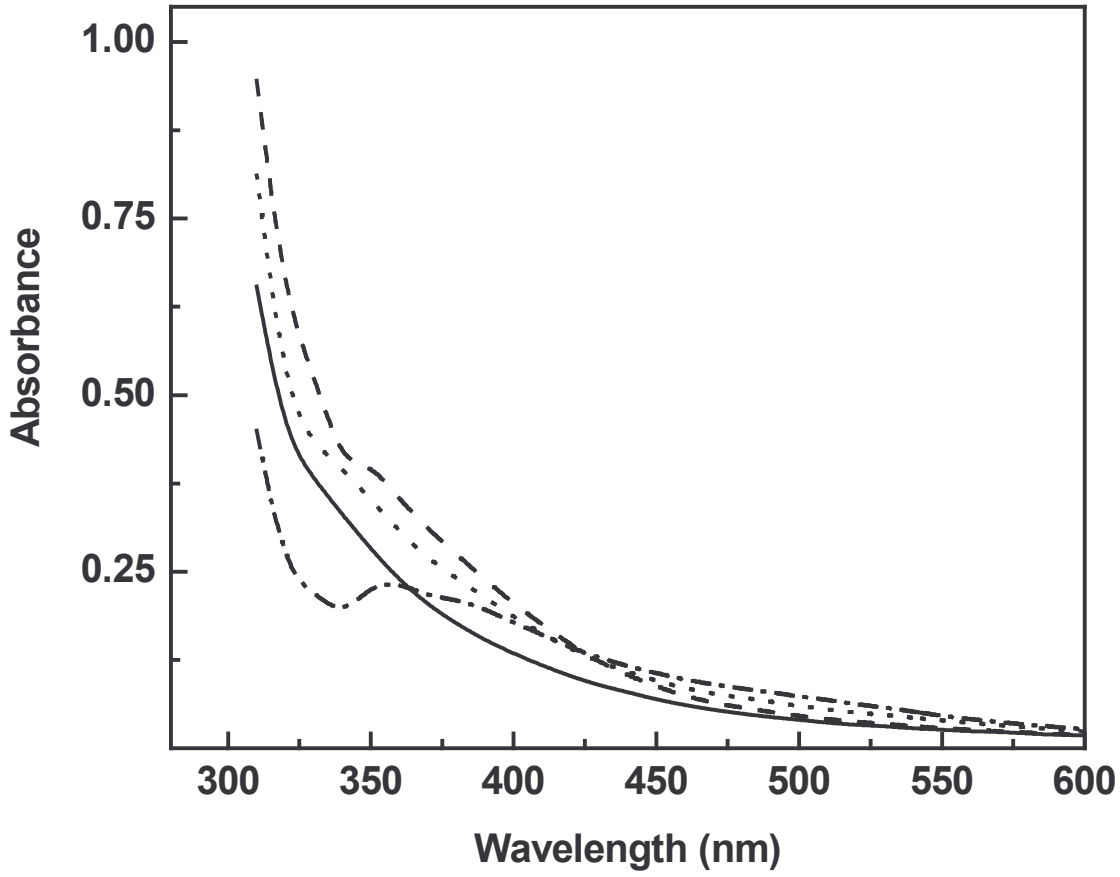

Figure 64. Effect of genistein on the absorption spectra of ferric lipoxygenase:

Absorption experiments were carried out in the region of 300-600 nm in 0.1 M borate buffer (pH 9.0). The cell path length was 1 cm and spectra were recorded in a double beam spectrophotometer. Native LOX-1 (160 μM) was treated with linoleic acid (160 μM) to convert it to active ferric form. To this genistein (160 and 320 μM) was added. Solid *Line:* Ferrous LOX-1 (Fe^{2+}), *Dashed Line*: Ferric LOX-1 (Fe^{3+}) Dotted *Line:* Genistein (160 μM) Short *dash:* Genistein (320 μM)

Circular Dichroism Measurements:

CD spectrum of soy LOX-1 in its active yellow form (Fe^{3+}), exhibited a positive CD band at 425 nm (Fig. 65) not seen in the ferrous form (resting state) (Spaapen *et. al.,* 1979). Chelation of ferric iron by amino acid residues of LOX could be the underlying reason for the appearance of the positive CD band in active LOX. This was reported in other non-heme iron containing enzymes (Slappendel *et. al.,* 1981).

The appearance of positive CD band is due to His-Fe (III) ligand-to-metal charge transfer (LCMT) transition (Holman *et. al.,* 1998). Addition of genistein and daidzein has resulted in the disappearance of the band at 425 nm (Fig. 65 & 66), indicating that genistein reduces the active Fe^{3+} yellow enzyme to its resting Fe^{2+} form. The inhibition of LOX activity by isoflavones may be by alteration of the redox chemistry of iron, suggestive of redox inhibition. Thus, our experiments have established that the isoflavones inhibit lipoxygenase by converting the active ferric enzyme to its resting form.

EPR measurements:

The EPR spectrum of lipoxygenase in resting state, active state and the effect of isoflavones at 20 K are shown (Fig. 67). In addition to the g= 4.3 signal, seen in the resting lipoxygenase (Fig. 67a), an EPR feature around g = 6.1 (Slappendel et. al., 1982) that can be attributed to the high-spin Fe^{3+} in an axial field can be seen (Fig. 67b). In the case of active state, addition of genistein (2 and 4 molar equivalents) to the active lipoxygenase shows a decrease in the g= 6.1 signal, indicating the conversion of the active state

lipoxygenase to its resting state (Fig. 67c and d). The addition of linoleic acid in molar excess (800 μM) to soy LOX-1 containing 400 μM genistein has led to the reappearance of the *g*= 6.1 signal (Fig. 67e). Similar results have been observed with daidzein (Fig. 68). The increase in *g* = 4.3 signal (in samples treated with genistein) probably, indicates the formation of an enzyme – genistein complex. Thus, the inhibition of LOX-1 by genistein is reversible. Genistein undergoes base catalyzed auto-oxidation at pH 9.0 and gives an EPR signal (Fig. 69). Since genistein undergoes auto-oxidation, formation of free radical metabolites or phenoxy radical of genistein could not be followed in the reaction between lipoxygenase/linoleic acid and genistein. The auto-oxidation of genistein might be prevented below pH 7.4. But detection of radicals requires high concentration of inhibitors and owing to the very low solubility of genistein and daidzein; experiments could not be done at low pH (pH 7.4 or below that) conditions using lipoxygenase/ linoleic acid system to generate free radicals from genistein and daidzein.

HPLC Measurements:

The detectability of genistein at 262 nm was used for studying the interaction of isoflavone in the course of LOX reaction with linoleic acid. Soy LOX-1 was assayed in the presence of genistein (100 μM) for a period of 5 min. The reaction was stopped; genistein was extracted into ether and estimated by RP-HPLC. There was no change in the retention time of genistein (52.09 min) and genistein is quantitatively recovered (Fig. 70) suggesting that the

genistein is not consumed during the course of the reaction and remains in its resting state.

Mass Spectrometry:

Genistein may undergo oxidation and this oxidized product may have similar retention time and resemble native genistein in its spectral properties. To rule out this possibility, genistein treated with lipoxygenase-linoleic acid system was analyzed by mass spectra. Mass spectra analysis reveals that genistein has mol. wt of 269 Da, which is the molecular weight of genistein ion. This further confirms that genistein remains in its resting state (Fig. 70 inset).

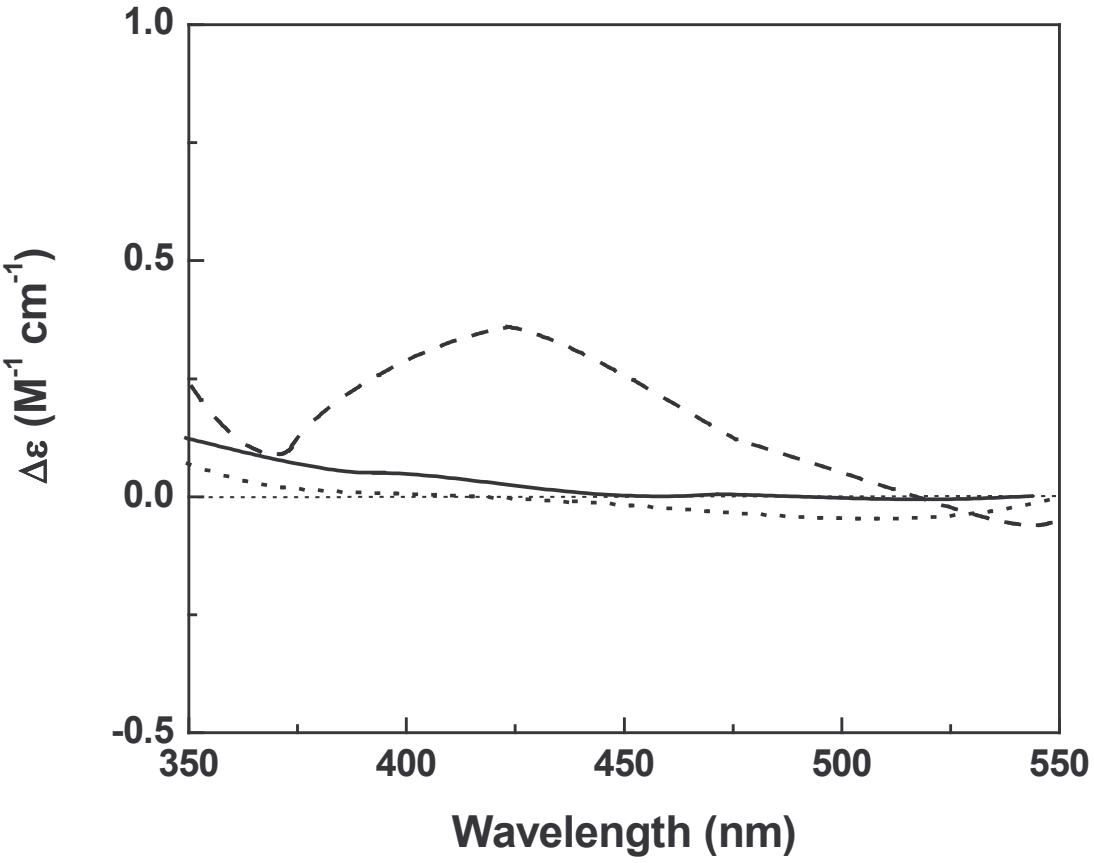

Figure 65. Effect of genistein on the CD spectrum ferric lipoxygenase:
CD measurements were carried out in the visible region of 350 – 550 nm in 0.1 M borate buffer (pH 9.0). The cell path length was 1 cm and spectra were recorded at a speed of 10 nm min^{-1}. All scans are an average of 3 runs. A mean residue weight of 115 was used for calculating the molar ellipticity values. Native LOX-1 (150 μM) was treated with linoleic acid (150 μM) to convert it to optically active ferric form. To this genistein (300 μM) was added. *Dotted Line:* Native Ferrous LOX-1 *Dashed Line*: Ferric LOX-1, band at 425 nm, Solid *Line:* CD Spectrum of LOX treated with genistein showing the disappearance of positive dichroic band.

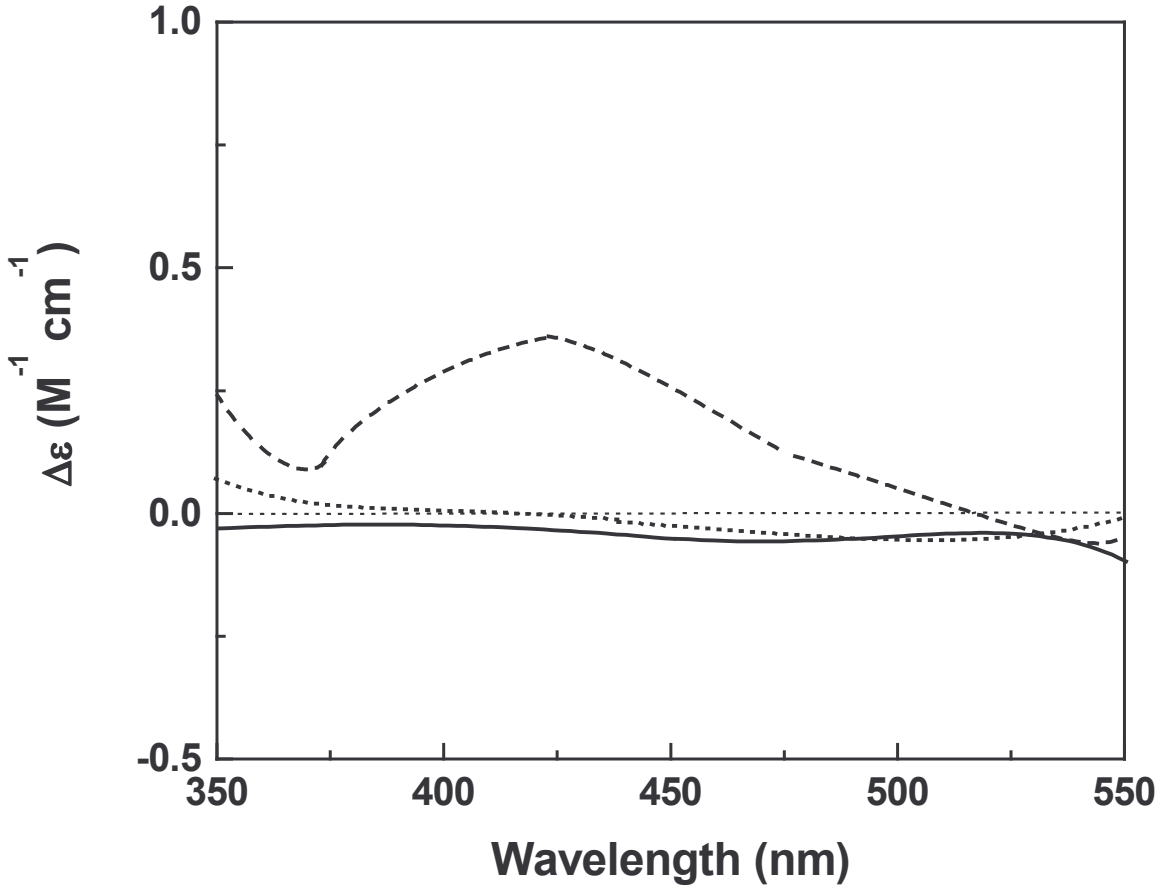

Figure 66. Effect of daidzein on the CD spectrum ferric lipoxygenase:
CD measurements were carried out in the visible region of 350 – 550 nm in 0.1 M borate buffer (pH 9.0). The cell path length was 1 cm and spectra were recorded at a speed of 10 nm min^{-1}. All scans are an average of 3 runs. A mean residue weight of 115 was used for calculating the molar ellipticity values. Native LOX-1 (150 μM) was treated with linoleic acid (150 μM) to convert it to optically active ferric form. To this daidzein (300 μM) was added. *Dotted Line:* Native Ferrous LOX-1 Dashed *Line*: Ferric LOX-1, band at 425 nm,*: Solid Line* CD Spectrum of LOX treated with daidzein showing the disappearance of positive dichroic band.

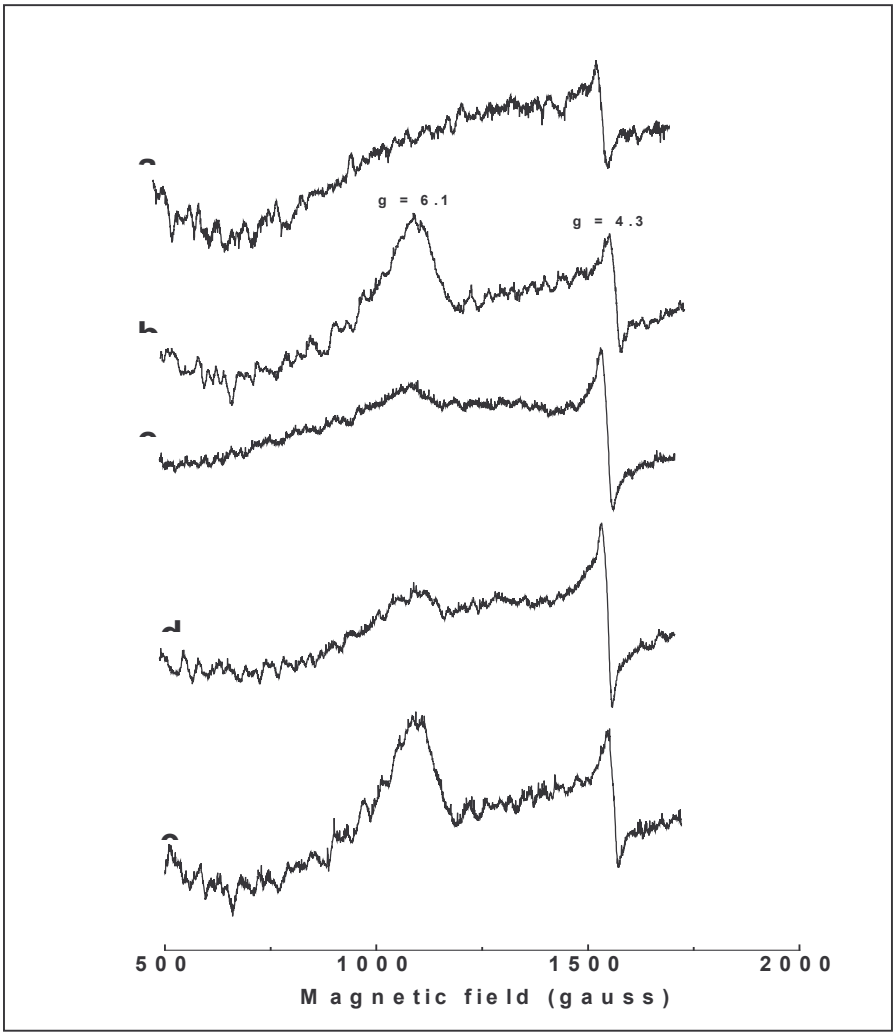

Figure 67. Effect of genistein on the EPR spectrum of ferric soybean lipoxygenase:

(**a**) Resting (Fe^{2+}) lipoxygenase (200 μM). (**b**) Ferric (Fe^{3+}) lipoxygenase obtained with addition of 200 μM of linoleic acid. (**c**) Ferric lipoxygenase treated with 400 μM of genistein. (**d**) Ferric lipoxygenase treated with 800 μM of genistein. (**e**) Ferric lipoxygenase treated with 400 μM of genistein and 1 min later, treated with 800 μM of linoleic acid. All the solutions were in 0.1 M borate buffer (pH 9.0) containing 3% methanol. Spectra were recorded in the range of 500-2500 gauss at 20 K under the following conditions: Spectrometer frequency 9.39 GHz; modulation frequency 100 KHz; modulation amplitude 10.0 G; microwave power 66 mW.

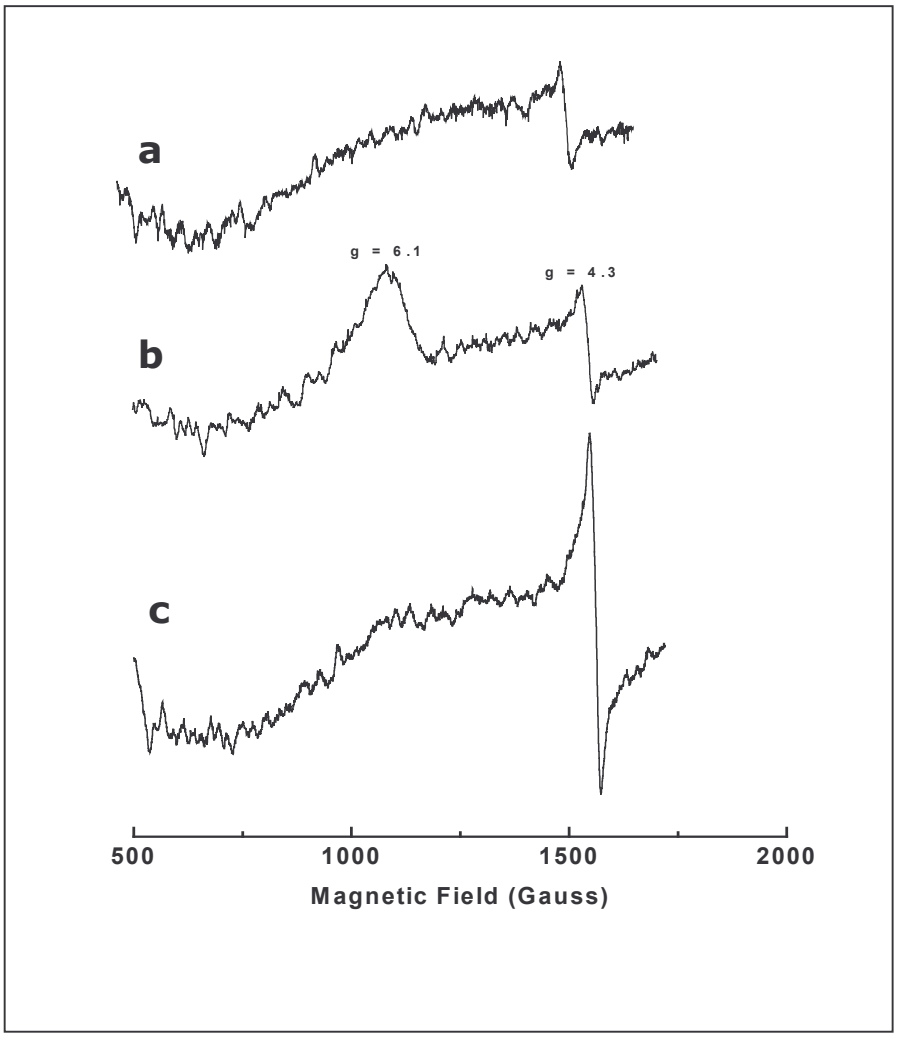

Figure 68. Effect of daidzein on the EPR spectrum of ferric soybean lipoxygenase:

(**a**) Resting (Fe^{2+}) lipoxygenase (200 μM). (**b**) Ferric (Fe^{3+}) lipoxygenase obtained with addition of 200 μM of linoleic acid. (**c**) Ferric lipoxygenase treated with 800 μM of daidzein. All the solutions were in 0.1 M borate buffer (pH 9.0) containing 3% methanol. Spectra were recorded in the range of 500-2500 gauss at 20 K under the following conditions: Spectrometer frequency 9.39 GHz; modulation frequency 100 KHz; modulation amplitude 10.0 G; microwave power 66 mW.

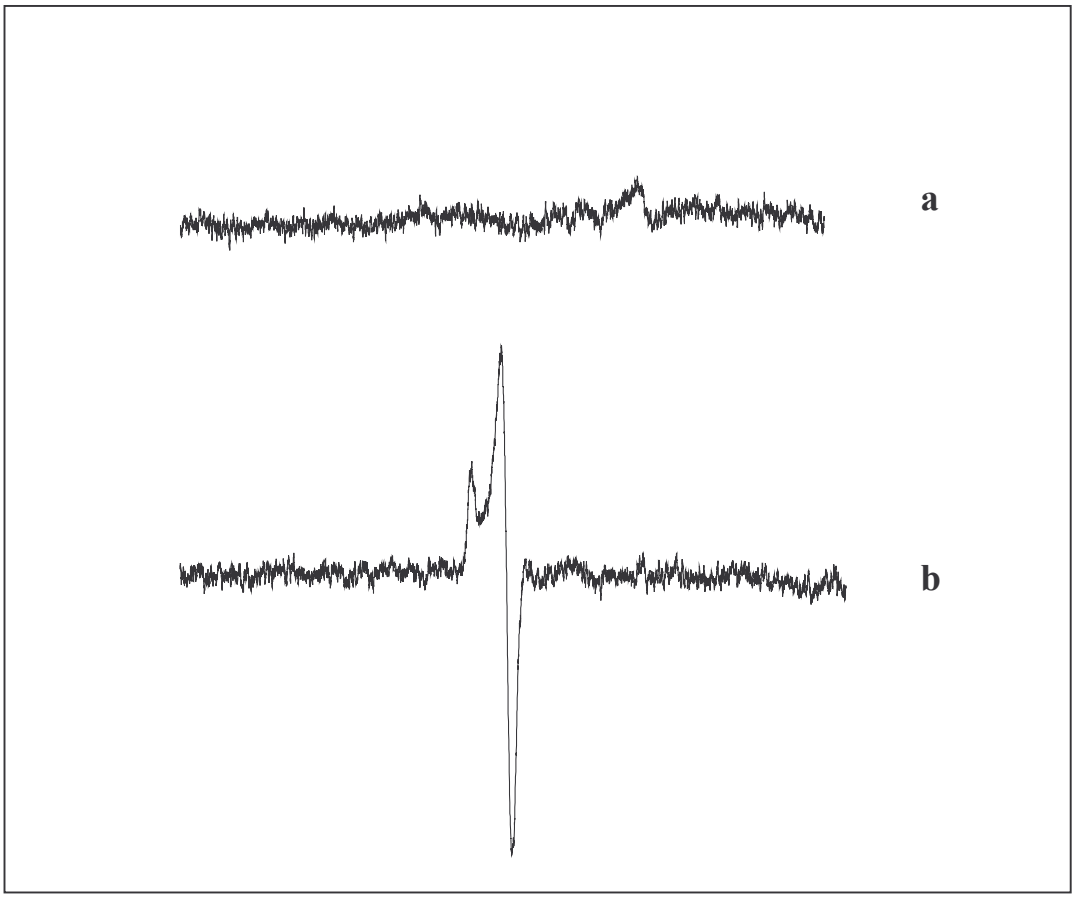

Figure 69. EPR spectra of genistein due to base-catalyzed auto oxidation: Genistein (1mM) was dissolved in 0.1 M borate buffer (pH 9.0) containing 120mM $MgCl_2$.The spectra was scanned under the following conditions at 100 ± 0.5 K, 9.389 GHz frequency, 100 KHz modulation frequency, 0.5G modulation amplitude, 2mW microwave power and sweep width of 40G**.**

a. Spectra of 0.1 M borate buffer (pH 9.0) containing 120mM $MgCl_2$.

b. Spectra of genistein (1mM) dissolved in 0.1 M borate buffer (pH 9.0) containing 120mM $MgCl_2$.

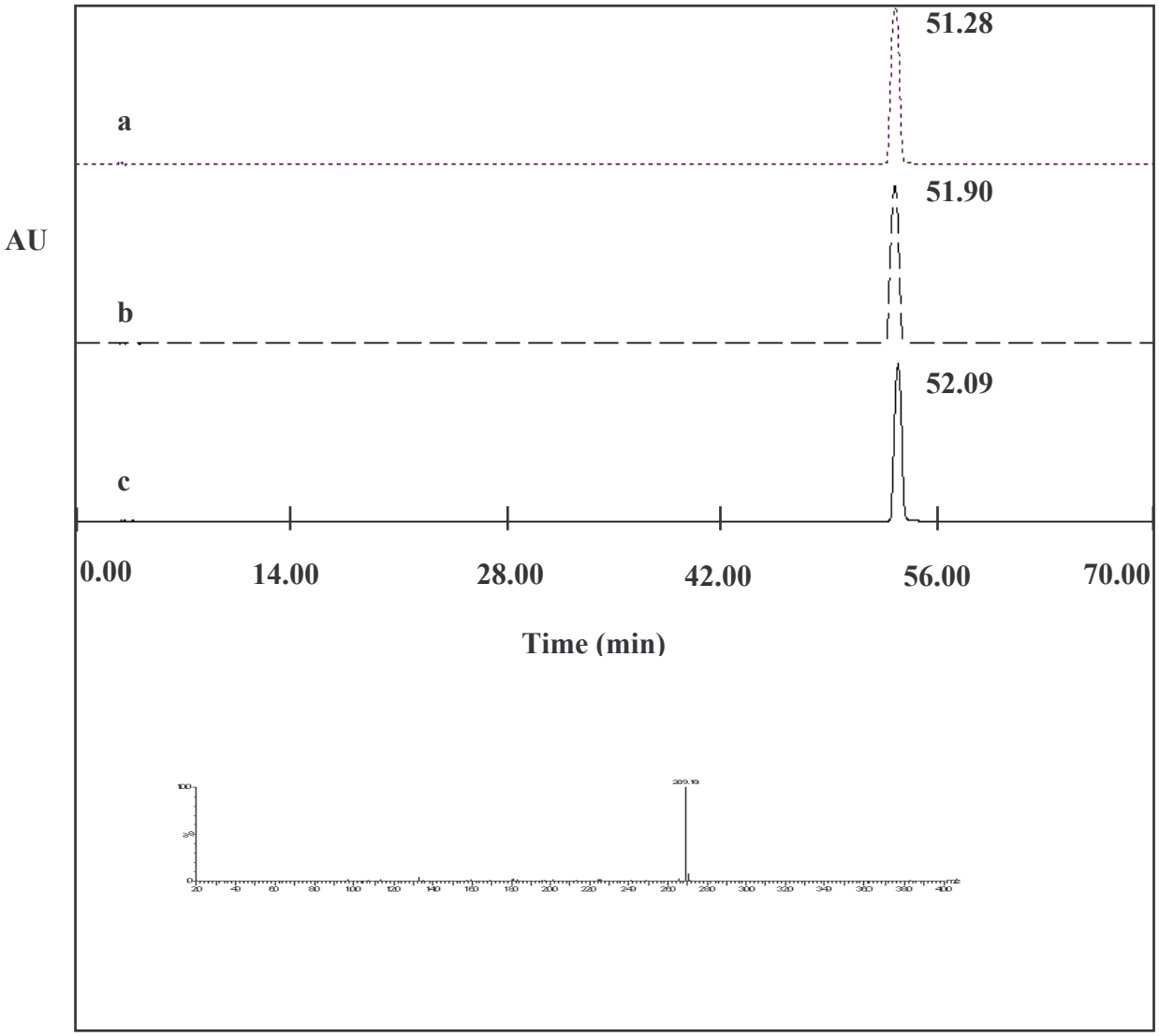

Figure 70. HPLC profile of genistein in presence of soy LOX-1 and linoleic acid: (A) Genistein in 0.2 M borate buffer (pH 9.0). (B) Genistein in presence of soy LOX-1 (C) Genistein in presence of soy LOX-1 and 100 μM linoleic acid. **Inset:** Mass Spectrum of genistein. Genistein was incubated in presence of soy LOX-1 and 100 μM linoleic acid. Genistein was extracted from the reaction mixture by ether. The ether was evaporated under nitrogen and genistein was dissolved in small amount of methanol and subjected to HPLC. Genistein fraction was collected and its mass was analyzed by mass spectrum. The figure shows the selected ion monitoring for the m/z = 269 ion for genistein.

Discussion

Hydroperoxides, products of LOX reaction with unsaturated fatty acids, are the key molecules responsible for the initiation of many diseases and disorders. Inhibition studies have been performed on lipoxygenases with a view to understand the key mechanistic aspects of its inactivation. Soy LOX–1 contains a nonheme ferrous ion that is oxidized by hydroperoxides to yield the catalytically active ferric enzyme (Papatheofanis and Lands, 1985). The ferric enzyme can be distinguished from the ferrous form by its unique CD and EPR features - appearance of a positive band at 425 nm (Slappendel *et. al.,* 1981) and signal at g = 6.1 (Slappendel *et. al.,* 1981), respectively. Antioxidants inhibit lipoxygenase activity by reducing the enzyme bound fatty acid radical intermediates - $L^{\bullet}$ and $LOO^{\bullet}$ (Papatheofanis and Lands, 1985; Takahama, 1985). It has been suggested that both radicals bind to the ferrous form of soy LOX-1 and the reduction of these intermediates is equivalent to the reduction of the ferric enzyme to its resting ferrous state (Feiters *et. al.,* 1985).

The requirement of hydroperoxide implies that the enzyme remains in its resting state in the absence of substrate. This also implies the existence of pathways for the conversion of ferric enzyme to its resting ferrous form. In the normal enzymic reaction, the reversion of ferric soybean LOX-1 to the resting ferrous form may occur due to leakage of linoleate radical ($LOO^{\bullet}$) from the catalytic cycle intermediate (Kemal *et. al.,* 1987). An alternate way of switching off lipoxygenase could be the reduction of the ferric to ferrous form by using physiologically relevant reducing agents.

Results of the present study indicate that isoflavones inhibit lipoxygenase-catalyzed oxidation (Fe^{2+} form) of fatty acid noncompetitively (Fig. 61 & 62). Hence, the substrate and inhibitor complex independently and reversibly, at different sites, with the enzyme. Thus, isoflavones exert dual actions that combine to make them efficient inhibitors. It competes with the hydroperoxide (HPOD) to prevent the conversion of enzyme from ferrous state to its active ferric state and is also capable of reducing the ferric enzyme to its resting form, thereby preventing the oxygenation of ferric enzyme. Stopped-flow inhibition studies confirm genistein inhibits active ferric (Fe^{3+}) form of enzyme.

One of the roles contemplated for isoflavones, is to act as free radical scavengers, wherein the Fe^{3+} of the active enzyme, accepts an electron and lipoxygenase returns to its resting state. It has earlier been reported that reaction started with the resting enzyme (Fe^{2+}) has a very small initial rate of 4 s^{-1}. In contrast, reaction started with active LOX (Fe^{3+}) has a rate of 150 s^{-1} (Schilstra *et. al.,* 1994).

Among the isoflavones studied, genistein is a more potent inhibitor of LOX-1, compared to daidzein. The glycosylated forms - genistin and daidzin- are as potent as their aglycone forms (Table 7). Glycosylation has no effect on the inhibitory potential. Earlier, it has been reported that antioxidants, like isoflavones, are scavengers of peroxyl radicals (Patel *et. al.,* 2001). Structure activity relationship (SAR) that characterizes the free radical scavenging properties of flavonoids is known (Bors *et. al.,* 1990). Isoflavones have similar structural features as flavonoids. In general, they include 2, 3-double

bond with a 4-oxo group and a 3-hydroxyl group in the C-ring. They also have 5, 7-dihydroxyl structures in the A-ring and an ortho-dihydroxyl structure in the *B* ring. Polyphenols are known to chelate with iron; this may also lead to inactivation of lipoxygenase (Schewe *et. al.,* 1986). Isoflavones are very effective against metal-ion induced peroxidation. Due to inherent polyphenolic structures, they can convert deleterious oxy radicals to less harmful phenoxyl radicals, by donating hydrogen atoms. The same inherent structure also contributes to the ability of isoflavonoids to chelate metal ions or alter the iron redox chemistry.

Genistein, with hydroxyl groups at 5, 7 & 4' (Fig. 1), exhibits the highest antioxidant activity in a liposomal system (Arora *et. al.,* 1998). Glycosylation does not affect the antioxidant activity of genistein. Daidzein and daidzin also have identical antioxidant activities. Daidzein, lacking C-5 hydroxyl group, is a less potent antioxidant than genistein with hydroxyl groups at 5, 7 & 4' (Fig. 1). This suggests the likelihood of the hydroxyl group at the C-5 position in genistein playing a very important role in its antioxidant activity. It is clear from the IC_{50} values of the present study, that glycosylation of the genistein and daidzein at C-7 position has no effect on the inhibitory potential of isoflavones. This matches with the reported data (Arora *et. al.,* 1998).

Nordihydroguaiaretic acid (NDGA) is a catecholic antioxidant having hydroxyl groups similar to isoflavones. NDGA has been shown to inhibit lipoxygenase by reducing the catalytically active ferric enzyme to the resting ferrous form thereby acting as an efficient redox inhibitor (Kemal *et. al.,* 1987). The

resting form of the enzyme, when treated with linoleic acid, is converted into active ferric form, which shows an increase in absorbance at 300-600 nm. Addition of genistein is found to decrease the absorbance of active lipoxygenase (Fig. 64), which is possible only if the inhibitor is redox in nature. The ferric form of lipoxygenase exhibits a positive dichroic band at 425 nm, while the ferrous form has no bands in the visible region (Fig. 65 & 66). Spectroscopic experiments clearly indicate that genistein and daidzein are capable of reducing the catalytically active ferric enzyme to the resting ferrous form. This is evident from the disappearance of the 425 nm positive dichroic band on addition of genistein to the soy LOX-1–linoleic acid complex. This confirms that isoflavones are redox inhibitors of lipoxygenase. We have been able to clearly demonstrate that genistein and daidzein prevents the formation of the active LOX by reducing the ferric form to its ferrous state (as shown by a decrease in the g = 6.1 signal) (Fig. 67c & d, 68). The formation of a complex (scheme 1) is indicated by the increase in the g = 4.3 signal. The inhibition of LOX is reversible as the addition of molar excess of linoleic acid to LOX having genistein resulted in the conversion of the resting form of LOX to its active form (Fig. 67e).

Isoflavones may inhibit lipoxygenase by trapping or reducing the enzyme bound fatty acid radical intermediate, $LOO^{\bullet}$, which is equivalent to reducing the Fe^{3+} form to Fe^{2+} form. Phenolic antioxidants reportedly inhibit auto-oxidation by trapping peroxyl radicals ($LOO^{\bullet}$). They cannot trap alkyl radicals ($L^{\bullet}$) as they react with oxygen at diffusion-controlled rates (Ingold, 1969). Genistein undergoes base-catalyzed auto-oxidation at pH 9.0 (Fig. 69).

Trapping of radicals by EPR requires very high concentration of these inhibitors (>1mM). Genistein has limited solubility below pH 7.4. The fact that genistein is able to form phenoxy radical in the absence of lipoxygenase and linoleic acid indicates that genistein may be getting converted to its one-electron oxidation products, when it interacts with lipoxygenase/linoleic acid system.

Soybean lipoxygenase inhibitors, p-aminophenol, catechol. hydroquinone and NDGA, are oxidized to free radical metabolites or one-electron oxidation products. They reduce the catalytically active ferric lipoxygenase to its resting ferrous form. It has been reported the inhibitors undergo base-catalyzed auto-oxidation in the pH range 6.5-9.0 (Van der Zee *et. al.,* 1989). Isoflavones can form phenoxy radicals, which is demonstrated by the consumption of genistein when incubated with 2, 2'-Azobis-amidino-propane hydrochloride (AAPH). The genistein/AAPH system produce phenoxy radicals, however the yield of the radicals is low which implies that either they are difficult to form or labile in nature (Patel *et. al.,* 2001). Genistein is a powerful and potent radical scavenger. The dissociation constant for genistein (pKa: 7.2, 10.0, 13.1) has been evaluated spectroscopically and the monoanionic form of genistein existing at physiological pH is more powerful radical scavenger than the neutral molecule (Zielonka *et. al.,* 2003). All these studies show that genistein can form phenoxy radical and probably genistein reacts with hydroperoxides to form phenoxy radicals and donates the electron to ferric form converting it to ferrous form. It is probable that genistein scavenges lipid peroxyl radicals derived from the enzyme reaction.

It also converts the active form of enzyme to the resting state. According to our mechanism (scheme 1), an electron donated by isoflavones is accepted by the ferric form (Fe^{3+}) of LOX, which is reduced to resting ferrous form (Fe^{2+}), thus inhibiting LOX. This report on the redox inhibition of lipoxygenase by isoflavones may be first of its kind. Isoflavones are natural redox inhibitors and can reductively regulate lipoxygenase activity by preventing the activation of resting lipoxygenase to its reactive state and at the same time they also convert the active form of lipoxygenase to its resting state. Genistein is neither consumed nor does its state change during the course of this reaction.

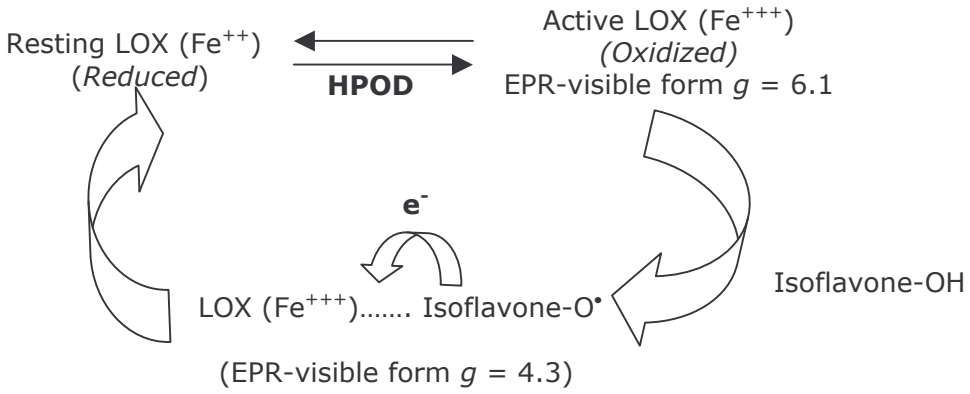

Scheme 1 Complex formation between Lipoxygenase-isoflavone

Section D: Interaction of isoflavones with glycinin and conglycinin

Results and Discussion

SDS-PAGE analysis of Glycinin and conglycinin:

The purity of glycinin and conglycinin was determined by reducing SDS-PAGE electrophoresis (Fig. 71). A resolving gel of 15% and a stacking gel of 5% were used. The purity of isolated glycinin and conglycinin was >95%.

Fluorescence measurements:

Isoflavones genistein, daidzein, genistin and daidzin did not quench the protein fluorescence of glycinin and conglycinin. This suggests that either they are not able to interact or protein has intrinsically bound polyphenols, which prevents the interaction. Daidzein fluorescence was also unaffected in the presence of glycinin and conglycinin, thereby suggesting the absence of binding sites on the protein molecule.

Equilibrium Dialysis:

Genistein did interact both with glycinin and conglycinin as there was no difference in genistein concentration between "blank" and protein containing solutions. This suggests that there are no binding sites for genistein on the protein molecule.

Quantification of Intrinsically bound isoflavones:

The presence of isoflavones was detected in the methanolic extract of glycinin and conglycinin. Glycinin HPLC profile shows that genistin is the most abundant isoflavones present. Genistein could not be detected (Fig.72). Conglycinin also showed the presence of four isoflavones genistein, daidzein, genistin and daidzin used in the interaction studies (Fig.73). Glycinin had 0.062% of isoflavone and conglycinin had 0.0502% of isoflavones.

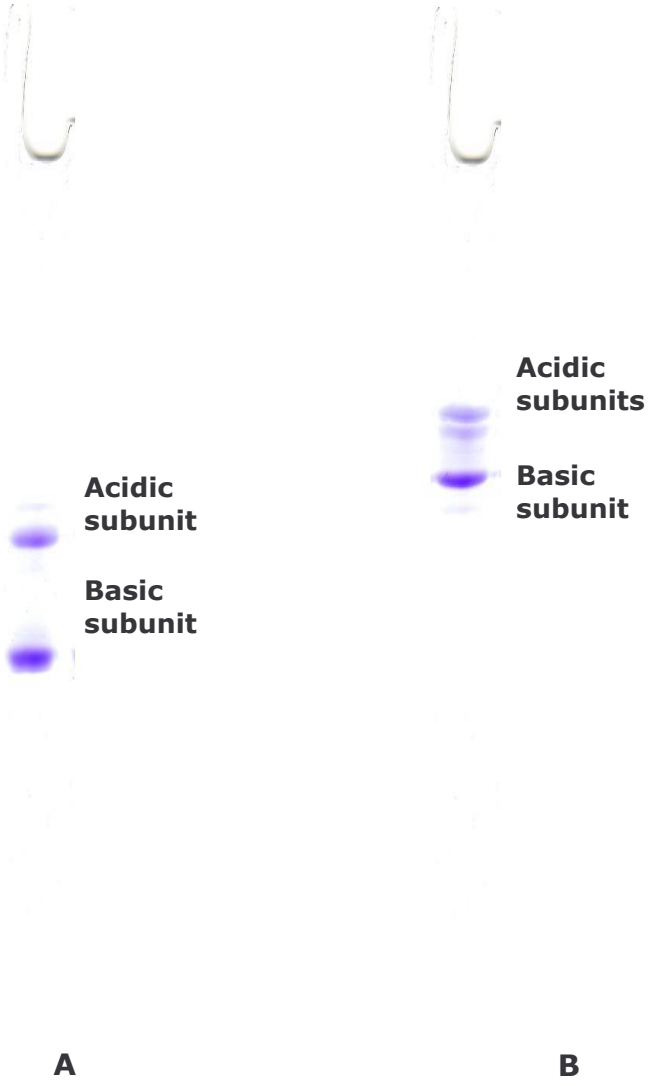

Figure 71. Gel electrophoresis of soy glycinin and conglycinin: **A** SDS-PAGE of glycinin, **B.** SDS-PAGE of conglycinin. A 5% stacking gel and 15% resolving gel was used and electrophoresis was run according to Laemmelli (1970).

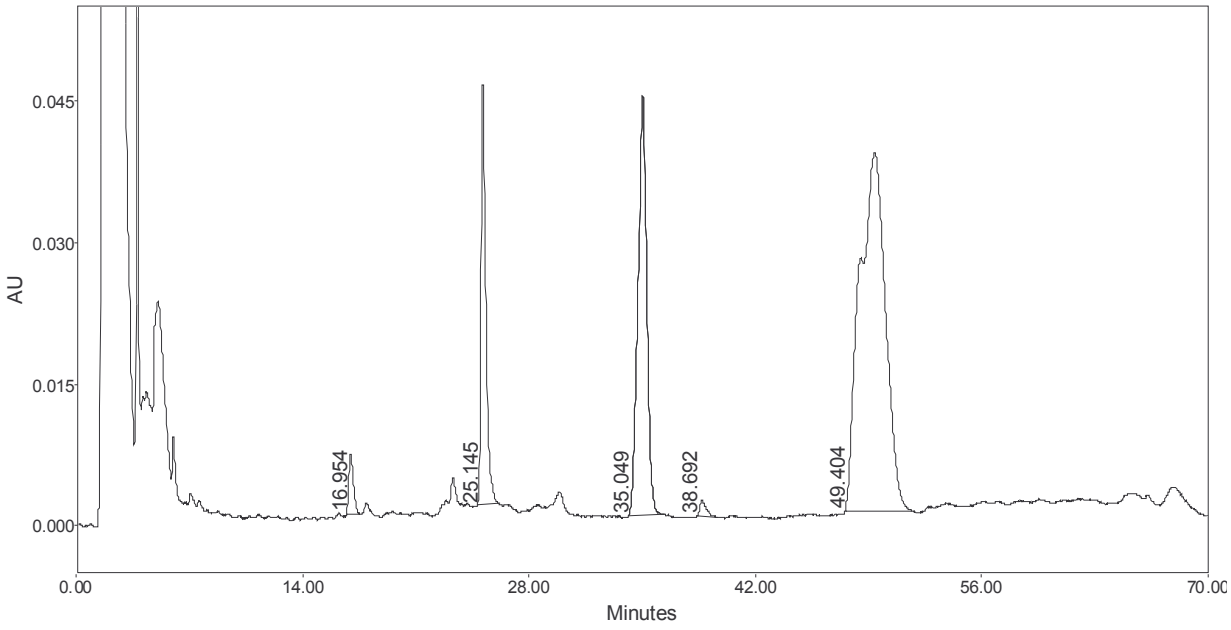

Figure 72. HPLC profile 11S extract showing the presence of isoflavones: Retention time of isoflavones is as follows 16.954-daidzin, 25.145-genistin, and 38.692-daidzein. A gradient elution using acetonitrile-water (15-35%) was run over a period of 50 min at a flow rate of 1ml/min.

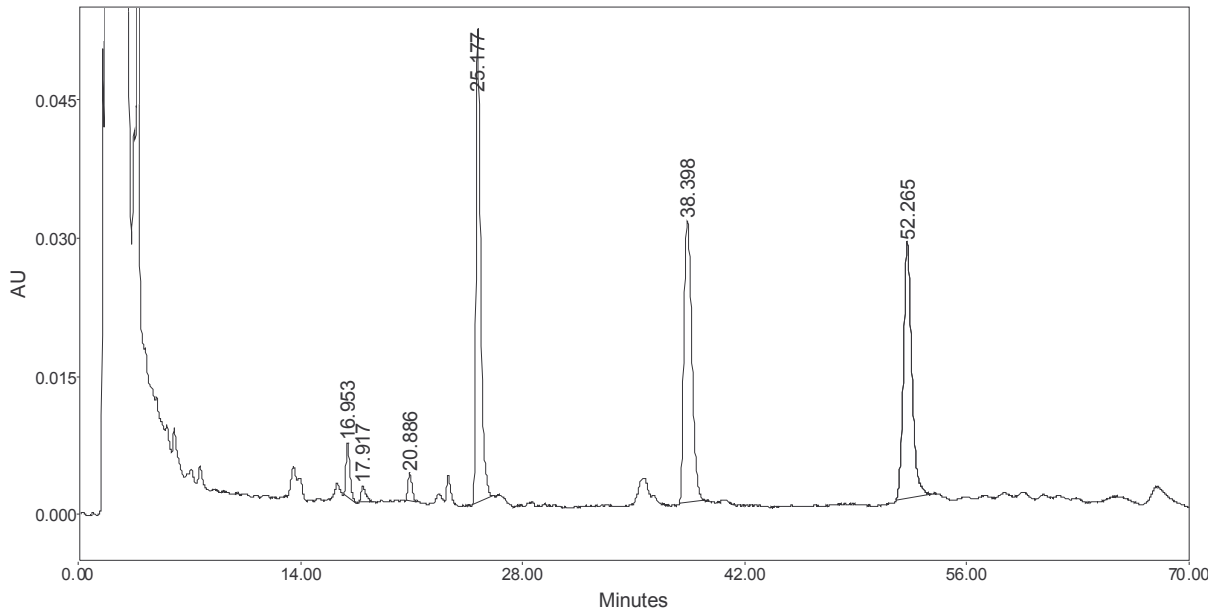

Figure 73. HPLC profile 7S extract showing the presence of isoflavones: Retention time of isoflavones is as follows 16.954-daidzin, 25.177-genistin, 38.398-daidzein, and 52.265-genistein. A gradient elution using acetonitrile-water (15-35%) was run over a period of 50 min at a flow rate of 1ml/min.

Discussion

Polyphenols are secondary metabolites synthesized by plants. They are undoubtedly the most useful of all plant chemical defenses. These are potent anti-fungal, anti-bacterial and anti-viral agents. These polyphenolic polymers combine with proteins leading to inhibition of enzymes and reducing the nutrionally available proteins in food. These are difficult to degrade and because of their molecular size, it is impossible to sequester into vesicles so that their activity may be stopped (Swain, 1978). The association of polyphenols with proteins is principally a surface phenomenon. The polyphenols are multidentate ligands with phenolic groups are capable of interacting with proteins. Polyphenol protein complexes can be dissociated by the addition of hydrophobic solvents or hydrogen bond acceptor solvents (e. g. acetone), polyvinylpyrrolidine, polyethylene glycols, non-ionic detergents and nitrogen heterocycles. Complex formation is pH dependent and each protein has a distinctive pH optimum and usually lies at or very near to the isoelectric point of the particular protein. It has been shown that extent of complex formation rapidly declines as the pH of the medium is raised above 9.0. These observations suggest that protein-polyphenolic interaction is dominated by formation of strong non-covalent bonds than by ionic or covalent linkages (White, 1957; Gustavson and Holm, 1952). The interaction between protein and polyphenol is depends upon three features (a) molecular size of the phenol, (b) conformational flexibility of the polyphenol and (c) water solubility of the polyphenol, a inverse relationship exists between the strength of association with protein and the solubility of the

polyphenol in water. Low solubility of polyphenol favours strong association. Protein-polyphenol complexation is surface phenomenon and takes place in two discrete steps. In the first step, polyphenol interacts with regions of protein rich in numerous aromatic amino acids by developing hydrophobic contacts. Due to this interaction there is a change in the polypeptide conformation bringing several aromatic groups or hydrophobic side chains in a close juxtaposition forming a hydrophobic pocket or a hydrophobic environment. In the second step, hydrophobic interaction is reinforced by hydrogen bonds between the phenolic residues and polar groups in the vicinity of hydrophobic cavity (Spencer *et. al.,* 1988). Isoflavones are also sparingly soluble polyphenols. When soy is defatted, isoflavones remain in the meal and does not partition into the oil phase. No isoflavones are present in the soybean oil thereby confirming that isoflavones have very high affinity for proteins present in the defatted meal. Glycinin and conglycinin are the major storage proteins of soy and understanding the partitioning of isoflavones among these proteins is of great importance in preparation of functional foods rich in isoflavones. Results of the present study indicate that isoflavones are unable to bind to glycinin and conglycinin. The probable reason may be the tight complexation between isoflavones and soybean storage proteins. The resulting protein-polyphenol complexation has no ligand binding sites available for the binding of isoflavones. The presence of intrinsically bound isoflavones has been confirmed by the extraction of the pure proteins and quantification of isoflavones present. Both glycinin and conglycinin are found to have intrinsically bound isoflavones and other

unidentified compounds like saponins. Both glycinin and conglycinin have been subjected to various methods of removing the intrinsically bound isoflavones. These treatments are found insufficient to remove the intrinsically bound isoflavones. This probably suggests that isoflavones are tightly bound to the glycinin and conglycinin. Glycinin (0.062%) has slightly higher content of isoflavones compared to conglycinin (0.0502%).

.

SUMMARY

AND

CONCLUSIONS

SUMMARY AND CONCLUSIONS

The salient features of the present investigation are as follows.

- Genistein, daidzein and their glycosylated forms genistin and daidzin were purified to homogeneity from defatted soy flour by solvent extraction, solvent partition and adsorption chromatography. The homogeneity of the purified isoflavones was established by high performance liquid chromatography.
- The interaction of purified isoflavones was followed with serum albumin (bovine and human), lipoxygenase (soy lipoxygenase-1 and mammalian PMNL 5-lipoxygenase) and soybean storage proteins (glycinin and conglycinin) by biophysical and enzyme kinetic measuements.
- The binding of genistein to bovine serum albumin (BSA) and human serum albumin (HSA) has been investigated by equilibrium dialysis, fluorescence measurements, circular dichroism and molecular visualization.
- Among the isoflavones genistein and daidzein interacted with serum albumin (bovine and human) as evidenced both by direct and indirect ligand binding measurements. The glycosylated isoflavones genistin and daidzin did not bind to serum albumin.
- Equilibrium dialysis measurements showed that genistein bound to bovine and human serum albumin with binding constants of $1.78 \pm 0.2 \times 10^5\ M^{-1}$ and $1.0 \pm 0.2 \times 10^5\ M^{-1}$ respectively.

- The binding constants obtained by fluorescence quenching measurements for genistein and daidzein to BSA are $1.5 \pm 0.2 \times 10^5\ M^{-1}$ and $1.2 \pm 0.2 \times 10^5\ M^{-1}$; HSA are $1.5 \pm 0.2 \times 10^5\ M^{-1}$ and $1.4 \pm 0.2 \times 10^5\ M^{-1}$, respectively. There is good agreement in the binding constants obtained for genistein-BSA and genistein-HSA interaction by both direct and indirect methods.
- One molecule of genistein is bound per mole of serum albumin (bovine and human).
- The ability of serum albumin (bovine and human) to bind genistein is found to be lost when the tryptophan residue of albumin is modified with N-bromosuccinimide.
- At 27°C (pH 7.4), van't Hoff's enthalpy, entropy and free energy changes that accompany the binding are found to be -13.16 kcal. mol^{-1}, –21 cal $mol^{-1}K^{-1}$ and –6.86 kcal mol^{-1}, for human serum albumin respectively. For bovine serum albumin van't Hoff enthalpy, entropy and free energy changes that accompany the binding are found to -11.5 kcal mol^{-1}, -15.5 cal mol^{-1} K^{-1} and –6.9 kcal mol^{-1} respectively.
- Temperature and ionic strength dependence and competitive binding measurements of genistein with HSA in presence of fatty acids and 8 – Anilino-1- naphthalene sulfonic acid have suggested the involvement of both hydrophobic and ionic interactions in the genistein-BSA and genistein-HSA binding.
- Binding measurements of genistein with BSA (Bovine serum albumin) and HSA, and those in the presence of warfarin and 2,3,5-tri-

iodobenzoic acid and Förster energy transfer measurements have been used for deducing the binding pocket on serum albumin.

- Fluorescence anisotropy measurements of daidzein bound and then displaced with warfarin, 2,3,5-tri-iodobenzoic acid or diazepam confirm the binding of daidzein and genistein to sub domain IIA of HSA, which is well supported by molecular visualization.
- The interaction of isoflavones (genistein and daidzein) with CNBr cleaved albumin fragments – N, M and C (amino acid residues 1-123, 124-298 and 299-585, respectively) was followed by intrinsic protein fluorescence and daidzein fluorescence.
- Genistein quenched the tryptophan fluorescence of the M domain, which contains the lone W_{214} with a binding constant of $0.45 \pm 0.2 \times 10^5$ M^{-1}. The binding constant was invariant with temperature in the range of 17 to 47°C, suggesting the role of hydrophobic interactions in the binding of genistein to M domain of HSA.
- Daidzein fluorescence and anisotropy, which remained unaffected in the presence of N domain, showed enhancement in the presence of M domain and a marginal increase in the presence of C domain. This suggested that isoflavones have greater affinity towards the M domain; domain M and C correspond to the domains II and III, respectively, of intact serum albumin molecule. These studies support our findings with HSA that isoflavones bind to domain IIA of serum albumin.

- Isoflavones are found to inhibit the activity of both soy lipoxygenase 1 and human polymorpho nuclear lymphocyte 5-lipoxygenase in a concentration dependent manner.
- Genistein, genistin, daidzein and daidzin inhibited soy lipoxygenase 1 with IC_{50} values of 107 μM, 109μM, 136μM and 140 μM, respectively. Glycosylation had no effect on the inhibitory potential of isoflavones.
- Genistein and daidzein inhibited 5- lipoxygenase with IC_{50} values of 125 μM and 157 μM, respectively.
- Both genistein and daidzein are found to be noncompetitive inhibitors of soy lipoxygenase 1 with inhibition constants, K_i, of 60 and 80 μM, respectively.
- Spectroscopic studies showed that isoflavones are redox inhibitors inhibiting lipoxygenase by reducing the active state iron to the ferrous state and also prevent the activation of the resting enzyme.
- From absorbance measurements, the addition of genistein shows a decrease in the peak at 350 nm (present only in active enzyme), indicating a change in the state of iron from the active ferric to ferrous state.
- CD spectrum of soy LOX-1 in its active yellow form (Fe^{3+}), revealed a positive CD band at 425 nm. Addition of genistein or daidzein resulted in a decreased band at 425 nm. Thus, genistein reduces the active Fe^{3+} yellow enzyme to its resting Fe^{2+} form.

- The EPR spectrum of lipoxygenase exhibits a *g*= 4.3 signal, seen in the resting lipoxygenase and EPR feature around *g*= 6.1 attributed to the high-spin Fe^{3+} in an axial field.
- Addition of genistein or daidzein to the active lipoxygenase showed a decrease in the *g*= 6.1, signal indicating the conversion of the active state lipoxygenase to its resting state. The addition of linoleic acid in molar excess to soy LOX-1 containing genistein has led to the reappearance of the *g*= 6.1 signal showing that the inhibition is reversible. The increase in *g*= 4.3 signal in samples treated with genistein, probably, indicates the formation of an enzyme–genistein complex.
- Stopped-flow inhibition studies also confirm genistein inhibits active ferric (Fe^{3+}) form of enzyme. The reaction in presence of inhibitor resembles the reaction of LOX in its resting Fe^{2+} form by exhibiting a lag phase, thereby conforming that isoflavones are redox inhibitors of LOX.
- Genistein may be getting converted to its one-electron oxidation products, when it interacts with lipoxygenase/linoleic acid system. HPLC and mass spectrometry show that genistein remains in its native state. Genistein can form phenoxy radical and it reacts with hydroperoxides to form phenoxy radicals and donates the electron to ferric form converting it to ferrous form.
- Isoflavones are unable to interact with purified glycinin and conglycinin. The resulting protein-polyphenol complexation has no

ligand binding sites available for the binding of isoflavones. Purified glycinin and conglycinin contain tightly bound isoflavones. The presence of intrinsically bound isoflavones was confirmed by the extraction of the pure proteins and quantification of isoflavones present.

- Isoflavones did not interact with isolated glycinin and conglycinin probably because of the tightly pre-occupied molecules.

BIBLIOGRAPHY

BIBLIOGRAPHY

1. Aceto A, Sacchetta P, Bucciarelli T, Dragani B, Angelucci S, Radatti GL & Diilio C (1995) Structural and functional properties of the 34kDa fragment produced by the N-Terminal chymotryptic cleavage of Glutathione transferase P1-1. *Arch Biochem Biophy* **316***,* 873-878.

2. Adlercreutz H, Fotsis T & Lampe J (1993) Quantitative determination of liganans and isoflavones in plasma of omnivorous and vegetarian women by isotope-dilution gas chromatography-mass spectrometry. *Scand J Clin Lab Invest* **53**, 5-18.

3. Adlercreutz H, Goldin BR, Gorbach SL, Höckerstedt KAV & Watanabe S (1995) Soybean phytoestrogen intake and cancer risk. *J Nutr* **125**, 757-770S.

4. Aharony D & Stein RL (1986) Kinetic mechanism of guinea pig neutrophil 5-lipoxygenase. *J Biol Chem* **261**, 11512-11519.

5. Akiyama T, Ishida J, Nakagawa S, Ogawara H, Watanabe SN, Shibuya M & Fukami Y (1987) Genistein, a specific inhibitor of tyrosine-specific protein kinases. *J Biol Chem* **262**, 5592-5595.

6. Anderson JW, Johnstone BM & Cook-Newell ME (1995) Meta-analysis of the effects of soy protein intake on serum lipids. *N Engl J Med* **333**, 276-82.

7. André C, Jacquot Y, Truong TT, Thomassin M, Robert JF and Guillaume YC (2003) Analysis of the progesterone displacement of its human serum albumin binding site by beta-estradiol using biochromatographic approaches: effect of two salt modifiers. *J Chromatogr B Analyt Technol Biomed Life Sci* **796(2)**, 267-81.

8. Anthony MS, Clarkson TB, Hughes CL Jr, Morgan TM & Burke GL (1996) Soybean isoflavones improve cardiovascular risk factors

without affecting the reproductive system of peripubertal rhesus monkeys. *J Nutr* **126**, 43-50.

9. Aoyama T, Fukui K, Takamatsu K, Hashimoto Y & Yamamoto T (2000) Soy protein isolate and its hydrolysate reduce body fat of dietary obese rats and genetically obese mouse (yellow KK). *Nutrition* **16 (5)**, 349-354.

10. Arora M, Nair G & Strasburg GM (1998) Antioxidant activities of isoflavones and their biological metabolites in a liposomal system. *Arch Biochim Biophys* **356**, 133-141.

11. Argos P (1985) Structural similarity between legumin and vicilin storage proteins from legumes. *EMBO J* **4(5)**, 1111-7.

12. Aurbach GD, Marx SJ & Spiegel AM (1992) Metabolic bone disease. In Williams Textbook of Endocrinology, ed, JD Wilson &DW Foster **28**, 1477-517. Philadelphia, Saunders 8th ed.

13. Axelrod B, Cheesbrough TM & Laakso S (1981) Lipoxygenase from soybeans. *Meth Enzymol* **71**, 441-451.

14. Bagatolli LA, Kivatinitz SC, Aguilar F, Soto MA, Sotomayor P & Fidelo GD (1996) Two distinguishable fluorescent modes of 1-anilino-8-napthalenesulfonate bound to human albumin. *J Fluoresc* **6**, 33-40.

15. Barnes S, Peterson G, Grubbs C & Setchell K (1994) Potential role of dietary isoflavones in the prevention of cancer. *Adv Exp Med Biol* **354**, 135-47.

16. Bennetts HW, Underwood EJ & Shier FL (1946) A specific breeding problem of sheep on subterranean clover pastures in western Australia. *Aust Vet J* **22**, 2-12.

17. Berde CB, Hudson BS, Simoni RD & Sklar LA (1979) Human serum albumin. Spectroscopic studies of binding and proximity relationships for fatty acids and bilirubin. *J Biol Chem* **254**, 391-400.

18. Bergamaschi G, Rosti V, Danova M, Ponchio L, Lucotti C & Cazzola M (1993) Inhibitors of tyrosine phosphorylation induce apoptosis in human leukemic cell lines. Leukemia **7**, 2012-2018.

19. Bhattacharya AA, Grűne T & Curry S (2000) Crystallographic analysis reveals common modes of binding of medium and long-chain fatty acids to human serum albumin. *J Mol Biol* **303**, 721-732.

20. Bi S, Ding L, Tian Y, Song D, Zhou X, Liu X & Zhang H (2004) Investigation of the interaction between flavonoids and human serum albumin*. J Mol Struct* **703***,* 37-45.

21. Bierman EL & Glomset JA (1992) Disorders of lipid metabolism. In Williams Textbook of Endocrinology, ed. JD Wilson, DW Foster, 26, 1367-95. Philadelphia: Saunders, 8th ed.

22. Borras C, Gambini J, Gomez-Cabrera MC, Sastre J, Pallardo FV, Mann GE & Vina J (2006) Genistein, a soy isoflavone, up-regulates expression of antioxidant genes: involvement of estrogen receptors, ERK1/2, and NF kappaB. *Faseb J* **20(12)**, 2136-8.

23. Borthakur A, Ramadoss CS & Appu Rao AG (1988) Physico-chemical studies on two forms of Bengal gram lipoxygenase: implication of structural differences. *Biochim Biophys Acta* **958**, 40-51.

24. Boyington JC, Gaffney BJ & Amzel LM (1990) Crystallization and preliminary X-ray analysis of soybean lipoxygenase-1, a non-heme iron-containing dioxygenase. *J Biol Chem* **265**, 12771-12773.

25. Boyington JC, Gaffney BJ & Amzel LM (1990) The three-dimensional structure of an arachidonic acid 15-lipoxygenase. *Science* **260**, 1482-1486.

26. Borgeat P, Fruteau de Laclos P & Maclouf J (1983) New concepts in the modulation of leukotrienes synthesis. *Biochem Pharmacol* **92**, 381-387.

27. Borowski T & Broclawik E (2003) Catalytic reaction mechanism of lipoxygenase. A density functional theory study. *J Phys Chem B* **107**, 4639-4646.

28. Boyum A (1976) Isolation of lymphocytes, granulocytes and macrophages. *Scand J Immunol Suppl* **5**, 9-15.

29. Bors W, Heller W, Michel C & Saran M (1990) Flavonoids as antioxidants: Determination of radical scavenging efficacies. *Meth Enzymol* **186**, 343-381.

30. Bradbury RB & White DE (1954) Oestrogens and related substances in plants. *Vitam Horm* **12**, 207-33.

31. Braden AWH, Hart NK & Lamberton JA (1967) The estrogenic activity and metabolism of certain isoflavones in sheep. *Aust J Agric Res* **18**, 335-48.

32. Brash AR (1999) Lipoxygenases: occurrence, functions, catalysis and acquisition of substrate. *Science* **260**, 1482-1486.

33. Brown JR (1975) Structure of bovine serum albumin. *Fedn Proc Fedn Am Socs exp Biol* **34**, 591.

34. Butenko IG, Gladtchenko SV & Galushko SV (1993) Anti-inflammatory properties and inhibition of leukotriene C4 biosynthesis *in vitro* by flavonoid baicalein from *Scutellaria baicalensis* Georgy roots. *Agents Actions* **39**, C49–C51.

35. Carter DC & Ho JC (1994) Structure of serum albumin. *Adv Prot Chem* **45**, 153-203.

36. Cassidy AS, Bingham S & Setchell KDR (1994) Biological effects of diet of soy protein rich in isoflavones on the menstrual cycle of premenopausal women. *Am J Clin Nutr* **60**, 333-40.

37. Chaudry A, McClinton S, Moffat LEF & Wahle KWJ (1991) Essential fatty acid distribution in the plasma and tissue phospholipids of patients with benign and malignant prostatic disease. *Br J Cancer* **64**, 1157–1160.

38. Chaudry AA, Wahle KWJ, McClinton S & Moffat LEF (1994) Arachidonic acid metabolism in benign and malignant prostatic tissue *in vitro*: effects of fatty acids and cyclooxygenase inhibitors. *Int J Cancer* **57**, 176–180.

39. Chang W-C, Liu Y-W, Ning C-C, Suzuki H, Yoshimoto T & Yamamoto S (1993) Induction of arachidonate 12-lipoxygenase mRNA by epidermal growth factor in A431 cells. *J Biol Chem* **268**, 18734–18739.

40. Chen GZ, Huang XZ, Xu JG, Wang ZB & Zheng ZZ (1990) *Method of fluorescent analysis*, 2nd ed., Science Press, Beijing, p 126.

41. Chen GZ, Huang XZ, Xu JG, Wang ZB & Zheng ZZ, (1990a) *Method of fluorescent analysis*, 2nd ed., Science Press, Beijing, p 123.

42. Chen RF (1967) Removal of fatty acids from serum albumin by charcoal treatment. *J Biol Chem* **242**, 173-181.

43. Clark P, Rachinsky MR & Foster JF (1962) Moving boundary electrophoresis behavior and acid isomerization of human mercaptalbumin. *J Biol Chem* **237**, 2509-2513.

44. Clapp CH, Banerjee A & Rotenberg SA (1985) Inhibition of soybean lipoxygenase 1 by N-alkylhydroxylamines. *Biochemistry* **24(8)**, 1826-30.
45. Coates JB, Medeiros JS, Thanh VH & Nielsen NC (1985) Characterization of the subunits of beta-conglycinin. *Arch Biochem Biophys* **243(1)**, 184-94.
46. Cohen B-S, Grossman S, Pinksky A & Klein BP (1984) Chlorophyll inhibition of lipoxygenase in growing pea plants. *J Agric Food Chem* **32**, 516-519.
47. Cohen LA, Thompson DO, Maeura Y, Choi K, Blank ME & Rose DP (1986) Dietary fat and mammary cancer. Promoting effects of different dietary fats on *N*-nitrosomethylurea-induced rat mammary tumorigenesis. *J Natl Cancer Inst* **77**, 33–42.
48. Coldham NG, Darby C, Hows M, King LJ, Zhang AQ & Sauer MJ (2002) Comparative metabolism of genistin by human and rat gut microflora: detection and identification of the end products of metabolism. *Xenobiotica* **32(1)**, 45-62.
49. Coldham NG & Sauer MJ (2001) Identification, quantification and biological activity of phytoestrogens in a dietary supplement for breast enhancement. *Food Chem Toxicol* **39 (12)**, 1211-1224.
50. Cooper C, Campion G & Melton LJ III. (1992) Hip fractures in the elderly: a worldwide projection. *Osteoporos Int* 285-9.
51. Constantinou A & Huberman E (1995) Genistein as an inducer of tumor cell differentiation: possible mechanisms of action. *Proc Soc ExpBiol Med* **208(1)**, 109-15.
52. Constantinou A, Kiguchi K & Huberman E (1990) Induction of differentiation and DNA strand breakage in human HL-60 and K-562 leukemia cells by genistein. *Cancer Res* **50**, 2618-24.

53. Corey EJ & Nagata R (1987) Evidence in favor of an organoiron-mediated pathway for lipoxygenation of fatty acids by soybean lipoxygenase. *J Am Chem Soc* **109**, 8107-8108.

54. Coward L, Barnes NC & Setchell KDR (1993) Genistein, daidzein and their β-Glycoside conjugates: Antitumor isoflavones in soybean Foods from American and Asian Diets. *J Agric Food Chem* **41**, 1961-1967.

55. Curry S, Mandelkow H, Brick P & Franks N (1998) Crystal structure of human serum albumin complexed with fatty acid reveals an asymmetric distribution of binding sites. *Nat Struct Biol* **5 (9)**, 827-835.

56. Davies CGA, Netto FM, Glassenap N, Gallaher CM, Labuza TP & Gallaher DD (1998) Indication of the maillard reaction during storage of protein isolates. *J Agric Food Chem* **46**, 2485-2489.

57. Dangles O, Dufour C, Manach C, Morand C & Remesy C (2001) Binding of flavonoids to plasma proteins. *Methods Enzymol* **335**, 319-333.

58. Daughaday WH (1959) Steroid-protein interactions. *Physiol Rev* **39**, 885-902.

59. De Groot JJ, Garssen GJ, Vliegenthart JF & Boldingh J (1973) The detection of linoleic acid radicals in the anaerobic reaction of lipoxygenase. *Biochim Biophys Acta* **326(2)**, 279-84.

60. De Groot JJMC, Veldink GA, Vliegenthart JFG, Boldngh J, Wever R & Van Gelder BF (1975) Demonstration by EPR spectroscopy of the functional role of iron in soybean Lipoxygenase-1. *Biochim Biophys Acta* **377**, 71-79.

61. Devachand PR, Keller H, Peters JM, Vazquez M, Gonzalez FJ & Wahli W (1996) The PPARa-leukotriene B4 pathway to inflammation. *Nature* **384**, 39-43.

62. Earashi M, Noguchi M, Kinoshita K & Tanaka M (1995) Effects of eicosanoid synthesis inhibitors on the *in vitro* growth and prostaglandin E and leukotriene B secretion of a human breast cancer cell line. *Oncology* **52**, 150–155.

63. Edmond MR, Fasella PM, Veldink GA, Vliegenthart JFG & Boldingh J (1977) On the mechanism of action of soybean lipoxygenase-1. A stopped flow kinetic study of the formation and conversion of yellow and purple species. *Eur J Biochem* **76**, 469-479.

64. Eriksen EF, Colvard DS & Berg NJ (1988) Evidence of estrogen receptors in normal human osteoblast-like cells. *Scienc*e **241**, 84-6.

65. Evans SV (1993) SETOR: hardware-lighted three-dimensional solid model representations of macromolecules. *J Mol Graph* **11**, 127-128, 134-138.

66. Fehske KJ, Schläfer U, Wollert U & Muller WE (1982) Characterization of an important drug binding area on human serum albumin including the high-affinity binding sites of warfarin and azapropazone**.** *Mol Pharmacol* **21**, 387-393.

67. Feiters MC, Aasa R, Malmstrom BG, Slappendel S, Veldink GA & Vliegenthart JFG (1985) Substrate fatty acid activation in soybean lipoxygenase-1 catalysis. *Biochim Biophys Acta* **831**, 302-305.

68. Feldhoff RC & Peters T Jr (1976) Determination of the number and relative position of tryptophan residues in various albumins. *Biochem J* **159**, 529-533.

69. Feussner I & Wastermack C (2002) The Lipoxygenase pathway. *Annu Rev Plant Biol* **53**, 275-297.

70. Fischer SM, Conti CJ, Locniskar M, Belury MA, Maldve RE, Lee ML, Leyton J, Slaga TJ & Bechtel DH (1992) The effect of dietary fat on the rapid development of mammary tumors induced by 7,12-dimethylbenz (*a*) anthracene in SENCAR mice. *Cancer Res* **52**, 662–666.

71. Forman BM, Chen J & Evans RM (1997) Hypolipidemic drugs, polyunsaturated fatty acids and eicosanoids are ligands for peroxisome proliferator activated receptors alpha and delta*. Proc Natl Acad Sci (USA)* **94**, 4132-4137.

72. Ford-Hutchinson AW, Gresser M & Young RN (1991) Arachidonate 15-lipoxygenase; characteristics and potential biological significance. *Eicosanoids* **4**, 65-74.

73. Forman BM, Chen J & Evans RM (1997) Hypolipidemic drugs, polyunsaturated fatty acids and eicosanoids are ligands for peroxisome proliferator activated receptors alpha and delta. *Proc Natl Acad Sci (USA)* **94**, 4132-4137.

74. Förster T (1967) Mechanism of energy transfer in comprehensive biochemistry (Florkin M and Statz E H, eds.), Vol **22**, pp 61-77, Elsevier, New York.

75. Föster JF & Sterman MD (1956) Conformation changes in bovine serum albumin associated with hydrogen ion and urea binding. II Hydrogen titration curves. *J Am Chem Soc* **78**, 3656-3660.

76. Foster JF (1977) In "Albumin Structure, Function and Uses" (Rosenoer VM, Oratz M and Rothschild MA, eds) Pergamon, Oxford 53-84.

77. Fotsis T, Pepper M, Adlercreutz H, Flerischmann G & Hase T (1993) Genistein, a dietary-derived inhibitor of in vitro angiogenesis. *Proc Natl Acad Sci (USA)* **90**, 2690-94.

78. Funk MO Jr, Carroll RT, Thompson JF & Dunham RW (1986) The lipoxygenases in developing soybean seeds. Their characterization and synthesis *in vitro*. *Plant Physiol* **82**, 1139-1144.

79. Funk CD (1996) The molecular biology of mammalian lipoxygenases and the quest for eicosanoid functions using lipoxygenase-deficient mice. *Biochim Biophys Acta* **1304**, 65-84.

80. Funk CD & Loll PJ (1997) A molecular dipstick? *Nature Struct Biol* **4**, 966-968.

81. Gaffney BJ (1996) Lipoxygenase: structural principles and spectroscopy. *Annu Rev Biophys Biomol Struct* **25**, 431-459.

82. Gao X and Honn KV (1995) Biological properties of 12(*S*)-HETE in cancer metastasis. *Adv Prostaglandin Thromboxane Leukotriene Res* **23**, 439–444.

83. Galpini JR, Tielens LGM, Veldink GA, Vliegenthart JFG & Bolding J (1976) On the interaction of some catechol derivatives with the iron atom of soybean lipoxygenase. *FEBS Letters* **69**, 178-182.

84. Gardner HW (1991) Recent investigations into the lipoxygenase pathway of plants. *Biochim Biophys Acta* **1084**, 221-239.

85. Ghuman J, Zunszain PA, Petitpas I, Bhattacharya AA, Otagiri M & Curry S (2005) Structural basis of the drug-binding specificity of human serum albumin. *J Mol Biol* **353**, 38-52.

86. Gillmor SA, Villaseñor A, Fletterick R, Sigal E & Browner MF (1997) The structure of mammalian 15-lipoxygenase reveals similarity to the lipases and the determinants of substrate specificity. *Nature Struct Biol* **4**, 1003-1009.

87. Gill SC & von Hippel PH (1989) Calculation of protein extinction coefficients from amino acid sequence data. *Anal Biochem* **182**, 319-326.

88. Glickman MH & Klinman JP (1995) Nature of rate limiting steps in soybean L1 reaction. *Biochemistry* **34**, 14077-14092.

89. Glickman MH & Klinman JP (1996) Lipoxygenase reaction mechanism: Demonstration that hydrogen abstraction from substrate precedes dioxygen binding during catalytic turnover. *Biochemistry* **35**, 12882-12892.

90. Glickman MH, Cliff S, Thiemens M & Klinman JP (1997) Comparative study of ^{17}O and ^{18}O isotope effects as a probe for dioxygen activation: Application to the soybean lipoxygenase reaction. *J Am Chem Soc* **119**, 11357.

91. Grossman S, Trop M, Yaroni S & Wilchek M (1972) Purification of soybean lipoxygenase by affinity chromatography. *Biochim Biophys Acta* **289(1)**, 77-81.

92. Grossman S, Ben-Aziz A, Ascarelli I & Budowski P (1974) Lipoxygenase from Medicago sativa: Purification on hydroxyapatite. *Phytochemistry* **13**, 1379-1381.

93. Grossman S & Waksman EG (1984) New aspects of the inhibition of soybean lipoxygenase by alpha-tocopherol. Evidence for the existence of a specific complex. *Int J Biochem* **16(3)**, 281-9.

94. Guo Y, Wang S, Hoot DR & Clinton SK (2006) Suppression of VEGF-mediated autocrine and paracrine interactions between prostate

cancer cells and vascular endothelial cells by soy isoflavones. *J Nutr Biochem* (in press)

95. Gustavson KH & Holm B (1952) *J Am Leather Chem Ass* **47**, 700.

96. Hadley ME (1993) Endocrinology of pregnancy, parturation and lactation. In Endocrinology, ed. Pp. 505-29. Englewood Cliffs, NJ: Prentice Hall. 3rd ed.

97. Hausknecht EC & Funk MO (1984) The differential effect of disulfiram on lipoxygenase from *Glycine max*. *Phytochemistry* **23**, 1535-1539.

98. He XM & Carter DC (1992) Atomic structure and chemistry of human serum albumin. *Nature* **358**, 209-215.

99. He W, Li Y, Tian J, Liu H, Hu Z & Chen X (2005) Spectroscopic studies on binding of shikonin to human serum albumin. *Photochem Photobiol* **174***,* 53-61.

100. Holman TR, Zhou J & Solomon EI (1998) Spectroscopic and functional characterization of a ligand coordination mutant of soybean lipoxygenase-1: First coordination sphere analogue of human 15-lipoxygenase. *J Am Chem Soc* **120**, 12564-12572.

101. Huang R, Shi F, Lei T, Song Y, Hughes CL & Liu G (2007) Effect of the isoflavone genistein against galactose-induced cataracts in rats. *Exp Biol Med* **232(1)**, 118-25.

102. Hunter T & Cooper JA (1985) Protein tyrosine kinases. *Annu Rev Biochem* **54**, 897-930.

103. Husted S & Andreasen F (1979) *Acta Pharmacol Toxicol* **45**, 206-214.

104. Hwang CS, Kwak HS, Lim HJ, Lee SH, Kang YS, Choe TB, Hur HG & Han KO (2006) Isoflavone metabolites and their *in vitro* dual functions: they can act as an estrogenic agonist or antagonist depending on the estrogen concentration. *J Steroid Biochem Mol Biol* **101(4-5)**, 246-53.

105. Israel E, Cohn J, Dube L & Drazen JM (1996) Effect of treatment with Zileuton, a 5-lipoxygenese inhibitor in patients with asthma. *J Am Med Assn* **275**, 931-936.

106. Ingold KU (1969) Peroxyl radicals. *Acc Chem Res* **2**, 1-9.

107. Jaffé HH & Orchin M (1962) *Theory and Application of Ultraviolet Spectroscopy*, pp 581-583, John Wiley, New York.

108. Joannou GE, Kelly GE, Reeder AY, Waring MA & Nelson C (1995) A urinary profile study of dietary phytoestrogens. The identification and mode of metabolism of new isoflavonoids. *J Steroid Biochem Molec Biol* **54(3/4)**, 167-84.

109. Jovanovic SV, Steenken S, Tosic M, Marjanovic B & Simic MG (1994) Flavonoids as antioxidants. *J Am Chem Soc* **116**, 4846-4851.

110. Kang J, Liu Y, Xie M-X, Li S, Jiang M & Wang Y-D (2004) Interactions of human serum albumin with chlorogenic acid and ferulic acid. *Biochim Biophys Acta* **1674***,* 205-214.

111. Karmali RA (1987) Eicosanoids in breast cancer. *Eur J Cancer Clin Oncol* **23**, 5–7.

112. Kelly GE, Nelson C, Waring MA, Joannou GE & Reeder AY (1993) Metabolites of dietary (Soya) isoflavones in human urine. *Clin Chim Acta* **223**, 9-22.

113. Kemal C, Flamberg PL, Olsen RK & Shorter AL (1987) Reductive inactivation of soybean lipoxygenase 1 by catechols: A possible mechanism for regulation of lipoxygenase activity. *Biochemistry* **26**, 7064-7072.

114. Kimura Y, Okuda H, Arichi S, Baba K & Kozawa M (1985) Inhibition of the formation of 5-hydroxy-6,8,11,14-eicosatetraenoic acid from

arachidonic acid in polymorphonuclear leukocytes by various coumarins. *Biochim Biophys Acta* **834**, 224–229.

115. Kingston WP (1981) 15-Lipoxygenase: a rapid sensitive assay for lipoxygenase inhibitors. *Br J Pharmacol* **74**, 919.

116. Knapp MJ, Seebeck FP & Klinmann JP (2001) Steric control of oxygenation regiochemistry in soybean lipoxygenase-1. *J Am Chem Soc* **123**, 2931.

117. Knight DC & Eden JA (1994) A review of the clinical effects of phytoestrogens. *Obstet Gynecol* **87**, 897-904.

118. Komm BS, Terpening CM, Benz DJ, Graeme KA, Gallegos A, Korc M, Greene GL, O'Malley BW & Haussler MR (1988) Estrogen binding, receptor mRNA, and biologic response in osteoblast-like osteosarcoma cells. *Science* **241(4861)**, 81-4.

119. Koshiyama I (1972) A newer method for isolation of the 7S globulin in soybean seeds. *Agric Biol Chem* **36**, 2255-2257.

120. Kuiper GGJM, Carlsson B, Grandien K, Enmark E, Häggblad J, Nillson S & Gustafsson JÅ (1997) Comparison of the ligand binding specificity and transcript tissue distribution of estrogen receptors α and β. *Endocrinology* **138**, 863-870.

121. Kuiper GGJM, Enmark E, Pelto-Huikko M, Nilsson & Gustafsson JÅ (1996) Cloning of a novel estrogen receptor expressed in rat prostate and ovary. *Proc Natl Acad Sci (USA)* **93**, 5925-5930.

122. Kuhn H, Saam J, Eibach S, Holzhutter HG, Ivanov & Walther M (2005) Structural biology of mammalian Lipoxygenases: Enzymatic

consequences of targeted alterations of the protein structure. *Biochem Biophys Res Commun* **339**, 93-101.

123. Kuhn H & Theile BJ (1999) The diversity of plant Lipoxygenase family. Many sequence data but little information on biological significance. *FEBS Lett* **16**, 7-11.

124. Kragh-Hansen U (1988) Evidence for a large and flexible region of human serum albumin possessing high affinity binding sites for salicylate, warfarin, and other ligands. *Mol Pharmacol* **34**, 160-171.

125. Laemmli UK (1970) Cleavage of structural proteins during the assembly of the head of bacteriophage T4. *Nature* **277**, 680-685.

126. Lakemond CMM, de Jongh HHJ, Gruppen H & Voragen AGJ (2002) Differences in denaturation of genetic variants of soy glycinin. *J Agric Food Chem* **50**, 4275-4281.

127. Lakemond CMM, de Jongh HHJ, Paques M, van Vliet T, Gruppen H & Voragen AGJ (2003) Gelation of soy glycinin; influence of pH and ionic strength on network structure in relation to protein conformation. *Food Hydrocolloids* **17**, 365-377.

128. Lalles JP, Tukur HM, Salgado P, Mills ENC, Morgan MRA, Quillien L, Levieux D & Toullec R (1999) Immunochemical studies on gastric and intestinal digestion of soybean glycinin and β-conglycinin *in vivo*. *J Agric Food Chem* **47**, 2797-2806.

129. Lee CJ, Harrison D & Timasheff SN (1975) Interaction of vinblastine with calf brain microtubule protein. *J Biol Chem* **250**, 9276-9282.

130. Liu K, Bhalla K, Hill C & Priest DG (1994) Evidence for involvement of tyrosine phosphorylation in taxol-induced apoptosis in a human ovarian tumor cell line. *Biochem Pharmacol* **48**, 1265-1272.

131. Liu K *Soybeans: Chemistry, Technology and Utilization*; Chapman and Hall: New York, 1997.

132. Li W, Zhang M, Zhang JL, Li HQ, Zhang XC, Sun Q & Qiu CM (2006) Interactions of daidzin with intramolecular G-quadruplex. *FEBS Lett* **580(20)**, 4905-10.

133. Liu X-H, Connolly JM & Rose DP (1996) Eicosanoids as mediators of linoleic acid-stimulated invasion and type IV collagenase production by a metastatic human breast cancer cell line. *Clin Exp Metastasis* **14**, 145–152.

134. Liu Y-W, Asaoka Y, Suzuki H, Yoshimoto T, Yamamoto S & Chang W-C (1994) Induction of 12-lipoxygenase expression by epidermal growth factor is mediated by protein kinase C in A431 cells. *J Pharmacol Exp Ther* **271**, 567–573.

135. Lowry OH, Rosebrough NJ, Farr A & Randall RJ (1951) Protein measurement with the folin phenol reagent. *J Biol Chem* **143**, 265-271.

136. Maccarone M, Melino G & Finazzi-Agro A (2001) Lipoxygenase and their involvement in programmed cell death. *Cell Death and Differ* **8**,776-784.

137. Mahesha HG, Singh SA, Srinivasan N & Rao AGA (2006) A Spectroscopic study of the interaction of isoflavones with human serum albumin. *FEBS Journal* **273**, 451-467.

138. Maliwal BP, Appu Rao AG and Narasinga Rao MS (1985) Spectroscopic study of the interaction of gossypol with bovine serum albumin. *Int J Pep Protein Res* **25***,* 382-388.

139. Manjanatha MG, Shelton S, Bishop ME, Lyn-cook LE & Aidoo A (2006) Dietary effects of soy isoflavones daidzein and genistein on 7,12-dimethylbenz [a] anthracene-induced mammary mutagenesis and carcinogenesis in ovariectomized big blue transgenic rats. *Carcinogenesis* **27(12)**, 2555-64.

140. Markiewicz L, Garey J, Adlercreutz H & Gurpide E (1993) *In vitro* bioassays of non-steroidal phytoestrogens. *J of Steroid Biochem and Mol Biol* **45**, 399-405.

141. Markovits J, Linassier C, Fosse P, Couprie J & Pierre J (1989) Inhibitory effects of the tyrosine kinase inhibitor genistein on mammalian DNA topoisomerase II. *Cancer Res* **49**, 5111-17.

142. Martin PM, Horwitz KB, Ryan DS & McGuire WL (1978) Phytoestrogens interaction with estrogen receptors in human breast cancer cells. *Endocrinology* **103**, 1860-67.

143. Maruyana T, Link CC, Yamasaki K, Miyoshi T, Mai T, Yamasakii M & Otagiri M (1993) Binding of suprofen to human serum albumin. *Biochem Pharmacol* **45 (5)** 1017 – 1026.

144. Matulis D & Lovrien R (1998) 1-Anilino-8-Naphathalene Sulfonate Anion-Protein Binding Depends Primarily on Ion Pair Formation. *Biophy J* **74**, 422-429.

145. Meloun B, Saber MA & Kusnir J (1975) Structure of N-terminal cyanogen bromide fragment of plasma albumin. *Biochim Biophys Acta* **393**, 505-19.

146. Mezei O, Banz WJ, Steger RW, Peluso MR, Winters TA & Shay N (2003) Soy isoflavones exert antidiabetic and hypolipidemic effects

through the PPAR pathways in obese Zucker rats and murine RAW 264.7 cells. *J Nutr* **133**, 1238-1243.

147. Miksicek RJ (1993) Commonly occurring plant flavonoids have estrogenic activity. *Mol Pharmacol* **44**, 37-43.

148. Miksicek RJ (1994) Interaction of naturally occurring nonsteroidal estrogens with expressed recombinant human estrogen receptor. *J of Steroid Biochem and Mol Biol* **49**, 153-160.

149. Minor W, Steezko J, Stec B, Otwinowski Z, Bolin TJ, Walter R & Axelrod B (1996) Crystal structure of soybean lipoxygenase L1 at 1.4 Å resolution. *Biochemistry* **35**, 10687-10701.

150. Moody TR, Leyton J, Martinez A, Hong S, Malkinson A & Mulshine JL (1998) Lipoxygenase inhibitors prevent lung carcinogenesis and inhibit non-small cell lung cancer growth. *Exp Lung Res* **24**, 617–628.

151. Morton MS, Wilcox G, Wahlqvist ML & Griffiths K (1994) Determination of lignans and isoflavonoids in human female plasma following dietary supplementation. *J Endocrinol* **142**, 251-9.

152. Naim M, Gestetner B, Kirson I, Birk Y & Bondi A (1973) Antioxidative and antihemolytic activity of soybean isoflavones. *J Agric Food Chem* **24**, 1174-77.

153. Nagai M, Hashimoto T, Yanagawa H, Yokoyama H & Minowa M (1982) Relationship of diet to the incidence of esophageal and stomach cancer in Japan. *Nutr Cancer* **3(4)**, 257-68.

154. Nelson MJ, Seitz SP & Cowling RA (1990) Enzyme-bound pentadienyl & peroxyl radicals in purple lipoxygenase. *Biochemistry* **29**, 6897-6903.

155. Nelson MJ & Seitz SP (1994) The structure and function of lipoxygenase. *Curr Opin Struct Biol* **4**, 878-884.

156. Nguyen DT, Hernandez-Montes E, Vauzour D, Schonthal AH, Rice-Evans C, Cadenas E & Spencer JP (2006) The intracellular genistein metabolite 5,7,3',4'-tetrahydroxyisoflavone mediates G2-M cell cycle arrest in cancer cells via modulation of the p38 signaling pathway. *Free Radic Biol Med* **41(8)**, 1225-39.

157. Occhiuto F, Pasquale RG, Guglielmo G, Palumbo DR, Zangla G, Samperi S, Renzo A & Circosta C (2006) Effects of phytoestrogenic isoflavones from red clover (Trifolium pratense L.) on experimental osteoporosis*. Phytother Res* (in press)

158. Ohta N, Kuwata G, Akahori H & Watanbe T (1979) Isoflavonoid Constituents of soybean. *Agric Biol Chem* **43**, 1415-1419.

159. Papatheofanis FJ & Lands WEM (1985) Biochemistry of arachidonic acid metabolism, In: (Lands, W. E. M., Ed.) Martinus Nijhoff, Boston, 9-39.

160. Parker CW (1987) Lipid mediators produced through the lipoxygenase pathway. *Annu Rev Immunol* **5**, 65-84.

161. Park JS, Woo MS, Kim DH, Hyun JW, Kim WK, Lee JC & Kim HS (2006) Anti-inflammatory mechanisms of isoflavone metabolites in lipopolysaccharide-stimulated microglial cells. *J Pharmacol Exp Ther (in press).*

162. Pang HY, Yang LL, Shaung MS, Dong C & Thompson M (2005) Interaction of human serum albumin with bendroflumethiazide by fluorescence spectroscopy. Photochem *Photobiol* **80**, 139-144.

163. Panossian AG (1984) Inhibition of arachidonic acid 5-lipoxygenase of human polymorphonuclear leukocytes by esculetin. *Biochim Biophys Acta* **43**, 1351–1355.

164. Patel RP, Boersma BJ, Crawford JH, Hogg N, Kirk M, Kalyanaraman B, Parks, DA, Barnes S & Usmar DA (2001) Antioxidant mechanisms of isoflavones in lipid systems: Paradoxical effects of peroxyl radical scavenging. *Free Radic Biol Med* **31**, 1570-1581.

165. Pratt DE & Birac PM (1979) Source of antioxidant activity of soybeans and soy products. *J Food Sci* **44**, 1720-22.

166. Pereira IR, Faludi AA, Aldright JM, Bertolami MC, Saleh MH, Silva RA, Nakamura Y, Campos MF, Novaes N & Abdalla DS (2006) Effects of soy germ isoflavones and hormone therapy on nitric oxide derivatives, low-density lipoprotein oxidation, and vascular reactivity in hypercholesterolemic postmenopausal women. *Menopause* **13(6)**, 942-50.

167. Peters Jr T (1985) Serum albumin. *Adv Protein Chem* **37**, Acad Press NY 161-245.

168. Peterson G & Barnes S (1991) Genistein inhibition of the growth of human breast cancer cells: Independence from estrogen receptors and multi-drug resistance gene. *Biochem Biophys Res Commun* **179**, 661-667.

169. Petersson L, Slappendel S & Vilegenthart JFG (1985) The magnetic susceptibility of native soybean Lipoxygenase-1. Implication for the symmetry of the iron environment and the possible coordination of dioxygen FoFe (II). *Biochim Biophys Acta* **828**, 81-85.

170. Petitpas I, Bhattacharya AA, Twine S, East M & Curry S (2001) Crystal structure analysis of warfarin binding to human serum albumin–anatomy of drug site I. *J Biol Chem* **276**, 22804-22809.

171. Pistorius EK & Axelrod B (1974) Iron, an essential component lipoxygenase. *J Biol Chem* **249(10)**, 3183-6.

172. Pistorius EK, Axelord B & Palmer G (1976) Evidence for participation of iron in Lipoxygenase reaction from optical and electron spin resonance studies. *J Biol Chem* **251**, 7144-7148.

173. Prigge ST, Boyington JC, Gaffney BJ & Amzel LM (1996) Lipoxygenases: structure & function. In: Lipoxygenase & Lipoxygenase pathway enzymes (Piazza GJ ed) AOCS Press, 1-31.

174. Rao AGA and Cann JR (1981) A comparative study of the interaction of chlorpromazine, trifluoperazine, and promethazine with mouse brain tubulin. *Mol Pharmacol* **19**, 295-301.

175. Riblett AL, Herald TJ, Schmidt KA & Tilley KA (2001) Characterization of β-conglycinin and glycinin soy protein fractions from four selected soybean genotypes. *J Agric Food Chem* **49**, 4983-4989.

176. Rigas B, Goldman IS & Levine L (1993) Altered eicosanoid levels in human colon cancer. *J Lab Clin Med* **122(5)**, 518-23.

177. Rioux N & Castonguay A (1998) Inhibitors of lipoxygenase: a new class of cancer chemopreventive agents. *Carcinogenesis (Lond)* **19**, 1393–1400.

178. Rose P & Connolly JM (1991) Effects of fatty acids and eicosanoid synthesis inhibitors on the growth of two human prostate cancer cell lines. *Prostrate* **18**, 243–254.

179. Saber MA, Stöckbauer P, Moravek L & Meloun B (1977) Disulfide bonds in human serum albumin. *Collin Czech Chem Commun Engl Edn* **42**, 564-579.

180. Samuelsson B, Dahlen SE, Lindgren JA, Rouzer CA & Serhan CN (1987) Leukotrienes and lipoxins: Structures, biosynthesis and biological effects. *Science* **237**, 1171-1176.

181. Sartorelli AC (1985) Malignant cell differentiation as a potential therapeutic approach. *Br J Cancer* **52**, 293-302.

182. Scarrow RC, Trimitsis MG, Buck CP, Grove GN, Cowling RA & Nelson MJ (1994) X-ray spectroscopy of the iron site in soybean Lipoxygenase-1: changes in coordination upon oxidation or addition of methanol. *Biochemistry* **33**, 15023-15035.

183. Scatchard G (1949) The attractions of proteins for small molecules and ions. *Ann NY Acad Sci* **51**, 660-672.

184. Schewe T, Rapoport SM & Kuhn H (1986) Enzymology of reticulocyte Lipoxygenase: Comparison with other Lipoxygenases. *Adv Enzymol Relat Areas Mol Biol* **58**, 191-272.

185. Schewe T, Kühn H & Sies H (2002) Flavonoids of cocoa inhibit recombinant human 5-lipoxygenase. *J N*utr **132**, 1825-1829.

186. Schilstra MJ, Veldink GA & Vliegenthart JFG (1994) The Dioxygenation Rate In Lipoxygenase Catalysis Is Determined by the Amount of Iron (III) Lipoxygenase in Solution. *Biochemistry* **33**, 3974 – 3979.

187. Schultze HE & Heremans JF (1966) "Molecular biology of human proteins, with special reference to plasma proteins" Elsevier, Amsterdam.

188. Sekiya K, Okuda H & Arichi S (1982) Selective inhibition of platelet lipoxygenase by esculetin. *Biochim Biophys Acta* **713**, 68–72.

189. Severson RK, Nomura AMY, Grove JS & Stemmermann GN (1989) A prospective study of demographics, diet and prostate cancer among men in Japanese ancestry in Hawaii. *Cancer Res* **49**, 1857-60.

190. Setchell KDR & Adlercreutz H (1988) Mammalian lignans and phytoestrogens. Recent studies on their formation, metabolism and biological role in health and disease. In *Role of the Gut Flora in Toxicity and cancer*, ed, IR Rowland, pp315-45, London; Academic.

191. Setchell KDR and Cassidy A (1999) Dietary isoflavones: biological effects and relevance to human health. *J Nutr* **129**, 758S-767S.

192. Shannon VR, Stenson WF & Holtzman MJ (1993) Induction of epithelial arachidonate 12-Lipoxygenese at active sites of inflammatory bowel disease. *Am J Physiol* **264**, G104-111.

193. Shaw CF (1989) Comments Inorg Chem **8(6)**, 233-267.

194. Shutt DA & Cox RI (1972) Steroid and phyto-oestrogen binding to sheep uterine receptors *in vitro*. *J Endocrinol* **52(2)**, 299-310.

195. Siedow JN (1991) Plant Lipoxygenase: structure and function. *Annu Rev Plant Physiol Plant Mol Biol* **42**, 145-188.

196. Simard JR, Zunszain PA, Hamilton JA & Curry S (2006) Location of high and low affinity fatty acid binding sites on human serum albumin revealed by NMR drug-competition analysis. *J Mol Biol* **361**, 336-351.

197. Skrzypczak-Jankun E, Amzel LM, Kroa BA & Funk MO Jr (1997) Structure of soybean lipoxygenase L3 and a comparison with its L1 isoenzyme. *Proteins* **29(1)**, 15-31.

198. Slappendel S, Veldink GA, Vliegenthart JFG, Aasa R & Malmstrom BG (1981). EPR spectroscopy of soybean Lipoxygenase-1. Description & quantification of the high spin Fe (III) signals. *Biochim Biophys Acta* **667**, 77-86.

199. Slappendel S, Aasa R, Malmstrom BG, Veragen J, Veldink GA & Vliegenthart JFG (1982) Factors affecting the line shape of the EPR signal of high-spin Fe (III) in soybean lipoxygenase. *Biochim Biophys Acta* **708**, 259-265.

200. Spaapen LJM, Veldink GA, Liefkens TJ, Vliegenthart JFG & Kay CM (1979) Circular dichroism of lipoxygenase-1 from soybeans. *Biochim Biophys Acta* **574**, 301-311.

201. Spande TF & Witkop B (1967) Determination of the tryptophan content of proteins with N-bromosuccinimide. *Methods Enzymol* **11**, 498-506.

202. Spencer CM, Cai Y, Martin R, Gaffney SH, Goulding PN, Magnolato D, Lilley TH & Haslam E (1988) Polyphenol complexation-some thoughts and observations. *Phytochemistry* **27**, 2397-2409.

203. Spinozzi F, Pagliacci MC, Migliorati G, Moraca R, Grignami F, Riccardi C & Nicoletti I (1994) The natural tyrosine kinase inhibitor genistein produces cell cycle arrest and apoptosis in Jurket T-leukemia cells. *Leuk Res* **18**, 431-439.

204. Spector A (1975) Fatty acid binding to plasma albumin. *J Lipid Res* **16**, 165-179.

205. Stamler J (1979) Population studies. In Nutrition and Lipids and Coronary Heart Disease, ed. RI Levy. BM Rifkind, BH Dennis, N Ernst, New York: Raven 25-88.

206. St Angelo AJ & Ory RL (1984) Lipoxygenase inhibition by naturally occurring monoenoic fatty acids. *Lipids* **19**, 34-37.

207. Staswick PE, Hermodson MA & Nielsen NC (1984) Identification of the cystines which link the acidic and basic components of the glycinin subunits. *J Biol Chem* **259**, 3431-3435.

208. Steinberg D, Parathasarathy S, Carew TE, Khoo JC & Witztum MD (1989) Beyond cholesterol modifications of low-density lipoprotein that increases its atherigenicity. *N Eng J Med* **320**, 915-924.

209. Sugio S, Kashima A, Mochizuki S, Noda M & Kobayashi (1999) Crystal structure of human serum albumin at 2.5 Å resolution. *Protein Engineering* **12**, 439-446.

210. Sudlow G, Birkett DJ & Wade DN (1975) The characterization of two specific drug binding sites on human serum albumin. *Mol Pharmacol* **11**, 824-832.

211. Sudharshan E & Rao AGA (1997) Rapid Method to separate the domains of soybean lipoxygenase 1: Identification of the interdomain interactions. *FEBS Lett* **406**, 184-188.

212. Swain T (1978) In Biochemical aspects of plant and animal co-evolution (Harborne JB; ed) page-3, Academic Press, London.

213. Sytnik A & Litvinyuk I (1996) Energy transfer to a proton-transfer fluorescence probe: Tryptophan to a flavonol in human serum albumin. *Proc Nat Acad Sci (USA)* **93***,* 12959-12963.

214. Takahama U (1985) Inhibition of lipoxygenase-dependent lipid peroxidation by quercetin: Mechanism of antioxidative function. *Phytochemistry* **24**, 1443-1446.

215. Takahashi Y, Reddy GR, Ueda N, Yamamoto S & Arase S Arachidonate (1993) 12-lipoxygenase of platelet-type in human epidermal cells. *J Biol Chem* **268**, 16443–16448.

216. Tappel AL, Boyer PD & Lundberg WO (1952) The reaction mechanism of soybean lipoxidase. *J Biol Chem* **199(1)**, 267-81.

217. Tejero I, Viloca MG, Lafont AG, Lluch JM & York DM (2006) Enzyme dynamics and tunneling enhanced by compression in the hydrogen abstraction catalyzed by soybean lipoxygenase-1. *J Phys Chem* **110**, 24708-24719.

218. Thanh VP & Shibasaki K (1976) Major proteins of soybean seeds. A straightforward fractionation and their characterization. *J Agric Food Chem* **24**, 1117-1121.

219. Tikkanen M, Wahala K, Ojala S, Vihma V & Adlercreutz H (1998) Effect of soybean phytoestrogen intake on low-density lipoprotein oxidation resistance. *Proc Natl Acad Sci (USA)* **l95**, 3106-3110.

220. Tillement JP, Zini R, d'Athias P & Vassent G (1974) Binding of certain acidic drugs to human albumin: theoretical and practical estimation of fundamental parameters. *Eur J Clin Pharmacol* **7**, 307-313.

221. Tomchick DR, Phan P, Cymborowski M, Minor W & Holman TR (2001) Structural and functional characterization of second-coordination sphere mutants of soybean lipoxygenase-1. *Biochemistry* **40**, 7509-7517.

222. Traganos F, Ardelt B, Halko N, Bruno S & Darzynkiewicz Z (1992) Effects of genistein on the growth and cell cycle progression of normal human lymphocytes and human leukemic MOLT-4 and HL-60 cells. *Cancer Res* **52**, 6200-8.

223. Twine SM, Gore MG, Morton P, Fish BC, Lee AG & East JM (2003) Mechanism of binding of warfarin enantiomers to recombinant domains of human albumin. *Arch Biochem Biophy* **414**, 83-90.

224. Ungar Y, Oluwatooyin F, Osundahunsi & Shimoni E (2003) Thermal stability of genistein and daidzein and its effect on their antioxidant activity. *J Agric Food Chem* **51**, 4394-4399.

225. Van der Zee J, Eling TE & Mason RP (1989) Formation of free-radical metabolites in the reaction between soybean lipoxygenase and its inhibitors. An ESR study. *Biochemistry* **28**, 8363-8367.

226. Veldink GA, Vliegenthart JFG & Bolding J (1977) Plant Lipoxygenase. *Prog Chem Fat Other Lipids* **15**, 131-166.

227. Wang G, Kuan SS, Francis OJ, Ware GM & Carman AS (1990) A simplified HPLC method for the determination of phytoestrogens in soybean and its processed products. *J Agric Food Chem* **38**, 185-190.

228. Wang HJ & Murphy PA (1994) Isoflavone content in commercial soybean foods. *J Agric Food Chem* **42**, 1674-1677.

229. Wang Z-X, Killilea DS & Srivastava DK (1993) Kinetic evaluation of substrate dependent origin of the lag phase in soybean lipoxygenase-1 catalyzed reactions. *Biochemistry* **32**, 1500-1509.

230. Wang TTY, Sathyamoorthy N & Phang JM (1996) Molecular effects of genistein on estrogen receptor mediated pathways. *Carcinogenesis* **17(2)**, 271-275.

231. Weber G & Young LB (1964) Fragmentation of bovine serum albumin by pepsin: the origin of the acid expansion of the albumin molecule. *J Biol Chem* **239**, 1415-1423.

232. Wei H, Bowen R, Cai Q, Barnes S & Wang Y (1995) Antioxidant and antipromotional effects of the soybean isoflavone genistein. *Proc Soc Exp Biol Med* **208 (1)**, 124-30.

233. Welsch CW (1992) Relationship between dietary fat and experimental mammary tumorigenesis: a review and critique. *Cancer Res* **52**, 2040S–2048S.

234. Welshons WV, Rottinghaus GE, Nonneman DJ, Dolan-Timpe M & Ross PF (1990) A sensitive bioassay for detection of dietary estrogens in animal feeds. *J Vet Diagn Invest* **2**, 268-73.

235. White T (1957) *J Sci Food Agric* **8**, 377.

236. Wu P & Brand L (1994) Resonance energy transfer: Methods and applications. *Anal Biochem* **218**, 1-13.

237. Xiao CW, Mei J, Huang W, Wood C, L'abbe MR, Gilani GS, Cooke GM & Curran IH (2007) Dietary soy protein isolate modifies hepatic retinoic acid receptor-beta proteins and inhibits their DNA binding activity in rats. *J Nutr* **137(1)**, 1-6.

238. Xu X, Harris K, Wang H–J, Murphy P & Hendrich S (1995) Bioavailability of soybean isoflavones depends upon gut microflora in women. *J Nutr* **125**, 2307-2315.

239. Yamamoto S, Suzuki H & Veda N (1997) Arachidonate 12-lipoxygenases. *Prog Lipid Res* **36**, 23-41.

240. Yamasaki K, Maruyama T, Kragh-Hansen U & Otagiri M (1996) Characterization of site I on human serum albumin: concept about the structure of a drug binding site. *Biochim Biophys Acta* **1295**, 147-157.

241. Yasumato K, Yamamoto A & Mitsuda H (1970) Effect of phenolic antioxidants on lipoxygenase reaction *Agric Biol Chem* **34**, 1162-1168.

242. Yang JT, Wu CSC & Martinez HM (1986) Calculation of protein conformation from circular dichroism. *Methods Enzymol* **130**, 208-269.

243. Yang JY, Lee SJ, Park HW & Chay S (2006) Effect of Genistein with Carnitine administration on lipid parameters and obesity in C57Bl/6J Mice Fed a High-Fat Diet. *J Med Food* **9(4)**, 459-67.

244. Yokomizo T, Izumi T, Chang K, Takuwa Y & Shimizu T (1997) A G-protein coupled receptor for leukotriene B4 that mediates chemotaxis. *Nature* **387**, 620-624.

245. Zielonka J, Gebicki J & G Grynkiewicz (2003) Radical scavenging properties of genistein. *Free Radic Biol Med* **35**, 958-965.

246. Zhang GY, Tsunokawa S, Hayashi Y, Matsumoto S, Matsumura Y & Mori T (2003) Reconstitution of single molecular species from isolated subunits of glycinin. *J Am Oil Chem Soc* **80**, 497-501.

247. Zsila F, Bikádi Z & Simónyi M (2003) Probing the binding of the flavonoid, quercetin to human serum albumin by circular dichroism, electronic absorption spectroscopy and molecular modeling methods. *Biochem Pharmacol* **65**, 447-456.

PUBLICATIONS

[1] **Mahesha, H. G.,** Singh, S. A. Srinivasan, N. and Rao, A. G. A. (2006) A spectroscopic study of the interaction of isoflavones with human serum albumin. *FEBS Journal* **273**, 451-467.

[2] **Mahesha, H. G.,** Singh, S. A. and Rao, A. G. A. (2007) Inhibition of lipoxygenase by soy isoflavones: evidence of isoflavones as redox inhibitors. *Arch Biochem Biophy* (in press).